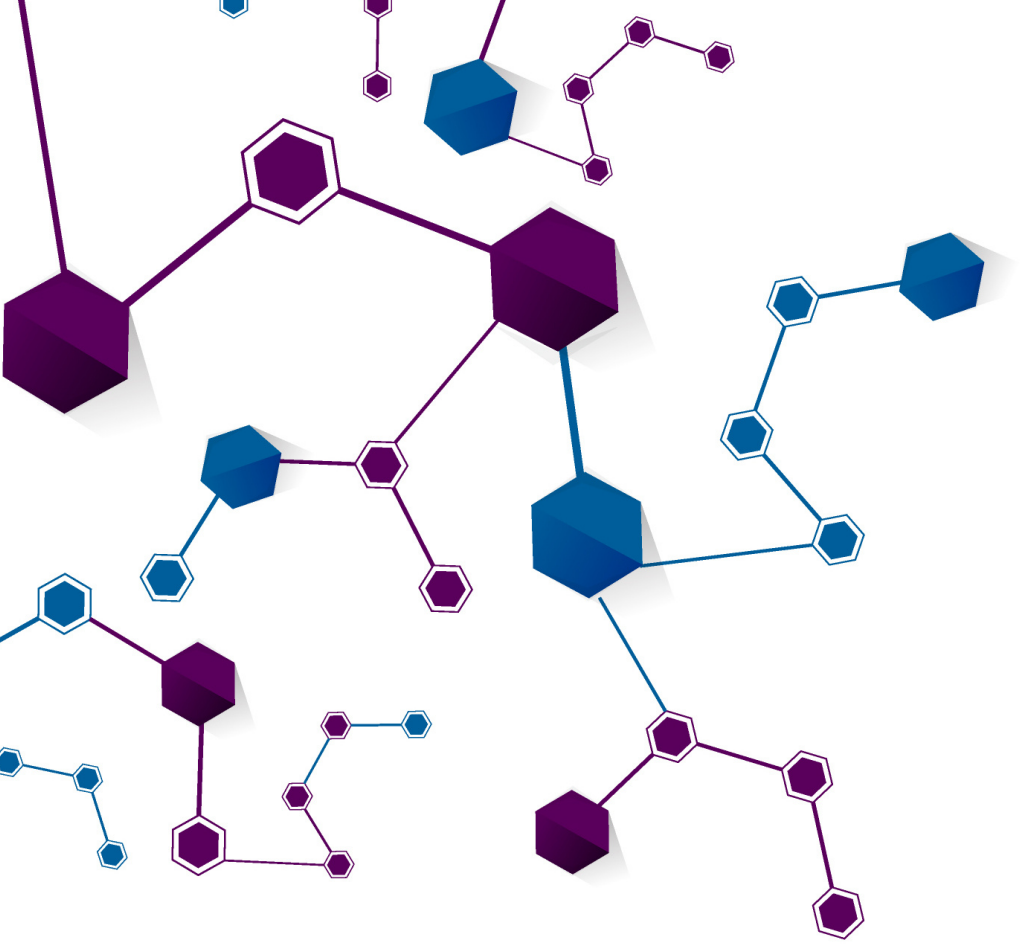

含溴药物品种 资料汇编

全面的含溴药物资料与合成方法、研发背景、药理、药代、安全性、临床试验等方面详细的研究结果展示

药智数据 编纂

https://db.yaozh.com/

含溴药物品种资料汇编

药智数据 编纂

简要说明：

本资料汇编由正文100页，附件112页构成。正文部分汇总了全部含溴药物，包括曾经研究过、曾经上市应用、目前尚在应用以及目前尚在研的含溴药物，计259种。对于其中15种重点药物，在附件部分给出其合成方法、研发背景、药理、药代、安全性、临床试验等方面详细的研究结果。

著录体例：

1，【别　　名】，包括药物的试验编号、商标名称及其英文异名；

2，【名称来源】，指的是 WHO DI 网站上公布的推荐 INN 表和建议 INN 表，例如，pINN-073,1995　rINN-036,1996　表示该 INN 名称来自于 1995 年的推荐 INN 第 73 表和 1996 年的建议 INN 第 36 表。

3，【中文 CADN】，指的是经国家药典委员会确定的中国药品通用名称，名后注(97)，表示该名称见于《中国药品通用名称》（1997 年版）；名后注(GB4)，表示该名称见于《国家药品标准工作手册》（第四版）。

4，【建议 CADN】，指的是第 3 条中所述两书均未收录，由《药智数据》根据 INN 和 CADN 命名规律而自拟的药品中文译名。

【英文 INN】acebrochol

【别　　名】acebrocol

【名称来源】pINN-001,1953　rINN-001,1955

【中文 CADN】醋溴考尔 (97)

【建议 CADN】

【化学表述】Cholestan-3-ol, 5,6-dibromo-, acetate, (3β,5α,6β)-

【CA 登记号】[514-50-1]

【分 子 式】C29H48Br2O2

【结 构 式】

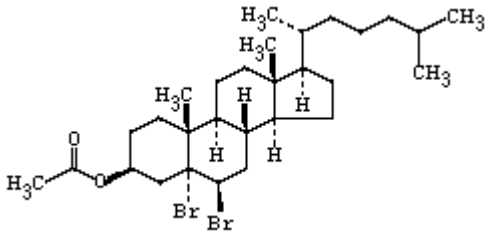

【品种类别】神经系统>催眠镇静药>其它

【英文 INN】azamethonium bromide

【别　　名】

【名称来源】pINN-001,1953　rINN-001,1955

【中文 CADN】阿扎溴铵(GB4)

【建议 CADN】

【化学表述】3-methyl-3-azapentane-1,5-bis(ethyl dimethyl ammonium) bromide

【CA 登记号】[306-53-6]

【分 子 式】C13H33Br2N3

【结 构 式】

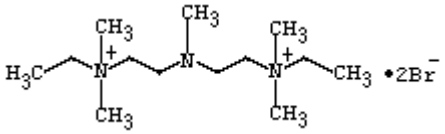

【品种类别】心血管系统>抗高血压药>双季铵盐类

【英文 INN】benzpyrinium bromide

【别　　名】

【名称来源】pINN-001,1953　rINN-001,1955

【中文 CADN】苄吡溴铵(GB4)

【建议 CADN】

【化学表述】Pyridinium, 1-benzyl-3-(dimethylcarbamyloxy)-, bromide

【CA 登记号】[587-46-2]

【分 子 式】C15H17BrN2O2

【结 构 式】

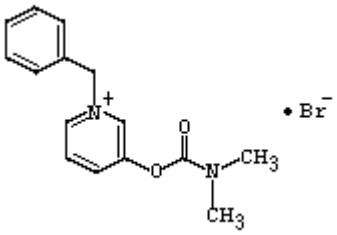

【品种类别】拟胆碱药

英文 INN】bibrocathol

【别　　名】Noviform

【名称来源】pINN-001,1953　rINN-001,1955

【中文 CADN】铋溴酚(97)

【建议 CADN】

【化学表述】4,5,6,7-Tetrabromo-2-hydroxy-1,3,2-Benzodioxabismole

【CA 登记号】[6915-57-7]

【分 子 式】C6HBiBr4O3

【结 构 式】

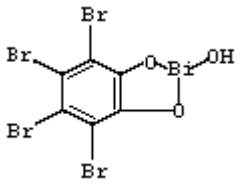

【品种类别】眼科用药>消毒防腐药>其它

【英文 INN】carbromal

【别　　名】

【名称来源】pINN-001,1953　rINN-001,1955

【中文 CADN】卡溴脲(97)

【建议 CADN】

【化学表述】Butanamide, N-(aminocarbonyl)-2-bromo-2-ethyl-

【CA 登记号】[77-65-6]

【分 子 式】C7H13BrN2O2

【结 构 式】

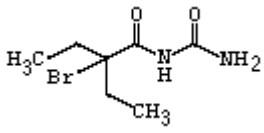

【品种类别】神经系统>催眠镇静药>酰脲类

【英文 INN】cetrimonium bromide

【别　　名】

【名称来源】pINN-001,1953　rINN-001,1955

【中文 CADN】西曲溴铵(GB4)

【建议 CADN】

【化学表述】1-Hexadecanaminium, N,N,N-trimethyl-, bromide

【CA 登记号】[57-09-0]

【分 子 式】C19H42BrN

【结 构 式】

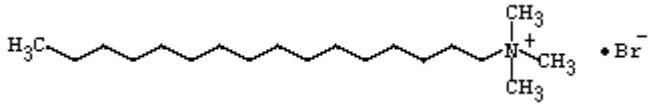

【品种类别】抗感染药>消毒防腐药>季铵盐类

【英文 INN】decamethonium bromide

【别　　名】

【名称来源】pINN-001,1953　rINN-001,1955

【中文 CADN】十烃溴铵(GB4)

【建议 CADN】

【化学表述】1,10-Decanediaminium, N,N,N,N',N',N'-hexamethyl-, bromide

【CA 登记号】[541-22-0]

【分 子 式】C16H38Br2N2

【结 构 式】

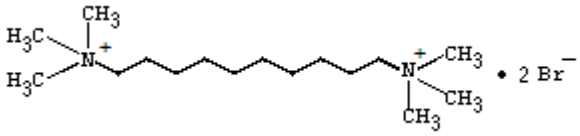

【品种类别】肌肉-骨骼系统>肌松药>季铵盐类

【英文 INN】hexamethonium bromide

【别　　名】

【名称来源】pINN-001,1953　rINN-001,1955

【中文 CADN】六甲溴铵(GB4)

【建议 CADN】

【化学表述】N,N,N,N',N',N'-Hexamethyl-1,6-hexanediaminium, dibromide

【CA 登记号】[55-97-0]

【分 子 式】C12H30Br2N2

【结 构 式】

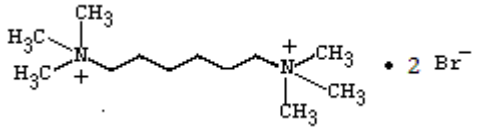

【品种类别】心血管系统>抗高血压药>双季铵盐类

【英文 INN】homatropine methylbromide

【别　　名】

【名称来源】pINN-001,1953　rINN-001,1955

【中文 CADN】甲溴后马托品(GB4)

【建议 CADN】

【化学表述】3-(2-hydroxy-2-phenylacetoxy)-8-methyl-8-azabicyclo[3.2.1]octane, bromide
【CA 登记号】[80-49-9]
【分 子 式】C17H24BrNO3
【结 构 式】

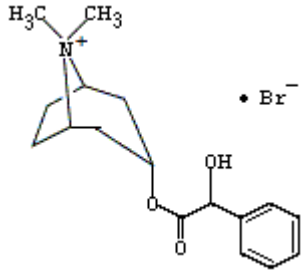

【品种类别】抗胆碱药>季铵盐类

【英文 INN】ibrotamide
【别　　名】
【名称来源】pINN-001,1953　rINN-001,1955
【中文 CADN】异溴米特(97)
【建议 CADN】
【化学表述】Butyramide, 2-bromo-2-ethyl-3-methyl-
【CA 登记号】[466-14-8]
【分 子 式】C7H14BrNO
【结 构 式】

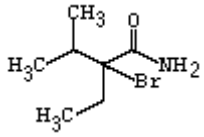

【品种类别】神经系统>催眠镇静药>酰胺类

【英文 INN】merbromin
【别　　名】Mercurochrome
【名称来源】pINN-001,1953　rINN-001,1955
【中文 CADN】汞溴红(GB4)
【建议 CADN】
【化学表述】Mercury, (2',7'-dibromo-3',6'-dihydroxy-3-oxospiro[isobenzofuran-1(3H),9'-[9H]xanthen]-4'-yl)hydroxy-, disodium salt
【CA 登记号】[129-16-8]
【分 子 式】C20H8Br2HgNa2O6
【结 构 式】

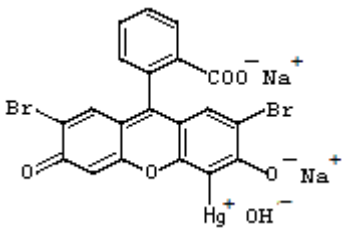

【品种类别】抗感染药>消毒防腐药>含汞化合物类

【英文 INN】oxyphenonium bromide
【别　　名】
【名称来源】pINN-001,1953　rINN-001,1955
【中文 CADN】奥芬溴铵(GB4)
【建议 CADN】
【化学表述】Ethanaminium,2-[(cyclohexylhydroxyphenylacetyl)oxy]-N,N-diethyl-N-methyl-, bromide
【CA 登记号】[50-10-2]
【分 子 式】C21H34BrNO3
【结 构 式】

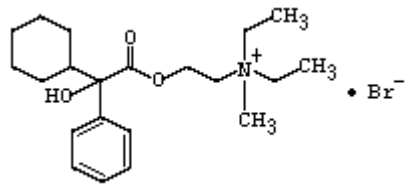

【品种类别】抗胆碱药>季铵盐类

【英文 INN】pentamethonium bromide
【别　　名】
【名称来源】pINN-001,1953　rINN-001,1955
【中文 CADN】五甲溴铵(GB4)
【建议 CADN】
【化学表述】1,5-Pentanediaminium, N,N,N,N',N',N'-hexamethyl-, dibromide
【CA 登记号】[541-20-8]
【分 子 式】C11H28Br2N2
【结 构 式】

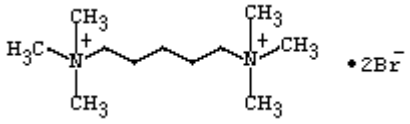

【品种类别】心血管系统>抗高血压药>双季铵盐类

【英文 INN】domiphen bromide
【别　　名】
【名称来源】pINN-001,1953　rINN-001,1955
【中文 CADN】度米芬(97)
【建议 CADN】
【化学表述】1-Dodecanaminium, N,N-dimethyl-N-(2-phenoxyethyl)-, bromide
【CA 登记号】[538-71-6]
【分 子 式】C22H40BrNO
【结 构 式】

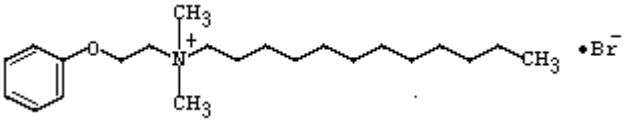

【品种类别】抗感染药>消毒防腐药>季铵盐类

【英文 INN】propantheline bromide
【别　　名】
【名称来源】pINN-001,1953　rINN-001,1955
【中文 CADN】溴丙胺太林(97)
【建议 CADN】
【化学表述】N,N-Diisopropyl-N-methyl-N-[2-(xanthen-9-ylcarbonyloxy)ethyl]ammonium bromide
【CA 登记号】[50-34-0]
【分 子 式】C23H30BrNO3
【结 构 式】

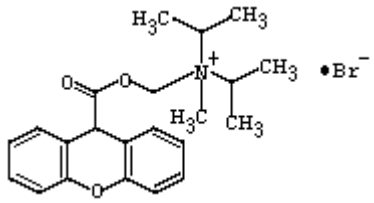

【品种类别】抗胆碱药>季铵盐类

【英文 INN】bromazine
【别　　名】Bromodiphenhydramine, Ambodryl
【名称来源】pINN-004,1956　rINN-003,1959
【中文 CADN】溴马秦(97)
【建议 CADN】
【化学表述】Ethanamine, 2-[(4-bromophenyl)phenylmethoxy]-N,N-dimethyl-
【CA 登记号】[118-23-0]
【分 子 式】C17H20BrNO
【结 构 式】

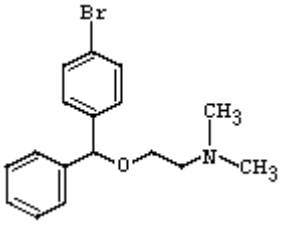

【品种类别】抗变态反应药>抗组胺药>氨乙基烷基醚类

【英文 INN】dibrompropamidine
【别　　名】
【名称来源】pINN-004,1956　rINN-003,1959
【中文 CADN】双溴丙脒(97)

【建议 CADN】

【化学表述】Benzenecarboximidamide, 4,4'-[1,3-propanediylbis(oxy)]bis[3-bromo-

【CA 登记号】[496-00-4]

【分 子 式】C17H18Br2N4O2

【结 构 式】

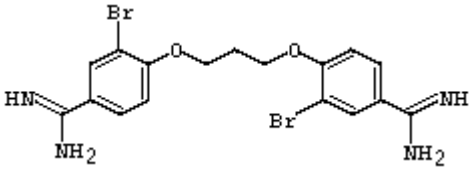

【品种类别】皮肤科用药>消毒防腐药>双胍及脒类

【英文 INN】pipenzolate bromide

【别　　名】

【名称来源】pINN-006,1958　rINN-003,1959

【中文 CADN】溴哌喷酯(97)

【建议 CADN】

【化学表述】1-Ethyl-3-hydroxy-1-methyl-piperidinium bromide benzilate

【CA 登记号】[125-51-9]

【分 子 式】C22H28BrNO3

【结 构 式】

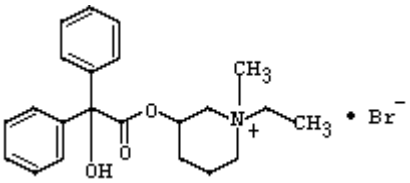

【品种类别】抗胆碱药>季铵盐类

【英文 INN】prodeconium bromide

【别　　名】

【名称来源】PZ　rINN-003,1959

【中文 CADN】丙癸溴铵(GB4)

【建议 CADN】

【化学表述】Ammonium, [decamethylenebis(oxyethylene)bis[(carboxymethyl)dimethyl-, dibromide, dipropyl ester

【CA 登记号】[3690-61-7]

【分 子 式】C28H58Br2N2O6

【结 构 式】

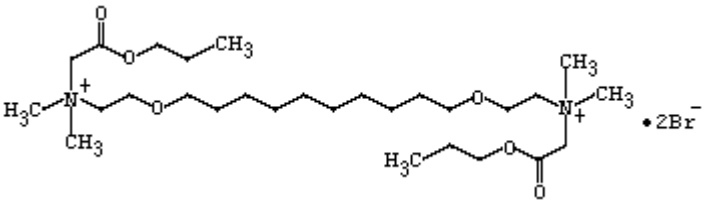

【品种类别】肌肉-骨骼系统>肌松药>季铵盐类

【英文 INN】pyridostigmine bromide
【别　　名】Mestinon
【名称来源】PZ　rINN-003,1959
【中文 CADN】溴吡斯的明(97)
【建议 CADN】
【化学表述】Pyridinium, 3-dimethylcarbamoyloxy-1-methyl-, bromide
【CA 登记号】[101-26-8]
【分 子 式】C9H13BrN2O2
【结 构 式】

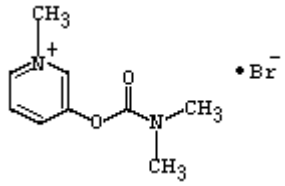

【品种类别】神经系统>抗痴呆药>乙酰胆碱酯酶抑制剂

【英文 INN】bretylium tosylate
【别　　名】Bretylium tosilate
【名称来源】pINN-010,1960　rINN-004,1962
【中文 CADN】托西溴苄铵(97)
【建议 CADN】
【化学表述】2-Bromo-N-ethyl-N,N-dimethylbenzenemethanaminium tosylate
【CA 登记号】[61-75-6]
【分 子 式】C11H17BrN.C7H7O3S
【结 构 式】

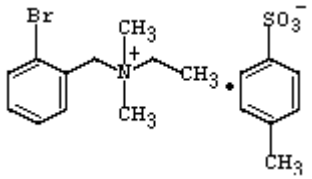

【品种类别】心血管系统>抗心律失常药(III 类)

【英文 INN】brompheniramine
【别　　名】
【名称来源】pINN-008,1959　rINN-004,1962
【中文 CADN】溴苯那敏(97)
【建议 CADN】
【化学表述】N-[(RS)-3-(4-Bromophenyl)-3-pyridin-2-ylpropyl]-N,N-dimethylamine
【CA 登记号】[86-22-6]
【分 子 式】C18H19BrN2
【结 构 式】

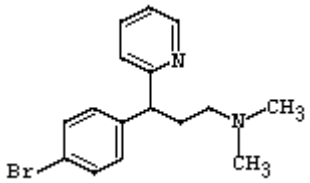

【品种类别】抗变态反应药>抗组胺药>乙二胺衍生物>非尼拉敏类

【英文 INN】clidinium bromide

【别　　名】

【名称来源】pINN-006,1958　rINN-004,1962

【中文 CADN】克利溴铵(GB4)

【建议 CADN】

【化学表述】3-Hydroxy-1-methylquinuclidinium bromide benzilate

【CA 登记号】[3485-62-9]

【分 子 式】C22H26BrNO3

【结 构 式】

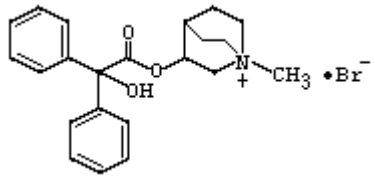

【品种类别】拟胆碱药>毒蕈碱受体激动剂/拮抗剂

【英文 INN】demecarium bromide

【别　　名】

【名称来源】pINN-010,1960　rINN-004,1962

【中文 CADN】地美溴铵(GB4)

【建议 CADN】

【化学表述】(3-Hydroxyphenyl)trimethylammonium bromide, decamethylenebis(methylcarbamate) ester

【CA 登记号】[56-94-0]

【分 子 式】C32H52Br2N4O4

【结 构 式】

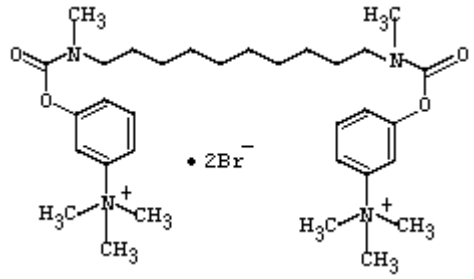

【品种类别】拟胆碱药

【英文 INN】dexbrompheniramine

【别　　名】d-BROMPHENIRAMINE, d-BROMPHENAMINE

【名称来源】pINN-010,1960　rINN-004,1962

【中文 CADN】右溴苯那敏(97)

【建议 CADN】

【化学表述】N-[(3S)-3-(4-Bromophenyl)-3-pyridin-2-ylpropyl]-N,N-dimethylamine

【CA 登记号】[132-21-8]

【分 子 式】C16H19BrN2

【结 构 式】

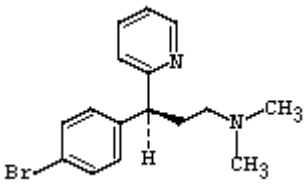

【品种类别】抗变态反应药>抗组胺药>乙二胺衍生物>非尼拉敏类

【英文 INN】halopenium chloride

【别　　名】

【名称来源】pINN-010,1960　rINN-004,1962

【中文 CADN】卤培氯铵(GB4)

【建议 CADN】

【化学表述】4-bromobenzyl-3-(4-chloro-5-methyl-2-isopropylphenoxy)propyldimethylammonium chloride

【CA 登记号】[7008-13-1]

【分 子 式】C22H30BrCl2NO

【结 构 式】

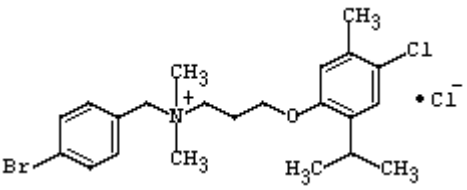

【品种类别】抗感染药>抗真菌药>其它

【英文 INN】hexadimethrine bromide

【别　　名】

【名称来源】pINN-008,1959　rINN-004,1962

【中文 CADN】海美溴铵(97)

【建议 CADN】

【化学表述】Poly[(dimethyliminio)-1,3-propanediyl(dimethyliminio)-1,6-hexanediyl dibromide]

【CA 登记号】[28728-55-4]

【分 子 式】(C13H30Br2N2)x

【结 构 式】

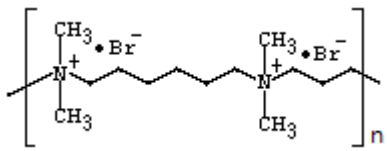

【品种类别】消化系统>保肝药

【英文 INN】hexcarbacholine bromide

【别　　名】Carbolonium bromide, Hexabiscarbacholine, BC 16, HC 406

【名称来源】pINN-010,1960　rINN-004,1962

【中文 CADN】溴己胺胆碱(97)

【建议 CADN】

【化学表述】N,N,N,N',N',N'-Hexamethyl-4,13-dioxa-3,14-dioxa-5,12-diazahexadecane-1,16-diaminium bromide

【CA 登记号】[306-41-2]

【分 子 式】C18H40Br2N4O4

【结 构 式】

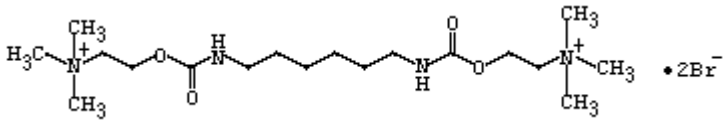

【品种类别】解痉药

【英文 INN】mepenzolate bromide

【别　　名】

【名称来源】pINN-010,1960　rINN-004,1962

【中文 CADN】溴美喷酯(97)

【建议 CADN】

【化学表述】(RS)-3-(Hydroxydiphenylacetoxy)-1,1-dimethylpiperidinium bromide

【CA 登记号】[76-90-4]

【分 子 式】C21H26BrNO3

【结 构 式】

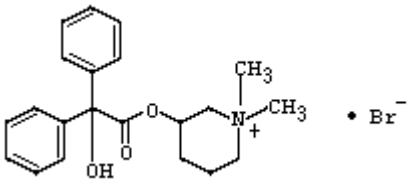

【品种类别】抗胆碱药>季铵盐类

【英文 INN】octatropine methylbromide

【别　　名】ANISOTROPINE METHYLBROMIDE

【名称来源】pINN-010,1960　rINN-004,1962

【中文 CADN】甲溴辛托品(GB4)

【建议 CADN】

【化学表述】8-Methyltropinium bromide 2-propylvalerate

【CA 登记号】[80-50-2]

【分 子 式】C17H23BrNO2

【结 构 式】

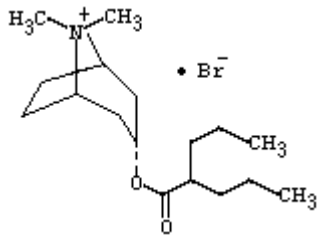

【品种类别】抗胆碱药>季铵盐类

【英文 INN】tetrylammonium bromide

【别　　名】

【名称来源】pINN-001,1953　rINN-004,1962

【中文 CADN】四乙溴铵(GB4)

【建议 CADN】

【化学表述】Ethanaminium, N,N,N-triethyl-, bromide

【CA 登记号】[71-91-0]

【分 子 式】C8H20BrN

【结 构 式】

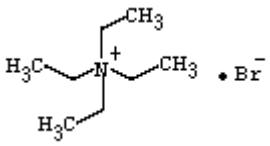

【品种类别】心血管系统>抗高血压药

【英文 INN】thihexinol methylbromide

【别　　名】

【名称来源】pINN-010,1960　rINN-004,1962

【中文 CADN】甲溴噻昔诺(97)

【建议 CADN】

【化学表述】Cyclohexanaminium,4-(hydroxydi-2-thienylmethyl)-N,N,N-trimethyl-, bromide (1:1)

【CA 登记号】[7219-91-2]

【分 子 式】C18H26BrNOS2

【结 构 式】

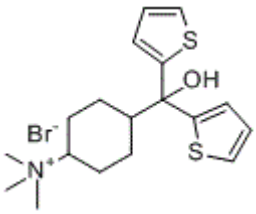

【品种类别】抗胆碱药>季铵盐类

【英文 INN】benzbromarone

【别　　名】Desuric, Hipurik, Max-Uric, Minuric, MJ-10061, Narcaricin, Uricovac, Urinorm

【名称来源】pINN-013,1963　rINN-005,1965

【中文 CADN】苯溴马隆(GB4)

【建议 CADN】

【化学表述】Methanone, (3,5-dibromo-4-hydroxyphenyl)(2-ethyl-3-benzofuranyl)-

【CA 登记号】[3562-84-3]

【分 子 式】C17H12Br2O3

【结 构 式】

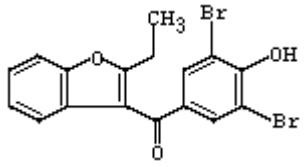

【品种类别】肌肉-骨骼系统>抗痛风药>增加尿酸分泌的

【英文 INN】benzilonium bromide

【别　　名】

【名称来源】pINN-013,1963　rINN-005,1965

【中文 CADN】苯咯溴铵(GB4)

【建议 CADN】

【化学表述】Pyrrolidinium, 1,1-diethyl-3-[(hydroxydiphenylacetyl)oxy]-, bromide

【CA 登记号】[1050-48-2]

【分 子 式】C22H28BrNO3

【结 构 式】

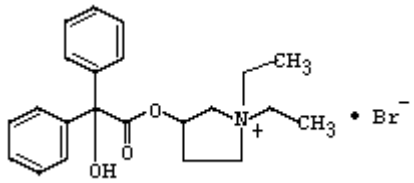

【品种类别】抗胆碱药>季铵盐类

【英文 INN】benzopyrronium bromide

【别　　名】

【名称来源】pINN-012,1962　rINN-005,1965

【中文 CADN】苯吡溴铵(GB4)

【建议 CADN】

【化学表述】Pyrrolidinium, 1,1-dimethyl-3-hydroxy-, bromide, benzilate

【CA 登记号】[13696-15-6]

【分 子 式】C20H24BrNO3

【结 构 式】

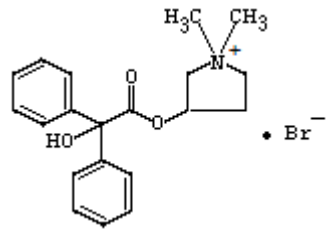

【品种类别】抗胆碱药>季铵盐类

【英文 INN】bibenzonium bromide

【别　　名】

【名称来源】pINN-012,1962　rINN-005,1965

【中文 CADN】比苯溴铵(GB4)

【建议 CADN】

【化学表述】Ethanaminium, 2-(1,2-diphenylethoxy)-N,N,N-trimethyl-, bromide

【CA 登记号】[15585-70-3]

【分 子 式】C19H26BrNO

【结 构 式】

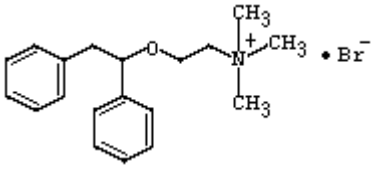

【品种类别】呼吸系统>镇咳药

【英文 INN】bromchlorenone

【别　　名】

【名称来源】pINN-012,1962　rINN-005,1965

【中文 CADN】溴氯唑酮(GB4)

【建议 CADN】

【化学表述】2(3H)-benzoxazolone, 6-bromo-5-chloro-

【CA 登记号】[5579-85-1]

【分 子 式】C7H3BrClNO2

【结 构 式】

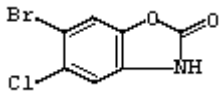

【品种类别】生殖泌尿系统>利尿药>其它，消毒防腐药>其它

【英文 INN】brometenamine

【别　　名】

【名称来源】pINN-012,1962　rINN-005,1965

【中文 CADN】溴美那明(97)

【建议 CADN】

【化学表述】1,3,5,7-Tetraazatricyclo[3.3.1.1^3,7]decane, complex with tribromomethane (1:1)

【CA 登记号】[15585-71-4]

【分 子 式】C6H12N4.CHBr3

【结 构 式】

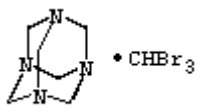

【品种类别】神经系统>镇静药

【英文 INN】bromindione

【别　　名】

【名称来源】pINN-012,1962　rINN-005,1965

【中文 CADN】溴茚二酮(97)

【建议 CADN】

【化学表述】1H-Indene-1,3(2H)-dione, 2-(4-bromophenyl)-

【CA 登记号】[1146-98-1]

【分 子 式】C15H9BrO2

【结 构 式】

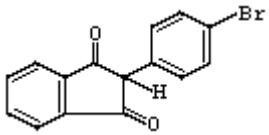

【品种类别】血液系统>抗凝血及溶栓药>茚二酮类

【英文 INN】broxyquinoline

【别　　名】

【名称来源】pINN-012,1962　rINN-005,1965

【中文 CADN】溴羟喹啉(GB4)

【建议 CADN】

【化学表述】8-Quinolinol, 5,7-dibromo-

【CA 登记号】[521-74-4]

【分 子 式】C9H5Br2NO

【结 构 式】

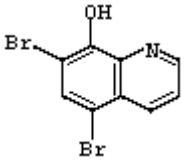

【品种类别】抗原虫药>抗阿米巴及其它原虫病药>羟基喹啉衍生物

【英文 INN】cyclopyrronium bromide

【别　　名】

【名称来源】pINN-012,1962　rINN-005,1965

【中文 CADN】

【建议 CADN】环吡溴铵

【化学表述】1-ethyl-3-hydroxy-1-methylpyrrolidinium bromide α-cyclopentylphenylacetate

【CA 登记号】[15599-22-1]

【分 子 式】C20H30BrNO2

【结 构 式】

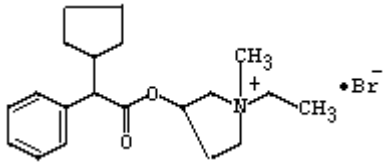

【品种类别】抗胆碱药>季铵盐类

【英文 INN】glycopyrronium bromide
【别　　名】GLYCOPYRROLATE
【名称来源】pINN-012,1962　rINN-005,1965
【中文 CADN】格隆溴铵(GB4)
【建议 CADN】
【化学表述】Pyrrolidinium 3-[(cyclopentylhydroxyphenylacetyl)oxy]-1,1-dimethyl-, bromide
【CA 登记号】[596-51-0]
【分 子 式】C19H28BrNO3
【结 构 式】

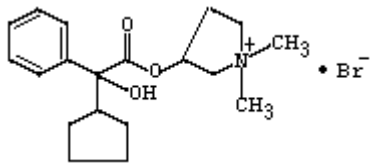

【品种类别】抗胆碱药>季铵盐类

【英文 INN】haloprogesterone
【别　　名】
【名称来源】pINN-011,1961　rINN-005,1965
【中文 CADN】卤孕酮(GB4)
【建议 CADN】
【化学表述】Pregn-4-ene-3,20-dione, 17-bromo-6-fluoro-, (6α)-
【CA 登记号】[3538-57-6]
【分 子 式】C21H28BrClO2
【结 构 式】

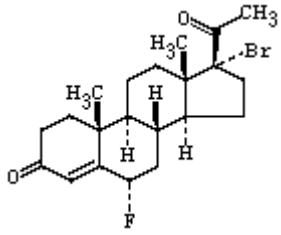

【品种类别】甾体激素>孕激素类

【英文 INN】hexafluronium bromide
【别　　名】HEXAFLUORENIUM BROMIDE
【名称来源】pINN-012,1962　rINN-005,1965
【中文 CADN】己芴溴铵(GB4)

【建议 CADN】

【化学表述】Hexamethylenebis(fluoren-9-yldimethylammonium bromide)

【CA 登记号】[317-52-2]

【分 子 式】C36H42Br2N2

【结 构 式】

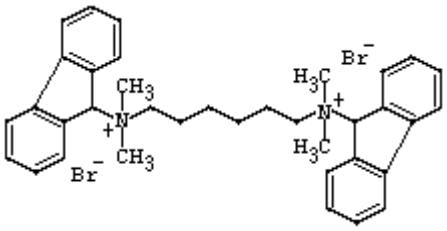

【品种类别】肌肉-骨骼系统>肌松药>季铵盐类

【英文 INN】hexopyrronium bromide

【别　　名】

【名称来源】pINN-013,1963　rINN-005,1965

【中文 CADN】海咯溴铵(GB4)

【建议 CADN】

【化学表述】Pyrrolidinium, 3-[(cyclohexylhydroxyphenylacetyl)oxy]-1,1-dimethyl-, bromide

【CA 登记号】[3734-12-1]

【分 子 式】C20H30BrNO3

【结 构 式】

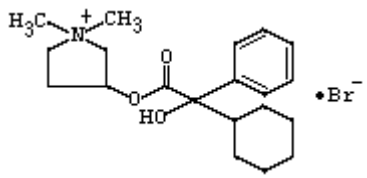

【品种类别】抗胆碱药>季铵盐类

【英文 INN】oxypyrronium bromide

【别　　名】OXIPYRRONIUM BROMIDE

【名称来源】pINN-013,1963　rINN-005,1965

【中文 CADN】羟吡溴铵(GB4)

【建议 CADN】

【化学表述】(2-Hydroxymethyl-1,1-dimethyl)-pyrrolidinium, bromide, α-phenylcyclohexaneglycolate

【CA 登记号】[561-43-3]

【分 子 式】C21H32BrNO3

【结 构 式】

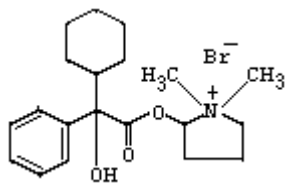

【品种类别】抗胆碱药>季铵盐类

【英文 INN】propyromazine

【别　　名】Diaspasmyl

【名称来源】pINN-012,1962　rINN-005,1965

【中文 CADN】溴吡马嗪(97)

【建议 CADN】

【化学表述】Pyrrolidinium, 1-methyl-1-[1-methyl-2-oxo-2-(10H-phenothiazin-10-yl)ethyl]-, bromide

【CA 登记号】[145-54-0]

【分 子 式】C20H23BrN2OS

【结 构 式】

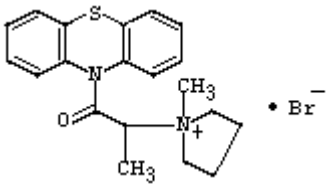

【品种类别】抗变态反应药>抗组胺药>吩噻嗪衍生物

【英文 INN】roflurane

【别　　名】

【名称来源】pINN-012,1962　rINN-005,1965

【中文 CADN】罗氟烷(GB4)

【建议 CADN】

【化学表述】Ethane, 2-bromo-1,1,2-trifluoro-1-methoxy-

【CA 登记号】[679-90-3]

【分 子 式】C2H4BrF3O

【结 构 式】

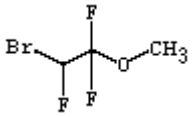

【品种类别】神经系统>全身麻醉药>卤代烃类

【英文 INN】teflurane

【别　　名】

【名称来源】pINN-012,1962　rINN-005,1965

【中文 CADN】替氟烷(GB4)

【建议 CADN】

【化学表述】Ethane, 2-bromo-1,1,1,2-tetrafluoro-

【CA 登记号】[124-72-1]

【分 子 式】C2HBrF4

【结 构 式】

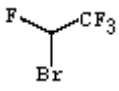

【品种类别】神经系统>全身麻醉药>卤代烃类

【英文 INN】trimedoxime

【别　　名】

【名称来源】pINN-012,1962　rINN-005,1965

【中文 CADN】双解磷(97)

【建议 CADN】

【化学表述】Pyridinium, 1,1'-(1,3-propanediyl)bis[4-[(hydroxyimino)methyl]-, dibromide

【CA 登记号】[56-97-3]

【分 子 式】C15H18Br2N4O2

【结 构 式】

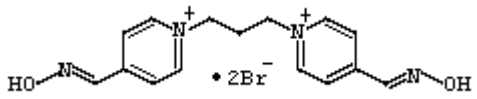

【品种类别】解毒剂

【英文 INN】tropenziline bromide

【别　　名】

【名称来源】pINN-011,1961　rINN-005,1965

【中文 CADN】溴托齐林(GB4)

【建议 CADN】

【化学表述】8-Azoniabicyclo[3.2.1]octane, 3-[(hydroxydiphenylacetyl)oxy]-6-methoxy-8,8-dimethyl-,bromide

【CA 登记号】[143-92-0]

【分 子 式】C24H30BrNO4

【结 构 式】

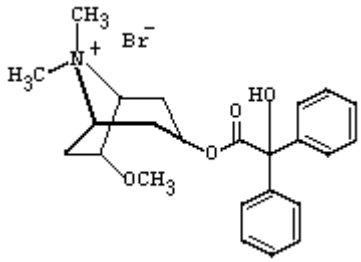

【品种类别】抗胆碱药>季铵盐类

【英文 INN】acecarbromal

【别　　名】Abasin，Sedamyl，acetylcarbromal

【名称来源】pINN-014,1964　rINN-006,1966

【中文 CADN】醋卡溴脲(97)

【建议 CADN】

【化学表述】Butanamide, N-[(acetylamino)carbonyl]-2-bromo-2-ethyl-

【CA 登记号】[77-66-7]

【分 子 式】C9H15BrN2O3

【结 构 式】

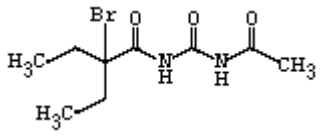

【品种类别】神经系统>催眠镇静药>酰脲类

【英文 INN】bromamide
【别　　名】
【名称来源】pINN-015,1965　rINN-006,1966
【中文 CADN】溴马酰胺(97)
【建议 CADN】
【化学表述】3-(p-bromoanilino)-N,N-dimethylpropionamide
【CA 登记号】[332-69-4]
【分 子 式】C11H15BrN2O
【结 构 式】

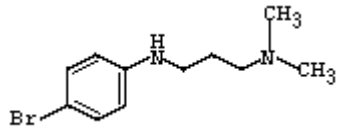

【品种类别】神经系统>催眠镇静药

【英文 INN】bronopol
【别　　名】
【名称来源】pINN-014,1964　rINN-006,1966
【中文 CADN】溴硝丙二醇(97)
【建议 CADN】
【化学表述】1,3-Propanediol, 2-bromo-2-nitro-
【CA 登记号】[52-51-7]
【分 子 式】C3H6BrNO4
【结 构 式】

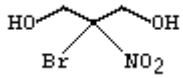

【品种类别】抗感染药>消毒防腐药>其它

【英文 INN】deditonium bromide
【别　　名】
【名称来源】pINN-015,1965　rINN-006,1966
【中文 CADN】地托溴铵(GB4)
【建议 CADN】
【化学表述】1,10-Decanediaminium, N,N,N',N'-tetramethyl-N,N'-bis[2-[5-methyl-2-(1-methylethyl)phenoxy]ethyl]-, dibromide
【CA 登记号】[2401-56-1]
【分 子 式】C38H66Br2N2O2
【结 构 式】

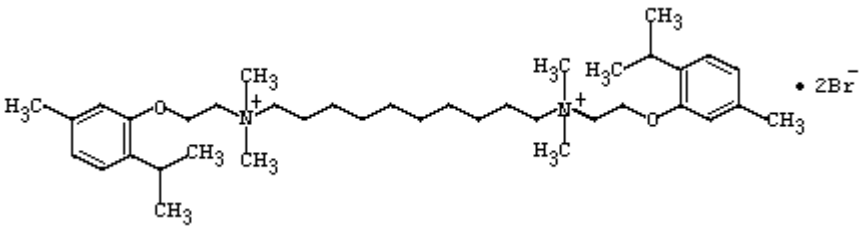

【品种类别】抗感染药>消毒防腐药>季铵盐类

【英文 INN】diponium bromide

【别　　名】

【名称来源】pINN-015,1965　rINN-006,1966

【中文 CADN】地泊溴铵(GB4)

【建议 CADN】

【化学表述】Ethanaminium, 2-[(dicyclopentylacetyl)oxy]-N,N,N-triethyl-, bromide

【CA 登记号】[2001-81-2]

【分 子 式】C20H30BrNO2

【结 构 式】

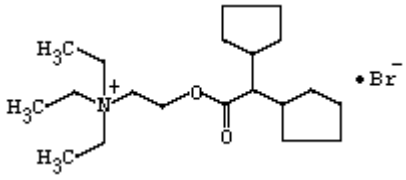

【品种类别】抗胆碱药>季铵盐类

【英文 INN】embramine

【别　　名】

【名称来源】pINN-015,1965　rINN-006,1966

【中文 CADN】恩布拉敏(97)

【建议 CADN】

【化学表述】2-[(p-bromo-α-methyl-α-phenylbenzyl)oxy]-N,N-dimethyl ethylamine

【CA 登记号】[3565-72-8]

【分 子 式】C18H22BrNO

【结 构 式】

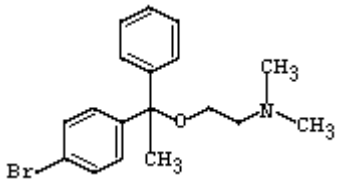

【品种类别】抗变态反应药>抗组胺药>氨乙基烷基醚类

【英文 INN】guanisoquine

【别　　名】

【名称来源】pINN-015,1965　rINN-006,1966

【中文 CADN】胍尼索喹(GB4)

【建议 CADN】

【化学表述】2(1H)-Isoquinolinecarboximidamide, 7-bromo-3,4-dihydro-

【CA 登记号】[154-73-4]

【分 子 式】C10H12BrN3

【结 构 式】

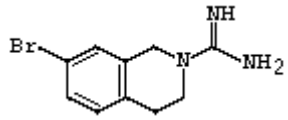

【品种类别】心血管系统>抗高血压药>胍衍生物

【英文 INN】heteronium bromide

【别　　名】

【名称来源】pINN-014,1964　rINN-006,1966

【中文 CADN】海特溴铵(GB4)

【建议 CADN】

【化学表述】Pyrrolidinium, 3-[(hydroxyphenyl-2-thienylacetyl)oxy]-1,1-dimethyl-, bromide

【CA 登记号】[7247-57-6]

【分 子 式】C18H12BrNO3S

【结 构 式】

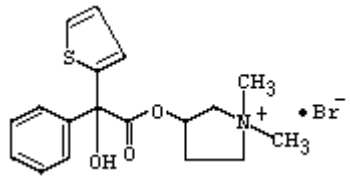

【品种类别】抗胆碱药>季铵盐类

【英文 INN】parapenzolate bromide

【别　　名】

【名称来源】pINN-014,1964　rINN-006,1966

【中文 CADN】溴帕拉喷酯(97)

【建议 CADN】

【化学表述】Piperidinium, 4-[(hydroxydiphenylacetyl)oxy]-1,1-dimethyl-, bromide

【CA 登记号】[5634-41-3]

【分 子 式】C21H26BrNO3

【结 构 式】

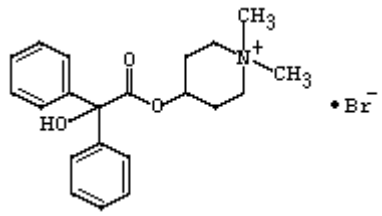

【品种类别】抗胆碱药>季铵盐类

【英文 INN】quindonium bromide

【别　　名】

【名称来源】pINN-014,1964　rINN-006,1966

【中文 CADN】喹度溴铵(GB4)

【建议 CADN】

【化学表述】1H-Benzo[a]cyclopenta[f]quinolizinium, 2,3,3a,5,6,11,12,12a-octahydro-8-hydroxy-, bromide

【CA 登记号】[130-81-4]

【分 子 式】C16H20BrNO

【结 构 式】

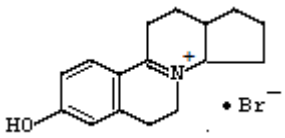

【品种类别】心血管系统>抗心律失常药>其它

【英文 INN】xenytropium bromide

【别　　名】

【名称来源】pINN-015,1965　rINN-006,1966

【中文 CADN】珍托溴铵(GB4)

【建议 CADN】

【化学表述】8-Azoniabicyclo[3.2.1]octane, 8-([1,1'-biphenyl]-4-ylmethyl)-3-(3-hydroxy-1-oxo-2-phenylpropoxy)-8-methyl-, bromide, (3-endo)-

【CA 登记号】[511-55-7]

【分 子 式】C30H32BrNO3

【结 构 式】

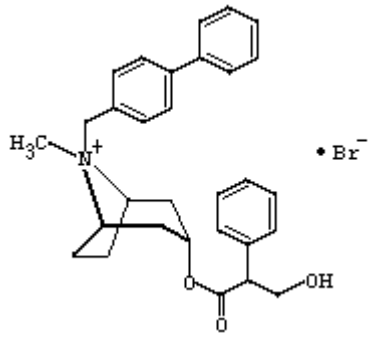

【品种类别】抗胆碱药>季铵盐类

【英文 INN】broquinaldol

【别　　名】

【名称来源】pINN-017,1967　rINN-007,1967

【中文 CADN】溴喹那多(GB4)

【建议 CADN】

【化学表述】5,7-dibromo-2-methyl-8-quinolinol

【CA 登记号】[15599-52-7]

【分 子 式】C10H7Br2NO

【结 构 式】

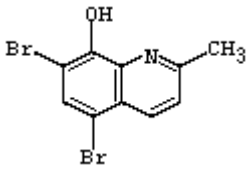

【品种类别】抗感染药>消毒防腐药>喹啉衍生物

【英文 INN】distigmine bromide

【别　　名】

【名称来源】pINN-016,1966　rINN-007,1967

【中文 CADN】溴地斯的明(97)

【建议 CADN】

【化学表述】3,3'-[Hexamethylenebis(methyliminocarbonyloxy)]bis(1-methylpyridinium) dibromide

【CA 登记号】[15876-67-2]

【分 子 式】C22H32Br2N4O4

【结 构 式】

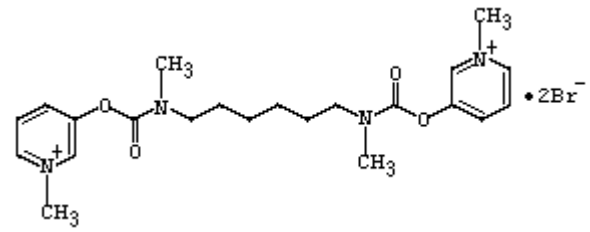

【品种类别】神经系统>抗痴呆药>乙酰胆碱酯酶抑制剂

【英文 INN】dodeclonium bromide

【别　　名】

【名称来源】pINN-016,1966　rINN-007,1967

【中文 CADN】多地溴铵(GB4)

【建议 CADN】

【化学表述】1-Dodecanaminium, N-[2-(4-chlorophenoxy)ethyl]-N,N-dimethyl-, bromide

【CA 登记号】[15687-13-5]

【分 子 式】C22H35BrClNO

【结 构 式】

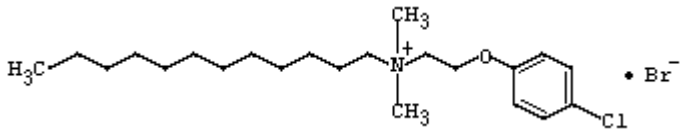

【品种类别】抗感染药>消毒防腐药>季铵盐类

【英文 INN】flusalan

【别　　名】Fluorosalan

【名称来源】pINN-016,1966　rINN-007,1967

【中文 CADN】氟沙仑(GB4)

【建议 CADN】

【化学表述】3,5-dibromo-α,α,α-trifluoro-m-salicylotoluidide

【CA 登记号】[4776-06-1]

【分 子 式】C14H9Br2F3NO2

【结 构 式】

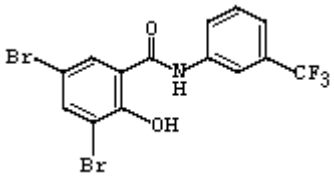

【品种类别】抗感染药>消毒防腐药>salan 类

【英文 INN】mitotenamine

【别　　名】

【名称来源】pINN-017,1967　rINN-007,1967

【中文 CADN】米托那明(GB4)

【建议 CADN】

【化学表述】5-bromo-N-(2-chloroethyl)-N-ethylbenzo[b]thiophene-3-methylamine

【CA 登记号】[7696-00-6]

【分 子 式】C13H15BrClNS

【结 构 式】

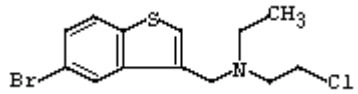

【品种类别】抗肿瘤药>核毒类/抗肿瘤药>烷基化剂>氯乙胺衍生物

【英文 INN】bensalan

【别　　名】

【名称来源】pINN-018,1967　rINN-008,1968

【中文 CADN】苯沙仑(GB4)

【建议 CADN】

【化学表述】Benzamide, 3,5-dibromo-2-hydroxy-N-[(4-bromophenyl)methyl]-

【CA 登记号】[15686-76-7]

【分 子 式】C14H10Br3NO2

【结 构 式】

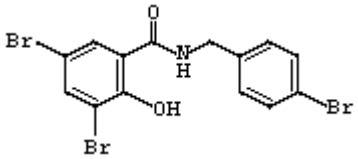

【品种类别】抗感染药>消毒防腐药>salan 类

【英文 INN】brocresine

【别　　名】

【名称来源】pINN-018,1967　rINN-008,1968

【中文 CADN】溴克立新(97)

【建议 CADN】

【化学表述】α-(aminooxy)-6-bromo-m-cresol

【CA 登记号】[555-65-7]

【分 子 式】C7H8BrNO2

【结 构 式】

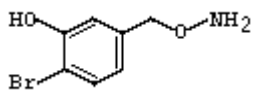

【品种类别】组胺酸脱羧酶抑制药

【英文 INN】ciclonium bromide

【别　　名】

【名称来源】pINN-019,1968　rINN-008,1968

【中文 CADN】环隆溴铵(GB4)

【建议 CADN】

【化学表述】2-[(α-Methyl-α-5-norbornen-2-ylbenzyl)oxyethyl]ammonium bromide

【CA 登记号】[29546-59-6]

【分 子 式】C22H34BrNO

【结 构 式】

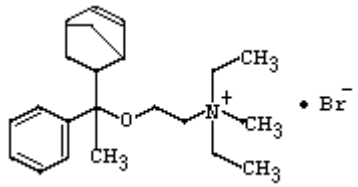

【品种类别】抗胆碱药>季铵盐类

【英文 INN】emepronium bromide

【别　　名】

【名称来源】pINN-018,1967　rINN-008,1968

【中文 CADN】依美溴铵(GB4)

【建议 CADN】

【化学表述】Benzenepropanaminium, N-ethyl-N,N,α-trimethyl-γ-phenyl-, bromide

【CA 登记号】[3614-30-0]

【分 子 式】C20H28BrN

【结 构 式】

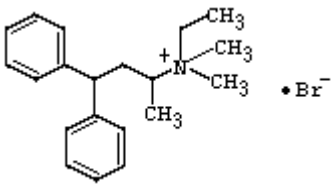

【品种类别】抗胆碱药>季铵盐类

【英文 INN】oxitefonium bromide

【别　　名】

【名称来源】pINN-018,1967　rINN-008,1968

【中文 CADN】奥封溴铵(GB4)

【建议 CADN】

【化学表述】diethyl(2-hydroxyethyl)methylammonium bromide α-phenyl-2-thiopheneglycolate

【CA 登记号】[17692-63-6]

【分 子 式】C19H26BrNO3S

【结 构 式】

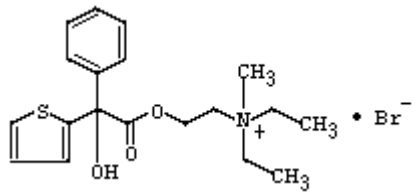

【品种类别】抗胆碱药>季铵盐类

【英文 INN】pancuronium bromide

【别　　名】

【名称来源】pINN-019,1968　rINN-008,1968

【中文 CADN】泮库溴铵(GB4)

【建议 CADN】

【化学表述】1,1'-(3α,17β-Diacetoxy-5α-androstan-2β,16β-diyl)bis(1-methylpiperidinium) dibromide

【CA 登记号】[15500-66-0]

【分 子 式】C35H60Br2N2O4

【结 构 式】

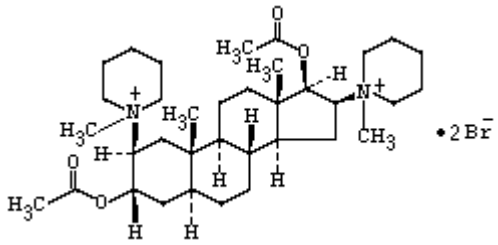

【品种类别】肌肉-骨骼系统>肌松药>季铵盐类

【英文 INN】penoctonium bromide

【别　　名】

【名称来源】pINN-019,1968　rINN-008,1968

【中文 CADN】喷辛溴铵(GB4)

【建议 CADN】

【化学表述】diethyl(2-hydroxyethyl)octyl ammonium bromide dicyclopentyl acetate

【CA 登记号】[17088-72-1]

【分 子 式】C26H50BrNO2

【结 构 式】

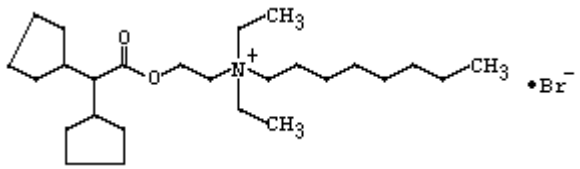

【品种类别】抗感染药>抗真菌药>其它

【英文 INN】pirralkonium bromide
【别　　名】
【名称来源】pINN-019,1968　rINN-008,1968
【中文 CADN】吡拉溴铵(GB4)
【建议 CADN】
【化学表述】bis[3-(2,5-dimethyl-1-pyrrolidinyl)propyl]hexadecylmethylammonium
【CA 登记号】[17243-65-1]
【分 子 式】C35H72BrN3
【结 构 式】

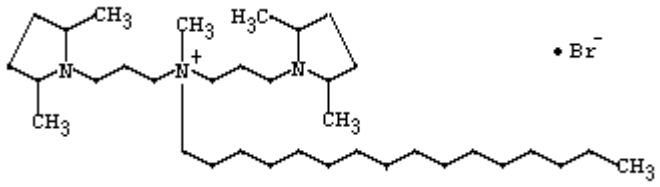

【品种类别】抗感染药>消毒防腐药>季铵盐类

【英文 INN】tetradonium bromide
【别　　名】Morpan T, Myristyltrimethylammonium bromide
【名称来源】pINN-018,1967　rINN-008,1968
【中文 CADN】替溴铵(GB4)
【建议 CADN】
【化学表述】Tetradecylammonium, N,N,N-trimethyl-, bromide
【CA 登记号】[1119-97-7]
【分 子 式】C17H38BrN
【结 构 式】

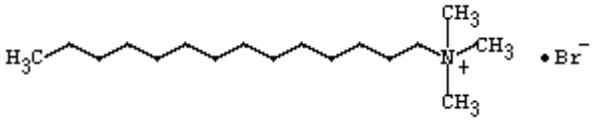

【品种类别】抗感染药>消毒防腐药>季铵盐类

【英文 INN】tibrofan
【别　　名】
【名称来源】pINN-018,1967　rINN-008,1968
【中文 CADN】替溴芬(97)
【建议 CADN】
【化学表述】2-Thiophenecarboxamide, 4,5-dibromo-N-(4-bromophenyl)-

【CA 登记号】[15686-72-3]

【分 子 式】C11H6Br3NOS

【结 构 式】

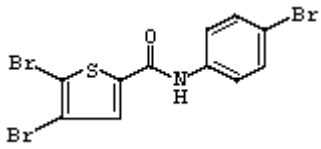

【品种类别】抗感染药>消毒防腐药>

【英文 INN】tiosalan

【别　　名】Thiosalan

【名称来源】pINN-018,1967　rINN-008,1968

【中文 CADN】硫沙仑(GB4)

【建议 CADN】

【化学表述】Benzamide, 3,5-dibromo-N-(4-bromophenyl)-2-mercapto-

【CA 登记号】[15686-78-9]

【分 子 式】C13H8Br3NOS

【结 构 式】

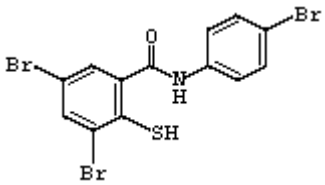

【品种类别】抗感染药>消毒防腐药>salan 类

【英文 INN】bromhexine

【别　　名】Bromohexine

【名称来源】pINN-020,1968　rINN-009,1969

【中文 CADN】溴己新(GB4)

【建议 CADN】

【化学表述】N-(2-Amino-3,5-dibromophenylmethyl)-N-cyclohexyl-N-methylamine

【CA 登记号】[3572-43-8]

【分 子 式】C14H20Br2N2

【结 构 式】

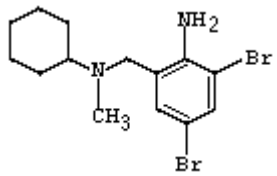

【品种类别】呼吸系统>祛痰药>溴己新类

【英文 INN】dacuronium bromide

【别　　名】

【名称来源】pINN-021,1969　rINN-009,1969

【中文 CADN】达库溴铵(GB4)

【建议 CADN】

【化学表述】Piperidinium, 1,1'-[(2β,3α,5α,16β,17β)-3-(acetyloxy)-17-hydroxyandrostane-2,6-diyl]bis[1-methyl-, dibromide

【CA 登记号】[27115-86-2]

【分 子 式】C33H58Br2N2O3

【结 构 式】

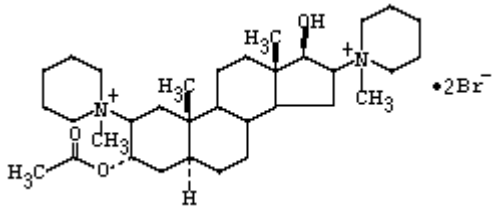

【品种类别】肌肉-骨骼系统>肌松药>季铵盐类

【英文 INN】mitobronitol

【别　　名】DBM, Dibromomannitol, Myebrol, Myelobromol

【名称来源】pINN-020,1968　rINN-009,1969

【中文 CADN】二溴甘露醇(GB4)

【建议 CADN】

【化学表述】D-Mannitol, 1,6-dibromo-1,6-dideoxy-

【CA 登记号】[488-41-5]

【分 子 式】C6H12Br2O4

【结 构 式】

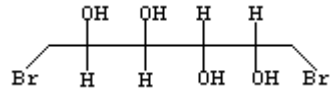

【品种类别】抗肿瘤药>核毒类

【英文 INN】prifinium bromide

【别　　名】

【名称来源】pINN-020,1968　rINN-009,1969

【中文 CADN】吡芬溴铵(GB4)

【建议 CADN】

【化学表述】Pyrrolidinium, 1,1-diethyl-3-(diphenylmethylene)-2-methyl-, bromide

【CA 登记号】[4630-95-9]

【分 子 式】C22H28BrN

【结 构 式】

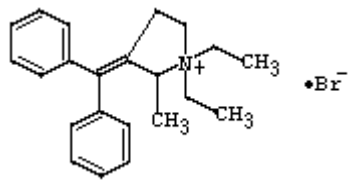

【品种类别】抗胆碱药>季铵盐类

【英文 INN】bromociclen

【别　　名】

【名称来源】pINN-023,1970　rINN-010,1970

【中文 CADN】溴西克林(97)

【建议 CADN】

【化学表述】5-(bromomethyl)-1,2,3,4,7,7-hexachloro-2-norbornene

【CA 登记号】[1715-40-8]

【分 子 式】C7H5BrCl4

【结 构 式】

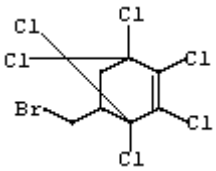

【品种类别】杀虫药和驱虫药>其它

【英文 INN】resorantel

【别　　名】

【名称来源】pINN-023,1970　rINN-010,1970

【中文 CADN】雷琐太尔(GB4)

【建议 CADN】

【化学表述】Benzamide, N-(4-bromophenyl)-2,6-dihydroxy-

【CA 登记号】[20788-07-2]

【分 子 式】C13H10BrNO3

【结 构 式】

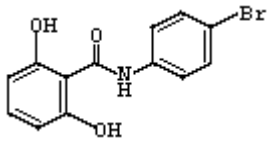

【品种类别】抗寄生虫药>驱虫药

【英文 INN】bromebric acid

【别　　名】

【名称来源】pINN-025,1971　rINN-011,1971

【中文 CADN】溴美酸(97)

【建议 CADN】

【化学表述】(E)-3-p-anisoyl-3-bromoacrylic acid

【CA 登记号】[5711-40-0]

【分 子 式】C11H9BrO4

【结 构 式】

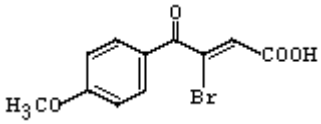

【品种类别】抗偏头痛药

【英文 INN】bromofos

【别　　名】

【名称来源】pINN-025,1971　rINN-011,1971

【中文 CADN】溴硫磷(GB4)

【建议 CADN】

【化学表述】O-(4-bromo-2,5-dichlorophenyl) O,O-dimethyl phosphorothioate

【CA 登记号】[2104-96-3]

【分 子 式】C8H8BrCl2O3PS

【结 构 式】

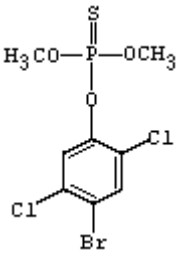

【品种类别】杀虫药和驱虫药>有机磷化合物

【英文 INN】dotefonium bromide

【别　　名】

【名称来源】pINN-024,1970　rINN-011,1971

【中文 CADN】多福溴铵(GB4)

【建议 CADN】

【化学表述】Pyrrolidinium, 1-methyl-1-[2-(N-methyl-α-2-thienylmandelamido)ethyl]-, bromide

【CA 登记号】[26058-50-4]

【分 子 式】C20H27BrN2O2S

【结 构 式】

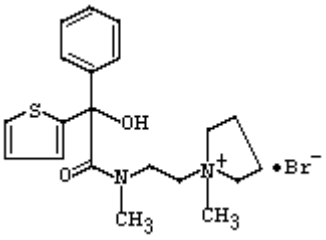

【品种类别】抗胆碱药>季铵盐类

【英文 INN】trantelinium bromide

【别　　名】

【名称来源】pINN-024,1970　rINN-011,1971

【中文 CADN】群替溴铵(GB4)

【建议 CADN】

【化学表述】8-methyltropinium bromide xanthene-9-carboxylate

【CA 登记号】[4047-34-1]

【分 子 式】C23H24BrNO3

【结 构 式】

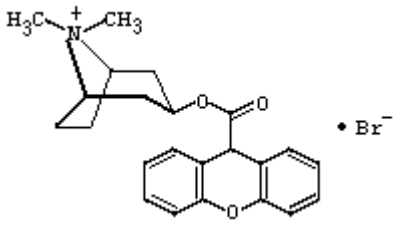

【品种类别】解痉药

【英文 INN】bromopride

【别　　名】Bentril, Cascapride, Digesan, Emepride, Emoril, Mepramide, Modulan, Plesium, Valopride, Viaben

【名称来源】pINN-027,1972　rINN-012,1973

【中文 CADN】溴必利(GB4)

【建议 CADN】

【化学表述】Benzamide, 4-amino-5-bromo-N-[2-(diethylamino)ethyl]-2-methoxy-

【CA 登记号】[4093-35-0]

【分 子 式】C14H22BrN3O2

【结 构 式】

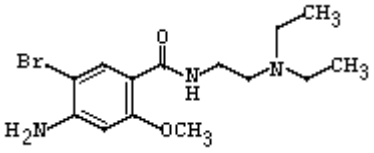

【品种类别】消化系统>胃肠道动力药>苯甲酰胺衍生物

【英文 INN】fenpiverinium bromide

【别　　名】Baralgin

【名称来源】PZ　rINN-012,1973

【中文 CADN】苯维溴铵(GB4)

【建议 CADN】

【化学表述】1-(3-Carbamoyl-3,3-diphenylpropyl)-1-methylpiperidinium bromide

【CA 登记号】[125-60-0]

【分 子 式】C22H29BrN2O

【结 构 式】

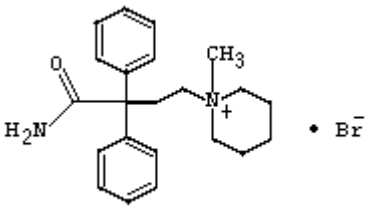

【品种类别】抗胆碱药>季铵盐类

【英文 INN】mitolactol

【别　　名】

【名称来源】pINN-026,1971　rINN-012,1973

【中文 CADN】二溴卫矛醇(GB4)

【建议 CADN】

【化学表述】Galactitol, 1,6-dibromo-1,6-dideoxy-

【CA 登记号】[10318-26-0]

【分 子 式】C6H12Br2O4

【结 构 式】

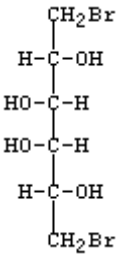

【品种类别】抗肿瘤药>核毒类

【英文 INN】nicergoline

【别　　名】

【名称来源】pINN-026,1971　rINN-012,1973

【中文 CADN】尼麦角林(GB4)

【建议 CADN】

【化学表述】(8β)-10-Methoxy-1,6-dimethyl-Ergoline-8-methanol 5-bromo-3-pyridinecarboxylate (ester)

【CA 登记号】[27848-84-6]

【分 子 式】C24H26BrN3O3

【结 构 式】

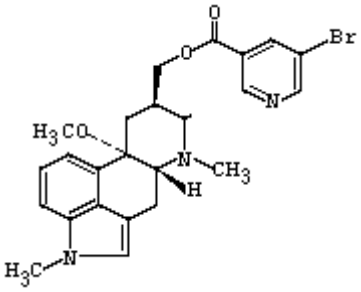

【品种类别】5-羟色胺受体拮抗剂>麦角生物碱衍生物

【英文 INN】bromocriptine

【别　　名】

【名称来源】pINN-029,1973　rINN-013,1973

【中文 CADN】溴隐亭(97)

【建议 CADN】

【化学表述】(5'α)-2-Bromo-12'-hydroxy-2'-(1-methylethyl)-5'-(2-methylpropyl)-Ergotaman-3',6',18-trione

【CA 登记号】[25614-03-3]

【分 子 式】C32H40BrN5O5

【结 构 式】

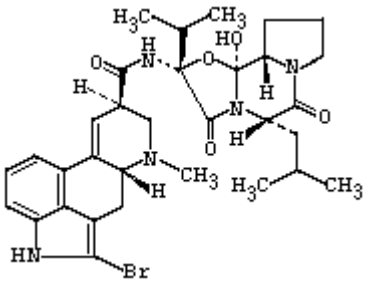

【品种类别】神经系统>抗震颤麻痹药>多巴胺能药>多巴胺激动剂

【英文 INN】brosotamide
【别　　名】
【名称来源】pINN-029,1973　rINN-013,1973
【中文 CADN】溴索胺(97)
【建议 CADN】
【化学表述】5-bromo-2,3-cresotamide
【CA 登记号】[40912-73-0]
【分 子 式】C8H8BrNO2
【结 构 式】

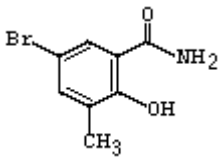

【品种类别】非甾体抗炎药>水杨酸衍生物

【英文 INN】fentonium bromide
【别　　名】
【名称来源】pINN-029,1973　rINN-013,1973
【中文 CADN】芬托溴铵(GB4)
【建议 CADN】
【化学表述】3α-hydroxy-8-(p-phenylphenacyl)-1αH,5αH-tropanium bromide(-) tropate
【CA 登记号】[5868-06-4]
【分 子 式】C31H34BrNO4
【结 构 式】

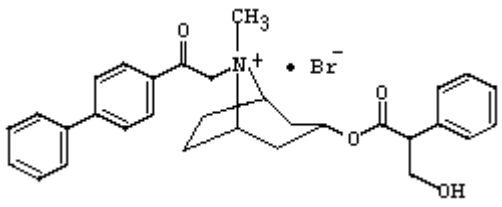

【品种类别】抗胆碱药>季铵盐类

【英文 INN】ipratropium bromide
【别　　名】Atrovent Inh

【名称来源】pINN-028,1972　rINN-013,1973

【中文 CADN】异丙托溴铵(GB4)

【建议 CADN】

【化学表述】(1R,3R,5S)-3-[(RS)-3-Hydroxy-2-phenylpropanoyloxy]-8-isopropyl-8-methyl-8-azoniabicyclo[3.2.1]octane bromide

【CA 登记号】[22254-24-6]

【分 子 式】C20H30BrNO3

【结 构 式】

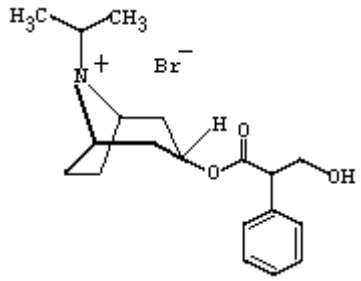

【品种类别】抗胆碱药>季铵盐类

【英文 INN】pirdonium bromide

【别　　名】

【名称来源】pINN-028,1972　rINN-013,1973

【中文 CADN】哌度溴铵(GB4)

【建议 CADN】

【化学表述】1,1-dimethyl-2-[[(p-methyl-α-phenylbenzyl)oxy]methyl]piperidinium bromide

【CA 登记号】[35620-67-8]

【分 子 式】C22H30BrNO

【结 构 式】

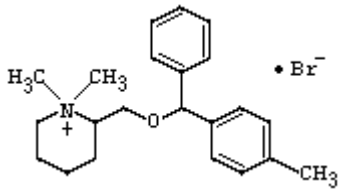

【品种类别】抗组胺药

【英文 INN】timepidium bromide

【别　　名】

【名称来源】pINN-029,1973　rINN-013,1973

【中文 CADN】噻哌溴铵(GB4)

【建议 CADN】

【化学表述】(RS)-3-(Dithien-2-ylmethylene)-5-methoxy-1,1-dimethylpiperidinium bromide

【CA 登记号】[35035-05-3]

【分 子 式】C17H22BrNOS2

【结 构 式】

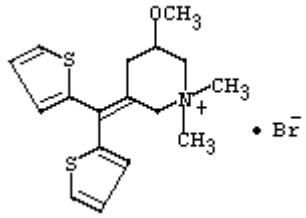

【品种类别】抗胆碱药>季铵盐类

【英文 INN】brofezil

【别　　名】

【名称来源】pINN-031,1974　rINN-014,1974

【中文 CADN】溴苯齐尔(97)

【建议 CADN】

【化学表述】4-(p-bromophenyl)-α-methyl-2-thiazoleacetic acid

【CA 登记号】[17969-45-8]

【分 子 式】C12H10BrNO2S

【结 构 式】

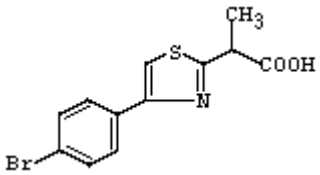

【品种类别】非甾体抗炎药>布洛芬衍生物

【英文 INN】brofoxine

【别　　名】

【名称来源】pINN-030,1973　rINN-014,1974

【中文 CADN】溴苯噁嗪酮

【建议 CADN】

【化学表述】6-bromo-1,4-dihydro-4,4-dimethyl-2H-3,1-benzoxazin-2-one

【CA 登记号】[21440-97-1]

【分 子 式】C10H10BrNO2

【结 构 式】

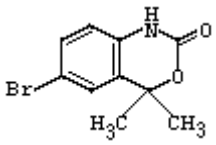

【品种类别】神经系统>安定药， 肌松药

【英文 INN】bromoxanide

【别　　名】

【名称来源】pINN-031,1974　rINN-014,1974

【中文 CADN】溴沙奈(GB4)

【建议 CADN】

【化学表述】Benzamide, N-[4-bromo-2-(trifluoromethyl)phenyl]-3-(1,1-dimethylethyl)-2-hydroxy-6-methyl-5-nitro-

【CA 登记号】[41113-86-4]

【分 子 式】C19H18BrF3N2O4

【结 构 式】

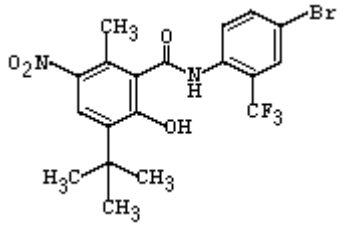

【品种类别】抗蠕虫药>抗绦虫药>水杨酰苯胺衍生物

【英文 INN】brotianide

【别　　名】

【名称来源】pINN-024,1970　rINN-014,1974

【中文 CADN】溴替尼特(97)

【建议 CADN】

【化学表述】3,4'-dibromo-5-chlorothiosalicylanilide acetate (ester)

【CA 登记号】[23233-88-7]

【分 子 式】C15H10Br2ClNO2S

【结 构 式】

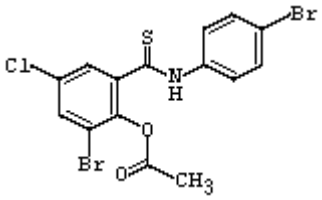

【品种类别】抗蠕虫药>抗绦虫药>其它

【英文 INN】brovanexine

【别　　名】

【名称来源】pINN-031,1974　rINN-014,1974

【中文 CADN】溴凡克新(GB4)

【建议 CADN】

【化学表述】2',4'-dibromo-α-(cyclohexylmethylamino)-o-vanillotoluidide (ester)

【CA 登记号】[54340-61-3]

【分 子 式】C24H28Br2N2O4

【结 构 式】

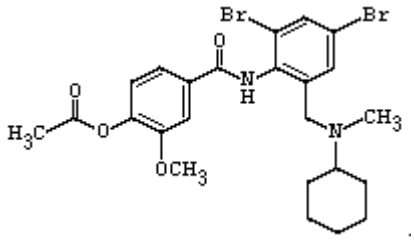

【品种类别】呼吸系统>祛痰药>溴己新类

【英文 INN】broxuridine

【别　　名】

【名称来源】pINN-030,1973　rINN-014,1974

【中文 CADN】溴尿苷(GB4)

【建议 CADN】

【化学表述】5-bromo-2'-deoxyuridine

【CA 登记号】[59-14-3]

【分 子 式】C9H11BrN2O5

【结 构 式】

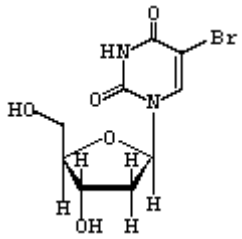

【品种类别】抗肿瘤药，抗病毒药>核苷及核苷酸类>逆转录酶抑制药>>尿苷衍生物

【英文 INN】butropium bromide

【别　　名】

【名称来源】pINN-030,1973　rINN-014,1974

【中文 CADN】布托溴铵(GB4)

【建议 CADN】

【化学表述】(1R,3R,5S)-8-(4-Butoxybenzyl)-3-[(2S)-hydroxy-2-phenylpropanoyloxy]-8-methyl-8-azoniabicyclo[3.2.1]octane bromide

【CA 登记号】[29025-14-7]

【分 子 式】C28H38BrNO4

【结 构 式】

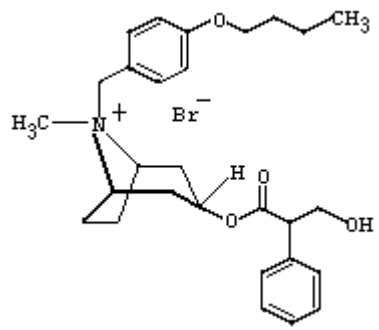

【品种类别】抗胆碱药>季铵盐类

【英文 INN】ambroxol

【别　　名】Mucosolvan, Ambrolitic, Bronchopront, Mucouent

【名称来源】pINN-032,1974　rINN-015,1975

【中文 CADN】氨溴索(97)

【建议 CADN】

【化学表述】Cyclohexanol, 4-[[(2-Amino-3,5-dibromophenyl)methyl]amino]-

【CA 登记号】[18683-91-5]

【分 子 式】C13H18Br2N2O

【结 构 式】

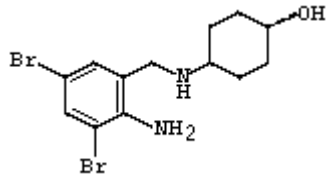

【品种类别】呼吸系统>祛痰药

【英文 INN】brindoxime

【别　　名】

【名称来源】pINN-032,1974　rINN-015,1975

【中文 CADN】溴茚肟

【建议 CADN】

【化学表述】2-[[(6,8-dibromo-9H-indeno[2,1-d]pyrimidin-9-ylidene)amino]oxy]-N-[2-(dimethylamino)ethyl]propionamide

【CA 登记号】[55837-17-7]

【分 子 式】C18H19Br2N5O2

【结 构 式】

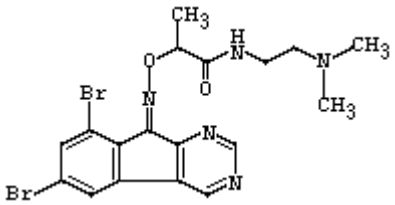

【品种类别】抗原虫药>抗疟药

【英文 INN】bromperidol

【别　　名】Azurene, Bromidol, Consilium, Impromen, R-1133, Tesoprel

【名称来源】pINN-033,1975　rINN-015,1975

【中文 CADN】溴哌利多(GB4)

【建议 CADN】

【化学表述】1-Butanone, 4-[4-(4-bromophenyl)-4-hydroxy-1-piperidinyl]-1-(4-fluorophenyl)-

【CA 登记号】[10457-90-6]

【分 子 式】C21H23BrFNO2

【结 构 式】

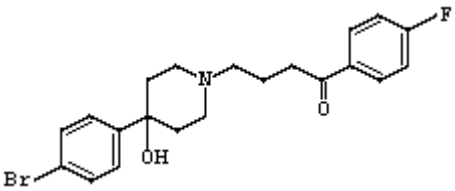

【品种类别】神经系统>抗精神病药>丁酰苯衍生物

【英文 INN】droclidinium bromide

【别　　名】

【名称来源】pINN-033,1975　rINN-015,1975

【中文 CADN】羟奎溴铵(GB4)

【建议 CADN】

【化学表述】3-hydroxy-1-methylquinuclidinium bromide α-phenylcyclohexaneglycolate

【CA 登记号】[29125-56-2]

【分 子 式】C22H32BrNO3

【结 构 式】

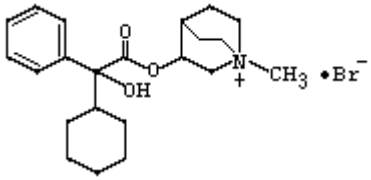

【品种类别】拟胆碱药>毒蕈碱受体激动剂/拮抗剂

【英文 INN】fazadinium bromide

【别　　名】AH-8165, Fazadon

【名称来源】pINN-032,1974　rINN-015,1975

【中文 CADN】法扎溴铵(GB4)

【建议 CADN】

【化学表述】1,1'-azobis[3-methyl-2-phenyl-1H-imidazo[1,2-a]pyridin-4-ium] dibromide

【CA 登记号】[49564-56-9]

【分 子 式】C28H24Br2N6

【结 构 式】

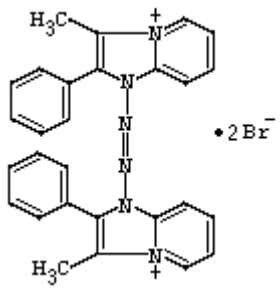

【品种类别】肌肉-骨骼系统>肌松药>季铵盐类

【英文 INN】halofuginone

【别　　名】

【名称来源】pINN-032,1974　rINN-015,1975

【中文 CADN】卤夫酮(97)

【建议 CADN】

【化学表述】rel-7-Bromo-6-chloro-3-[3-[(2R,3S)-3-hydroxy-2-piperidinyl]-2-oxopropyl]-4(3H)-quinazolinone

【CA 登记号】[55837-20-2]

【分 子 式】C16H17BrClN3O3

【结 构 式】

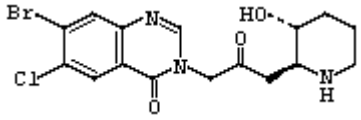

【品种类别】抗球虫药>喹唑啉酮类(兽药)

【英文 INN】pinaverium bromide

【别　　名】Dicetal, Dicetal, Eldicet, L-17

【名称来源】pINN-032,1974　rINN-015,1975

【中文 CADN】匹维溴铵(GB4)

【建议 CADN】

【化学表述】Morpholinium, 4-[[2-bromo-4,5-dimethoxyphenyl]methyl]-4-[2-[2-(6,6-dimethylbicyclo[3.1.1]hept-2-yl)ethoxy]ethyl]-, bromide

【CA 登记号】[53251-94-8]

【分 子 式】C26H41Br2NO4

【结 构 式】

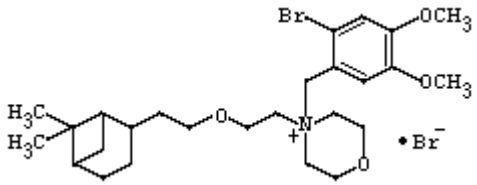

【品种类别】解痉药>罂粟碱类

【英文 INN】ritropirronium bromide

【别　　名】

【名称来源】pINN-033,1975　rINN-015,1975

【中文 CADN】利吡咯溴铵(GB4)

【建议 CADN】

【化学表述】erythro-3-hydroxy-1,1-dimethylpyrrolidinium bromide α-cyclopentylmandelate

【CA 登记号】[51186-83-5]

【分 子 式】C19H28BrNO3

【结 构 式】

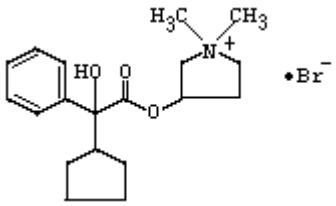

【品种类别】抗胆碱药>季铵盐类

【英文 INN】bromisoval
【别　　名】
【名称来源】pINN-001,1953　rINN-016,1976
【中文 CADN】溴米索伐(97)
【建议 CADN】
【化学表述】(RS)-(2-Bromo-3-methylbutanoyl)urea
【CA 登记号】[496-67-3]
【分 子 式】C6H11BrN2O2
【结 构 式】

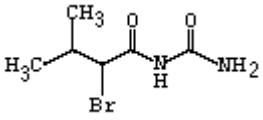

【品种类别】神经系统>催眠镇静药>酰脲类

【英文 INN】methylbenactyzium bromide
【别　　名】Benactyzium methobromide
【名称来源】pINN-034,1975　rINN-016,1976
【中文 CADN】溴甲贝那替嗪(GB4)
【建议 CADN】
【化学表述】N,N-Diethyl-N-[2-(hydroxydiphenylacetoxy)ethyl]-N-methylammonium bromide
【CA 登记号】[3166-62-9]
【分 子 式】C21H28BrNO3
【结 构 式】

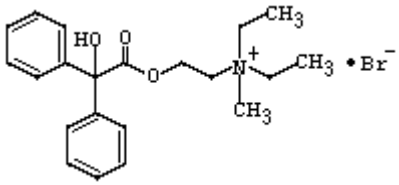

【品种类别】抗胆碱药>季铵盐类

【英文 INN】nibroxane
【别　　名】
【名称来源】pINN-035,1976　rINN-016,1976
【中文 CADN】硝溴生(GB4)
【建议 CADN】

【化学表述】5-bromo-2-methyl-5-nitro-m-dioxane

【CA 登记号】[53983-00-9]

【分 子 式】C5H8BrNO4

【结 构 式】

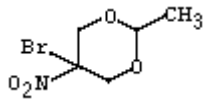

【品种类别】抗感染药>消毒防腐药>其它

【英文 INN】adamexine

【别　　名】

【名称来源】pINN-036,1976　rINN-017,1977

【中文 CADN】金刚克新(GB4)

【建议 CADN】

【化学表述】Acetamide, N-[2,4-dibromo-6-[(methyltricyclo[3.3.1.1^3,7]dec-1-ylamino)methyl]phenyl]-

【CA 登记号】[54785-02-3]

【分 子 式】C20H26Br2N2O

【结 构 式】

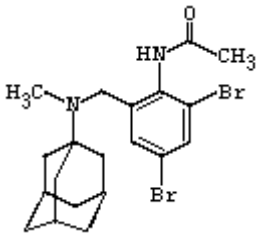

【品种类别】呼吸系统>祛痰药>溴己新类

【英文 INN】brazergoline

【别　　名】

【名称来源】pINN-037,1977　rINN-017,1977

【中文 CADN】溴麦角林(GB4)

【建议 CADN】

【化学表述】2-bromo-6-methylergoline-8β-methanol hexahydro-1H-azepine-1-carboxylate (ester)

【CA 登记号】[60019-20-7]

【分 子 式】C23H30BrN3O2

【结 构 式】

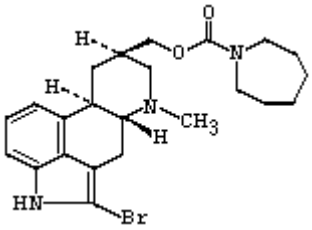

【品种类别】5-羟色胺受体拮抗剂>麦角生物碱衍生物

【英文 INN】cinromide

【别　　名】

【名称来源】pINN-037,1977　rINN-017,1977

【中文 CADN】桂溴胺(97)

【建议 CADN】

【化学表述】(E)-m-bromo-N-ethylcinnamamide

【CA 登记号】[58473-74-8]

【分 子 式】C11H12BrNO

【结 构 式】

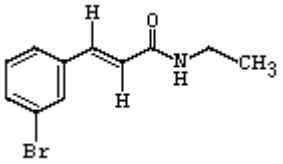

【品种类别】神经系统>抗惊厥药

【英文 INN】dimetipirium bromide

【别　　名】

【名称来源】pINN-037,1977　rINN-017,1977

【中文 CADN】地吡溴铵(GB4)

【建议 CADN】

【化学表述】1-(2-hydroxyethyl)-1,2,5-trimethylpyrrolidinium bromide benzilate

【CA 登记号】[51047-24-6]

【分 子 式】C23H30BrNO3

【结 构 式】

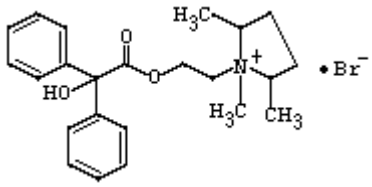

【品种类别】抗胆碱药>季铵盐类

【英文 INN】halopredone

【别　　名】

【名称来源】pINN-036,1976　rINN-017,1977

【中文 CADN】卤泼尼松(GB4)

【建议 CADN】

【化学表述】Pregna-1,4-diene-3,20-dione, 2-bromo-6,9-difluoro-11,17,21-trihydroxy-, (6β,11β)-

【CA 登记号】[57781-15-4]

【分 子 式】C21H25BrF2O5

【结 构 式】

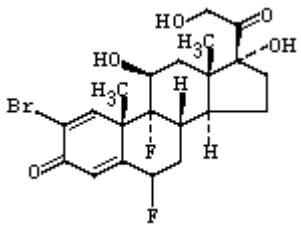

【品种类别】甾体激素>肾上腺皮质激素>泼尼松和泼尼松龙衍生物

【英文 INN】halothane

【别　　名】

【名称来源】pINN-006,1958　rINN-017,1977

【中文 CADN】氟烷(97)

【建议 CADN】

【化学表述】Ethane, 2-Bromo-2-chloro-1,1,1-trifluoro-, (RS)-

【CA 登记号】[151-67-7]

【分 子 式】C2HBrClF3

【结 构 式】

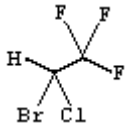

【品种类别】神经系统>全身麻醉药>卤代烃类

【英文 INN】homidium bromide

【别　　名】

【名称来源】pINN-036,1976　rINN-017,1977

【中文 CADN】胡米溴铵(GB4)

【建议 CADN】

【化学表述】3,8-diamino-5-ethyl-6-phenylphenanthridinium bromide

【CA 登记号】[1239-45-8]

【分 子 式】C21H20BrN3

【结 构 式】

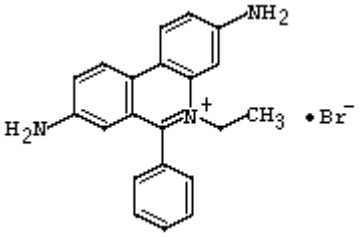

【品种类别】抗原虫药>抗黑热病和锥虫病药>其它

【英文 INN】nolinium bromide

【别　　名】

【名称来源】pINN-037,1977　rINN-017,1977

【中文 CADN】诺利溴铵(GB4)

【建议 CADN】

【化学表述】2-(3,4-dichloroanilino)quinolizinium bromide

【CA 登记号】[40759-33-9]

【分 子 式】C15H11BrCl2N2

【结 构 式】

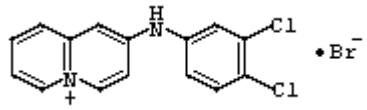

【品种类别】抗胆碱药>季铵盐类

【英文 INN】oxitropium bromide

【别　　名】Ventilat, Tersigat, Oxivent, Ba253BR

【名称来源】pINN-036,1976　rINN-017,1977

【中文 CADN】氧托溴铵(GB4)

【建议 CADN】

【化学表述】

(1R,2R,4S,5S,7s,9s)-9-ethyl-7-{[(2S)-3-hydroxy-2-phenylpropanoyl]oxy}-9-methyl-3-oxa-9-azoniatricyclo[3.3.1.0(2,4)]nonane bromide

【CA 登记号】[30286-75-0]

【分 子 式】C19H26BrNO4

【结 构 式】

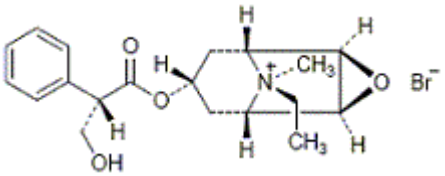

【品种类别】抗胆碱药>季铵盐类

【英文 INN】zimeldine

【别　　名】zimelidine

【名称来源】pINN-036,1976　rINN-017,1977

【中文 CADN】齐美定(97)

【建议 CADN】

【化学表述】Pyridine, 3-[1-(4-bromophenyl)-3-(dimethylamino)propenyl]-, (Z)-

【CA 登记号】[56775-88-3]

【分 子 式】C16H17BrN2

【结 构 式】

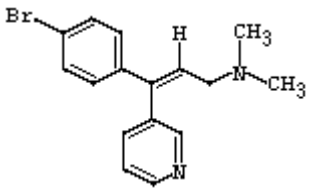

【品种类别】神经系统>抗抑郁药(1983 年撤市)

【英文 INN】amantanium bromide

【别　　名】Amantol, CR-898

【名称来源】pINN-039,1978　rINN-018,1978

【中文 CADN】金刚溴铵(GB4)

【建议 CADN】

【化学表述】1-Decanaminium, N,N-dimethyl-N-[2-[(tricyclo[3.3.1.1^3,7]dec-1-ylcarbonyl)oxy]ethyl]-, bromide

【CA 登记号】[58158-77-3]

【分 子 式】C25H48BrNO2

【结 构 式】

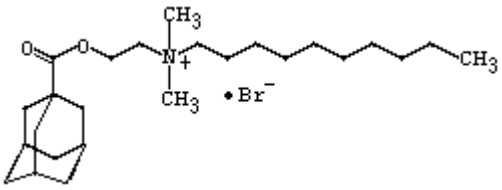

【品种类别】抗感染药>消毒防腐药>季铵盐类

【英文 INN】haloxazolam

【别　　名】Somelin，CS-430

【名称来源】pINN-038,1977　rINN-018,1978

【中文 CADN】卤沙唑仑(GB4)

【建议 CADN】

【化学表述】(RS)-10-Bromo-11b-(2-fluorophenyl)-2,3,7,11b-tetrahydrooxazolo[3,2-d]benzodiazepin-6(5H)-one

【CA 登记号】[59128-97-1]

【分 子 式】C17H14BrFN2O2

【结 构 式】

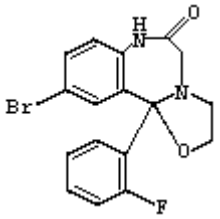

【品种类别】神经系统>抗焦虑药>苯并二氮杂卓衍生物

【英文 INN】otilonium bromide

【别　　名】

【名称来源】pINN-038,1977　rINN-018,1978

【中文 CADN】奥替溴铵(GB4)

【建议 CADN】

【化学表述】Ethanaminium, N,N-diethyl-N-methyl-2-[[4-[[2-(octyloxy)benzoyl]amino]benzoyl]oxy]-, bromide

【CA 登记号】[26095-59-0]

【分 子 式】C29H43BrN2O4

【结 构 式】

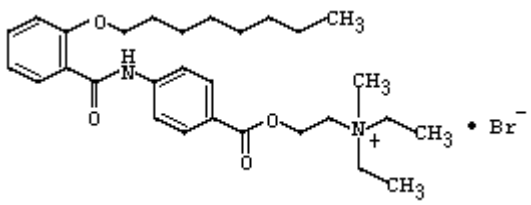

【品种类别】抗胆碱药>季铵盐类

【英文 INN】brallobarbital
【别　　名】
【名称来源】pINN-041,1979　rINN-019,1979
【中文 CADN】溴烯比妥(GB4)
【建议 CADN】
【化学表述】5-allyl-5-(2-bromoallyl)barbituric acid
【CA 登记号】[561-86-4]
【分 子 式】C10H11BrN2O3
【结 构 式】

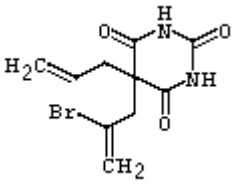

【品种类别】神经系统>催眠镇静药>巴比妥类

【英文 INN】brosuximide
【别　　名】
【名称来源】pINN-041,1979　rINN-019,1979
【中文 CADN】溴琥胺(97)
【建议 CADN】
【化学表述】2-(3-bromophenyl)succinimide
【CA 登记号】[22855-57-8]
【分 子 式】C10H8BrNO2
【结 构 式】

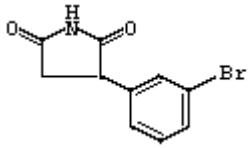

【品种类别】神经系统>抗癫痫药>琥珀酰亚胺衍生物

【英文 INN】brotizolam
【别　　名】Lendormin, Ladormimi, Indomyl, Bondormin, Dormex, Lendorm, WE-94
【名称来源】pINN-040,1978　rINN-019,1979
【中文 CADN】溴替唑仑(97)
【建议 CADN】

【化学表述】6H-Thieno[3,2-f][1,2,4]triazol[4,3-a][1,4]diazepine, 2-bromo-4-(2-chlorophenyl)-9-methyl-

【CA 登记号】[57801-81-7]

【分 子 式】C15H10BrClN4S

【结 构 式】

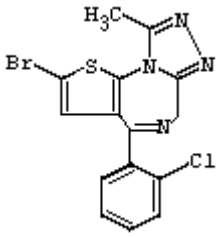

【品种类别】神经系统>抗焦虑药>噻吩并二氮杂卓衍生物

【英文 INN】ciclotizolam

【别　　名】

【名称来源】pINN-040,1978　rINN-019,1979

【中文 CADN】环氯唑仑(97)

【建议 CADN】

【化学表述】2-bromo-4-(2-chlorophenyl)-9-cyclohexyl-6H-thieno[3,2-f]-s-triazolo[4,3-a][1,4]diazepine

【CA 登记号】[58765-21-2]

【分 子 式】C20H18BrClN4S

【结 构 式】

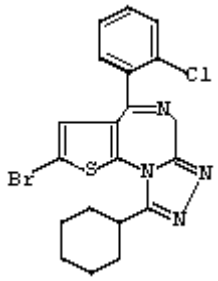

【品种类别】神经系统>抗焦虑药>噻吩并二氮杂卓衍生物

【英文 INN】nomelidine

【别　　名】Norzimelidine, Botiacrine, CPP-199, A-24356

【名称来源】pINN-040,1978　rINN-019,1979

【中文 CADN】诺美立定(97)

【建议 CADN】

【化学表述】(Z)-3-[1-(4-bromophenyl)-3-(methylamino)propenyl]pyridine

【CA 登记号】[60324-59-6]

【分 子 式】C15H15BrN2

【结 构 式】

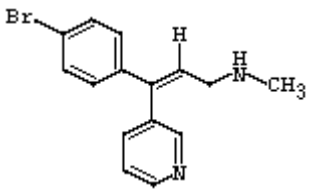

【品种类别】神经系统>抗抑郁药>

【英文 INN】oxabrexine

【别　　名】

【名称来源】pINN-040,1978　rINN-019,1979

【中文 CADN】奥溴克新(GB4)

【建议 CADN】

【化学表述】ethyl [[4,6-dibromo-α-(cyclohexylmethylamino)-o-tolyl]oxy]acetate

【CA 登记号】[65415-42-1]

【分 子 式】C18H25Br2NO3

【结 构 式】

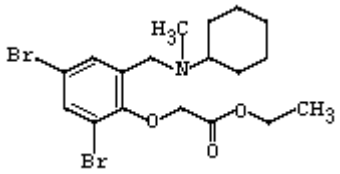

【品种类别】呼吸系统>祛痰药>溴己新类

【英文 INN】pipecuronium bromide

【别　　名】

【名称来源】pINN-041,1979　rINN-019,1979

【中文 CADN】哌库溴铵(GB4)

【建议 CADN】

【化学表述】4,4'-[3α,17β-di(acetyloxy)-5α-androstane-2β,16β-diyl]bis[1,1-dimethylpiperazinium] dibromide

【CA 登记号】[68399-57-5]

【分 子 式】C35H62Br2N4O4

【结 构 式】

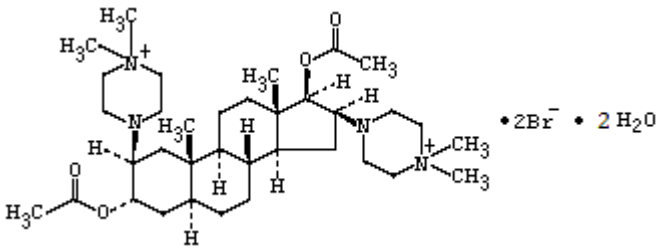

【品种类别】肌肉-骨骼系统>肌松药>季铵盐类

【英文 INN】quinuclium bromide

【别　　名】

【名称来源】pINN-040,1978　rINN-019,1979

【中文 CADN】奎纽溴铵(GB4)

【建议 CADN】

【化学表述】1-methyl-3-oxo-4-phenylquinuclidinium bromide hemihydrate

【CA 登记号】[64755-06-2]

【分 子 式】C14H18BrNO.1/2H2O

【结 构 式】

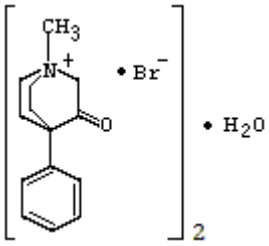

【品种类别】心血管系统>抗高血压药>季铵盐类/喹啉衍生物

【英文 INN】broclepride

【别　　名】

【名称来源】pINN-043,1980　rINN-020,1980

【中文 CADN】溴氯必利(GB4)

【建议 CADN】

【化学表述】4-amino-5-bromo-N-[1-(4-chlorobenzyl)-4-piperidyl]-o-anisamide

【CA 登记号】[71195-56-7]

【分 子 式】C20H23BrClN3O2

【结 构 式】

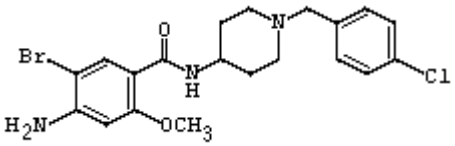

【品种类别】神经系统>抗精神病药>苯甲酰胺衍生物

【英文 INN】bromofenofos

【别　　名】

【名称来源】pINN-043,1980　rINN-020,1980

【中文 CADN】溴酚磷(GB4)

【建议 CADN】

【化学表述】3,3',5,5'-tetrabromo-2,2'-biphenyldiol, mono(dihydrogen phosphate)

【CA 登记号】[21466-07-9]

【分 子 式】C12H7Br4O5P

【结 构 式】

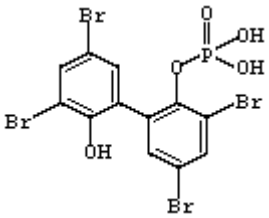

【品种类别】抗蠕虫药

【英文 INN】broperamole

【别　　名】

【名称来源】pINN-042,1979　rINN-020,1980

【中文 CADN】溴哌莫(97)

【建议 CADN】

【化学表述】Piperidine, 1-[3-[5-(3-bromophenyl)-2H-tetrazol-2-yl]-1-oxopropyl]-

【CA 登记号】[33144-79-5]

【分 子 式】C15H18BrN5O

【结 构 式】

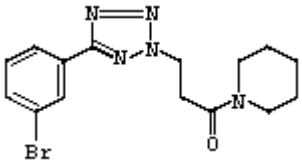

【品种类别】消炎药

【英文 INN】brovincamine

【别　　名】Sabromin, Buprozine, BV-26-723

【名称来源】pINN-042,1979　rINN-020,1980

【中文 CADN】溴长春胺(GB4)

【建议 CADN】

【化学表述】(3α,14β,16α)-l1-Bromo-14,15-dihydro-14-hydroxy eburnamenine-14-carboxylic acid methyl ester

【CA 登记号】[57475-17-9]

【分 子 式】C21H25BrN2O3

【结 构 式】

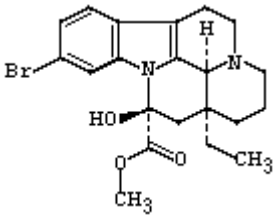

【品种类别】神经系统>脑血管和外周血管扩张药

【英文 INN】tipetropium bromide

【别　　名】

【名称来源】pINN-042,1979　rINN-020,1980

【中文 CADN】替托溴铵(GB4)

【建议 CADN】

【化学表述】3α-[(6,11-dihydrodlbenzo[b,e]thiepin-11-yl)oxy]-8-propyl-1αH,5αH-tropanium bromide

【CA 登记号】[54376-91-9]

【分 子 式】C25H32BrNOS

【结 构 式】

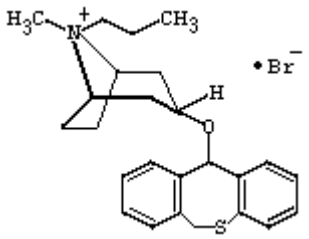

【品种类别】呼吸系统>平喘药

【英文 INN】brodimoprim

【别　　名】

【名称来源】pINN-044,1980　rINN-021,1981

【中文 CADN】溴莫普林(GB4)

【建议 CADN】

【化学表述】Pyrimidine, 2,4-diamino-5-(4-bromo-3,5-dimethoxybenzyl)-

【CA 登记号】[56518-41-3]

【分 子 式】C13H15BrN4O2

【结 构 式】

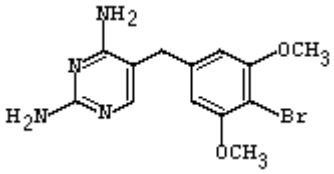

【品种类别】抗感染药>合成抗菌药>甲氧苄啶类

【英文 INN】mebrofenin

【别　　名】Choletec, SQ-26962

【名称来源】pINN-047,1982　rINN-022,1982

【中文 CADN】甲溴苯宁(GB4)

【建议 CADN】

【化学表述】Glycine, N-[2-[(3-bromo-2,4,6-trimethylphenyl)amino]-2-oxoethyl]-N-(carboxymethyl)-

【CA 登记号】[78266-06-5]

【分 子 式】C15H19BrN2O5

【结 构 式】

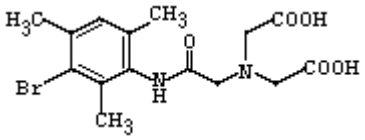

【品种类别】诊断用药>(苯氨甲酰)甲基亚氨二乙酸衍生物

【英文 INN】metaclazepam

【别　　名】Brometazepam, Ka-2547, KC-2547, Talis

【名称来源】pINN-040,1978　rINN-022,1982

【中文 CADN】美氯西泮(GB4)

【建议 CADN】

【化学表述】1H-1,4-Benzodiazepine, 7-bromo-5-(2-chlorophenyl)-2,3-dihydro-2-(methoxymethyl)-1-methyl-

【CA 登记号】[84031-17-4]

【分 子 式】C18H18BrClN2O

【结 构 式】

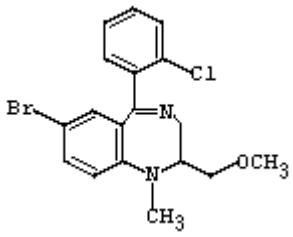

【品种类别】神经系统>抗焦虑药>苯并二氮杂卓衍生物

【英文 INN】sintropium bromide

【别　　名】

【名称来源】pINN-047,1982　rINN-022,1982

【中文 CADN】辛托溴铵(GB4)

【建议 CADN】

【化学表述】8-Azoniacyclo[3.2.1]octane, 3-[(dipropylacetyl)oxy]-8-methyl-8-(1-methylethyl)-, bromide, (3-endo,8-syn-)-

【CA 登记号】[79467-19-9]

【分 子 式】C19H36BrNO2

【结 构 式】

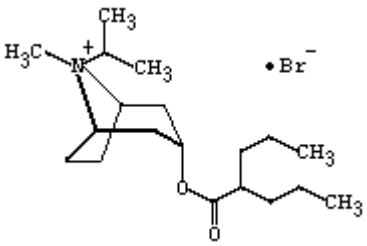

【品种类别】抗胆碱药>季铵盐类

【英文 INN】tiquizium bromide

【别　　名】Thiaton，HSR-902, HS-902

【名称来源】pINN-047,1982　rINN-022,1982

【中文 CADN】替喹溴铵(GB4)

【建议 CADN】

【化学表述】2H-Quinolizinium, trans-3-(di-2-thienylmethylene)octahydro-5-methyl-, bromide

【CA 登记号】[71731-58-3]

【分 子 式】C19H24BrNS2

【结 构 式】

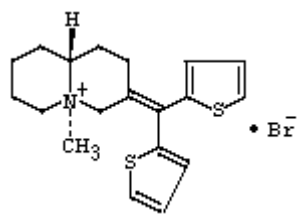

【品种类别】抗胆碱药>喹啉衍生物

【附件编号】 115074

【英文 INN】vecuronium bromide

【别 名】Musculax, NC-45, Norcuron, Org-NC-45, Vercuronium bromide

【名称来源】pINN-046,1981 rINN-022,1982

【中文 CADN】维库溴铵(GB4)

【建议 CADN】

【化学表述】Piperidinium, 1-[3,17-bis(acetyloxy)-2-(1-piperidinyl)androstan-18-yl]-1-methyl-, bromide

【CA 登记号】[50700-72-6]

【分 子 式】C34H57BrN2O4

【结 构 式】

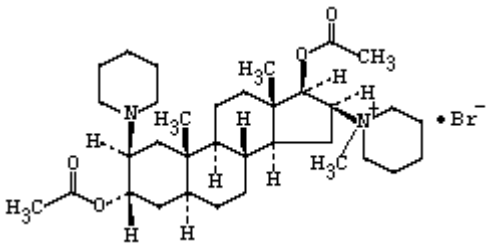

【品种类别】肌肉-骨骼系统>肌松药>季铵盐类

【英文 INN】bromadoline

【别 名】

【名称来源】pINN-049,1983 rINN-023,1983

【中文 CADN】溴朵林(97)

【建议 CADN】

【化学表述】Benzamide, 4-bromo-N-[(1R,2R)-2-(dimethylamino)cyclohexyl]-, rel-

【CA 登记号】[67579-24-2]

【分 子 式】C15H21BrN2O

【结 构 式】

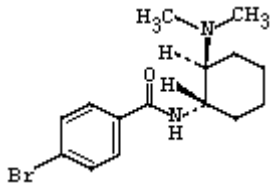

【品种类别】神经系统>镇痛药>混合阿片受体激动剂/拮抗剂类

【英文 INN】remoxipride

【别 名】Roxiam, FLA731, A33547

【名称来源】pINN-049,1983 rINN-023,1983

【中文 CADN】瑞莫必利(GB4)

【建议 CADN】

【化学表述】Benzamide, 3-Bromo-N-[[(2S)-1-ethyl-2-pyrrolidinyl]methyl]-2,6-dimethoxy-

【CA 登记号】[80125-14-0]

【分 子 式】C16H23BrN2O3

【结 构 式】

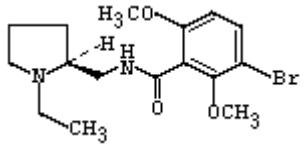

【品种类别】消化系统>胃肠道动力药>苯甲酰胺衍生物

【英文 INN】brocrinat

【别　　名】Halocrinic acid

【名称来源】pINN-047,1982　rINN-024,1984

【中文 CADN】溴克利那(GB4)

【建议 CADN】

【化学表述】Acetic acid, [[7-bromo-3-(2-fluorophenyl)-1,2-benzisoxazol-6-yl]oxo]-

【CA 登记号】[72481-99-3]

【分 子 式】C15H9BrFNO4

【结 构 式】

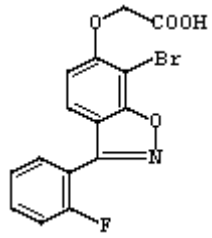

【品种类别】生殖泌尿系统>利尿药>苯氧乙酸衍生物

【英文 INN】bromerguride

【别　　名】

【名称来源】pINN-051,1984　rINN-024,1984

【中文 CADN】溴麦角脲(GB4)

【建议 CADN】

【化学表述】Urea, N'-[(8α)-2-bromo-9,10-didehydro-6-methylergolin-8-yl]-N,N-diethyl-

【CA 登记号】[83455-48-5]

【分 子 式】C20H25BrN4O

【结 构 式】

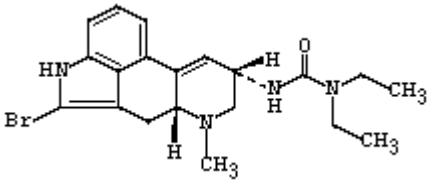

【品种类别】5-羟色胺受体拮抗剂>麦角生物碱衍生物

【英文 INN】broxaterol

【别　　名】

【名称来源】pINN-051,1984　rINN-024,1984

【中文 CADN】溴沙特罗(GB4)

【建议 CADN】

【化学表述】5-Isoxazolemethanol, 3-bromo-α-[[(1,1-dimethylethyl)amino]methyl]-

【CA 登记号】[76596-57-1]

【分 子 式】C9H13BrN2O2

【结 构 式】

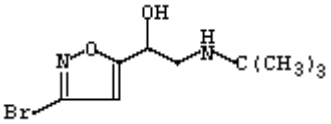

【品种类别】呼吸系统>支气管扩张药>苯乙胺衍生物>β2-肾上腺素受体激动剂

【英文 INN】ciclotropium bromide

【别　　名】

【名称来源】pINN-050,1983　rINN-024,1984

【中文 CADN】环托溴铵(GB4)

【建议 CADN】

【化学表述】8-Azoniacyclo[3.2.1]octane, 3-[(cyclopentylphenylacetyl)oxy]-8-methyl-8-(1-methylethyl)-, bromide, (3-endo,8-syn-)-

【CA 登记号】[85166-20-7]

【分 子 式】C24H36BrNO2

【结 构 式】

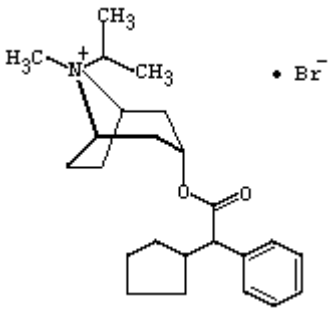

【品种类别】抗胆碱药>季铵盐类

【英文 INN】cimetropium bromide

【别　　名】N-Cyclopropylmethyl Scopolamide bromide, Alginor, DA3177

【名称来源】pINN-051,1984　rINN-024,1984

【中文 CADN】西托溴铵(GB4)

【建议 CADN】

【化学表述】3-Oxa-9-azoniatricyclo[3.3.1.$0^{2,4}$]nonane, 9-(cyclopropylmethyl)-[7-(2S)-3-hydroxy-1-oxo-2-phenylpropoxy]-9-methyl-, bromide, (1α,2β,4β,5α,7β)-

【CA 登记号】[51598-60-8]

【分 子 式】C21H28BrO4

【结 构 式】

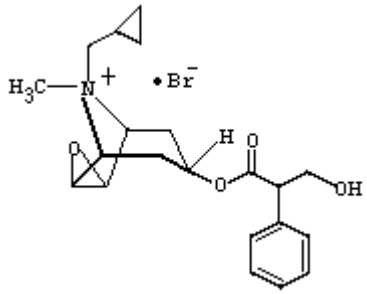

【品种类别】抗胆碱药>季铵盐类

【英文 INN】dibrospidium chloride

【别　　名】

【名称来源】pINN-051,1984　rINN-024,1984

【中文 CADN】二溴螺氯铵(GB4)

【建议 CADN】

【化学表述】3,12-bis(3-bromopropionyl)-3,12-diazoniadispiro[5.2.5.2]hexadecane dichloride

【CA 登记号】[86641-76-1]

【分 子 式】C18H32Br2Cl2N4O2

【结 构 式】

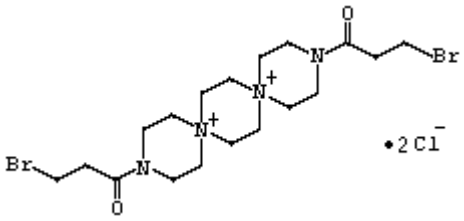

【品种类别】抗肿瘤药>烷基化剂>其它

【英文 INN】flutropium bromide

【别　　名】Flubron，Ba598BR

【名称来源】pINN-050,1983　rINN-024,1984

【中文 CADN】氟托溴铵(GB4)

【建议 CADN】

【化学表述】8-Azoniabicyclo[3.2.1]octane, 8-(2-fluoroethyl)-3-[(hydroxydiphenylacetyl)oxy]-8-methyl-, bromide, (3-endo,8-syn)-

【CA 登记号】[63516-07-4]

【分 子 式】C24H29BrFNO3

【结 构 式】

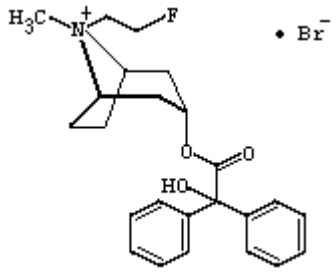

【品种类别】抗胆碱药>季铵盐类

【英文 INN】broxitalamic acid

【别　　名】

【名称来源】pINN-052,1984　rINN-025,1985

【中文 CADN】溴异酞酸(97)

【建议 CADN】

【化学表述】5-acetamido-2,4,6-tribromo-N-(2-hydroxyethyl)isophthalamic acid

【CA 登记号】[86216-41-3]

【分 子 式】C12H11Br3N2O5

【结 构 式】

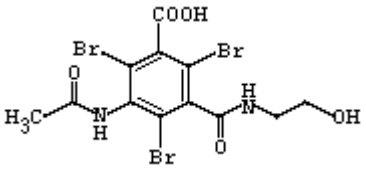

【品种类别】诊断用药

【英文 INN】ioxabrolic acid

【别　　名】

【名称来源】pINN-053,1985　rINN-025,1985

【中文 CADN】碘克溴酸(GB4)

【建议 CADN】

【化学表述】

N-(2-hydroxyethyl)-2,4,6-triiodo-5-[2-[2,4,6-tribromo-3-(N-methylacetamido)-5-(methylcarbamoyl)benzamido]acetamido]isophthalamic acid

【CA 登记号】[96191-65-0]

【分 子 式】C24H29Br3I3N5O8

【结 构 式】

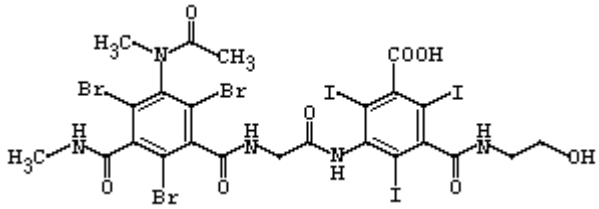

【品种类别】诊断用药>X 射线造影剂>碘代物

【英文 INN】brobactam

【别　　名】

【名称来源】pINN-053,1985　rINN-025,1985

【中文 CADN】溴巴坦(GB4)

【建议 CADN】

【化学表述】4-Thia-1-azabicyclo[3.2.0]heptane-2-carboxylic acid, 6-bromo-3,3-dimethyl-7-oxo-, (2S,5R,6R)-

【CA 登记号】[26631-90-3]

【分 子 式】C8H10BrNO3S

【结 构 式】

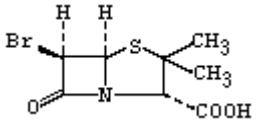

【品种类别】抗感染药>抗生素>β-内酰胺酶抑制剂

【英文 INN】isobromindione

【别　　名】

【名称来源】pINN-052,1984　rINN-025,1985

【中文 CADN】依溴二酮(97)

【建议 CADN】

【化学表述】1H-Indene-1,3(2H)-dione, 5-bromo-2-phenyl-

【CA 登记号】[1470-35-5]

【分 子 式】C15H9BrO2

【结 构 式】

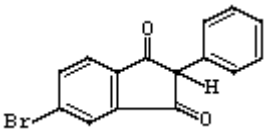

【品种类别】肌肉-骨骼系统>抗痛风药>增加尿酸分泌的

【英文 INN】brofaromine

【别　　名】

【名称来源】pINN-054,1985　rINN-026,1986

【中文 CADN】溴法罗明(97)

【建议 CADN】

【化学表述】4-(7-bromo-5-methoxy-2-benzofuranyl)piperidine

【CA 登记号】[63638-91-5]

【分 子 式】C14H16BrNO2

【结 构 式】

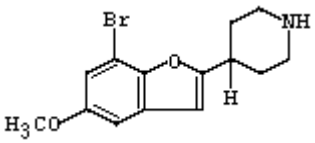

【品种类别】神经系统>抗抑郁药>

【英文 INN】brolamfetamine

【别　　名】

【名称来源】pINN-055,1986　rINN-026,1986

【中文 CADN】布苯丙胺(97)

【建议 CADN】

【化学表述】(±)-4-bromo-2,5-dimethoxy-α-methylphenethylamine

【CA 登记号】[64638-07-9]

【分 子 式】C11H16BrNO2

【结 构 式】

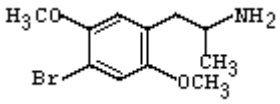

【品种类别】神经系统>中枢兴奋药

【英文 INN】bromfenac

【别　　名】

【名称来源】pINN-055,1986　rINN-026,1986

【中文 CADN】溴芬酸(GB4)

【建议 CADN】

【化学表述】[2-amino-3-(p-bromobenzoyl)phenyl]acetic acid

【CA 登记号】[91714-94-2]

【分 子 式】C15H12BrNO3

【结 构 式】

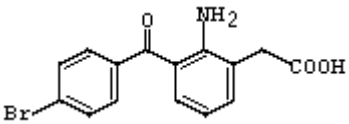

【品种类别】非甾体抗炎药>苯乙酸衍生物

【英文 INN】bropirimine

【别　　名】

【名称来源】pINN-055,1986　rINN-026,1986

【中文 CADN】溴匹立明(97)

【建议 CADN】

【化学表述】2-Amino-5-bromo-6-phenyl-4(1H)-pyrimidinone

【CA 登记号】[56741-95-8]

【分 子 式】C10H8BrN3O

【结 构 式】

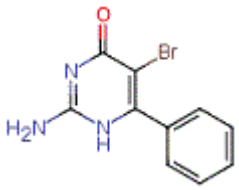

【品种类别】抗肿瘤药

【英文 INN】cistinexine

【别　　名】

【名称来源】pINN-054,1985　rINN-026,1986

【中文 CADN】西替克新(GB4)

【建议 CADN】

【化学表述】dibenzyl [dithiobis[（R）-1-[[4,6-dibromo-α-(cyclohexylmethylamino)-o-tolyl]carbamoyl]ethylene]]dicarbamate

【CA 登记号】[86042-50-4]

【分 子 式】C50H60Br4N6O6S2

【结 构 式】

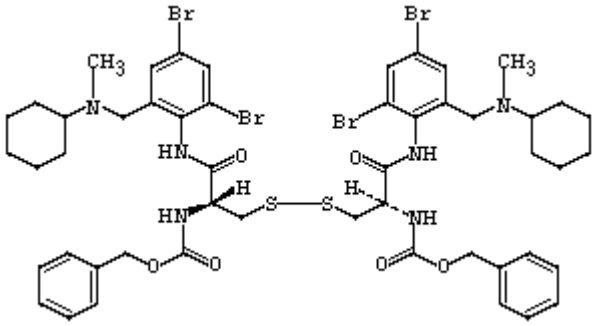

【品种类别】呼吸系统>祛痰药>溴己新类

【英文 INN】lodazecar

【别　　名】

【名称来源】pINN-054,1985　rINN-026,1986

【中文 CADN】氯达西卡(97)

【建议 CADN】

【化学表述】

1-[1,1-bis(hydroxymethyl)ethyl]-3-[(S)-6-bromo-5-(o-chlorophenyl)-2,3-dihydro-1,3-dimethyl-2-oxo-1H-1,4-benzodiazepin-7-yl]urea

【CA 登记号】[87646-83-1]

【分 子 式】C22H24BrClN4O4

【结 构 式】

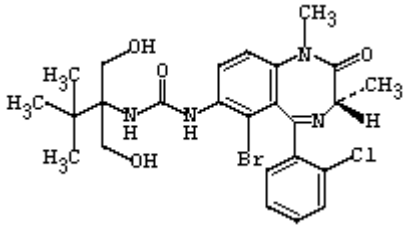

【品种类别】心血管系统>降血脂药

【英文 INN】temelastine

【别　　名】

【名称来源】pINN-054,1985　rINN-026,1986

【中文 CADN】替美斯汀(GB4)

【建议 CADN】

【化学表述】4(1H)-Pyrimidinone, 2-[[4-(5-bromo-3-methyl-2-piperidinyl)butyl]amino]-5-[(6-methyl-3-pyridinyl)methyl]-

【CA 登记号】[86181-42-2]

【分 子 式】C21H24BrN5O

【结 构 式】

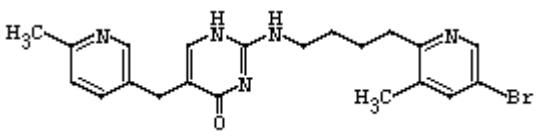

【品种类别】抗组胺药>组胺 H1 受体拮抗剂

【英文 INN】azumolene

【别　　名】

【名称来源】pINN-056,1986　rINN-027,1987

【中文 CADN】阿珠莫林(97)

【建议 CADN】

【化学表述】1-[[[5-(4-bromophenyl)-2-oxazolyl]methylene]amino]hydantoin

【CA 登记号】[64748-79-4]

【分 子 式】C13H9BrN4O3

【结 构 式】

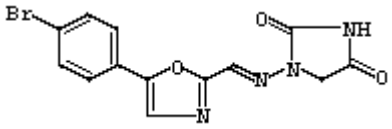

【品种类别】肌肉-骨骼系统>肌松药>其它

【英文 INN】dembroxol

【别　　名】Dembrexine

【名称来源】pINN-050,1983　rINN-027,1987

【中文 CADN】登溴克新(GB4)

【建议 CADN】

【化学表述】Phenol, 2,4-dibromo-6-[[(trans-4-hydroxycyclohexyl)amino]methyl]-

【CA 登记号】[83200-09-3]

【分 子 式】C13H17Br2NO2

【结 构 式】

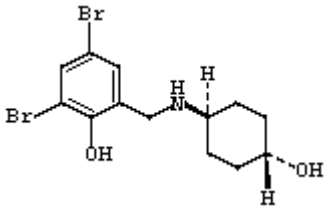

【品种类别】呼吸系统>祛痰药>溴己新类

【英文 INN】ebrotidine

【别　　名】Ebrocit, FI-3542

【名称来源】pINN-057,1987　rINN-027,1987

【中文 CADN】乙溴替丁(GB4)

【建议 CADN】

【化学表述】Benzenesulfonamide, N-[[[2-[[[2-[(aminoiminomethyl)amino]-4-thiazoly]methyl]thio]ethyl]amino]methylene]-4-bromo-

【CA 登记号】[100981-43-9]

【分 子 式】C14H17BrN6O2S3

【结 构 式】

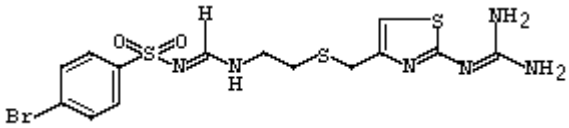

【品种类别】消化系统>抗溃疡病药>H2 受体拮抗剂>西咪替丁类

【英文 INN】brolaconazole

【别　　名】

【名称来源】pINN-058,1987　rINN-028,1988

【中文 CADN】溴康唑(GB4)

【建议 CADN】

【化学表述】(±)-1-(p-bromo-β-phenylphenethyl)imidazole

【CA 登记号】[108894-40-2]

【分 子 式】C17H15BrN2

【结 构 式】

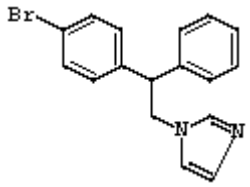

【品种类别】抗感染药>抗真菌药>咪唑衍生物

【英文 INN】ponalrestat

【别　　名】

【名称来源】pINN-058,1987　rINN-028,1988

【中文 CADN】泊那司他(GB4)

【建议 CADN】

【化学表述】3-(4-bromo-2-fluorobenzyl)-3,4-dihydro-4-oxo-1-phthalazineacetic acid

【CA 登记号】[72702-95-5]

【分 子 式】C17H12BrFN2O3

【结 构 式】

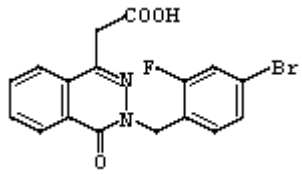

【品种类别】代谢系统>抗糖尿病药>醛糖还原酶抑制剂

【英文 INN】rilozarone

【别　　名】

【名称来源】pINN-058,1987　rINN-028,1988

【中文 CADN】利洛扎隆(GB4)

【建议 CADN】

【化学表述】1-bromo-2-phenyl-3-indolizinyl 3-chloro-4-[3-(dibutylamino)propoxy]phenyl ketone

【CA 登记号】[79282-39-6]

【分 子 式】C32H36BrClN2O2

【结 构 式】

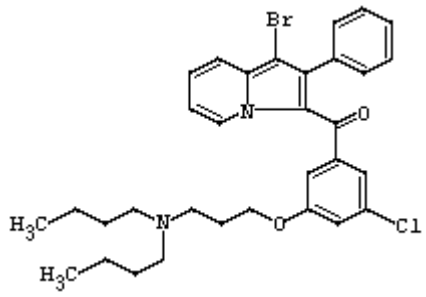

【品种类别】心血管系统>抗心律失常药>其它

【英文 INN】romifidine

【别　　名】

【名称来源】pINN-058,1987　rINN-028,1988

【中文 CADN】罗米非定(97)

【建议 CADN】

【化学表述】2-(2-bromo-6-fluoroanilino)-2-imidazoline

【CA 登记号】[65896-16-4]

【分 子 式】C9H9BrFN3

【结 构 式】

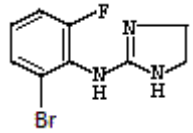

【品种类别】神经系统>镇痛药

【英文 INN】bretazenil

【别　　名】

【名称来源】pINN-060,1988　rINN-029,1989

【中文 CADN】溴他西尼(GB4)

【建议 CADN】

【化学表述】9H-imidazo[1,5-a]pyrrolo[2,1-c][1,4]benzodiazepine-1-carboxylic acid, 8-bromo-11,12,13,13a-tetrahydro-9-oxo-, 1,1-dimethylethyl ester, (13aS)-

【CA 登记号】[84379-13-5]

【分 子 式】C19H20BrN3O3

【结 构 式】

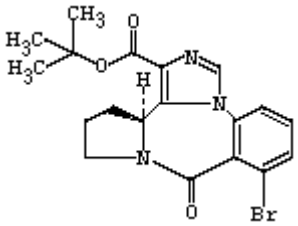

【品种类别】神经系统>抗焦虑药>苯并二氮杂卓衍生物

【英文 INN】brivudine

【别　　名】

【名称来源】pINN-059,1988　rINN-029,1989

【中文 CADN】溴夫定(GB4)

【建议 CADN】

【化学表述】(E)-5-(2-bromovinyl)-2'-deoxyuridine

【CA 登记号】[69304-47-8]

【分 子 式】C11H13BrN2O5

【结 构 式】

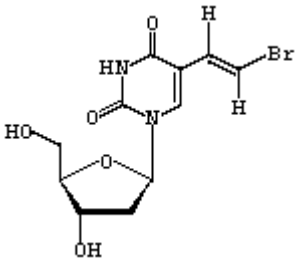

【品种类别】抗感染药>抗病毒药>核苷类逆转录酶抑制剂

【英文 INN】neltenexine

【别　　名】

【名称来源】pINN-062,1989　rINN-030,1990

【中文 CADN】奈替克新(GB4)

【建议 CADN】

【化学表述】4',6'-dibromo-α-[(trans-4-hydroxycyclohexyl)amino]-2-thiophenecarboxy-o-toluidide

【CA 登记号】[99453-84-6]

【分 子 式】C18H20Br2N2O2S

【结 构 式】

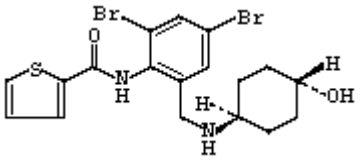

【品种类别】呼吸系统>祛痰药>溴己新类

【英文 INN】sorivudine

【别　　名】Brovavir，Usevir，BVAU

【名称来源】pINN-064,1990　rINN-031,1991

【中文 CADN】索立夫定(GB4)

【建议 CADN】

【化学表述】(+)-1-β-D-arabinofuranosyl-5-[(E)-2-bromovinyl]uracil

【CA 登记号】[77181-69-2]

【分 子 式】C11H13BrN2O6

【结 构 式】

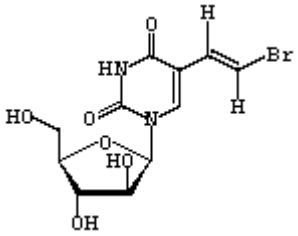

【品种类别】抗感染药>抗病毒药>核苷类逆转录酶抑制剂

【英文 INN】zenarestat

【别　　名】

【名称来源】pINN-064,1990　rINN-031,1991

【中文 CADN】折那司他(GB4)

【建议 CADN】

【化学表述】3-(4-bromo-2-fluorobenzyl)-7-chloro-3,4-dihydro-2,4-dioxo-1(2H)-quinazolineacetic acid

【CA 登记号】[112733-06-9]

【分 子 式】C17H11BrClFN2O4

【结 构 式】

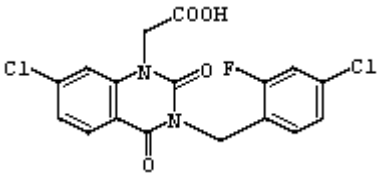

【品种类别】代谢系统>抗糖尿病药>醛糖还原酶抑制剂

【英文 INN】brimonidine

【别　　名】Alphagan, Alphagan P

【名称来源】pINN-066,1991　rINN-032,1992

【中文 CADN】溴莫尼定(GB4)

【建议 CADN】

【化学表述】5-bromo-6-(2-imidazolidinylidenamino)quinoxaline

【CA 登记号】[59803-98-4]

【分 子 式】C11H10BrN5

【结 构 式】

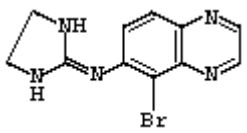

【品种类别】α2-肾上腺素受体激动剂

【英文 INN】perflubron

【别　　名】

【名称来源】pINN-066,1991　rINN-032,1992

【中文 CADN】全氟溴烷(GB4)

【建议 CADN】

【化学表述】1-bromoheptadecafluorooctane

【CA 登记号】[423-55-2]

【分 子 式】C8BrF17

【结 构 式】

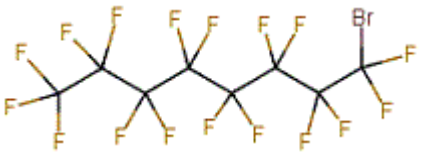

【品种类别】血液系统>携氧药；诊断用药>MRI 造影剂>其它

【英文 INN】rocuronium bromide

【别　　名】

【名称来源】pINN-066,1991　rINN-032,1992

【中文 CADN】罗库溴铵(GB4)

【建议 CADN】

【化学表述】1-allyl-1-(3α,17β-dihydroxy-2β-morpholino-5α-androstan-16β-yl)pyrrolidinium bromide, 17-acetate

【CA 登记号】[119302-91-9]

【分 子 式】C32H53BrN2O4

【结 构 式】

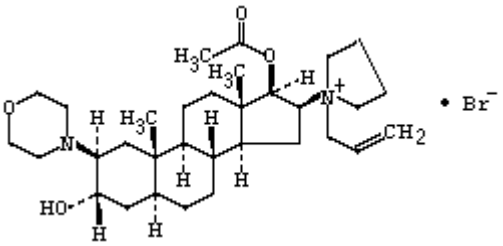

【品种类别】肌肉-骨骼系统>肌松药>季铵盐类

【英文 INN】tiotropium bromide

【别　　名】

【名称来源】pINN-067,1992　rINN-033,1993

【中文 CADN】噻托溴铵(GB4)

【建议 CADN】

【化学表述】6β,7β-epoxy-3β-hydroxy-8-methyl-1αH,5αH-tropanium bromide

【CA 登记号】[139404-48-1]

【分 子 式】C19H22BrNO4S2

【结 构 式】

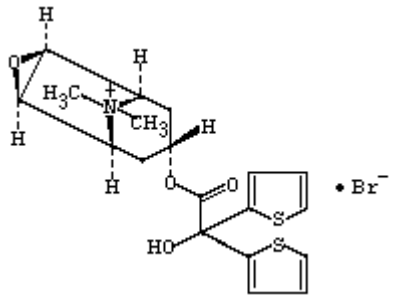

【品种类别】呼吸系统>平喘药>吸入剂>抗胆碱能药类

【英文 INN】laurcetium bromide

【别　　名】

【名称来源】pINN-070,1993　rINN-034,1994

【中文 CADN】劳塞溴铵(GB4)

【建议 CADN】

【化学表述】(carboxymethyl)dodecyldimethylammonium bromide, ethyl ester

【CA 登记号】[1794-75-8]

【分 子 式】C18H36BrNO2

【结 构 式】

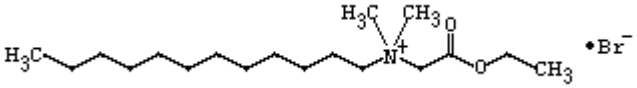

【品种类别】抗感染药>消毒防腐药>季铵盐类

【英文 INN】zolasartan

【别　　名】

【名称来源】pINN-070,1993　rINN-034,1994

【中文 CADN】佐拉沙坦(GB4)

【建议 CADN】

【化学表述】1-[[3-bromo-2-(o-1H-tetrazol-5-ylphenyl)-5-benzofuranyl]methyl]-2-butyl-4-chloroimidazole-5-carboxylic acid

【CA 登记号】[145781-32-4]

【分 子 式】C24H20BrClN6O3

【结 构 式】

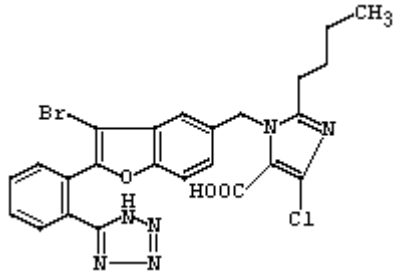

【品种类别】心血管系统>抗高血压药>血管紧张素 II 拮抗剂

【英文 INN】berupipam

【别　　名】

【名称来源】pINN-071,1994　rINN-035,1995

【中文 CADN】贝芦匹泮

【建议 CADN】

【化学表述】(+)-(5S)-5-(5-bromo-2,3-dihydro-7-benzofuranyl)-8-chloro-2,3,4,5-tetrahydro-3-methyl-1H-3-benzazepin-7-ol

【CA 登记号】[150490-85-0]

【分 子 式】C19H19BrClNO2

【结 构 式】

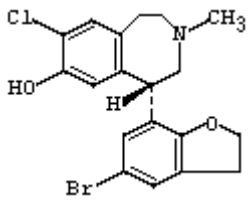

【品种类别】神经系统>抗精神病药>其它

【英文 INN】saprisartan

【别　　名】

【名称来源】pINN-072,1994　rINN-035,1995

【中文 CADN】沙普立沙坦(GB4)

【建议 CADN】

【化学表述】

1-[[3-bromo-2-[o-(1,1,1-trifluoromethanesulfonamido)phenyl]-5-benzofuranyl]methyl]-4-cyclopropyl-2-ethylimidazole-5-carboxamide

【CA 登记号】[146623-69-0]

【分 子 式】C25H22BrF3N4O4S

【结 构 式】

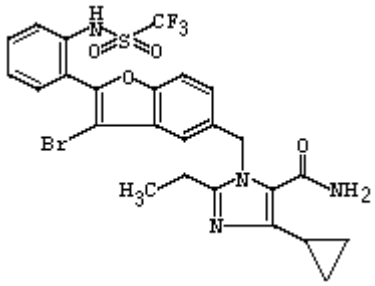

【品种类别】心血管系统>抗高血压药>血管紧张素 II 拮抗剂

【英文 INN】trovirdine

【别　　名】

【名称来源】pINN-073,1995　rINN-036,1996

【中文 CADN】卓韦啶

【建议 CADN】

【化学表述】1-(5-bromo-2-pyridyl)-3-[2-(2-pyridyl)ethyl]-2-thiourea

【CA 登记号】[149488-17-5]

【分 子 式】C13H13BrN4S

【结 构 式】

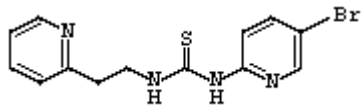

【品种类别】抗感染药>抗病毒药>非核苷类>逆转录酶抑制药

【英文 INN】minalrestat

【别　　名】

【名称来源】pINN-076,1996　rINN-038,1997

【中文 CADN】米那司他(GB4)

【建议 CADN】

【化学表述】(±)-2-(4-bromo-2-fluorobenzyl)-6-fluorospiro[isoquinoline-4(1H),3'-pyrrolidine]-1,2',3,5'(2H)-tetrone

【CA 登记号】[129688-50-2]

【分 子 式】C19H11BrF2N2O4

【结 构 式】

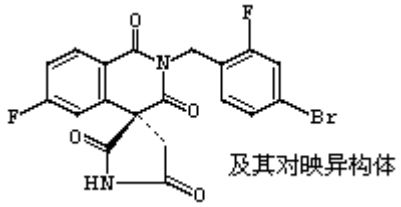

【品种类别】代谢系统>抗糖尿病药>醛糖还原酶抑制剂

【英文 INN】rapacuronium bromide

【别　　名】

【名称来源】pINN-078,1997　rINN-040,1998

【中文 CADN】雷库溴铵(GB4)

【建议 CADN】

【化学表述】1-allyl-1-(3α,17β-dihydroxy-2-piperidino-5α-androstan-16β-yl)piperidinium bromide, 3-acetate 17-propionate

【CA 登记号】[156137-99-4]

【分 子 式】C37H61BrN2O4

【结 构 式】

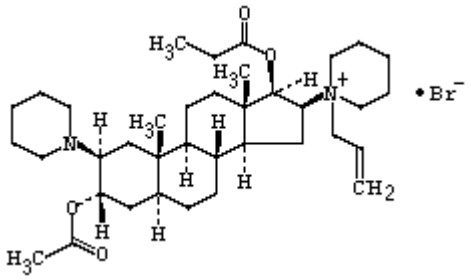

【品种类别】肌肉-骨骼系统>肌松药>季铵盐类(2001 年撤市)

【英文 INN】pibrozelesin

【别　　名】

【名称来源】pINN-081,1999　rINN-043,2000

【中文 CADN】哌溴来新

【建议 CADN】

【化学表述】methyl (S)-8-(bromomethyl)-3,6,7,8-tetrahydro-4-hydroxy-2-methyl-6-[(5,6,7-trimethoxyindol-2-yl)carbonyl]benzo[1,2-b:4,3-b']dipyrrole-1-carboxylate, 4-methyl-1-piperazinecarboxylate (ester)

【CA 登记号】[154889-68-6]

【分 子 式】C32H36BrN5O8

【结 构 式】

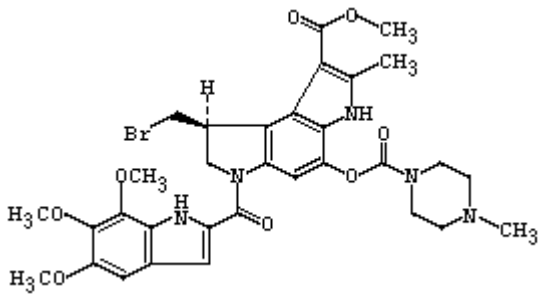

【品种类别】抗肿瘤药>

【英文 INN】brostallicin
【别　　名】PNU-166196A
【名称来源】pINN-084,2000　rINN-046,2001
【中文 CADN】
【建议 CADN】溴他立星
【化学表述】4-(2-bromoacrylamido)-N'''-(2-guanidinoethyl)-1,1',1",1'''-tetramethyl-N,4':N',4":N",4'''-quarter[pyrrole-2-carboxamide]
【CA 登记号】[203258-60-0]
【分 子 式】C30H35BrN12O5
【结 构 式】

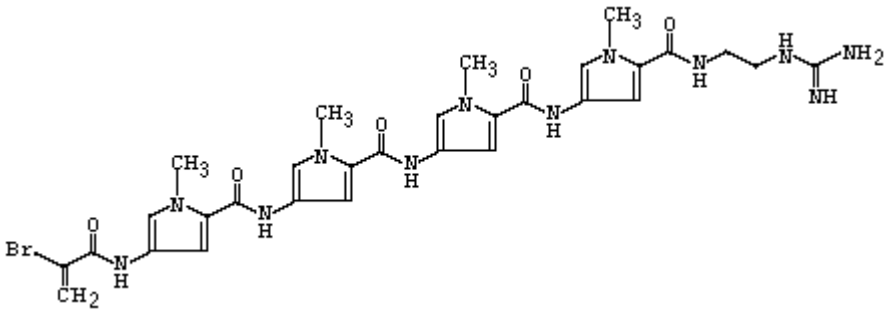

【品种类别】抗肿瘤药>
【附件编号】　262512

【英文 INN】gadomelitol
【别　　名】
【名称来源】pINN-085,2001　rINN-047,2002
【中文 CADN】钆美利醇(GB4)
【建议 CADN】
【化学表述】hydrogen
[2,2',2",2'''-[1,4,7,10-tetraazacyclododecane-1,4,7,10-triyl]tetrakis[5-[[2-[[4-[[4-[[2-[[3,5-bis[bis[(2S,3R,4R,5R)-2,3,4,5,6-pentahydroxyhexyl-2,4,6-tribromo]carbamoyl]phenyl]amino]-2-oxoethyl]carbamoyl]phenyl]carbamoyl]phenyl]amino]-2-oxoethyl]amino]-5-oxopentanoato](4-)]gadolinate(1-)
【CA 登记号】[308814-41-7]
【分 子 式】C228H313Br12GdN32O116
【结 构 式】

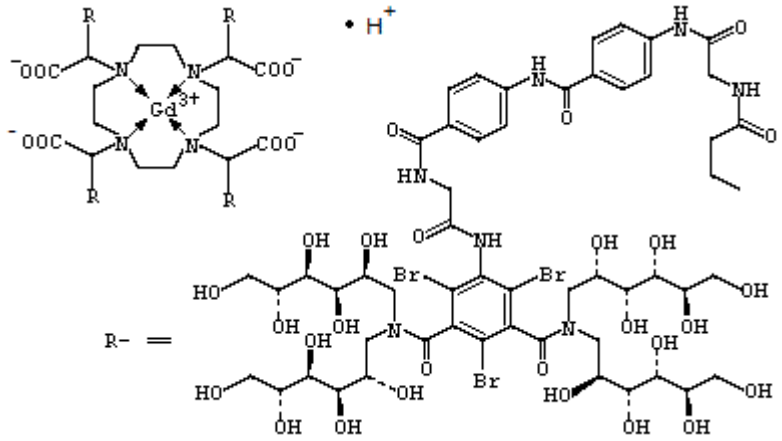

【品种类别】诊断用药>钆衍生物

【英文 INN】lonafarnib

【别　　名】SCH 66336, Sarasar

【名称来源】pINN-086,2002　rINN-048,2002

【中文 CADN】

【建议 CADN】洛那法尼

【化学表述】

(+)-4-[2-[4-[(11R)-3,10-dibromo-8-chloro-6,11-dihydro-5H-benzo[5,6]cyclohepta[1,2-b]pyridin-11-yl]piperidin-1-yl]-2-oxoethyl]piperidine-1-carboxamide

【CA 登记号】[193275-84-2]

【分 子 式】C27H31Br2ClN4O2

【结 构 式】

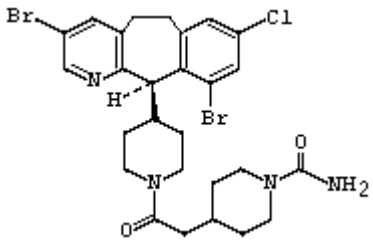

【品种类别】抗肿瘤药>法呢基转移酶抑制剂类

【附件编号】　254680

【英文 INN】olcegepant

【别　　名】BIBN-4096BS

【名称来源】pINN-086,2002　rINN-048,2002

【中文 CADN】

【建议 CADN】奥塞戈潘

【化学表述】

N-[(1R)-2-[[(1S)-5-amino-1-[[4-(pyridin-4-yl)piperazin-1-yl]carbonyl]pentyl]amino]-1-(3,5-dibromo-4-hydroxybenzyl)-2-oxoethyl]-4-(2-oxo-1,4-dihydroquinazolin-3(2H)-yl)piperidine-1-carboxamide

【CA 登记号】[204697-65-4]

【分 子 式】C38H47Br2N9O5

【结 构 式】

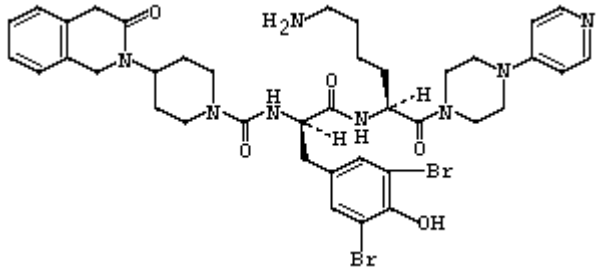

【品种类别】抗偏头痛药>降钙素基因相关肽受体拮抗剂

【附件编号】 285741

【英文 INN】ertiprotafib

【别 名】PTP-112

【名称来源】pINN-087,2002 rINN-049,2003

【中文 CADN】*

【建议 CADN】厄替洛他非

【化学表述】(2R)-2-[4-(9-bromo-2,3-dimethylnaphtho[2,3-b]thiophen-4-yl)-2,6-dimethylphenoxy]-3-phenylpropanoic acid

【CA 登记号】[251303-04-5]

【分 子 式】C31H27BrO3S

【结 构 式】

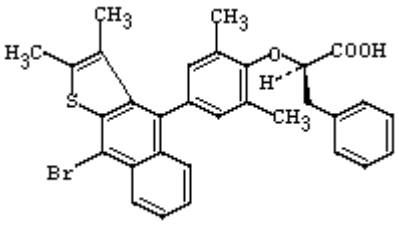

【品种类别】代谢系统>抗糖尿病药>蛋白酪氨酸磷酸酶 β 抑制剂

【英文 INN】perflubrodec

【别 名】Component of AF0144，Component of Oxygent

【名称来源】pINN-087,2002 rINN-049,2003

【中文 CADN】全氟溴癸烷(GB4)

【建议 CADN】

【化学表述】1-bromohenicosafluorodecane

【CA 登记号】[307-43-7]

【分 子 式】C10BrF21

【结 构 式】

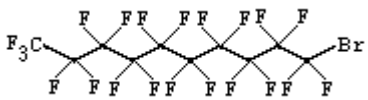

【品种类别】血液系统>携氧药

【英文 INN】etravirine

【别 名】TMC- 125, R-165335

【名称来源】pINN-088,2003　rINN-050,2003

【中文 CADN】

【建议 CADN】依曲韦林

【化学表述】4-[6-amino-5-bromo-2-(4-cyanoanilino)pyrimidin-4-yloxy]-3,5-dimethylbenzonitrile

【CA 登记号】[269055-15-4]

【分　子　式】C20H15BrN6O

【结　构　式】

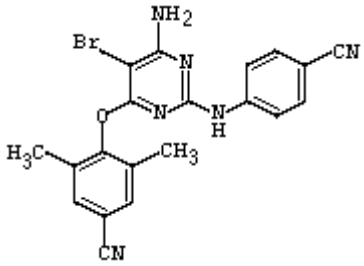

【品种类别】抗感染药>抗病毒药>嘧啶及咪唑衍生物>非核苷逆转录酶抑制剂

【附件编号】　290137

【英文　INN】ibrolipim

【别　　名】NO-1886; OPF 009

【名称来源】pINN-088,2003　rINN-050,2003

【中文 CADN】

【建议 CADN】艾溴利平

【化学表述】diethyl {4-[(4-bromo-2-cyanophenyl)carbamoyl]benzyl}phosphonate

【CA 登记号】[133208-93-2]

【分　子　式】C19H20BrN2O4P

【结　构　式】

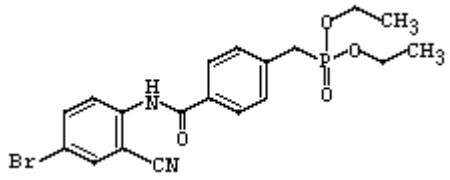

【品种类别】心血管系统>抗动脉粥样硬化药

【英文　INN】lomeguatrib

【别　　名】

【名称来源】pINN-089,2003　rINN-051,2004

【中文 CADN】

【建议 CADN】洛美呱曲

【化学表述】6-(4-bromothenyloxy)-7H-purin-2-amine

【CA 登记号】[192441-08-0]

【分　子　式】C10H8BrN5OS

【结　构　式】

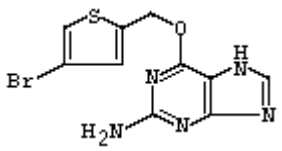

【品种类别】烷基鸟嘌呤 DNA 烷基转移酶抑制剂

【英文 INN】dasantafil

【别　　名】SCH 446132

【名称来源】pINN-091,2004　rINN-053,2005

【中文 CADN】达生他非(GB4)

【建议 CADN】

【化学表述】

7-(3-bromo-4-methoxyphenylmethyl)-1-ethyl-8-{[(1R,2R)-2-hydroxycyclopentyl]amino}-3-(2-hydroxyethyl)-3,7-dihydro-1H-purine-2,6-dione

【CA 登记号】[569351-91-3]

【分 子 式】C22H28BrN5O5

【结 构 式】

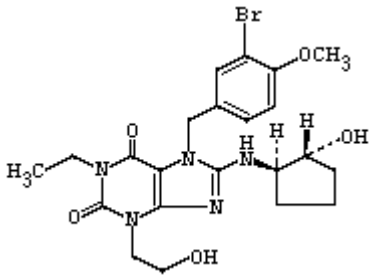

【品种类别】生殖泌尿系统>勃起机能障碍用药>血管扩张药类>PDE5 抑制剂

【英文 INN】ranirestat

【别　　名】AS-3201, SX-3201

【名称来源】pINN-091,2004　rINN-053,2005

【中文 CADN】雷尼司他(GB4)

【建议 CADN】

【化学表述】(3R)-2'-(4-bromo-2-fluorobenzyl)spiro[pyrrolidine-3,4'(1'H)-pyrrolo[1,2-a]pyrazine]-1',2,3',5(2'H)-tetrone

【CA 登记号】[147254-64-6]

【分 子 式】C17H11BrFN3O4

【结 构 式】

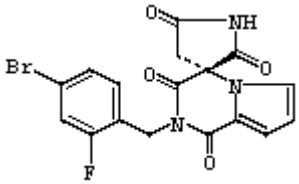

【品种类别】代谢系统>抗糖尿病药>醛糖还原酶抑制剂

【附件编号】　199625

【英文 INN】vandetanib

【别　　名】AZD-6474，ZD-6474

【名称来源】pINN-091,2004　rINN-053,2005

【中文 CADN】凡德他尼(GB4)

【建议 CADN】

【化学表述】N-(4-bromo-2-fluorophenyl)-6-methoxy-7-[(1-methylpiperidin-4-yl)methoxy]quinazolin-4-amine

【CA 登记号】[338992-00-0]

【分 子 式】C22H24BrFN4O2

【结 构 式】

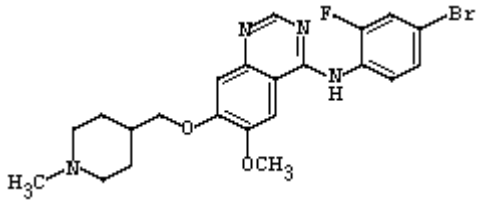

【品种类别】抗肿瘤药>血管生成抑制剂类

【附件编号】　304792

【英文 INN】ancriviroc

【别　　名】SCH351125

【名称来源】pINN-092,2004　rINN-054,2005

【中文 CADN】

【建议 CADN】安利韦洛

【化学表述】3-({4-[(Z)-(4-bromophenyl)(ethoxyimino)methyl]-4'-methyl-[1,4'-bipiperidin]-1'-yl}carbonyl)-2,4-dimethylpyridine, 1-oxide

【CA 登记号】[370893-06-4]

【分 子 式】C28H37BrN4O3

【结 构 式】

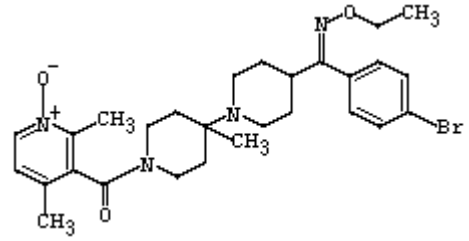

【品种类别】抗感染药>抗病毒药>CC 趋化因子主受体 5 拮抗剂

【英文 INN】surinabant

【别　　名】

【名称来源】pINN-093,2005　rINN-055,2006

【中文 CADN】

【建议 CADN】舒利纳班

【化学表述】5-(4-bromophenyl)-1-(2,4-dichlorophenyl)-4-ethyl-N-(piperidin-1-yl)-1H-pyrazole-3-carboxamide

【CA 登记号】[288104-79-0]

【分 子 式】C23H23BrCl2N4O

【结 构 式】

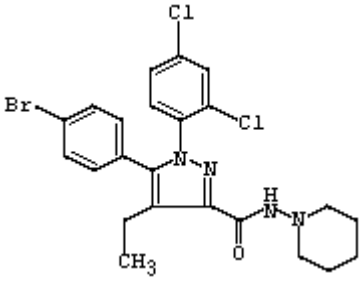

【品种类别】消化系统>减肥药>大麻素受体拮抗剂

【英文 INN】parogrelil

【别　　名】

【名称来源】pINN-094,2005　rINN-056,2006

【中文 CADN】

【建议 CADN】帕洛格雷

【化学表述】4-bromo-6-[3-(4-chlorophenyl)propoxy]-5-[(pyridin-3-ylmethyl)amino]pyridazin-3(2H)-one

【CA 登记号】[139145-27-0]

【分 子 式】C19H18BrClN4O2

【结 构 式】

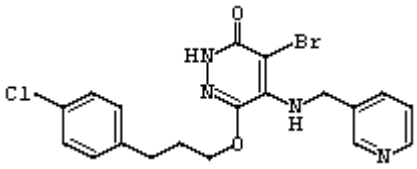

【品种类别】血液系统>抗凝血及溶栓药>血小板凝集抑制剂

【英文 INN】debropol

【别　　名】

【名称来源】pINN-065,1991

【中文 CADN】溴硝丙醇

【建议 CADN】

【化学表述】(±)-2-bromo-2-nitro-1-propanol

【CA 登记号】[24403-04-1]

【分 子 式】C3H6BrNO3

【结 构 式】

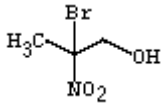

【品种类别】防腐药

【英文 INN】tilbroquinol

【别　　名】

【名称来源】pINN-045,1981

【中文 CADN】甲溴羟喹(GB4)

【建议 CADN】

【化学表述】8-Quinolinol, 7-bromo-5-methyl-

【CA 登记号】[7175-09-9]

【分 子 式】C10H8BrNO

【结 构 式】

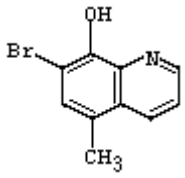

【品种类别】抗原虫药>抗阿米巴及其它原虫病药>羟基喹啉衍生物

【英文 INN】fubrogonium iodide

【别　　名】Fubromegan

【名称来源】pINN-018,1967

【中文 CADN】呋波碘铵(GB4)

【建议 CADN】

【化学表述】1-Butanaminium, 3-[[(5-bromo-2-furanyl)carbonyl]oxy]-N,N-diethyl-N-methyl-, iodide

【CA 登记号】[3690-58-2]

【分 子 式】C14H28BrINO3

【结 构 式】

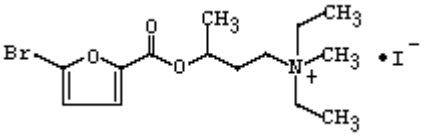

【品种类别】抗胆碱药

【英文 INN】fursalan

【别　　名】

【名称来源】pINN-018,1967

【中文 CADN】呋沙仑(GB4)

【建议 CADN】

【化学表述】Benzamide, 3,5-dibromo-2-hydroxy-N-[(tetrahydro-2-furanyl)methyl]-

【CA 登记号】[15686-77-8]

【分 子 式】C12H12Br2NO2

【结 构 式】

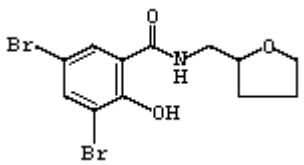

【品种类别】抗感染药>消毒防腐药>salan 类

【英文 INN】metabromsalan

【别　　名】

【名称来源】pINN-016,1966

【中文 CADN】美溴沙仑(GB4)

【建议 CADN】

【化学表述】3,5-dibromosalicylanilide

【CA 登记号】[2577-72-2]

【分 子 式】C13H9Br2NO2

【结 构 式】

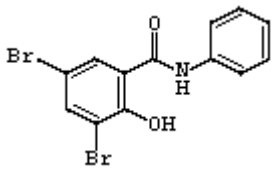

【品种类别】抗感染药>消毒防腐药>salan 类

【英文 INN】pipobroman

【别　　名】

【名称来源】pINN-016,1966

【中文 CADN】哌泊溴烷(97)

【建议 CADN】

【化学表述】Piperazine, 1,4-bis(3-bromopropionyl)-

【CA 登记号】[54-91-1]

【分 子 式】C10H16Br2N2O2

【结 构 式】

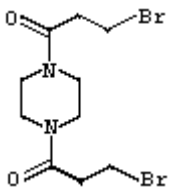

【品种类别】抗肿瘤药>烷基化剂>其它

【英文 INN】pyritidium bromide

【别　　名】

【名称来源】pINN-016,1966

【中文 CADN】匹立溴铵(GB4)

【建议 CADN】

【化学表述】3-amino-8-[(2-dimethylamino-6-methyl-4-pyrimidinyl)amino]-6-(p-aminophenyl)-5-methylphenanthridinium bromide-1'-metho-bromide

【CA 登记号】[14222-46-9]

【分 子 式】C25H27Br2N7

【结 构 式】

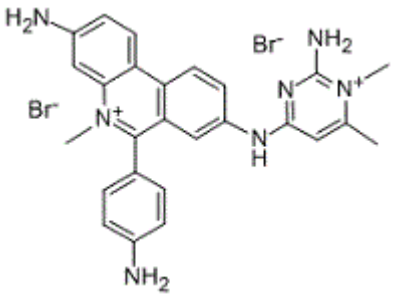

【品种类别】抗原虫药>抗黑热病和锥虫病药>其它

【英文 INN】dibromsalan
【别　　名】
【名称来源】pINN-014,1964
【中文 CADN】二溴沙仑(GB4)
【建议 CADN】
【化学表述】3-bromo-6-hydroxybenz-p-bromanilide
【CA 登记号】[87-12-7]
【分 子 式】C13H9BrNO2
【结 构 式】

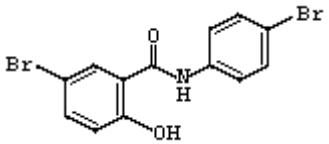

【品种类别】抗感染药>消毒防腐药>salan 类

【英文 INN】tonzonium bromide
【别　　名】Thonzonium bromide
【名称来源】pINN-014,1964
【中文 CADN】通佐溴铵(GB4)
【建议 CADN】
【化学表述】hexadecyl[2-(p-methoxybenzyl)-2-pyrimidinylamino]ethyl dimethyl ammonium bromide
【CA 登记号】[553-08-2]
【分 子 式】C31H55BrN4O
【结 构 式】

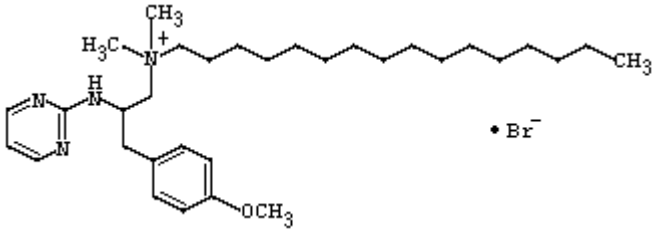

【品种类别】抗感染药>消毒防腐药>季铵盐类

【英文 INN】tribromsalan
【别　　名】

【名称来源】pINN-014,1964

【中文 CADN】三溴沙仑(GB4)

【建议 CADN】

【化学表述】Benzamide, 3,5-dibromo-N-(4-bromophenyl)-2-hydroxy-

【CA 登记号】[87-10-5]

【分 子 式】C13H8Br3NO2

【结 构 式】

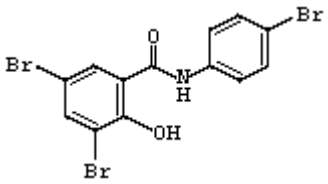

【品种类别】抗感染药>消毒防腐药>salan 类

【英文 INN】broxaldine

【别　　名】

【名称来源】pINN-012,1962

【中文 CADN】溴沙定(97)

【建议 CADN】

【化学表述】8-Quinolinol, 5,7-dibromo-2-methyl-, benzoate (ester)

【CA 登记号】[3684-46-6]

【分 子 式】C17H11Br2NO2

【结 构 式】

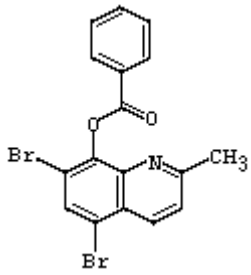

【品种类别】抗感染药>消毒防腐药>喹啉衍生物

【英文 INN】neostigmine bromide

【别　　名】

【名称来源】pINN-004,1956

【中文 CADN】溴新斯的明(97)

【建议 CADN】

【化学表述】N-(3-Dimethylcarbamoyloxyphenyl)-N,N,N-trimethylammonium monobromide

【CA 登记号】[114-80-7]

【分 子 式】C12H19BrN2O2

【结 构 式】

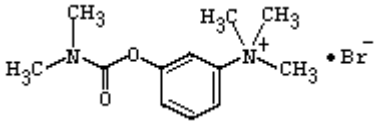

【品种类别】神经系统>抗痴呆药>乙酰胆碱酯酶抑制剂

【英文 INN】hydroxyamphetaminium bromide

【别　　名】

【名称来源】pINN-001,1953

【中文 CADN】氢溴酸羟苯丙胺(97)

【建议 CADN】

【化学表述】1-p-hydroxyphenyl-2-aminopropane hydrobromide

【CA 登记号】[306-21-8]

【分 子 式】C9H13NO.HBr

【结 构 式】

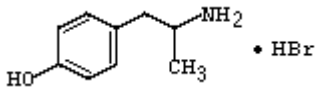

【品种类别】心血管系统>抗低血压药>α-肾上腺素能激动剂

【英文 INN】methanthelinium bromide

【别　　名】

【名称来源】pINN-001,1953

【中文 CADN】溴甲胺太林(97)

【建议 CADN】

【化学表述】Ethanaminium, N,N-diethyl-N-methyl-2-[(9H-xathen-9-ylcarbonyl)oxy]-, bromide

【CA 登记号】[53-46-3]

【分 子 式】C21H26BrNO3

【结 构 式】

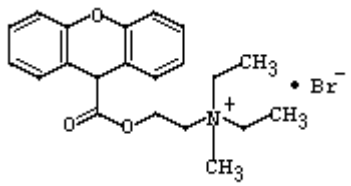

【品种类别】抗胆碱药>季铵盐类

【英文 INN】aclidinium bromide

【别　　名】

【名称来源】pINN-095,2006　rINN-057,2007

【中文 CADN】

【建议 CADN】阿利溴铵

【化学表述】(3R)-3-[(hydroxy)di(thiophen-2-yl)acetyloxy]-1-(3-phenoxypropyl)-1λ^5-azabicyclo[2.2.2]octan-1-ylium bromide

【CA 登记号】[320345-99-1]

【分 子 式】C26H30BrNO4S2

【结 构 式】

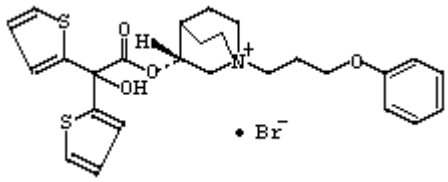

【品种类别】拟胆碱药>毒蕈碱受体激动剂/拮抗剂

【英文 INN】methylnaltrexone bromide

【别　　名】MRZ- 2663BR,　MOA-728,　MNTX-302

【名称来源】pINN-096,2006　rINN-058,2007

【中文 CADN】*

【建议 CADN】甲纳曲酮溴铵

【化学表述】(17R)-17-(cyclopropylmethyl)-4,5-epoxy-3,14-dihydroxy-17-methyl-6-oxomorphinanium bromide

【CA 登记号】[916055-92-0]

【分 子 式】C21H26BrNO4

【结 构 式】

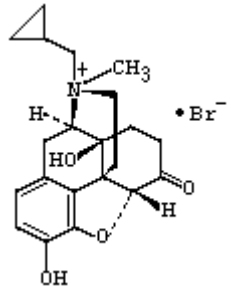

【品种类别】神经系统>镇痛药>阿片受体拮抗/激动剂>去甲吗啡类

【附件编号】　284766

【英文 INN】azoximer bromide

【别　　名】

【名称来源】pINN-097,2007　rINN-059,2008

【中文 CADN】*

【建议 CADN】阿佐西姆溴铵

【化学表述】poly{[1-(carboxymethyl)piperazin-1-ium-1,4-diyl bromide]ethylene-co-[(piperazin-1,4-diyl 1-oxide)ethylene]}

【CA 登记号】[892497-01-7]

【分 子 式】[[C8H15BrN2O2]x[C6H12N2O]y]n

【结 构 式】

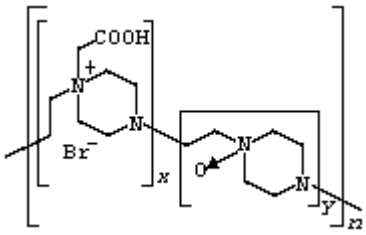

【品种类别】免疫调节剂

【英文 INN】intiquinatine

【别　　名】tiliquinatine

【名称来源】pINN-097,2007　rINN-061,2009

【中文 CADN】*

【建议 CADN】英替喹那汀

【化学表述】(2R)-2-{4-[(7-bromoquinolin-2-yl)oxy]phenoxy}propanoic acid

【CA 登记号】[445041-75-8]

【分 子 式】C18H14BrNO4

【结 构 式】

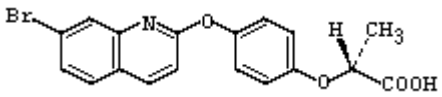

【品种类别】抗肿瘤药>喹啉衍生物

【英文 INN】bederocin

【别　　名】

【名称来源】pINN-099,2008　rINN-061,2009

【中文 CADN】*

【建议 CADN】贝德罗辛

【化学表述】2-{[3-({[4-bromo-5-(1-fluoroethenyl)-3-methylthiophen-2-yl]methyl}amino)propyl]amino}quinolin-4(1H)-one

【CA 登记号】[757942-43-1]

【分 子 式】C20H21BrFN3OS

【结 构 式】

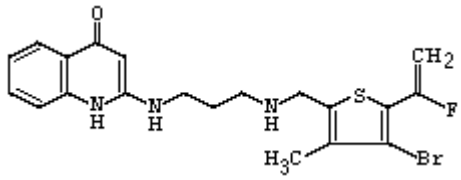

【品种类别】抗感染药>抗菌药

【英文 INN】darotropium bromide

【别　　名】

【名称来源】pINN-099,2008　rINN-061,2009

【中文 CADN】*

【建议 CADN】达托溴铵

【化学表述】(1R,3R,5S)-3-(2-cyano-2,2-diphenylethyl)-8,8-dimethyl-8-azabicyclo[3.2.1]octan-8-ium bromide

【CA 登记号】[850607-58-8]

【分 子 式】C24H29BrN2

【结 构 式】

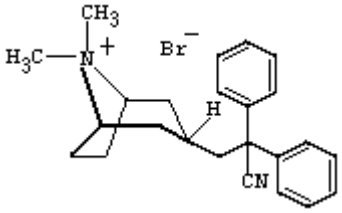

【品种类别】抗胆碱能药

【英文 INN】eprotirome

【别　　名】

【名称来源】pINN-099,2008　rINN-061,2009

【中文 CADN】*

【建议 CADN】依普替罗

【化学表述】3-({3,5-dibromo-4-[4-hydroxy-3-(propan-2-yl)phenoxy]phenyl}amino)-3-oxopropanoic acid

【CA 登记号】[355129-15-6]

【分 子 式】C18H17Br2NO5

【结 构 式】

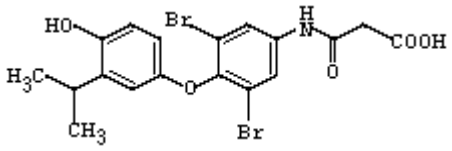

【品种类别】心血管系统>降血脂药>拟甲状腺素衍生物

【英文 INN】macitentan

【别　　名】

【名称来源】pINN-099,2008　rINN-061,2009

【中文 CADN】*

【建议 CADN】玛西腾坦

【化学表述】N-[5-(4-bromophenyl)-6-{2-[(5-bromopyrimidin-2-yl)oxy]ethoxy}pyrimidin-4-yl]-N'-propylsulfuric diamide

【CA 登记号】[441798-33-0]

【分 子 式】C19H20Br2N6O4S

【结 构 式】

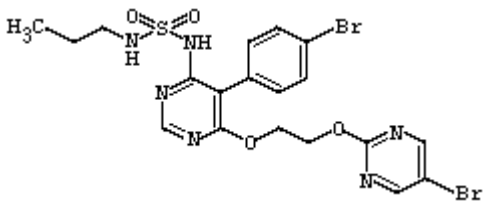

【品种类别】心血管系统>血管扩张药>内皮素受体拮抗剂

【英文 INN】tasisulam

【别　　名】

【名称来源】pINN-099,2008　rINN-061,2009

【中文 CADN】*

【建议 CADN】他西舒兰

【化学表述】N-(5-bromothiophene-2-sulfonyl)-2,4-dichlorobenzamide

【CA 登记号】[519055-62-0]

【分 子 式】C11H6BrCl2NO3S2

【结 构 式】

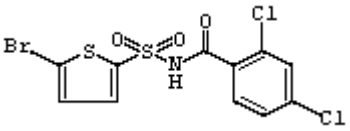

【品种类别】抗肿瘤药>细胞凋亡诱导剂>磺酰胺衍生物

【英文 INN】selumetinib

【别　　名】ARRY-142886

【名称来源】pINN-100,2008　rINN-062,2009

【中文 CADN】

【建议 CADN】舍美替尼

【化学表述】5-[(4-bromo-2-chlorophenyl)amino]-4-fluoro-N-(2-hydroxyethoxy)-1-methyl-1H-benzimidazole-6-carboxamide

【CA 登记号】[606143-52-6]

【分 子 式】C17H15BrClFN4O3

【结 构 式】

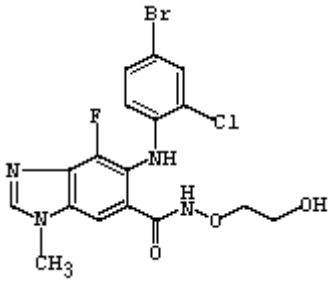

【品种类别】抗肿瘤药>MEK 酪氨酸激酶抑制剂

【附件编号】　355417

【英文 INN】albitiazolium bromide

【别　　名】

【名称来源】pINN-101,2009　rINN-063,2010

【中文 CADN】

【建议 CADN】阿比噻唑溴铵

【化学表述】3,3'-(dodecan-1,12-diyl)bis[5-(2-hydroxyethyl)-4-methyl-1,3-thiazol-3-ium] dibromide

【CA 登记号】[321915-72-4]

【分 子 式】C24H42Br2N2O2S2

【结 构 式】

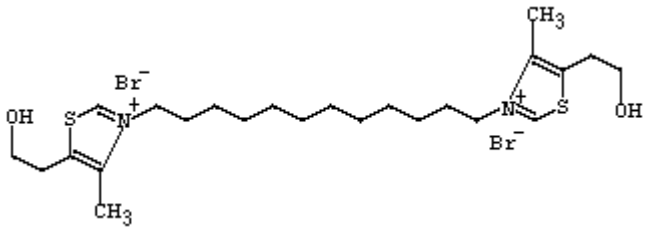

【品种类别】抗原虫药>抗疟药

【英文 INN】nelotanserin

【别　　名】

【名称来源】pINN-101,2009　rINN-063,2010

【中文 CADN】

【建议 CADN】奈罗色林

【化学表述】1-[3-(4-bromo-1-methyl-1H-pyrazol-5-yl)-4-methoxyphenyl]-3-(2,4-difluorophenyl)urea

【CA 登记号】[839713-36-9]

【分 子 式】C18H15BrF2N4O2

【结 构 式】

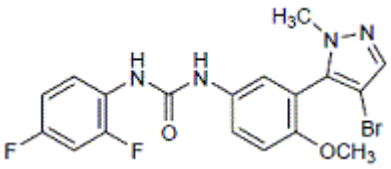

【品种类别】心血管系统>抗高血压药>羟色胺 5-HT2 受体拮抗剂

【英文 INN】zaurategrast

【别　　名】

【名称来源】pINN-101,2009　rINN-063,2010

【中文 CADN】

【建议 CADN】扎泰司特

【化学表述】(2S)-2-[(2-bromo-3-oxospiro[3.5]non-1-en-1-yl)amino]-3-{4-[(2,7-naphthyridin-1-yl)amino]phenyl}propanoic acid

【CA 登记号】[455264-31-0]

【分 子 式】C26H25BrN4O3

【结 构 式】

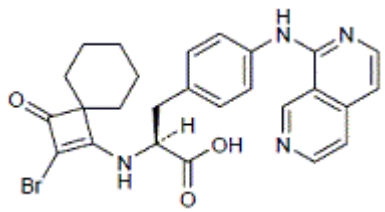

【品种类别】非甾体抗炎药>整联蛋白拮抗剂

【英文 INN】zibrofusidic acid

【别　　名】

【名称来源】pINN-102,2009　rINN-064,2010

【中文 CADN】

【建议 CADN】齐洛夫西地酸

【化学表述】(17Z)-16β-(acetyloxy)-24-bromo-3α,11α-dihydroxy-29-norprotosta-17(20),24-dien-21-oic acid

【CA 登记号】[827603-95-2]

【分 子 式】C31H47BrO6

【结 构 式】

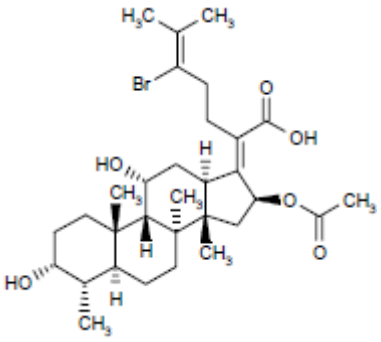

【品种类别】抗感染药>抗生素>

【英文 INN】remimazolam

【别　　名】CNS-7056，ONO-2745

【名称来源】pINN-102,2009　rINN-064,2010

【中文 CADN】

【建议 CADN】瑞米唑仑

【化学表述】methyl 3-{(4S)-8-bromo-1-methyl-6-(pyridin-2-yl)-4H-imidazo[1,2-a][1,4]benzodiazepin-4-yl}propanoate

【CA 登记号】[308242-62-8]

【分 子 式】C21H19BrN4O2

【结 构 式】

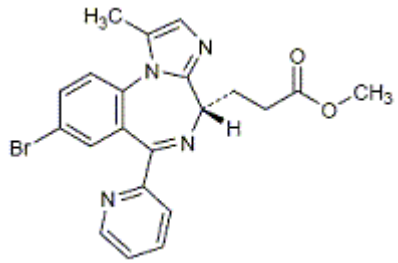

【品种类别】神经系统>麻醉药>苯并二氮杂卓衍生物

【附件编号】　297752

【英文 INN】bedaquiline

【别　　名】R-207910，TMC-207

【名称来源】pINN-103,2010　rINN-065,2011

【中文 CADN】

【建议 CADN】贝达喹啉

【化学表述】(1R,2S)-1-(6-bromo-2-methoxyquinolin-3-yl)-4-(dimethylamino)-2-(naphthalen-1-yl)-1-phenylbutan-2-ol

【CA 登记号】[843663-66-1]

【分 子 式】C32H31BrN2O2

【结 构 式】

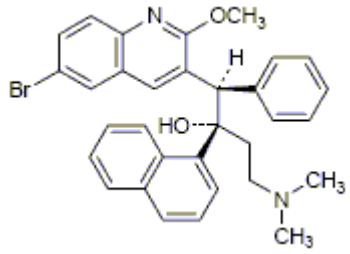

【品种类别】抗感染药>抗菌药>

【附件编号】 386239

【英文 INN】umifenovir

【别 名】

【名称来源】pINN-103,2010 rINN-065,2011

【中文 CADN】

【建议 CADN】乌芬诺韦

【化学表述】ethyl 6-bromo-4-[(dimethylamino)methyl]-5-hydroxy-1-methyl- 2-[(phenylsulfanyl)methyl]-1H-indole-3-carboxylate

【CA 登记号】[131707-25-0]

【分 子 式】C22H25BrN2O3S

【结 构 式】

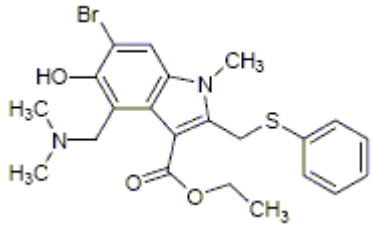

【品种类别】抗感染药>抗病毒药>

【英文 INN】Crolibulin

【别 名】

【名称来源】pINN-104,2010 rINN-066,2011

【中文 CADN】

【建议 CADN】克洛布林

【化学表述】(4R)-2,7,8-triamino-4-(3-bromo-4,5-dimethoxyphenyl)-4H-chromene-3-carbonitrile

【CA 登记号】[1000852-17-4]

【分 子 式】C18H17BrN4O3

【结 构 式】

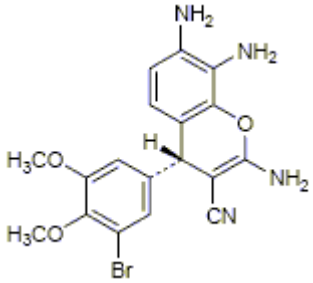

【品种类别】抗肿瘤药>抗有丝分裂药>γ-微管蛋白聚合抑制剂

【英文 INN】lesinurad

【别　　名】

【名称来源】pINN-105,2011　rINN-067,2012

【中文 CADN】

【建议 CADN】来西努雷

【化学表述】2-{[5-bromo-4-(4-cyclopropylnaphthalen-1-yl)-4H-1,2,4-triazol-3-yl]sulfanyl}acetic acid

【CA 登记号】[878672-00-5]

【分 子 式】C17H14BrN3O2S

【结 构 式】

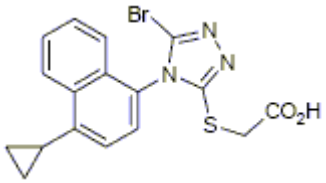

【品种类别】抗通风药>尿酸转运蛋白抑制剂

【英文 INN】sepantronium bromide

【别　　名】YM-155

【名称来源】pINN-105,2011　rINN-067,2012

【中文 CADN】

【建议 CADN】塞托溴铵

【化学表述】1-(2-methoxyethyl)-2-methyl-4,9-dioxo-3-[(pyrazin-2-yl)methyl]-4,9-dihydro-1H-naphtho[2,3-d]imidazolium bromide

【CA 登记号】[781661-94-7]

【分 子 式】C20H19BrN4O3

【结 构 式】

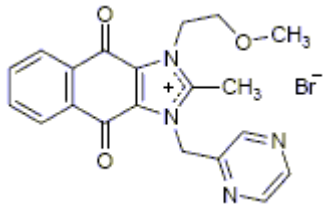

【品种类别】抗肿瘤药>细胞毒素类抗生素>蒽醌衍生物类

【附件编号】　413279

【英文 INN】faldaprevir

【别　　名】BI-201335

【名称来源】pINN-106,2011　rINN-068,2012

【中文 CADN】

【建议 CADN】法达瑞韦

【化学表述】

(1R,2S)-1-{[(2S,4R)-4-[{8-bromo-7-methoxy-2-[2-(2-methylpropanamido)-1,3-thiazol-4-yl]quinolin-4-yl}oxy]-1-[(2S)-2-{[(cyclopentyloxy)carbonyl]amino}-3,3-dimethylbutanoyl]pyrrolidine-2-carboxamido]-2-ethenylcyclopropane-1-carboxylic acid

【CA 登记号】[801283-95-4]

【分 子 式】C40H49BrN6O9S

【结 构 式】

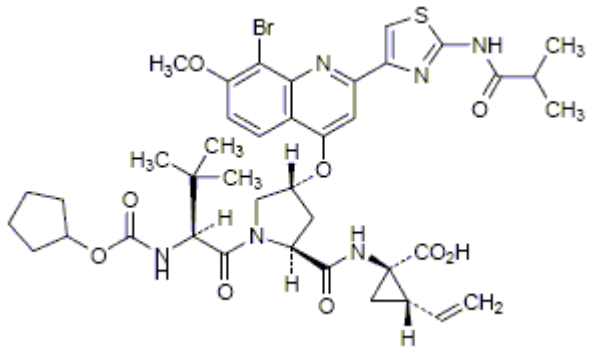

【品种类别】抗感染药>抗病毒药>丙型肝炎病毒蛋白酶抑制剂

【附件编号】　644871

【英文 INN】umeclidinium bromide

【别　　名】GSK-573719

【名称来源】pINN-106,2011　rINN-068,2012

【中文 CADN】

【建议 CADN】乌美利溴铵

【化学表述】1-{2-[(benzyl)oxy]ethyl}4-[hydroxydi(phenyl)methyl]-1-azabicyclo[2.2.2]octan-1-ium bromide

【CA 登记号】[869113-09-7]

【分 子 式】C29H34BrNO2

【结 构 式】

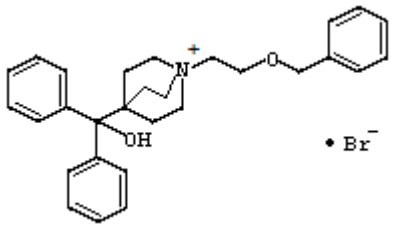

【品种类别】拟胆碱药>毒蕈碱受体激动剂/拮抗剂

【附件编号】　447223

【英文 INN】rabusertib

【别　　名】

【名称来源】pINN-107,2012　rINN-069,2013

【中文 CADN】

【建议 CADN】雷布舍替

【化学表述】1-(2-chloro-3-fluorophenyl)-3-[4-chloro-2-hydroxy-3-(piperazine-1-sulfonyl)phenyl]urea

【CA 登记号】[911222-45-2]

【分 子 式】C18H22BrN5O3

【结 构 式】

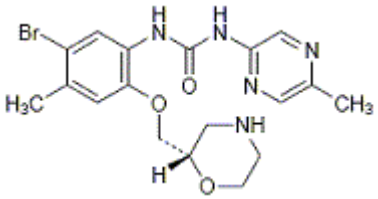

【品种类别】抗肿瘤药>丝氨酸/苏氨酸激酶抑制剂

【英文 INN】deleobuvir

【别　　名】

【名称来源】pINN-108,2012　rINN-070,2013

【中文 CADN】

【建议 CADN】迪来布韦

【化学表述】

(2E)-3-(2-{1-[2-(5-bromopyrimidin-2-yl)-3-cyclopentyl-1-methyl-1H-indole-6-carboxamido]cyclobutyl}-1-methyl-1H-benzimidazol-6-yl)prop-2-enoic acid

【CA 登记号】[863884-77-9]

【分 子 式】C34H33BrN6O3

【结 构 式】

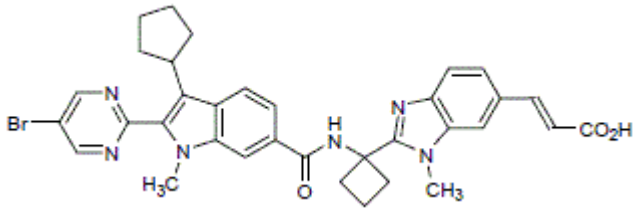

【品种类别】抗感染药>抗病毒药>RNA 聚合酶(NS5B)抑制剂

【英文 INN】firtecan peglumer

【别　　名】

【名称来源】pINN-108,2012　rINN-070,2013

【中文 CADN】

【建议 CADN】培谷姆-菲尔替康

【化学表述】-{3-[(α-N-acetylpoly-L-glutamyl)amino]propyl}-ω-methoxypoly(oxyethan-1,2-diyl) where the free γ-carboxyl groups are partially esterified by

(4S)-4,11-diethyl-4-hydroxy-3,14-dioxo-3,4,12,14-tetrahydro-1H-pyrano[3',4':6,7]indolizino[1,2-b]quinolin-9-yl, partially converted to an amide with (propan-2-yl)[(propan-2-yl)carbamoyl]amino and partially unchanged

【CA 登记号】[1204768-03-5]

【分 子 式】C6H13NO2 [C5H6NO2]a [C2H4O]n

(C22H19N2O5)x (C7H15N2O)y (HO)z

a = x + y + z

【结 构 式】

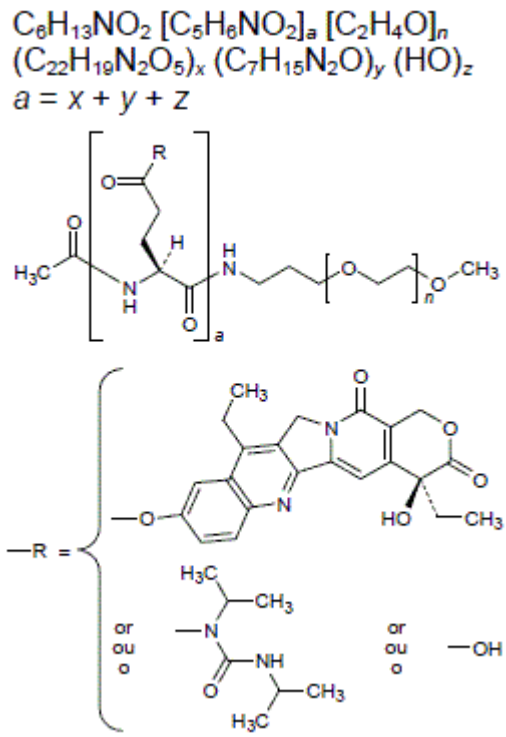

【品种类别】抗肿瘤药>拓扑异构酶抑制剂>喜树碱衍生物类

【英文 INN】binimetinib

【别　　名】ARRY-162，ARRY-438162，MEK-162

【名称来源】pINN-109,2013　rINN-071,2014

【中文 CADN】

【建议 CADN】比美替尼

【化学表述】5-[(4-bromo-2-fluorophenyl)amino]-4-fluoro-N-(2-hydroxyethoxy)-1-methyl-1H-benzimidazole-6-carboxamide

【CA 登记号】[606143-89-9]

【分 子 式】C17H15BrF2N4O3

【结 构 式】

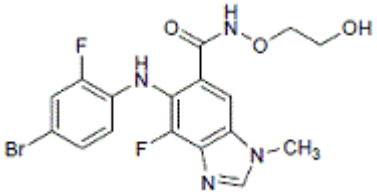

【品种类别】抗肿瘤药>MEK 酪氨酸激酶抑制剂类

【附件编号】　349927

【英文 INN】remeglurant

【别　　名】

【名称来源】pINN-109,2013　rINN-071,2014

【中文 CADN】

【建议 CADN】瑞美谷兰

【化学表述】(6-bromopyrazolo[1,5-a]pyrimidin-2-yl)[(1R)-1-methyl-3,4-dihydroisoquinolin-2(1H)-yl]methanone

【CA 登记号】[1309783-00-3]

【分 子 式】C17H15BrN4O

【结 构 式】

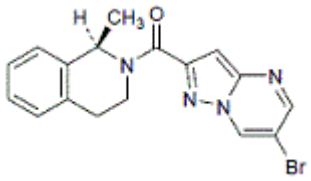

【品种类别】神经系统>代谢型谷氨酸受体拮抗剂/负变构调节剂

【英文 INN】evofosfamide

【别　　名】HAP-302，TH-302

【名称来源】pINN-111,2014　rINN-073,2015

【中文 CADN】

【建议 CADN】依磷酰胺

【化学表述】(1-methyl-2-nitro-1H-imidazol-5-yl)methyl N,N'-bis(2-bromoethyl)phosphorodiamidate

【CA 登记号】[918633-87-1]

【分 子 式】C9H16Br2N5O4P

【结 构 式】

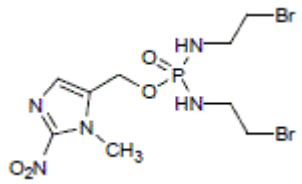

【品种类别】抗肿瘤药>烷基化剂>异磷酰胺氮芥衍生物

【附件编号】　442503

【英文 INN】epacadostat

【别　　名】

【名称来源】pINN-114,2015　rINN-076,2016

【中文 CADN】

【建议 CADN】依多司他

【化学表述】(Z)-N-(3-bromo-4-fluorophenyl)-N'-hydroxy-4-{[2-(sulfamoylamino)ethyl]amino}-1,2,5-oxadiazole-3-carboximidamide

【CA 登记号】[1204669-58-8]

【分 子 式】C11H13BrFN7O4S

【结 构 式】

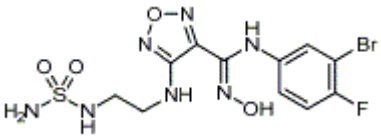

【品种类别】抗肿瘤药>酶抑制剂类>氨肽酶抑制剂

【英文 INN】tarloxotinib bromide

【别　　名】

【名称来源】pINN-114,2015　rINN-076,2016

【中文 CADN】

【建议 CADN】溴化他罗替尼

【化学表述】

(2E)-4-{[4-(3-bromo-4-chloroanilino)pyrido[3,4-d]pyrimidin-6-yl]amino}-N,N-dimethyl-N-[(1-methyl-4-nitro-1H-imidazol-5-yl)methyl]-4-oxobut-2-en-1-aminium bromide

【CA 登记号】[1636180-98-7]

【分 子 式】C24H24Br2ClN9O3

【结 构 式】

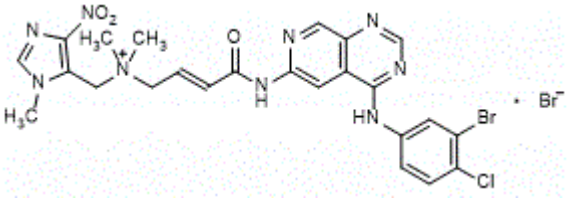

【品种类别】抗肿瘤药>酪氨酸激酶抑制剂

【英文 INN】sofpironium bromide

【别　　名】

【名称来源】pINN-115,2016

【中文 CADN】

【建议 CADN】索吡溴铵

【化学表述】1-ambo-(3R)-3-{[(R)-(cyclopentyl)hydroxy(phenyl)acetyl]oxy}-1-(2-ethoxy-2-oxoethyl)-1-methylpyrrolidinium bromide

【CA 登记号】[1628106-94-4]

【分 子 式】C22H32BrNO5

【结 构 式】

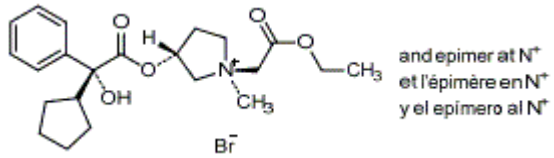

【品种类别】抗胆碱药>季铵盐类

【英文 INN】aprocitentan

【别　　名】

【名称来源】pINN-116,2016

【中文 CADN】

【建议 CADN】阿普洛腾坦

【化学表述】N-[5-(4-bromophenyl)-6-{2-[(5-bromopyrimidin-2-yl)oxy]ethoxy}pyrimidin-4-yl]sulfuric diamide

【CA 登记号】[1103522-45-7]

【分 子 式】C16H14Br2N6O4S

【结 构 式】

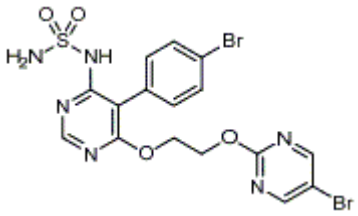

【品种类别】心血管系统>抗高血压药>内皮素受体拮抗剂

【英文 INN】teslexivir

【别　　名】

【名称来源】pINN-116,2016

【中文 CADN】

【建议 CADN】特来昔韦

【化学表述】4-(2-{2-(4-benzylphenyl)-2-[2-methyl-6-(piperidin-1-yl)phenyl]hydrazin-1-yl}-2-oxoethyl)-5-bromo-2-methoxybenzoic acid

【CA 登记号】[1075798-37-6]

【分 子 式】C35H36BrN3O4

【结 构 式】

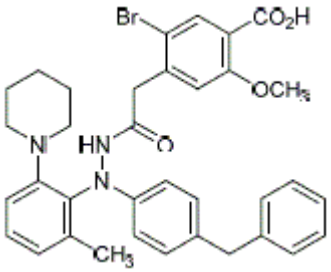

【品种类别】抗感染药>抗病毒药

【英文 INN】elsulfavirine

【别　　名】

【名称来源】pINN-117,2017

【中文 CADN】

【建议 CADN】依磺韦林

【化学表述】N-(4-{2-[4-bromo-3-(3-chloro-5-cyanophenoxy)-2-fluorophenyl]acetamido}-3-chlorobenzenesulfonyl)propanamide

【CA 登记号】[868046-19-9]

【分 子 式】C24H17BrCl2FN3O5S

【结 构 式】

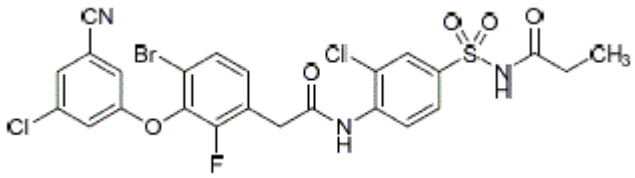

【品种类别】抗感染药>抗病毒药>非核苷逆转录酶抑制剂

【英文 INN】epaminurad

【别　　名】

【名称来源】pINN-118,2018

【中文 CADN】

【建议 CADN】依帕努雷

【化学表述】(3,5-dibromo-4-hydroxyphenyl)(2,3-dihydro-4H-pyrido[4,3-b]-1,4-oxazin-4-yl)methanone

【CA 登记号】[1198153-15-9]

【分 子 式】C14H10Br2N2O3

【结 构 式】

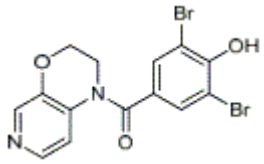

【品种类别】抗通风药>尿酸转运蛋白抑制剂

【英文 INN】danicopan

【别　　名】

【名称来源】pINN-119,2018

【中文 CADN】

【建议 CADN】达尼可泮

【化学表述】

(2S,4R)-1-{[3-acetyl-5-(2-methylpyrimidin-5-yl)-1H-indazol-1-yl]acetyl}-N-(6-bromopyridin-2-yl)-4-fluoropyrrolidine-2-carboxamide

【CA 登记号】[1903768-17-1]

【分 子 式】C26H23BrFN7O3

【结 构 式】

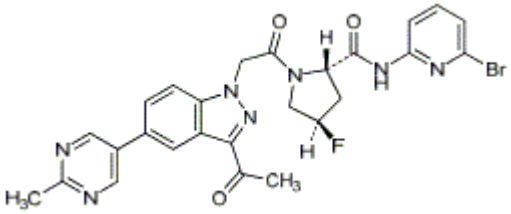

【品种类别】补体因子 D 抑制剂

【英文 INN】masupirdine

【别　　名】

【名称来源】pINN-119,2018

【中文 CADN】

【建议 CADN】玛舒吡啶

【化学表述】1-(2-bromobenzene-1-sulfonyl)-5-methoxy-3-[(4-methylpiperazin-1-yl)methyl]-1H-indole

【CA 登记号】[701205-60-9]

【分 子 式】C21H24BrN3O3S

【结 构 式】

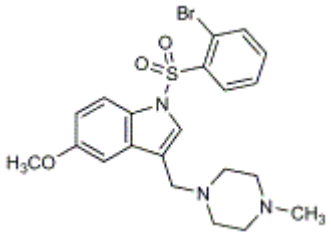

【品种类别】神经系统>抗痴呆症药>5-HT6 受体拮抗剂

【英文 INN】ripretinib

【别　　名】

【名称来源】pINN-119,2018

【中文 CADN】

【建议 CADN】利瑞替尼

【化学表述】N-{4-bromo-5-[1-ethyl-7-(methylamino)-2-oxo-1,2-dihydro-1,6-naphthyridin-3-yl]-2-fluorophenyl}-N'-phenylurea

【CA 登记号】[1442472-39-0]

【分 子 式】C24H21BrFN5O2

【结 构 式】

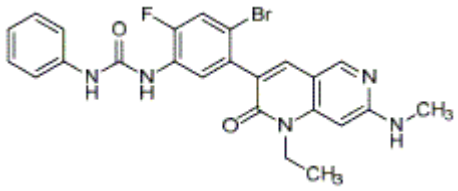

【品种类别】抗肿瘤药>酪氨酸激酶抑制剂

Drugs of the Future 2000, 25(2): 131-136

CCC: 0377-8282/2000

AS-3201

Aldose Reductase Inhibitor

SX-3201

(–)-(*R*)-2-(4-Bromo-2-fluorobenzyl)spiro[1,2,3,4-tetrahydropyrrolo[1,2-*a*]pyrazine-4,3'-pyrrolidine]-1,2',3,5'-tetraone

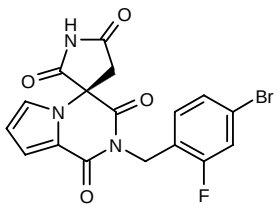

$C_{17}H_{11}BrFN_3O_4$ Mol wt: 420.1929

CAS: 147254-64-6
CAS: 147193-59-7 (as racemate)
CAS: 147254-65-7 (as (+)-enantiomer)

EN: 199625

Synthesis

The synthesis of AS-3201 has been performed according to the method shown in Scheme 1. The alkylation of ethyl 2-(benzyloxycarbonylamino)cyanoacetate (I) with ethyl bromoacetate and anhydrous potassium carbonate in acetone gives diethyl 2-(benzyloxycarbonylamino)-2-cyanosuccinate (II), which is hydrolyzed by means of hydrogen peroxide and sodium carbonate in acetone/water, yielding 3-(benzyloxycarbonylamino)-3-(ethoxycarbonyl)pyrrolidine-2,5-dione (III). Racemic (III) is then resolved by means of crystallization with cinchonidine in ethanol to give the (–)-enantiomer (IV) (>99.5% e.e.). Hydrogenolysis of (IV) over Pd/C in ethanol, followed by treatment with 2,5-dimethoxytetrahydrofuran in acetic acid, affords (–)-3-(ethoxycarbonyl)-3-(pyrrol-1-yl)pyrrolidine-2,5-dione (VI). Treatment of (VI) with trichloroacetyl chloride in ethyl acetate, followed by condensation with 4-bromo-2-fluorobenzylamine in the presence of triethylamine, gives AS-3201 (>99.4% e.e.) (1).

Description

Light yellow solid, m.p. 192-3 °C, $[\alpha]^{28}_{405}$ –33.0° (c 1.0, MeOH).

Introduction

Derangements of glucose metabolism, especially abnormalities in the polyol pathway, under conditions of diabetic hyperglycemia are thought to play an important role in the pathogenesis of diabetic complications, as the incidence of neuropathy, retinopathy, nephropathy and cataract in diabetic patients is directly correlated with the duration and severity of hyperglycemia (2, 3). The polyol pathway involves the enzyme aldose reductase (AR), which reduces glucose to sorbitol, and sorbitol dehydrogenase (SDH), which oxidizes sorbitol to fructose. There is little flux through this pathway at blood glucose levels that are kept within the normal range. At elevated blood glucose levels, however, a significant flux through the polyol pathway is induced in tissues including the nerve, retina, lens and kidney. The intense flux of glucose results in a correspondingly high rate of AR-catalyzed sorbitol production. The intracellular accumulation of sorbitol, an organic osmolyte, causes hypertonicity, together with a decrease in myo-inositol contents or impairment of Na^+/K^+-ATPase activity, which is thought to lead to cell dysfunction and structural damage in these tissues (4). In addition to the sorbitol accumulation, the redox imbalance caused by the activated polyol pathway has been implicated as another important factor for the pathogenesis of diabetic complications (5-7). The decrease of NADPH/NADP ratio, which results from increased reduction of glucose to sorbitol, could cause oxidative stress by lowering glutathione levels or cause a decrease in nitric oxide (NO) synthesis in the tissues. Also, the increase of

Yoshiyuki Ono[1]*, Toshiyuki Negoro[2], Masanobu Komiya[2]. [1]Clinical Development Division and [2]Discovery Research Laboratories, Dainippon Pharmaceutical Co., Ltd., 33-94, Enokicho, Suita, Osaka 564-0053, Japan. *Correspondence.

Scheme 1: Synthesis of AS-3201

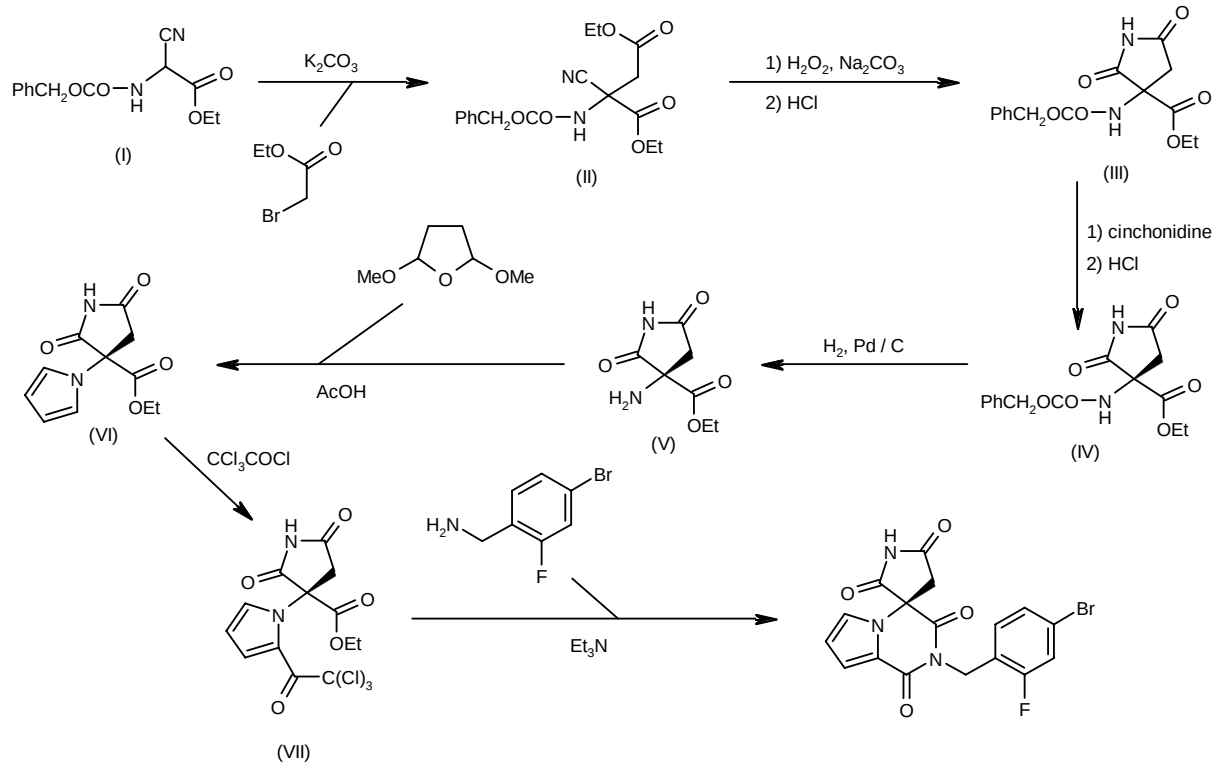

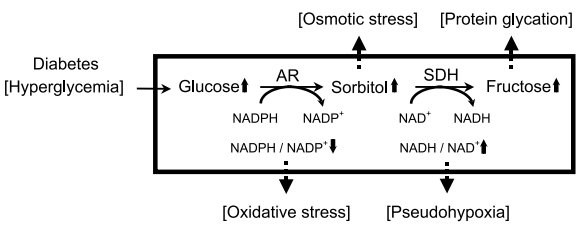

Fig. 1. Scheme of the polyol pathway and pathogenic factors in diabetic neuropathy.

NADH/NAD ratio, which results from increased oxidation of sorbitol to fructose, could give rise to pseudohypoxia. Additionally, it seems likely that the increase in fructose levels accelerates the development of diabetic complications since fructose may serve as a major source of advanced glycation end products (AGEs), which are implicated in the pathogenesis of the complications (8).

Thus, activation of the polyol pathway affects various pathogenic factors including osmotic regulation (Fig. 1). Therefore, a strict control of the polyol pathway activation in hyperglycemia is necessary to restrain not only the tissue sorbitol accumulation but also the increase in fructose level and the redox imbalance.

Various experimental indications suggesting that interruption of the polyol pathway by inhibition of AR may be an effective therapeutic approach to prevent or ameliorate diabetic complications have led to the discovery of several classes of AR inhibitors, and some of them are undergoing clinical studies at the present time (Table I). These AR inhibitors have been suggested to be effective in the treatment of diabetic complications in a number of studies using experimental models. However, the development of many AR inhibitors has been discontinued due to their poor efficacy or adverse effects in clinical studies. Sorbinil was discontinued (9) due to its potential to induce hypersensitivity reactions. Tolrestat has also been withdrawn due to its lack of efficacy and possible toxic effects on the liver (10). Ponalrestat has been discontinued as a result of no beneficial effects found in the clinical studies. However, in a subsequent study it was suggested that ponalrestat failed to penetrate the human nerves in a concentration sufficient to decrease nerve sorbitol levels (11). From the results of these clinical studies and recent animal studies on polyol metabolism, development of a new class of AR inhibitors with far more potent *in vivo* activity and fewer adverse effects than the classical AR inhibitors is desirable in order to provide direct evidence supporting the polyol pathway hypothesis.

With the aim of developing new AR inhibitors with such properties, we examined a series of pyrrolo[1,2-*a*]-

Table I: Aldose reductase inhibitors.

Compound	Status	Originator
1. Sorbinil	Phase III (Discontinued)	Pfizer
2. Ponalrestat	Phase III (Discontinued)	Zeneca
3. Tolrestat	Launched (Discontinued)	Wyeth-Ayerst
4. Epalrestat	Launched	Ono
5. Imirestat	Phase II (Discontinued)	Alcon
6. Zenarestat	Phase III	Fujisawa
7. Fidarestat	Phase III	Sanwa Kagaku
8. Zopolrestat	Phase II	Pfizer
9. Minalrestat	Phase II	Wyeth-Ayerst

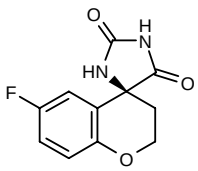
(1)

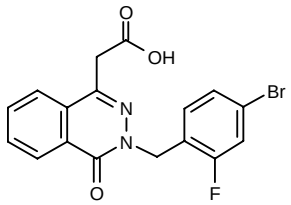
(2)

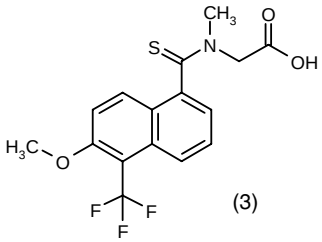
(3)

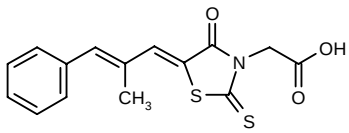
(4)

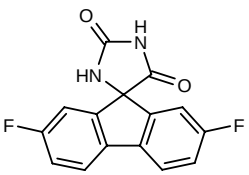
(5)

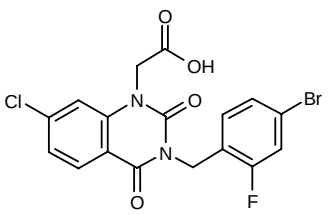
(6)

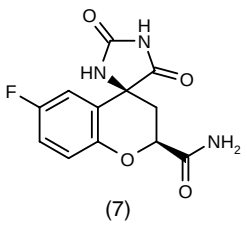
(7)

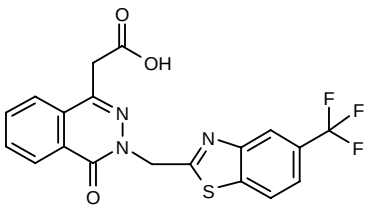
(8)

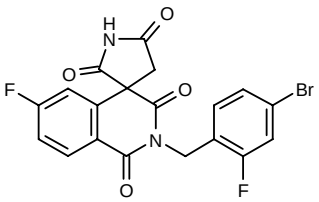
(9)

pyrazine derivatives and selected AS-3201, which is predicted to have distinct therapeutic potential in man (12-15).

Pharmacological Actions

Inhibitory activity on aldose reductase

AS-3201 potently inhibited ARs derived from organs of various kinds of animals in a reversible manner. This inhibition was uncompetitive and increased with increasing substrate (glucose) concentration. AS-3201 had high affinity for human recombinant AR with a K_i value (inhibition constant) of 0.38 nM. The inhibitory potency of AS-3201 in terms of K_i value was approximately 2.3, 5, 9, 234 and 237 times greater than that of fidarestat, zenarestat, zopolrestat, epalrestat and ponalrestat, respectively.

AS-3201 was found to form a stable noncovalent complex with human recombinant AR, which was dissociable at a slow rate. Inhibition of AR by AS-3201 was reversed by dialysis at 37 °C for 48 h but not at 4 °C. AS-3201 has been shown to have a very high selectivity for AR; among the various kinds of enzymes tested, only aldehyde reductase (an AR-related enzyme) was inhibited, with about 500 times less affinity than that for AR. Possible interaction of AS-3201 with neurotransmission receptors was examined with various transmitter ligands in binding experiments. AS-3201 showed no significant affinity for the receptors examined.

Inhibitory effect on activated polyol pathway in vivo

After rats were made diabetic by injection of streptozotocin (STZ), the polyol pathway in their tissues was soon activated and thereafter the sorbitol and fructose

levels in tissues increased significantly within 1 week. AS-3201 potently inhibited the activated polyol pathway in diabetic rats at low doses. Repeated oral administration of AS-3201, once a day for 21 days starting 7 days after the diabetes induction, reversed the elevated sorbitol levels in the sciatic nerve. The ED_{50} value for normalization of sorbitol levels was 0.034 mg/kg/day. AS-3201 at a dose of 0.3 mg/kg/day caused a decrease in sorbitol to levels lower than those in normal, nondiabetic control rats. This effect was more pronounced in comparison with other AR inhibitors. AS-3201 was about 3.5, 9, 226 and 259 times more potent than minalrestat, fidarestat, zopolrestat and ponalrestat, respectively.

AS-3201 significantly decreased elevated fructose levels in the sciatic nerve of diabetic rats at doses (> 0.03 mg/kg/day) somewhat higher than those necessary to lower sorbitol levels. It normalized the elevated fructose levels at a dose of 0.3 mg/kg/day.

AS-3201 decreased sorbitol levels not only in the sciatic nerve but also in other target tissues in diabetic rats. It inhibited sorbitol accumulation in the erythrocytes, retina and lens at doses similar to those effective for the sciatic nerve. The ED_{50} values ranged from 0.010-0.07 mg/kg/day. In the lens, existing AR inhibitors, even at high doses, showed only weak effects on sorbitol accumulation. The reason for this is that these inhibitors are not readily transported into the lens due to low permeability. On the other hand, AS-3201 showed dose-related inhibition of lens sorbitol accumulation at doses of 0.01-0.3 mg/kg/day and suppressed the sorbitol level nearly to normal at 0.1 mg/kg/day. These results indicate that AS-3201 has marked penetration to reach sufficiently high levels in target organs and completely inhibit AR. Pfeifer *et al.* reviewed 47 clinical studies with AR inhibitors which had hitherto been tried for diabetic neuropathy and pointed out that profound penetration into nerves is a prerequisite for therapeutic agents (16).

Duration of action

Following single oral administration (0.3 mg/kg) of AS-3201 to diabetic rats, the maximum decrease in sorbitol levels in the sciatic nerve was achieved after 7 days and the effect lasted beyond 14 days. On the other hand, the effect on sorbitol levels in the erythrocytes reached a maximum 24 h after administration and then disappeared rapidly. This indicates that AS-3201 is an inhibitor with long-lasting action in target tissues of nerves. This long duration of action appears to reflect its potent effects with repeated administration.

Enhancing effect on motor nerve conduction velocity

Early nerve dysfunction in diabetic patients is manifested by a slowing of nerve conduction velocity in a variety of voluntary and autonomic nerves. In diabetic rats (3 weeks after STZ administration), the motor nerve conduction velocity (MNCV) at the sciatic nerves decreased from 46.8 ± 0.7 m/sec (value before STZ injection) to 40.6 ± 0.4 m/sec. AS-3201, given orally (0.1-1.0 mg/kg/day) once a day for 3 weeks, significantly and dose-dependently improved the decrease in MNCV. These values correlated well with sorbitol levels in the sciatic nerve of rats. Sorbitol levels in diabetic rats with improved MNCV after treatment with AS-3201 were similar to those in nondiabetic control rats or even lower (Fig. 2). These results suggest that the polyol pathway should be completely normalized and should remain unchanged within normal levels for a long period of time by strict inhibition of AR in order to achieve significant improvement in the MNCV.

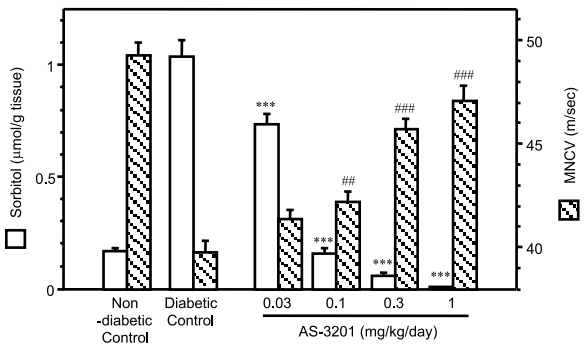

Fig. 2. Effects of AS-3201 on sorbitol levels and motor nerve conduction velocity (MNCV) in sciatic nerves of diabetic rats. AS-3201 was orally administered to 3-week streptozotocin-induced diabetic rats once a day for 21 days. After the final administration, the MNCV at the sciatic nerves was measured under halothane anesthesia, and then the sciatic nerves were removed to determine their sorbitol contents. Values are mean ± SE (n = 10-12). $^{\#\#}p < 0.01$, $^{***,\#\#\#}p < 0.001$ compared with the diabetic control by Dunnett's multiple comparison test.

Cameron and Cotter (17) have reported that there is a dissociation between the effective dose that decreases sorbitol levels and the effective dose that improves the MNCV in diabetic rats. In clinical trials with ponalrestat, doses higher than 10 times the clinical dose (600 mg) would be necessary to achieve improvement in the MNCV. This dose had been estimated on the basis of the effective dose (ED_{50}) for sorbitol levels in erythrocytes in diabetic rats.

AS-3201 has more potent *in vivo* activity than existing AR inhibitors. It should be able to substantially block polyol pathway activation in hyperglycemia by potently inhibiting AR in nerves, retina and lens because of its high affinity for AR and high penetration into these tissues. Additionally, its long-lasting action could be beneficial for long-term treatment as it would continuously block the polyol pathway in diabetic complications that develop slowly over a long period of time. AS-3201 possesses a high degree of selectivity for AR, which could be associated with its safety. In fact, no adverse effects of AS-3201

were observed in acute or chronic toxicity tests in rats and dogs even at a dose 100 times higher than the pharmacologically effective dose. Therefore, AS-3201 is considered to be a selective AR inhibitor without side effects.

Pharmacokinetics

When [^{14}C]-AS-3201 was orally administrated to rats, the concentration of radioactivity in the plasma reached a maximum 2-4 h after administration and thereafter decreased with an apparent half-life of 5-11 h and subsequently with an apparent half-life of approximately 130 h (18). In most tissues, concentrations of radioactivity reached a maximum between 4-10 h after administration. However, in the sciatic nerve and the lens, radioactivity concentrations peaked later than in other tissues and elimination was much slower. Metabolites of AS-3201 were not detected in the plasma or tissues including the sciatic nerve, lens, testicle and kidney. After oral or intravenous administration, approximately 14% and 82% of the administrated amount were recovered from the urine and the feces, respectively, throughout the entire 480 h. The bioavailability for oral administration was 90% or more.

Clinical Studies

Two phase I clinical trials of AS-3201 have been performed in healthy male volunteers. One trial consisted of single administration of 6 doses ranging from 2.5-60 mg and the other of repeated administration of a once-daily dose of 20 mg for 14 days. No significant adverse events attributable to AS-3201 were observed in either trial. At present, AS-3201 is under early phase II clinical evaluation for diabetic peripheral neuropathy.

Conclusions

Many clinical studies of AR inhibitors, preferentially for diabetic neuropathy, have been performed thus far. Nevertheless, the therapeutic value of AR inhibitors has not yet been sufficiently verified. Recent clinical and preclinical studies (19) indicated that the ambiguous therapeutic effects of AR inhibitors could be due to underdosing of the drugs, which does not completely suppress activation of the polyol pathway. This suggests that a strict control of the polyol metabolism by AR inhibitors, for example, inhibiting more than 90% of sorbitol increase in the nerve, is critical for obtaining definite therapeutic effects for diabetic complications. Thus, the development of new AR inhibitors with much higher potencies than those of classical AR inhibitors is desirable.

AS-3201 is a novel, highly potent AR inhibitor with a good safety profile. It may be the most suitable drug to achieve complete and continuous inhibition of elevated polyol pathway in diabetic patients. Therefore, AS-3201 is expected to provide an effective treatment for diabetic complications such as neuropathy.

Manufacturer

Dainippon Pharmaceutical Co., Ltd. (JP).

References

1. Negoro, T., Murata, M., Ueda, S., Fujitani, B., Ono, Y., Kuromiya, A., Komiya, M., Suzuki, K., Matsumoto, J. *Novel, highly potent aldose reductase inhibitors: (R)-(-)-2-(4-Bromo-2-fluorobenzyl)-1,2,3,4-tetrahydropyrrolo[1,2-a]pyrazine-4-spiro-3'-pyrrolidine-1,2',3,5'-tetrone (AS-3201) and its congeners.* J Med Chem 1998, 41: 4118-29.

2. Pirart, J. *Diabetes mellitus and its degenerative complications: A prospective study of 4,400 patients observed between 1947 and 1973.* Diabetes Care 1978, 1: 168-88.

3. Ziegler, D., Mayer, P., Mühlen, H., Gries, F.A. *The natural history of somatosensory and autonomic nerve dysfunction in relation to glycaemic control during the first 5 years after diagnosis of type 1 (insulin-dependent) diabetes mellitus.* Diabetologia 1991, 34: 822-9.

4. Greene, D.A., Lattimer, S.A. *Impaired rat sciatic nerve sodium-potassium adenosine triphosphatase in acute streptozotocin diabetes and its correction by dietary myo-inositol supplementation.* J Clin Invest 1983, 72: 1058-63.

5. Van Dam, P.S., Van Asbeck, B.S., Erkelens, D.W., Marx, J.J.M., Gispen, W.H., Bravenboer, B. *The role of oxidative stress in neuropathy and other diabetic complications.* Diabetes Metab Rev 1995, 11: 181-92.

6. Stevens, M.J., Dananberg, J., Feldman, E.L., Lattimer, S.A., Kamijo, M., Thomas, T.P., Shindo, H., Sima, A.A.F., Greene, D.A. *The linked roles of nitric oxide, aldose reductase and (Na^+, K^+)-ATPase in the slowing of nerve conduction in the streptozotocin diabetic rat.* J Clin Invest 1994, 94: 853-9.

7. Williamson, J.R., Chang, K., Frangos, M., Hasan, K.S., Ido, Y., Kawamura, T., Nyengaard, J.R., Van den Enden, M., Kilo, C., Tilton, R.G. *Hyperglycemic pseudohypoxia and diabetic complications.* Diabetes 1993, 42: 801-13.

8. Brownlee, M. *Glycation and diabetic complications.* Diabetes 1994, 43: 836-41.

9. Jaspan, J.B., Towle, V.L., Maselli, R., Herold, K. *Clinical studies with an aldose reductase inhibitor in the autonomic and somatic neuropathies of diabetes.* Metabolism 1986, 35(Suppl. 1): 83-92.

10. Foppiano, M., Lombardo, G. *Worldwide pharmacovigilance systems and tolrestat withdrawal.* Lancet 1997, 349: 399-400.

11. Greene, D.A., Sima, A.A.F. *Effects of aldose reductase inhibitors on the progression of nerve damage.* Diabet Med 1993, 10(Suppl. 2): S31-2.

12. Negoro, T., Murata, M., Ueda, S., Mizuta, H., Ono, Y., Fujitani, B., Matsumoto, J. *A new aldose reductase inhibitor: Synthesis and biological activities of pyrrolo[1,2-a]pyrazine derivatives.* 206th ACS Natl Meet (Aug 22-27, Chicago) 1993, Abst MEDI 238.

13. Ono, Y., Fujitani, B., Kuromiya, A., Nakamura, K., Komiya, M., Karasawa, T. *Effect of a novel, highly potent aldose reductase inhibitor, SX-3201 in diabetic rats.* 15th Int Diabetes Fed Cong (Nov 6-11, Kobe) 1994, Abst 10A5-0873.

14. Nakamura, K., Fujitani, B., Ono, Y., Komiya, M., Negoro, T., Kuromiya, A., Karasawa, T. *Enzymological study of SX-3201, a potent and long-lasting aldose reductase inhibitor.* Can J Physiol Pharmacol 1994, 72(Suppl. 1): Abst P5.2.32.

15. Kurono, M., Yoshida, K., Naruto, S. *Interaction between SX-3201, a potent aldose reductase (AR) inhibitor, and recombinant human AR.* 209th ACS Natl Meet (April 2-6, Anaheim) 1995, Abst MEDI 197.

16. Pfeifer, M.A., Schumer, M.P., Gelber, D.A. *Aldose reductase inhibitors: The end of an era or the need for different trial designs?* Diabetes 1997, 46(Suppl. 2): S82-89.

17. Cameron, N.E., Cotter, M.A. *Dissociation between biochemical and functional effects of the aldose reductase inhibitor, ponalrestat, on peripheral nerve in diabetic rats.* Br J Pharmacol 1992, 107: 939-44.

18. Fujii, T., Matsushita, H., Matsunaga, Y., Nomura, N., Kasai, H., Matsumoto, S., Miyazaki, H. *Disposition and metabolism of [^{14}C]SX-3201, an aldose reductase inhibitor, in rats.* 4th Int ISSX Meet (Aug 27-31, Seattle) 1995, Abst 313.

19. Cameron, N.E., Cotter, M.A. *Metabolic and vascular factors in the pathogenesis of diabetic neuropathy*. Diabetes 1997, 46(Suppl. 2): S31-7.

Drugs of the Future 2003, 28(12): 1168-1181

CCC: 0377-8282/2003

Lonafarnib

Prop INN; USAN

Farnesyltransferase Inhibitor
Solid Tumor Therapy
Leukemia Therapy

Sch-66336
Sarasar™

(+)-(*R*)-4-[2-[4-(3,10-Dibromo-8-chloro-5,6-dihydro-11*H*-benzo[5,6]cyclohepta[1,2-*b*]pyridin-11-yl)piperidin-1-yl]-2-oxoethyl]piperidine-1-carboxamide

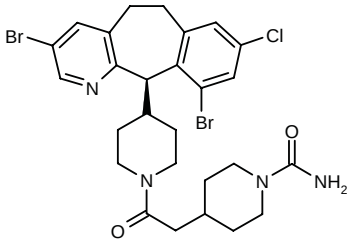

$C_{27}H_{31}Br_2ClN_4O_2$

Mol wt: 638.8289

CAS: 193275-84-2

EN: 254680

Abstract

Ras proteins are involved in many crucial as well as housekeeping cellular processes such as growth, differentiation, apoptosis, cytoskeletal organization and membrane trafficking. Mutations of Ras proteins have been observed in as many as 30% of human cancers. Thus, interruption of Ras signaling has become a focus for the development of anticancer agents. One potentially effective approach that is currently being followed involves the prevention of the localization of Ras through inhibition of protein farnesyltransferase (FTase), the enzyme which catalyzes post-translational modification (*i.e.*, farnesylation) of Ras to enable localization of Ras proteins to the inner plasma membrane. Lonafarnib (Sch-66336) is a novel, orally active, heterocyclic peptidomimetic FTase inhibitor that competes with the enzyme for the CAAX portion of Ras. The agent has shown marked *in vitro* and *in vivo* antitumor activity and was chosen for further development. Lonafarnib has demonstrated efficacy and tolerability in numerous phase I and II trials as monotherapy or in combination with other chemotherapeutics, and is currently undergoing phase II/III development for the treatment of cancer.

Synthesis

The nitration of loratadine (I) (1) by means of tetrabutylammonium nitrate and trifluoroacetic anhydride (TFAA) in dichloromethane gives the 3-nitro derivative (II), which is reduced with iron filings and $CaCl_2$ in refluxing ethanol/water to yield the 3-amino derivative (III). Treatment of compound (III) with $NaNO_2$, HBr and Br_2 provides 4-(3-bromo-8-chloro-5,6-dihydro-1*H*-benzo[5,6]-cyclohepta[1,2-*b*]pyridin-11-ylidene)piperidine-1-carboxylic acid ethyl ester (IV) (2). Scheme 1.

Introduction of a bromine atom at the 10-position of the benzocycloheptapyridine (IV) is achieved by the following sequence: Nitration of (IV) using $NaNO_3$ and H_2SO_4 affords a mixture of nitro compounds (V) and (VI), from which the major 9-nitro isomer (VI) is separated by silica gel chromatography. Reduction of the nitro group of (VI) with iron filings and $CaCl_2$ in refluxing aqueous ethanol gives the 9-amine derivative (VII), which is brominated at position 10 with Br_2 in AcOH. The brominated aniline (VIII) is then deaminated by diazotization, followed by reduction of the resulting diazonium salt with hypophosphorous acid to give the trihalogenated compound (IX), which by hydrolysis of the carbamate group in boiling concentrated HCl affords the piperidine derivative (X). Subsequent reduction of the C-11 double bond of compound (X) using DIBAL-H in refluxing toluene affords the corresponding racemic piperidine, which is submitted to enantiomeric separation by means of either HPLC on a ChiralPak AD column or chemical resolution using *N*-acetyl-L-phenylalanine as the resolving agent. The appropriate (+)-(*R*)-enantiomer (XI) is coupled with *N*-Boc-4-piperidineacetic acid (XII) in the presence of EDC and HOBt to yield the protected amide (XIII), which by hydrolysis of the Boc protecting group with trifluoroacetic acid results in the piperidine derivative (XIV) (3-5). Finally, this

L.A. Sorbera, J. Castañer. Prous Science, P.O. Box 540, 08080 Barcelona, Spain.

Scheme 1: Synthesis of Intermediate (IV)

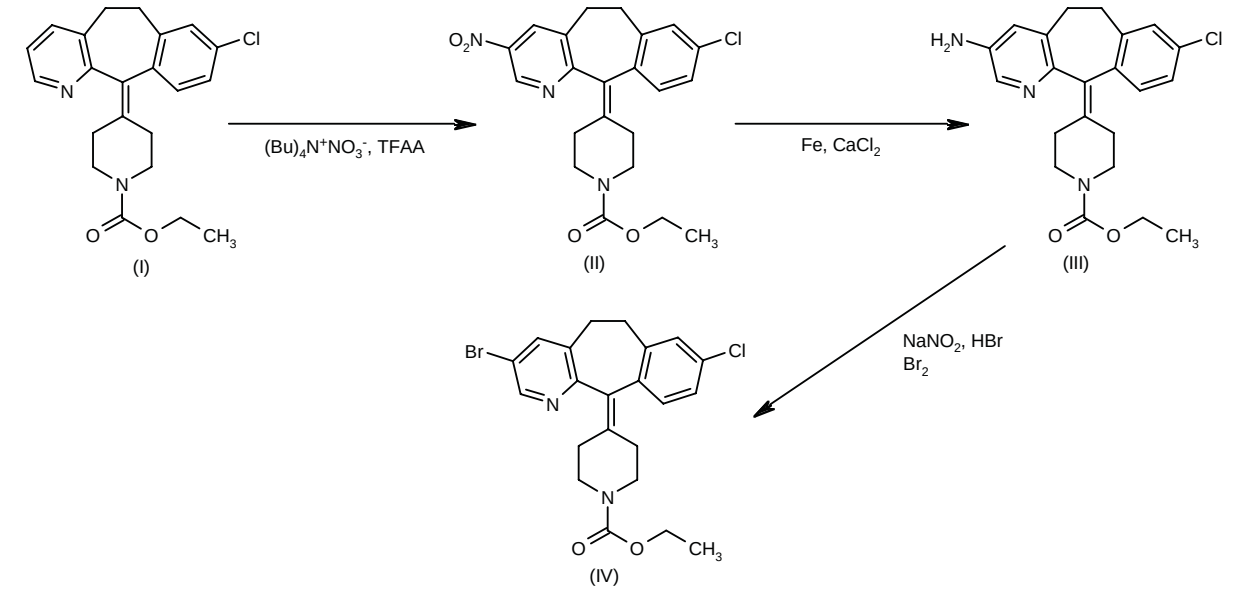

compound is treated with either trimethylsilyl isocyanate in dichloromethane (3-5) or urea in refluxing water (5). Scheme 2.

Alternatively, compound (X) can be resolved into its atropoisomers by digestion with Toyobo LIP-300 enzyme in the presence of trifluroethyl isobutyrate (XV) to give a mixture of the unreacted compound (–)-(XVI) and the acylated compound (+)-(XVII), which are separated by acid extraction. The undesired atropoisomer (–)-(XVI) is recovered by thermal razemization in diethyleneglycol dibutyl ether at 210 °C and new enzymatic separation. Acid hydrolysis of the separated amide (+)-(XVII) provides the desired atropoisomer (+)-(XVIII), which is finally reduced with DIBAL-H to the (+)-(*R*)-enantiomer (XI) (6, 7). Scheme 3.

Introduction

Genetic mutations are the underlying cause of tumorigenesis where they can cause the activation of oncogenes or the inactivation of tumor suppressor genes, leading to expression of a malignant phenotype. Ras oncogenes are known to be involved in signal transduction pathways regulating cell growth and differentiation in many human cancers, so that mutations of Ras protein are seen in about 30% of all cancers. There are 3 *ras* proto-oncogenes (H-*ras*, K-*ras* and N-*ras*) which encode 4 related and highly conserved 21-kDa Ras proteins (H-Ras, N-Ras, K-Ras4A and K-Ras4B). Ras proteins are members of the superfamily of GTPases comprised of proteins regulating protein synthesis and signal transduction involved in growth, differentiation, apoptosis, cytoskeletal organization and membrane trafficking. They are localized on the inner surface of the plasma membrane, where they act as molecular switches that cycle between an inactive GDP-bound form and an active GTP-bound state. In its active state, Ras mediates proliferative signals mainly upstream of receptor tyrosine kinases to a downstream cascade of protein kinases and their associated downstream pathways, including the mitogen-activated protein kinase (MAPK) cascade via Raf1, cell morphology via Rac/Rho, cell survival via phosphatidylinositol 3'-kinase (PI3-kinase) and stress response via mitogen-activated protein/ERK kinase kinase (MEKK) (8-12).

Localization of the Ras protein to the inner surface of the plasma membrane is required for signaling. Ras proteins are synthesized as inactive cytosolic precursors, after which they undergo a series of post-translational modifications at the C-terminus which yield the mature Ras protein that can be localized to the plasma membrane. The first post-translational modification is farnesylation, a prenylation reaction where a 15-carbon farnesyl isoprenoid moiety is added to Ras. This process is catalyzed by the zinc metalloenzyme protein farnesyltransferase (FTase), which transfers a farnesyl moiety from farnesyl pyrophosphate to the cysteine residue of CAAX-containing proteins (C = cysteine; A = aliphatic amino acid [leucine, isoleucine or valine]; X = methionine, serine, leucine or glutamine; Fig. 1). So far, studies have identified over 300 candidate peptides that contain CAAX and can undergo farnesylation, suggesting that a significant

Scheme 2: Synthesis of Lonafarnib

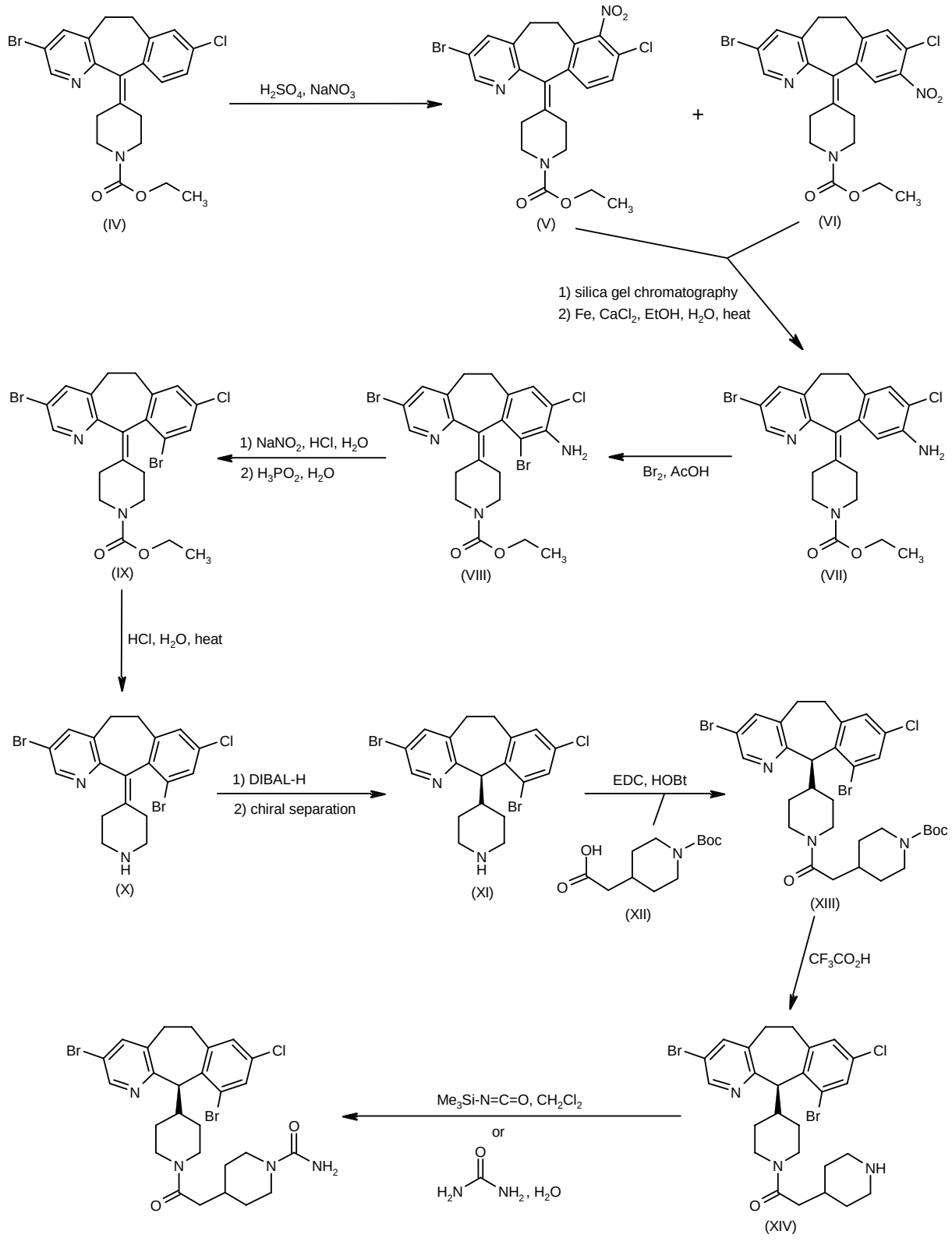

Scheme 3: Synthesis of Intermediate (XI)

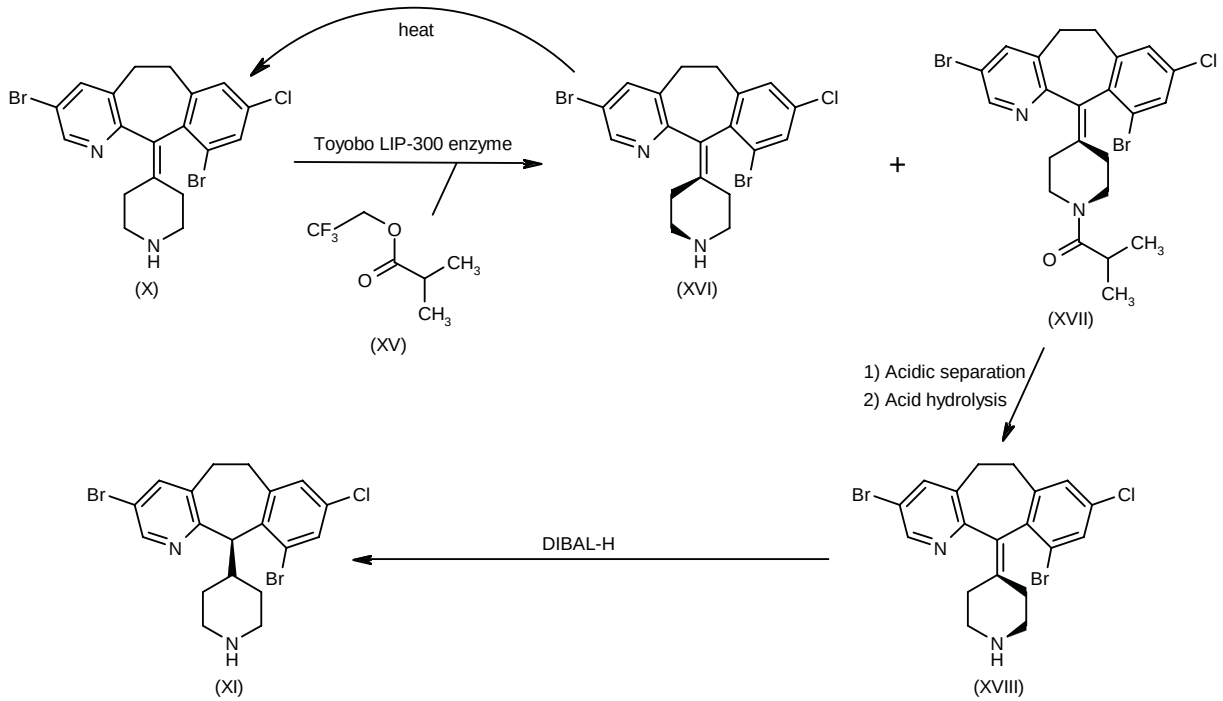

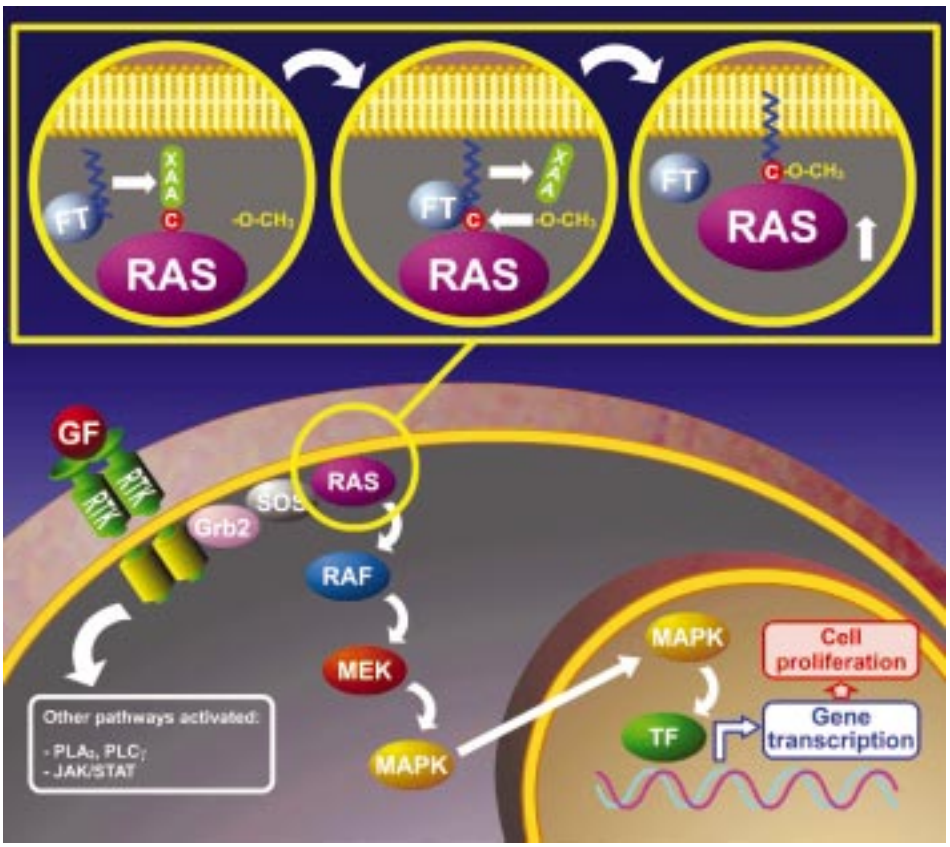

Fig. 1.

number of these proteins may be oncogenic and involved in mitogenic signaling (13, 14).

As mentioned above, a number of human tumors harbor Ras mutations which maintain Ras in a locked, activated state. K-*ras* is the most common, found with relative frequencies of 90, 55, 50, 35 and 23% in pancreatic, thyroid, colon, lung and ovarian carcinomas, respectively. N-*ras* mutations are less common, found with relative frequencies of 55, 43, 35, 30 and 20% in thyroid carcinoma, seminoma, lung cancer, myelodysplastic syndrome (MDS)/ acute myeloid leukemia (AML) and malignant melanoma, respectively, although they are more common than rare H-*ras* mutations (9, 10, 15-19). Because a large number of human cancers harbor mutated Ras, interruption of Ras signaling has become a focus for the development of anticancer agents. Approaches being developed include preventing membrane localization of Ras (*e.g.*, inhibition of FTase), inhibition of Ras protein expression through ribozyme, antisense nucleotides and inhibition of Ras downstream effectors. Small-molecule FTase inhibitors in particular are a novel class of antineoplastic agents of which at least 7 are currently under clinical development. Two of these agents, R-115777 (20) and lonafarnib (Sch-66336), are orally active heterocyclic peptidomimetics that compete with FTase for the CAAX portion of Ras. Lonafarnib in particular has exhibited marked antitumor activity *in vitro* and *in vivo* and has reached phase II/III development (3, 21).

Pharmacological Actions

Results from *in vitro* enzyme assays showed that lonafarnib potently and selectively inhibited the transfer of [^{3}H]-farnesyl pyrophosphate to activated H-Ras (IC_{50} = 1.9 nM); on the other hand, at concentrations up to 50 μM it was inactive in inhibiting protein geranylgeranyltransferase (GGPT)-mediated prenyl transfer. Lonafarnib also markedly inhibited farnesylation of H-Ras proteins in COS-7 cells transiently expressing H-ras[Val^{12}]-CVLS (IC_{50} = 10 nM) and inhibited anchorage-independent growth of tumor cell lines with and without H-*ras* and K-*ras* mutations. The IC_{50} values obtained from these colony-forming soft agar assays were 0.07, 0.50, 0.07, 0.25, 0.05 and 0.05 μM against H-*ras* NIH, K-*ras* NIH, colon HCT 116 bearing K-*ras*, pancreatic MIA PaCa-2 bearing K-*ras*, breast MCF7 and lung NCI-H146 cell lines, respectively (3, 21).

Lonafarnib was shown to have a good *in vitro* safety profile. Results from bacterial mutagenicity, human peripheral blood lymphocyte chromosome aberration and mouse bone marrow micronucleus assays indicated that the agent has no genotoxic potential and thus has an improved safety profile over other genotoxic anticancer agents (22).

Further studies examined the ability of lonafarnib to inhibit human tumor colony-forming units *in vitro*, with results indicating potent, broad-spectrum activity against ovarian, breast and non-small cell lung (NSCLC) cancers. The study using soft agar cloning assays and 70 primary tumor specimens from patients showed that 14-day exposure to lonafarnib (0.1-2.5 μM) resulted in concentration-related inhibition of tumor colony-forming units. At the highest concentration, lonafarnib was active against 3 of 6 (50%) breast tumors, 6 of 15 (40%) ovarian tumors and 5 of 13 (38%) NSCLC. Of the 69 specimens, lonafarnib showed activity against 27, 38, 33 and 27% of those samples resistant to doxorubicin, cisplatin, paclitaxel and etoposide, respectively (23).

In vitro studies using human head and neck squamous cell carcinoma (HNSCC) lines demonstrated the efficacy of lonafarnib in inhibiting Ras activity. In sulforhodamine B assays, the growth of 6 cell lines was time- and concentration-dependently inhibited with treatment (> 50% inhibition at 1 μM for 4 days). Anchorage-independent growth of all 6 cell lines was also inhibited in soft agar assays after 14 days of treatment with the agent. Reductions in cell number after treatment were found to be due to apoptosis. Experiments using the UMSCC38 cell line demonstrated that lonafarnib (1.5 μM) effectively inhibited Ras activity, since decreased phosphorylated Raf expression was observed at 5, 15 and 30 min and 1 h after treatment. Phosphorylated Akt expression was also reduced in a pattern similar to that observed for phosphorylated Raf, indicating an alteration of the PI3-kinase/Akt pathway activity. Similar effects were observed in 4 other HNSCC cell lines. A reduction in phosphorylated Bad, a proapoptotic protein which is phosphorylated and inactivated by Akt, was also observed in studies using SqCC/Y1 cells; reductions in expression of Bcl-xL and Bcl-2, but not Bax, cyclin D1 or cyclin B1, were also observed with treatment (24, 25).

An *in vitro* study using Ras-transformed Rat2 fibroblasts examining the mechanism of action of lonafarnib-induced apoptosis reported that treatment of H-Ras-CVLS-transformed fibroblasts with MEK1/2 (MAPK/ERK kinase) inhibitors (*e.g.*, PD-098059) significantly enhanced lonafarnib-induced apoptosis (approximately 60% vs. 30%). Combination treatment also resulted in markedly increased caspase 3 activity and a more complete and sustained inhibition of MAPK pathway activity than either agent alone; lonafarnib alone or in combination with the MEK1/2 inhibitor had no effect on Rat2 cells transformed with a geranylgeranylated form of H-Ras (H-Ras-CVLL). Interestingly, lonafarnib had no effect on K-Ras-transformed cells, although these cells underwent apoptosis in response to exposure to the MEK1/2 inhibitor (26).

The broad-spectrum antitumor efficacy of lonafarnib has been demonstrated *in vitro* in studies using several human cancer cell lines and *in vivo* in murine human tumor xenograft models. Antiproliferative activity (IC_{50} = 7.1-32.3 μM) was observed against 5 established human glioblastoma multiforme cell lines; cell lines expressing a large amount of H-Ras (*e.g.*, U-87 MG) and lesser amounts of K-Ras and N-Ras were more sensitive to the agent (27). Moreover, lonafarnib (2.5, 10 or 40 mg/kg q.i.d. p.o.) was effective in inhibiting tumor growth in nude

mice bearing human tumor xenografts including lung (A549, HTB-177), pancreatic (AsPC-1, HPAF-II, Hs 700T, MIA PaCa-2), colon (HCT 116, DLD-1) and prostate (DU 145) carcinomas. Significant inhibition of tumor volume was observed with all doses (*e.g.*, 67-86% inhibition at 40 mg/kg) (28).

Lonafarnib was also effective against chronic myeloid leukemia (CML) LLC-MK2 and LLC-MK1 Philadelphia chromosome (Ph)-positive cell lines, with increased apoptotic effects observed with increased exposure (96 h vs. 48 h) (29). Lonafarnib was also effective *in vivo* in reverting signs of leukemia and significantly increasing survival rates in a transgenic murine model of Bcr/Abl-positive lymphoblastic leukemia. Treatment (40 mg/kg p.o. b.i.d.) was well tolerated and no adverse events were noted. While all untreated control animals died within 103 days, 80% of the animals treated with lonafarnib survived until discontinuation of treatment at a median of 200 days. These animals showed no signs of leukemia or lymphoma (30).

Lonafarnib was shown to effectively prevent membrane association of H-Ras but not K-Ras or N-Ras in several human tumor cell lines in a study using cell fractionation and Western blot analysis (31). However, as mentioned above, the agent prevented anchorage-independent growth of cell lines harboring H-*ras*, K-*ras* and N-*ras* mutations in soft agar, and in an MTT assay it exhibited time- and concentration-dependent activity against NSCLC cell lines bearing 2 different K-*ras* mutations (A549: K-ras mutation GGT>AGT, codon 12; LX-1: GGT>GTT, codon 12) and against Calu-6 cells bearing wild-type K-*ras* (32). These observations suggest that lonafarnib may also block the farnesylation of other proteins in addition to Ras. A study has demonstrated that lonafarnib-sensitive human tumor cell lines (*e.g.*, lung NCI-H460, colon HCT 116, pancreatic MIA PaCa-2, breast MCF7) accumulated in the G_2/M phase following exposure to the agent (1 μM). However, those cell types with activated H-Ras (*e.g.*, H-*ras*-transformed NIH/3T3, bladder T24) accumulated in the G_1 phase, with the population of cells in the G_2/M phase unaffected. Genotypic analysis of the sensitive human tumor cell lines revealed that cells with wild-type *p53* were particularly sensitive to lonafarnib, and after exposure to the agent for 24 h, $p21^{Cip1}$, the downstream target of *p53*, was induced. It was concluded that *p53* status influences the sensitivity of cells to lonafarnib (33).

Treatment of the leukogenic murine cell line Bcr/Abl-BaF3A also resulted in accumulation of cells in the G_2/M phase, indicating an action of the agent on other proteins. It has been suggested that centromere-associated proteins CENP-E and CENP-F, which are involved in mitosis and regulate the G_2/M checkpoint, are critical farnesylated targets of lonafarnib (34, 35). Other farnesylated proteins such as the heat shock protein HDJ2 and the nuclear lamin prelamin A have also been implicated as farnesylated targets for lonafarnib. Experiments using biopsies or surgical tumor specimens from patients with head and neck cancer, melanoma or metastatic colorectal carcinoma who had been treated for 1-2 weeks with oral lonafarnib showed an accumulation of prelamin A and unfarnesylated HDJ2 (36). G_2/M arrest and accumulation of HDJ2 protein were also observed in B16 and COLO 853 human melanoma cells treated with the agent (37).

Further studies have also implicated other possible direct or indirect targets for the anticancer activity of lonafarnib. Treatment *in vitro* of melanoma LOX, breast carcinoma MDA-MB-231, NSCLC carcinoma NCI-H460, H-*ras*-transformed fibroblasts and *wap-ras* transgenic tumors resulted in concentration-dependent downregulation of expression of the angiogenic factors VEGF (vascular endothelial growth factor), IL-8 and angiogenin. Thus, inhibition of angiogenesis may also contribute to the potent antineoplastic effects of the agent (38). In addition, treatment of the MS-1 chronic myelomonocytic leukemia (CMML) cell line with lonafarnib (10 nM-1 μM) concentration-dependently upregulated LFA-1 integrin expression and induced inside-out activation of β_1 (to promote heterotypic adhesion) and β_2 integrin (to promote heterotypic adhesion). Lonafarnib had no stimulatory effects on antiinflammatory cytokines such as TNF-α, IL-1β, IL-8, SDF-1α or VEGF in these cells (39).

Results from an *in vitro* study using NIH-G185 cells which overexpress the gene product of human MDR1 (human transporter P-glycoprotein [Pgp]) indicate that lonafarnib should have synergistic activity when combined with Pgp substrate/inhibitors such as paclitaxel, tamoxifen and vinblastine by significantly enhancing their inhibitory effects on Pgp. In this study, lonafarnib was shown to directly interact with the substrate binding site of Pgp. Lonafarnib significantly inhibited daunorubicin transport (IC_{50} ~ 3 μM) and reduced Pgp-mediated ATP hydrolysis by more than 70% (K_m = 3 μM) (40).

The possible synergistic effects of lonafarnib with other chemotherapeutic agents were confirmed in several *in vitro* and *in vivo* studies. Lonafarnib enhanced the antitumor activity of paclitaxel in 10 of 11 (except breast adenocarcinoma MDA-MB-231) human breast, colon, lung, ovary, prostate and pancreatic tumor cell lines examined and was synergistic with docetaxel in 4 of 5 (except MDA-MB-231) cell lines tested. Synergistic activity was also observed *in vivo* with combination treatment including lonafarnib (20 mg/kg p.o. for 14 days) and paclitaxel (5 mg/kg i.p. once daily for 4 days) against human lung tumor NCI-H460 xenografts in nude mice. Moreover, lonafarnib (2.5, 10 or 40 mg/kg q.i.d. for 4 weeks) not only dose-dependently inhibited tumor growth in male *wap-ras*/F transgenic mice that spontaneously develop paclitaxel-resistant mammary tumors, but treatment with the agent also sensitized the tumors to paclitaxel. Tumor regression was observed with lonafarnib and was associated with increased apoptosis and a reduction in DNA synthesis (28, 41).

The antiproliferative effects *in vitro* of a combination of lonafarnib and cisplatin were additive or synergistic in A549 NSCLC and T98G human glioblastoma cells, with enhanced apoptosis observed, but they were less than

additive in breast MCF7, colon HCT 116 and pancreatic adenocarcinoma BxPC-3 cells. The synergistic effects of lonafarnib were drug sequence-dependent since treatment of A549 cells with cisplatin followed by lonafarnib resulted in antagonistic activity (42). Additive antiproliferative effects were observed in human lung cancer cell lines A549 and NCI-H460 treated with a combination of lonafarnib and cisplatin or carboplatin. Significantly enhanced antitumor efficacy was also observed *in vivo* in nude mice bearing human tumor xenografts and treated with lonafarnib + cisplatin (A549 xenograft model) or lonafarnib + temozolomide (human melanoma LOX xenograft model) (43).

Combination treatment of several human tumor cell lines *in vitro* with lonafarnib and Sch-58500, a replication-deficient recombinant *p53*, resulted in synergistic or additive cytotoxicity. Further synergy was not observed when paclitaxel was added to this combination, although additive effects were noted (44). Additive or synergistic effects were also seen when lonafarnib was combined with imatinib or cytosine arabinoside in a proliferation assay using imatinib-resistant Bcr/Abl-positive cells, indicating a possible efficacy for the agent in treating patients with imatinib-resistant Ph-positive leukemias. Moreover, lonafarnib potently sensitized imatinib-resistant cells to imatinib-induced apoptosis. In contrast, antagonistic effects were seen in these cells when lonafarnib was combined with daunorubicin or etoposide (45-48).

Synergistic activity in NSCLC cells was also observed when lonafarnib was combined with an adenovirus expressing insulin-like growth factor-binding protein 3 (IGFBP-3; Ad5CMV-BP3), which targets Ras and Akt (49).

Pharmacokinetics

Two HPLC methods were developed to determine levels of lonafarnib in plasma and its chiral inversion. The achiral method was found to be linear over a concentration range of 0.1-20 μg/ml in cynomolgus monkey plasma. The chiral method was linear in rat and cynomolgus monkey plasma over a concentration range of 0.25-10 μg/ml for both enantiomers and showed that the agent was not subjected to chiral inversion in these animals (50).

The pharmacokinetics of lonafarnib were determined in athymic nude mice, rats and cynomolgus monkeys. A serum C_{max} of 8.8 μM and an $AUC_{(0\text{-}24\ h)}$ value of 24.1 μg·h/ml were obtained in mice following oral administration of the agent (25 mg/kg); oral bioavailability was 76%. The half-life following i.v. administration was 1.4 h. Plasma C_{max} values in rats were 3, 10 and 30 μM following oral administration of 10, 30 and 100 mg/kg, respectively. In monkeys, C_{max} values were 1.8-2.5 μM following oral or i.v. administration of 10 mg/kg and the $AUC_{(0\text{-}48\ h)}$ value after oral administration was 14.7 μg·h/ml; the oral bioavailability was about 50% (3, 51).

The pharmacokinetics of lonafarnib (300 and 400 mg p.o. once daily in 28-day cycles) were determined in a phase I trial conducted in 12 patients with advanced solid tumors; pharmacokinetic analysis was performed on days 1 and 15. Grade 3 diarrhea was reported in 1 patient at 400 mg. However, 3 of 6 patients discontinued early at this dose level due to grade 1-3 diarrhea, uremia, creatinine elevation, asthenia, vomiting and/or weight loss. Similar toxicities were observed with 300 mg, although they were all grade 1-2; 300 mg once daily was the recommended dose for phase II studies. C_{max} and AUC values were dose-related and were increased on day 15 as compared to day 1, indicating drug accumulation. Steady state was achieved by day 14. A large volume of distribution was observed at steady state, suggesting marked distribution outside the plasma compartment. The plasma half-life appeared to increase with dose and was 5-9 h (52).

Similar pharmacokinetic results were obtained with a twice-daily dosing schedule. The pharmacokinetics of lonafarnib (25, 50, 100, 200, 300 and 400 mg p.o. b.i.d. in 28-day cycles) were examined in a dose-escalation phase I trial conducted in 24 patients with advanced solid tumors; pharmacokinetic analysis was performed on days 1 and 15. The dose-limiting toxicities (DLTs) were grade 4 vomiting, grade 4 neutropenia and thrombocytopenia and a combination of grade 3 anorexia and diarrhea with reversible grade 3 plasma creatinine elevation at 400 mg b.i.d., and grade 4 neutropenia, grade 3 neurocortical toxicity and a combination of grade 3 fatigue with grade 2 nausea and diarrhea at 300 mg b.i.d. The recommended dose for phase II studies was 200 mg b.i.d. Steady-state plasma concentrations of the agent were achieved at days 7-14. The volume of distribution was large at steady state, suggesting that there was extensive distribution of the agent outside the plasma compartment. A greater-than-dose-proportional increase in drug exposure and plasma C_{max} values was observed, so that higher values were obtained on day 15 as compared to day 1; these results suggest drug accumulation. Plasma half-life values appeared to increase with dose and ranged from 4 to 11 h (53).

The effects of food on the pharmacokinetic profile of lonafarnib were examined in 2 randomized, crossover phase I studies: a single-dose (100 mg after an overnight fast or a high-fat breakfast) study in 12 subjects and a multiple-dose (200 mg b.i.d. for a 28-day cycle under fasted conditions and a 28-day cycle under fed conditions separated by a 2-week washout period) in 12 patients with advanced cancer. The agent was safe and generally well tolerated in both studies. Results from the single-dose study showed that food intake reduced the rate (about 50%) and extent of absorption (about 23%) (C_{max} = 323 and 154 ng/ml, AUC = 2077 and 1556 ng·h/ml, t_{max} = 3 and 8 h, respectively, for fasted and fed states). However, in the multiple-dose study, no significant difference in the pharmacokinetics on day 15 were observed between fasted and fed states (C_{max} = 2.77 and 2.27 ng/ml, AUC = 24.1 and 21.6 ng·h/ml, t_{max} = 4 and 4 h, respectively, for fasted and fed states) (54, 55).

A phase I/II study conducted in patients with solid tumors (n=3-8/dose) showed that a single dose of paclitaxel (135 or 175 mg/m^2 by single 3-h i.v. infusion on a 3-week cycle) did not influence the pharmacokinetics of multiple-dose lonafarnib (100, 125 or 150 mg p.o. b.i.d. in 3-week cycles). Similarly, multiple-dose lonafarnib did not alter the pharmacokinetics of paclitaxel (56).

Results from an open-label phase I study conducted in patients (n=3-7/dose) indicated that multiple lonafarnib doses (100, 150 or 200 mg p.o. b.i.d. for 15 days) did not affect the pharmacokinetics of gemcitabine (600, 750 or 1000 mg/m^2 i.v. once a week) (57).

Clinical Studies

Phase I studies

A phase I dose-escalation trial in 20 patients with solid tumors determined the maximum tolerated dose (MTD) and efficacy of lonafarnib (25, 50, 100, 200, 300, 350 and 400 mg p.o. b.i.d. for 7 days on a 21-day cycle). Patients received 92 courses. At the highest dose, moderate, reversible renal insufficiency secondary to dehydration from gastrointestinal toxicity was observed. The DLTs at this dose level were gastrointestinal toxicities (nausea, vomiting and diarrhea) and fatigue. A patient with previously treated metastatic NSCLC who was on the study for 14 months had a partial response. Analysis of buccal mucosa cells of treated patients showed inhibition of prelamin A farnesylation, indicating successful inhibition of FTase (58).

A randomized phase IB trial in 22 previously untreated patients with squamous cell carcinoma of the head and neck who were scheduled for surgical resection examined the efficacy of induction therapy with lonafarnib (100, 200 or 300 mg p.o. b.i.d. for 8-14 days before surgery). Seventeen patients were treated with the agent and 5 were randomized to no therapy before surgery. Only moderate toxicity was observed, which included grade 1 nausea (n=4), grade 1/2 diarrhea (n=5) with grade 3 dehydration (n=1), grade 1/2 anemia (n=9) and grade 1 thrombocytopenia (n=7). Of the 17 treated patients, 3 patients with skin, oral cavity and oropharynx as primary sites (2 of whom received the highest dose) had partial remission before surgery. Resected surgical specimens from all treated patients showed inhibition of DNA-J (11-50% increases in unfarnesylated DNA-J) and prelamin A (59).

The efficacy of lonafarnib (200 mg p.o. b.i.d.) was examined in a pilot study involving 12 previously treated patients with chronic- or accelerated-phase CML resistant or refractory to imatinib. Because 2 patients experienced a rapid increase in white blood cells (WBCs) at 7-10 days after the initiation of therapy, transient use of hydroxyurea was allowed. Median duration of therapy was 10 weeks. Two patients continued on therapy after 13 and 17 weeks, respectively. Diarrhea was the most common adverse event seen in 10 patients, with grade 3 or greater reported in 4 patients requiring dose adjustments. One patient developed grade 3 nausea. One patient with accelerated-phase CML and who received hydroxyurea for 2 weeks had hematological remission and resolution of splenomegaly lasting for 3 months. Another patient with chronic-phase CML who did not receive hydroxyurea also had a response and continues to receive treatment after 4 months. An alteration in differential count was noted so that increases in myelocytes and promelocytes, and sometimes WBCs, were observed in 6 patients, possibly indicative of an effect on differentiation (60).

A phase I trial examined the tolerability and efficacy of lonafarnib (200 or 300 mg p.o. b.i.d.) in 19 patients with hematological malignancies including acute myelogenous leukemia (AML), acute lymphocytic leukemia (ALL), CML-BC (blast crisis), CMML and myelodysplastic syndrome (MDS). A DLT of grade 3 diarrhea and hypokalemia unresponsive to diarrhea therapy was seen at the higher dose. Other adverse events noted at both dose levels included grade 2 diarrhea, nausea, fatigue and weakness. The lower dose was concluded to be well tolerated. During the first cycle, 2 deaths occurred due to disease progression. Of 17 evaluable patients, 3 of 5 with CMML, 2 of 4 with Ph-positive CML-BC or ALL, and 1 of 7 with AML had clinical responses (*e.g.*, erythroid, neutrophil, platelet responses and/or a > 50% decrease in blast or monocyte count). Inhibition of DNA-J farnesylation was observed at both dose levels (61).

A phase I study in 24 patients with solid tumors examined the safety and efficacy of combination therapy with lonafarnib (100, 125 or 150 mg p.o. b.i.d.) and paclitaxel (135 or 175 mg/m^2). No grade 3 or higher toxicities were observed in the 3 patients receiving 100 mg lonafarnib + 135 mg/m^2 paclitaxel. However, 2 of 8 patients receiving 100 mg lonafarnib + 175 mg/m^2 paclitaxel had grade 3 dehydration and grade 3 hyperbilirubinemia and 1 of 3 patients given 150 mg lonafarnib + 175 mg/m^2 paclitaxel had grade 4 neutropenia with fever. Of the 18 evaluable patients, partial responses were obtained in 3 of 6 previously untreated patients (2 stage IV NSCLC and 1 metastatic salivary gland tumor) and 3 of 6 extensively pretreated patients with metastatic NSCLC. The maximum tolerated dose (MTD) was determined to be 100 mg lonafarnib + 175 mg/m^2 paclitaxel (62).

Another phase I trial in 27 patients with advanced malignancies (colon, NSCLC, renal, melanoma, pancreatic, adrenal, prostate, sarcoma, hepatoma, biliary tract and unknown) examined the tolerability of lonafarnib (100, 125, 150 or 200 mg p.o. b.i.d. on days 3-28 of cycle 1 and days 1-28 for subsequent cycles) combined with paclitaxel (40, 60 or 80 mg/m^2/week on day 1 of each week). A total of 87 cycles were administered. A DLT of myelosuppression was seen in 2 of 3 patients given 150 mg lonafarnib + 80 mg/m^2 paclitaxel. Other toxicities reported included nausea, vomiting, diarrhea, fatigue/weakness and taste alterations. The MTD was determined to be 125 mg lonafarnib + 80 mg/m^2 paclitaxel (63).

The tolerability of combination treatment including lonafarnib (75, 100, 125 or 100 mg b.i.d. on days 6-21 of

cycle 1 and days 1-21 for subsequent cycles), paclitaxel (125, 150, 175 or 200 mg/m^2 as 3-h i.v. infusion on day 1) and carboplatin (AUC = 5 as 30-min i.v. infusion following paclitaxel) was examined in a phase I trial conducted in 27 patients with solid tumors. Twenty-six patients have completed a total of 86 cycles (1 patient withdrew prior to treatment). Treatment was well tolerated. DLTs of neutropenia and diarrhea were seen in 2 patients receiving 75 mg lonafarnib + 125 mg/m^2 paclitaxel + carboplatin, and diarrhea was reported in 1 patient administered 125 mg lonafarnib + 175 mg/m^2 paclitaxel + carboplatin. Other toxicities observed were fatigue, nausea/vomiting, diarrhea, alopecia, neuropathy and dry mouth. One patient discontinued carboplatin in cycle 13 for hypersensitivity reactions. Patient enrollment continues (64).

The tolerability of lonafarnib (50, 100, 125, 150 or 200 mg p.o. b.i.d. continuously starting on day 1) combined with docetaxel (60 or 75 mg/m^2 as 1-h i.v. infusion every 3 weeks starting on day 8) was studied in a phase I trial in 13 patients with solid malignancies (NSCLC, esophageal, head and neck, mesothelioma, SCLC and thyroid) and no more than 2 prior chemotherapy regimens. Treatment was well tolerated. A DLT of diarrhea/fatigue was seen in 1 of 6 patients administered 125 mg lonafarnib + 75 mg/m^2 docetaxel. Other adverse events reported included nausea, vomiting, diarrhea, neutropenia, thrombocytopenia and fatigue. Patient enrollment continues (65).

A phase I dose-escalation trial conducted in 25 patients with advanced malignancies reported the tolerability and efficacy of lonafarnib (100, 150 or 200 mg p.o. b.i.d. continuously) combined with gemcitabine (600, 750 or 1000 mg/m^2 on days 1, 8 and 15 every 28 days). The median duration of treatment was 6 months. Dose-limiting toxicities seen included nausea, vomiting, diarrhea and moderate myelosuppression, which were controlled with dose changes. Two partial responses were obtained in patients with pancreatic malignancies. Two patients with pancreatic malignancies and mesothelioma achieved minor responses. Long-term disease stability of greater than 6 months was reported for 11 patients. Examination of buccal smears from patients showed accumulation of prelamin A (66).

A phase I trial in 14 patients with advanced cancers examined the tolerability and efficacy of combination treatment including lonafarnib (75-125 mg p.o. b.i.d.), cisplatin (75-100 mg/m^2) and increasing doses of gemcitabine (750-1000 mg/m^2 weekly x 3) in 28-day cycles. A total of 27 courses have been administered. Non-hematological toxicities reported were nausea/vomiting (grade 1/2 in 52% of the courses; grade 3 in 37%), grade 1/2 fatigue (in 41%), grade 1 transaminase elevations (in 41%), grade 1 tinnitus (in 26%) and grade 1/2 diarrhea (in 15%). Dose-limiting toxicities of grade 2 thrombocytopenia and neutropenic fever were seen in 2 patients receiving 75 mg lonafarnib + 75 mg/m^2 cisplatin + 1000 mg/m^2 gemcitabine and in 2 patients receiving 100 mg lonafarnib + 100 mg/m^2 cisplatin + 1000 mg/m^2 gemcitabine. Lonafarnib was discontinued for nausea/vomiting in 1 patient who had received 100 mg lonafarnib + 75 mg/m^2 cisplatin + 1000 mg/m^2 gemcitabine and 2 other patients withdrew due to persistent nausea/vomiting or fatigue. Analysis of peripheral blood mononuclear cells revealed a reduction in FTase (37.5 ± 16.7%) activity in 7 of 8 patients receiving a regimen including 75 mg lonafarnib. Accrual continues (67).

Phase I/II studies

The efficacy and tolerability of lonafarnib (200 mg p.o. b.i.d. for 3 courses of 4 weeks separated by 1-4 weeks off treatment) as a treatment for MDS or secondary AML were examined in a phase I/II trial conducted in 16 patients. The major adverse events reported were gastrointestinal toxicities (diarrhea, nausea and anorexia) and myelosuppression. Other adverse events included infections, fatigue, elevations in liver enzymes, arrhythmia and skin rash. One patient was discontinued due to atrial fibrillation and another died from infection. Dose reductions were required in all but 1 patient treated with more than 1 course. Of the 12 patients evaluable for response, 2 partial responses were observed in patients who did not present Ras mutations. One of these patients, who had secondary AML with complex chromosome abnormalities, had reductions in blasts of 8% after the first course and remained stable after the second course. However, the patient discontinued due to gastrointestinal toxicity. The other patient had RAEB (with 5q- and 20 q-) and experienced reductions in blasts of 3% with normal karyotype and FISH (fluorescence *in situ* hybridization) screening after 1 course. However, excess blasts and chromosomal abnormalities returned despite continued treatment (68).

A phase I/II trial examined the efficacy and tolerability of lonafarnib (100 mg p.o. b.i.d.) in combination with paclitaxel (175 mg/m^2 i.v. over 3 h) in patients with NSCLC who failed previous therapy with paclitaxel (76%), docetaxel (39%), or both (15%). A median of 5 treatment cycles were administered. Combination treatment was well tolerated. Only minimal toxicity was observed, which included grade 3 fatigue in 3 patients, diarrhea, dyspnea and weakness in 2 patients and neutropenia in 1 patient. Two patients suffered grade 4 respiratory insufficiency and 1 patient each had grade 4 fatigue or neutropenic fever, respectively. Of the 34 evaluable patients, 5 and 15 patients had partial responses and stable disease, respectively (69).

Phase II studies

A phase II trial examining the efficacy and tolerability of lonafarnib monotherapy (starting dose of 200 mg p.o. b.i.d. as continuous daily dosing) in 21 patients with metastatic colorectal cancer who were refractory to first- and second-line therapy (5-fluorouracil and irinotecan) did not recommend future development of the agent for

this indication. The major adverse events reported were grade 1 (42%), 2 (42%) and 3 (14%) fatigue, grade 1 (23%) and 3 (42%) diarrhea and grade 2 (16%) nausea. Grade 2 or 3 elevations in serum creatinine, probably due to diarrhea-induced dehydration, were seen in 19% of the patients. No significant hematological toxicities were observed, although 19% of the patients developed grade 1 thrombocytopenia and 28% had grade 2 or 3 anemia. No objective responses were obtained, although 3 patients did have stable disease lasting for months (70).

A multicenter, randomized phase II trial in 15 patients with unresectable or metastatic transitional cell carcinoma of the urothelial tract who failed prior chemotherapy examined the efficacy and tolerability of lonafarnib (200 mg p.o. b.i.d. daily repeated every 28 days with allowance for dose escalation). Fourteen patients were evaluable, with 7, 3 and 4 receiving less than 4 weeks, 4-7 weeks and 8 weeks of therapy, respectively. Grade 3 and 4 toxicities related to treatment were fatigue, anorexia, nausea/vomiting, confusion, dehydration and dyspnea. Significant hematological toxicities were less common and included grade 3 and 4 anemia, neutropenia and thrombocytopenia. Four patients were discontinued and 3 required hospitalization for toxicities. Of the 7 patients evaluable for response, 1 had stable disease while 6 had disease progression. The trial will be stopped if more than 9 patients of the total 15 patients have progressive disease at 8 weeks (71).

An ongoing, open-label phase II trial in 54 adult patients with CML-BC, CMML, ALL, advanced MDS or relapsed, refractory or poor-risk AML examined the tolerability and efficacy of lonafarnib (200 mg p.o. b.i.d. continuously). Treatment was well tolerated. Ten patients have developed hematological toxicities. One of the 19 patients with AML had a pathological response (decrease in marrow blast count from 64% to 32%). Of the 15 patients with MDS, 1 patient had minor erythroid improvement and major platelet improvement, 1 patient had minor erythroid improvement and 1 patient had minor platelet improvement. Normalization of monocyte counts was seen in 6 of the 12 patients with CMML (72).

The safety and efficacy of lonafarnib (200 mg p.o. b.i.d.) were compared to gemcitabine (1000 mg/m^2 weekly for 7 weeks followed by 1 week of rest) in a randomized phase II trial in 63 patients with metastatic adenocarcinoma of the pancreas. A similar incidence of nausea, vomiting and diarrhea was seen in both treatment groups, although cases were more severe with gemcitabine. Moreover, fewer cases of thrombocytopenia and neutropenia were seen in the group receiving lonafarnib (0% vs. 17% and 3% vs. 17%, respectively). The 3-month progression-free survival rate for patients administered lonafarnib was 23% as compared to 31% for gemcitabine. Partial responses and stable disease were seen in 2 and 6 patients receiving lonafarnib, respectively, while 1 and 11 patients receiving gemcitabine had a partial response and stable disease, respectively. Due to the favorable results obtained in this study, future evaluation of lonafarnib in combination with gemcitabine will be performed in patients with advanced pancreatic cancer (73).

Source

Schering-Plough Corp. (US).

References

1. Prous, J., Castañer, J. *Loratadine.* Drugs Fut 1987, 12: 544-9.

2. Njoroge, F.G., Vibulbhan, B., Rane, D.F. et al. *Structure-activity relationship of 3-substituted N-(pyridinylacetyl)-4-(8-chloro-5,6-dihydro-11H-benzo[5,6]cyclohepta[1,2-b]pyridin-11-ylidene)-piperidine inhibitors of farnesyl-protein transferase: Design and synthesis of in vivo active antitumor compounds.* J Med Chem 1997, 40: 4290-301.

3. Njoroge, F.G., Taveras, A.G., Kelly, J. et al. *(+)-4-[2-[4-(8-Chloro-3,10-dibromo-6,11-dihydro-5H-benzo[5,6]cyclohepta[1,2-b]-pyridin-11(R)-yl)-1-piperidinyl]-2-oxo-ethyl]-1-piperidinecarboxamide (SCH-66336): A very potent farnesyl protein transferase inhibitor as a novel antitumor agent.* J Med Chem 1998, 41: 4890-902.

4. Doll, R.J., Kelly, J.M., Njoroge, F.G., Mallams, A.K., Remiszewski, S.W., Taveras, A.G. (Schering Corp.). *Tricyclic amides useful for inhibition of G-protein function and for treatment of proliferative diseases.* EP 1019392, JP 1999501671, WO 9723478.

5. Mallams, A.K. (Schering Corp.). *Method for preparing substd. 1-piperidinecarboxamide derivs.* WO 9804549.

6. Njoroge, F.G., Vibulbhan, B., Girijavallabhan, V.M. (Schering Corp.). *Process for producing (8-chloro-3,10-dibromo-6,11-dihydro-5H-benzo[5,6]cyclohepta[1,2-b]pyridin-11-yl)-1-piperidine.* EP 1091954, JP 2002519419, WO 0001689.

7. Morgan, B., Zaks, A., Dodds, D.R. et al. *Enzymatic kinetic resolution of piperidine atropisomers: Synthesis of a key intermediate of the farnesyl protein transferase inhibitor, SCH66336.* J Org Chem 2000, 65: 5451-9.

8. Bos, J.L. *Ras oncogenes in human cancer: A review.* Cancer Res 1989, 49: 4682-9.

9. Lowy, D.R., Willumsen, B.M. *Function and regulation of ras.* Annu Rev Biochem 1993, 62: 851-91.

10. Rowinsky, E.K., Windle, J.J., Von Hoff, D.D. *Ras protein farnesyltransferase: A strategic target for anticancer therapeutic development.* J Clin Oncol 1999, 17: 3631-52.

11. Rowinsky, E.K. *Inhibiting farnesyl transferase: Rehauling the notion for optimal therapeutic development.* Cancer Invest 2003, 21(Suppl. 1): Abst 66.

12. Hahn, S.M., Bernhard, E., McKenna, W.G. *Farnesyltransferase inhibitors.* Semin Oncol 2001, 28(5, Suppl. 16): 86-93.

13. Adjei, A.A. *Protein farnesyl transferase as a target for the development of anticancer drugs.* Drugs Fut 2000, 25: 1069-79.

14. Ashar, H.R., James, L., Gray, K. et al. *Farnesyl transferase inhibitors block the farnesylation of CENP-E and CENP-F*

and alter the association of CENP-E with the microtubules. J Biol Chem 2000, 275: 30451-7.

15. Hruban, R.H., van Mansfeld, A.D., Offerhaus, G.J. et al. *K-ras oncogene activation in adenocarcinoma of the human pancreas. A study of 82 carcinomas using a combination of mutant-enriched polymerase chain reaction analysis and allele-specific oligonucleotide hybridization.* Am J Pathol 1993, 143: 545-54.

16. Breivik, J., Meling, G.I., Spurkland, A., Rognum, T.O., Gaudernack, G. *K-ras mutation in colorectal cancer: Relations to patient age, sex and tumour location.* Br J Cancer 1994, 69: 367-71.

17. Slebos, R.J., Kibbelaar, R.E., Dalesio, O. et al. *K-ras oncogene activation as a prognostic marker in adenocarcinoma of the lung.* New Engl J Med 1990, 323: 561-5.

18. Abo, J., Inokuchi, K., Dan, K., Nomura, T. *p53 and N-ras mutations in two new leukemia cell lines established from a patient with multilineage CD7-positive acute leukemia.* Blood 1993, 82: 2829-36.

19. Barbacid, M. *Ras genes.* Annu Rev Biochem 1987, 56: 779-827.

20. Sorbera, L.A., Fernández, R., Castañer, J. *R-115777.* Drugs Fut 2001, 25: 453-61.

21. Ganguly, A.K., Doll, R.J., Girijavallabhan, V.M. *Farnesyl protein transferase inhibition: A novel approach to anti-tumor therapy. The discovery and development of SCH 66336.* Curr Med Chem 2001, 8: 1419-36.

22. Choy, W.N., Murli, H., Morrissey, R.E., MacDonald, J.S. *Absence of genotoxic potential of an anticancer agent: A farnesyl transferase inhibitor (SCH 66336).* Mutat Res 2001, 483(Suppl. 1): S98.

23. Petit, T., Izbicka, E., Lawrence, R.A., Bishop, W.R., Weitman, S., Von Hoff, D.D. *Activity of SCH 66336, a tricyclic farnesyltransferase inhibitor, against human tumor colony-forming units.* Ann Oncol 1999, 10: 449-53.

24. Jun, K.H., Lee, H.-Y., Hassan, K., Khuri, F., Hong, W.K.I., Lotan, R. *The farnesyltransferase inhibitor SCH66336 induces apoptosis through down-regulation of AKT signaling pathway in human head and neck squamous cell carcinoma (HNSCC) cell lines.* Proc Am Assoc Cancer Res 2002, 43: Abst 4034.

25. Hassan, K.A., Wu, W., Wang, L. et al. *Dephosphorylation and downregulation of Akt is associated with farnesyltransferase inhibitor (SCH66336) treatment in head and neck squamous cell carcinoma cell lines.* Proc Am Assoc Cancer Res 2002, 43: Abst 4666.

26. Brassard, D.L., English, J.M., Malkowski, M., Kirschmeier, P., Nagabhushan, T.L., Bishop, W.R. *Inhibitors of farnesyl protein transferase and MEK1,2 induce apoptosis in fibroblasts transformed with farnesylated but not geranylgeranylated H-Ras.* Exp Cell Res 2002, 273: 138-46.

27. Feldkamp, M.M., Lau, N., Guha, A. *The farnesyl transferase inhibitor SCH66336 inhibits the growth of human astrocytoma cell lines and xenografts implanted in NOD-SCID mice.* Proc Am Assoc Cancer Res 2000, 41: Abst 2834.

28. Liu, M., Bryant, M.S., Chen, J. et al. *Antitumor activity of SCH 66336, an orally bioavailable tricyclic inhibitor of farnesyl protein transferase, in human tumor xenograft models and wap-ras transgenic mice.* Cancer Res 1998, 58: 4947-56.

29. Grafone, T., Martinelli, G., Ottaviani, E. et al. *Different effects of the farnesyl protein transferase inhibitors in vitro against MK2 and MK1 cell lines Philadelphia chromosome (Ph)-positive.* Blood 2002, 100(11, Part 1): Abst 3115.

30. Reichert, A., Heisterkamp, N., Daley, G.Q., Groffen, J. *Treatment of Bcr/Abl-positive acute lymphoblastic leukemia in P190 transgenic mice with the farnesyl transferase inhibitor SCH66336.* Blood 2001, 97: 1399-403.

31. Whyte, D.B., Kirschmeier, P., Hockenberry, T.N. et al. *K- and N-Ras are geranylgeranylated in cells treated with farnesyl protein transferase inhibitors.* J Biol Chem 1997, 272: 14459-64.

32. Loprevite, M., Favoni, R.E., Mazzanti, P., de Cupis, A., Pirani, P., Grossi, F., Ardizzoni, A. *Pre-clinical evaluation of the farnesyltransferase inhibitor SCH 66336 in non-small cell lung cancer (NSCLC) cell lines.* Clin Cancer Res 2000, 6(Suppl.): Abst 400.

33. Ashar, H.R., James, L., Gray, K. et al. *The farnesyl transferase inhibitor SCH 66336 induces a G2→M or G1 pause in sensitive human tumor cell lines.* Exp Cell Res 2001, 262: 17-27.

34. Peters, D.G., Hoover, R.R., Gerlach, M.J. et al. *Activity of the farnesyl protein transferase inhibitor SCH66336 against BCR/ABL-induced murine leukemia and primary cells from patients with chronic myeloid leukemia.* Blood 2001, 97: 1404-12.

35. Bishop, W.R. *Preclinical and translational studies of the farnesyl transferase inhibitor SCH 66336 (lonafarnib).* Proc Am Assoc Cancer Res 2003, 44(2nd ed): Invited Abstracts.

36. Bishop, W.R., Patton, R., Bohanon, S. et al. *Evaluation of biochemical markers of protein farnesylation in human tumor specimens following treatment with oral SCH 66336, an inhibitor of farnesyl protein transferase.* Proc Am Assoc Cancer Res 2001, 42: Abst 1400.

37. Smalley, K.S.M., Eisen, T.G. *Farnesyl transferase inhibitor SCH66336 is cytostatic, pro-apoptotic and enhances chemosensitivity to cisplatin in melanoma cells.* Int J Cancer 2003, 105: 165-75.

38. Lee, S., Mayer-Ezell, R., Sanchez, R. et al. *SCH66336, a farnesyl transferase inhibitor, decreases the levels of angiogenic growth factors in various tumor models.* Proc Am Assoc Cancer Res 2001, 42: Abst 2636.

39. List, A.F., Tache-Tallmadge, C., Tate, W. et al. *Lonafarnib (Sarasar®) modulates integrin affinity to promote homotypic and heterotypic adhesion of chronic myelomonocytic leukemia (CMML) cells.* Proc Am Assoc Cancer Res 2003, 44: Abst 4620.

40. Wang, E.-J., Casciano, C.N., Clement, R.P., Johnson, W.W. *The farnesyl protein transferase inhibitor SCH66336 is a potent inhibitor of MDR1 product P-glycoprotein.* Cancer Res 2001, 61: 7525-9.

41. Shi, B., Yaremko, B., Hajian, G., Terracina, G., Bishop, W.R., Liu, M., Nielsen, L.L. *The farnesyl protein transferase inhibitor SCH66336 synergizes with taxanes in vitro and enhances their antitumor activity in vivo.* Cancer Chemother Pharmacol 2000, 46: 387-93.

42. Adjei, A.A., Davis, J.N., Bruzek, L.M., Erlichman, C., Kaufmann, S.H. *Synergy of the protein farnesyltransferase inhibitor SCH66336 and cisplatin in human cancer cell lines.* Clin Cancer Res 2001, 7: 1438-45.

43. Liang, L., Gheyas, F., Lee,S. et al. *SCH 66336 (lonafarnib), a farnesyl transferase inhibitor, demonstrates enhanced antitumor efficacy in combination with the alkylating agents temozolomide, cisplatin, and carboplatin.* Proc Am Assoc Cancer Res 2003, 44(2nd ed): Abst 807.

44. Nielsen, L.L., Shi, B., Hajian, G. et al. *Combination therapy with the farnesyl protein transferase inhibitor SCH66336 and SCH58500 (p53 adenovirus) in preclinical cancer models.* Cancer Res 1999, 59: 5896-901.

45. Nakajima, A., Tauchi, T., Sumi, M., Bishop, R.W., Ohyashiki, K. *Efficacy of SCH66336, the farnesyl transferase inhibitor, against Gleevec-resistant BCR-ABL-positive cells.* Proc Am Assoc Cancer Res 2002, 43: Abst 4235.

46. Hoover, R.R., Mahon, F.-X., Melo, J.V., Daley, G.Q. *Overcoming STI571 resistance with the farnesyltransferase inhibitor SCH66336.* Blood 2001, 98(11, Part 1): Abst 2585.

47. Hoover, R.R., Mahon, F.-X., Melo, J.V., Daley, G.Q. *Overcoming STI571 resistance with the farnesyl transferase inhibitor SCH66336.* Blood 2002, 100: 1068-71.

48. a) Brodsky, A.L. *Apoptotic synergism between STI571 and the farnesyl transferase inhibitor SCH66336 on an imatinib-sensitive cell line.* Blood 2003, 101: 2070. b) Daley, G.Q., Hoover, R.R., Carr, D., Kirschmeier, P. *SCH66336/lonafarnib together with STI571/imatinib shows synergistic killing of BCR/ABL transformed leukemia cells.* Blood 2003, 101: 2070-1.

49. Chang, Y.S., Khuri, F.R., Hassan, K.A. et al. *IGFBP-3 and the farnesyl transferase inhibitor SCH66336 act synergistically to induce apoptosis in non-small cell lung cancer (NSCLC) cells.* Proc Am Assoc Cancer Res 2003, 44(2nd ed): Abst 6177.

50. Kim, H., Likhari, P., Lin, C.-C., Nomeir, A.A. *High-performance liquid chromatographic analysis of the anti-tumor agent SCH 66336 in cynomolgus monkey plasma and evaluation of its chiral inversion in animals.* J Chromatogr B - Biomed Sci Appl 1999, 728: 133-41.

51. Bryant, M.S., Liu, M., Wang, S. et al. *Pharmacokinetics of a potent orally bioavailable inhibitor of farnesyl protein transferase in the mouse, rat and cynomolgus monkey.* Proc Am Assoc Cancer Res 1998, 39: Abst 2177.

52. Awada, A., Eskens, F.A.L.M., Piccart, M. et al. *Phase I and pharmacological study of the oral farnesyltransferase inhibitor SCH 66336 given once daily to patients with advanced solid tumours.* Eur J Cancer 2003, 38: 2272-8.

53. Eskens, F.A.L.M., Awada, A., Cutler, D.L. et al. *Phase I and pharmacokinetic study of the oral farnesyl transferase inhibitor SCH 66336 given twice daily to patients with advanced solid tumors.* J Clin Oncol 2001, 19: 1167-75.

54. Zhu, Y., Statkevich, P., Cutler, D.L., Pember, L., Curtis, D., Batra, V.K. *Effect of food on the pharmacokinetics of lonafarnib, a farnesyl protein transferase inhibitor.* Clin Pharmacol Ther 2002, 71(2): Abst WPIII-23.

55. Zhu, Y., Statkevich, P., Cutler, D.L., Calzetta, A., Rosen, L.S., Curtis, D., Batra, V.K. *Reduced effect of food on the pharmacokinetics of lonafarnib following multiple oral doses.* Clin Pharmacol Ther 2003, 73(2): Abst PIII-18.

56. Statkevich, P., Zhu, Y., Curtis, D. et al. *Pharmacokinetics of lonafarnib and paclitaxel when coadministered to patients with solid tumors.* Annu Meet Am Assoc Pharm Sci (AAPS) (Nov 10-14, Toronto) 2002, Abst T2259.

57. Zhu, Y., Statkevich, P., Cutler, D.L., Calzetta, A., Curtis, D., Batra, V.K. *Lonafarnib, a farnesyl protein transferase inhibitor, does not affect the pharmacokinetics of gemcitabine.* Annu Meet Am Assoc Pharm Sci (AAPS) (Nov 10-14, Toronto) 2002, Abst T2263.

58. Adjei, A.A., Erlichman, C., Davis, J.N. et al. *A phase I trial of the farnesyl transferase inhibitor SCH66336: Evidence for biological and clinical activity.* Cancer Res 2000, 60: 1871-7.

59. Kies, M.S., Clayman, G.L., El-Naggar, A.K. et al. *Induction therapy with SCH 66336, a farnesyltransferase inhibitor, in squamous cell carcinoma (SCC) of the head and neck.* Proc Am Soc Clin Oncol 2001, 20(Part 1): Abst 896.

60. Cortes, J.E., Daley, G., Talpaz, M. et al. *Pilot study of SCH66336 (lonafarnib), a farnesyl transferase inhibitor (FTI), in patients with chronic myeloid leukemia (CML) in chronic or accelerated phase resistant or refractory to imatinib.* Blood 2002, 100(11, Part 1): Abst 614.

61. List, A. , Cortes, J., DeAngelo, D., O'Brien, S., Zaknoen, S., Baum, C., Wilson, J. *Phase I study of continuous oral administration of lonafarnib (SCH66336) in patients with advanced myelodysplastic syndrome (MDS), acute myeloid leukemia (AML), chronic myeloid leukemia blast crisis (CML-BC), and acute lymphoblastic leukemia (ALL).* Cancer Invest 2003, 21(Suppl. 1): Abst 67.

62. Khuri, F.R., Glisson, B.S., Meyers, M.L., Statkevich, P., Bangert, S., Hong, W.K. *Phase I study of farnesyl transferase inhibitors (FTI) SCH66336 with paclitaxel in solid tumors: Dose finding, pharmacokinetics, efficacy/safety.* Clin Cancer Res 2000, 6(Suppl.): Abst 403.

63. Lipton, A., Ready, N., Bukowski, R.M., Zaknoen, S., Heck, K.-A., Statkevich, P., Zhu, Y. *Phase I study of continuous oral lonafarnib plus weekly paclitaxel for advanced cancer.* Proc Am Soc Clin Oncol 2002, 21(Part 1): Abst 364.

64. Sprague, E., Vokes, E.E., Garland, L.L. et al. *Phase I study of continuous lonafarnib plus paclitaxel and carboplatin in refractory or advanced solid tumors.* Proc Am Soc Clin Oncol 2002, 21(Part 2): Abst 1920.

65. Zaknoen, S.L., Crawford, J., Shepherd, F., Bennett, D., Statkevich, P., Zhu, Y., Khuri, F. *Phase I study of oral lonafarnib plus docetaxel as second-line treatment for advanced solid tumors.* Proc Am Soc Clin Oncol 2002, 21(Part 2): Abst 2136.

66. Hurwitz, H., Amado, R., Prager, D. et al. *Phase I pharmacokinetic trial of the farnesyl transferase inhibitor SCH66336 plus gemcitabine in advanced cancers.* Proc Am Soc Clin Oncol 2000, 19: Abst 717.

67. Pierson, A.S., Holden, S.N., Basche, M. et al. *A phase I pharmacokinetic (PK) and biological study of the farnesyl transferase inhibitor (FTI) Sarasar (lonafarnib, SCH66336), cisplatin (C), and gemcitabine (G) in patients (pts) with advanced solid tumors.* Proc Am Soc Clin Oncol 2002, 21(Part 1): Abst 365.

68. Ravoet, C., Mineur, P., Robin, V. et al. *Phase I-II study of a farnesyl transferase inhibitor (FTI), SCH66336, in patients with myelodysplastic syndrome (MDS) or secondary acute myeloid leukemia (sAML).* Blood 2002, 100(11, Part 1): Abst 3136.

69. Khuri, F. *Phase I/II trials of Sarasar™ (lonafarnib) in non-small cell lung cancer.* Cancer Invest 2003, 21(Suppl 1): Abst 55.

70. Sharma, S., Kemeny, N., Kelsen, D.P. et al. *A phase II trial of farnesyl protein transferase inhibitor SCH 66336, given by twice-daily oral administration, in patients with metastatic colorectal cancer refractory to 5-fluorouracil and irinotecan.* Ann Oncol 2002, 13: 1067-71.

71. Winquist, E., Moore, M.J., Chi, K. et al. *NCIC CTG IND.128: A phase II study of a farnesyl transferase inhibitor (SCH 66336) in patients with unresectable or metastatic transitional cell carcinoma of the urothelial tract failing prior chemotherapy*. Proc Am Soc Clin Oncol 2001, 20(Part 1): Abst 785.

72. Cortes, J., Holyoake, T.L., Silver, R.T. et al. *Continuous oral lonafarnib (Sarasar™) for the treatment of patients with advanced hematologic malignancies: A phase II study.* Blood 2002, 100(11, Part 1): Abst 3132.

73. Lersch, C., Van Cutsem, E., Amado, R. et al. *Randomized phase II study of SCH 66336 and gemcitabine in the treatment of metastatic adenocarcinoma of the pancreas.* Proc Am Soc Clin Oncol 2001, 20(Part 1): Abst 608.

Additional References

Feldkamp, M., Nelson, L., Guha, A. *The farnesyl transferase inhibitor SCH66336 inhibits the growth of human astrocytoma cell lines and xenografts implanted in NOD-SCID mice.* Can J Neurol Sci 2000, 27(Suppl. 2): Abst P-092.

Khuri, F., Glisson, B., Meyers, M. et al. *Phase I study of farnesyl transferase inhibitor (FTI) SCH66336 with paclitaxel in solid tumors: Dose finding, pharmacokinetics, efficacy/safety.* Proc Am Soc Clin Oncol 2000, 19: Abst 799.

Kim, E.S., Kies, M.S., Fossella, F.V. et al. *A phase I/II study of the farnesyl transferase inhibitor (FTI) SCH66336 (lonafarnib) with paclitaxel in taxane-refractory/resistant patients with non-small cell lung cancer (NSCLC): Final report.* Proc Am Assoc Cancer Res 2002, 43: Abst 2735.

Kim, E.S., Glisson, B.S., Meyers, M.L. et al. *A phase I/II study of the farnesyl transferase inhibitor (FTI) SCH66336 with paclitaxel in patients with solid tumors.* Proc Am Assoc Cancer Res 2001, 42: Abst 2629.

Liu, M., Lee, S., Yaremko, B. et al. *SCH 66336, an orally bioavailable tricyclic farnesyl protein transferase inhibitor, demonstrates broad and potent in-vivo antitumor activity.* Proc Am Assoc Cancer Res 1998, 39: Abst 1843.

Kirschmeier, P., Carr, D., Gray, K. et al. *SCH 66336, an orally bioavailable tricyclic farnesyl transferase inhibitor blocks anchorage-independent growth of ras-transformed fibroblasts and human tumor cell lines.* Proc Am Assoc Cancer Res 1998, 39: Abst 2175.

Njoroge, F.G., Taveras, A., Kelly, J. et al. *Orally active, trihalobenzocycloheptapyridine farnesyl protein transferase inhibitor antitumor agents.* Proc Am Assoc Cancer Res 1998, 39: Abst 2176.

Adjei, A., Erlichman, C., Davis, J.N. et al. *A phase I and pharmacologic study of the farnesyl protein transferase (FPT) inhibitor SCH 66336 in patients with locally advanced or metastatic cancer.* Proc Am Soc Clin Oncol 1999, 18: Abst 598.

Hurwitz, H., Colvin, O.M., Petros, W. et al. *Phase I and pharmacokinetic study of SCH66336, a novel FPTI, using a 2-week on, 2-week off schedule.* Proc Am Soc Clin Oncol 1999, 18: Abst 599.

Eskens, F., Awada, A., Verweij, J., Cutler, D.L., Hanauske, A., Piccart, M. *Phase 1 and pharmacological study of continuous daily oral SCH 66336, a novel farnesyl transferase inhibitor, in patients with solid tumors.* Proc Am Soc Clin Oncol 1999, 18: Abst 600.

Awada, A., Eskens, F., Piccart, M.J. et al. *A clinical, pharmacodynamic and pharmacokinetic phase I study of SCH 66336 (SCH) an oral inhibitor of the enzyme farnesyl transferase given once daily in patients with solid tumors.* AACR-NCI-EORTC Int Conf Mol Targets Cancer Ther (Nov 16-19, Washington DC) 1999, Abst 20.

Izbicka, E., Lawrence, R., Davidson, K. et al. *Activity of a farnesyl protein transferase inhibitor (SCH 66336) against a broad range of tumors taken directly from patients.* Proc Am Assoc Cancer Res 1999, 40: Abst 3454.

Brassard, D.L., Kirschmeier, P., Nagabhushan, T.L., Bishop, W.R. *Proapoptotic effects of the farnesyl transferase inhibitor, SCH 66336, on Ras-transformed Rat2 fibroblasts.* Proc Am Assoc Cancer Res 1999, 40: Abst 3455.

Ashar, H., James, L., Gray, K. et al. *A potential role for centromere-associated proteins and the nuclear phosphatase PTP-CAAX-1 in cell cycle changes and p53 induction by the farnesyl transferase inhibitor SCH 66336.* Proc Am Assoc Cancer Res 1999, 40: Abst 3456.

Shi, B., Gurnani, M., Yaremko, B. et al. *Enhanced efficacy of the farnesyl protein transferase inhibitor SCH66336 in combination with paclitaxel.* Proc Am Assoc Cancer Res 1999, 40: Abst 3457.

Nielsen, L.L., Shi, B., Gurnani, M. et al. *Combination therapy using SCH58500 (p53 adenovirus) and SCH66336 (farnesyl protein transferase inhibitor) has enhanced efficacy in preclinical cancer models.* Proc Am Assoc Cancer Res 1999, 40: Abst 3458.

Ashar, H.R., James, L., Gray, K. et al. *The farnesyl transferase inhibitor SCH 66336 induces cell cycle changes in sensitive human tumor cell lines and prevents the farnesylation of the centromere associated proteins CENP-E and CENP-F*. Proc Am Assoc Cancer Res 2000, 41: Abst 1398.

Taveras, A.G., Njoroge, F.G., Kelly, J. et al. *Advancing the frontiers of anticancer therapy: Discovery of the farnesyl protein transferase inhibitor SCH-66336.* 219th ACS Natl Meet (March 26-30, San Francisco) 2000, Abst MEDI 293.

Peters, D.G., Hoover, R.R., Koh, E.Y. et al. *Activity of the farnesyl transferase inhibitor SCH66336 against BCR-ABL-induced murine leukemia, STI571-resistant CML cell lines, and primary cells from CML patients.* Blood 2000, 96(11, Part 1): Abst 2193.

Nakajima, A., Tauchi, T., Sumi, M., Bishop, W.R., Ohyashiki, K. *Efficacy of SCH66336, the farnesyl transferase inhibitor, in conjunction with other antileukemic agents against Glivec-resistant BCR-ABL-positive cells.* Blood 2001, 98(11, Part 1): Abst 2409.

Johnson, W.W., Wang, E.-J., Obrocea, M., Casciano, C., Clement, R. *The farnesyl protein transferase inhibitor SCH66336 is a potent inhibitor of MDR1 product P-glycoprotein.* Proc Am Assoc Cancer Res 2001, 42: Abst 1409.

List, A.F., DeAngelo, D., O'Brien, S. et al. *Phase I study of continuous oral administration of lonafarnib (Sarasar™) in patients*

with advanced hematologic malignancies. Blood 2002, 100(11, Part 1): Abst 3120.

Smalley, K.S.M., Eisen, T. *The farnesyltransferase inhibitor SCH 66336 induces apoptosis and augments the effects of cisplatin in meloma cells.* Proc Am Assoc Cancer Res 2002, 43: Abst 4665.

Wu, W., Hassan, K.A., Hong, W.K., Mao, L., Khuri, F.R. *Proteomic identification of proteins associated with farnesyltransferase inhibitor treatment.* Proc Am Assoc Cancer Res 2002, 43: Abst 4667.

Liu, M., Bishop, W.R., Nielsen, L.L., Bryant, M.S., Kirschmeier, P. *Orally bioavailable farnesyltransferase inhibitors as anticancer agents in transgenic and xenograft models.* Methods Enzymol 2001, 333: 306-18.

Johnston, S.R.D., Kelland, L.R. *Farnesyl transferase inhibitors - A novel therapy for breast cancer.* Endocr-Relat Cancer 2001, 8: 227-35.

Hudes, G.R. *Signaling inhibitors in the treatment of prostate cancer.* Invest New Drugs 2002, 20: 159-73.

Herrera, R., Sebolt-Leopold, J.S. *Unraveling the complexities of the Raf/MAP kinase pathway for pharmacological intervention.* Trends Mol Med 2002, 8(4, Suppl.): S27-31.

Drugs of the Future 2008, 33(6): 478-488

CCC: 0377-8282/2008
DOI: 10.1358/dof.2008.033.06.1217989

Brostallicin Hydrochloride

Minor Groove-Binding Agent
Oncolytic

Rec INNM

PNU-166196A

2-[4-[4-[4-[4-(2-Bromo-2-propenamido)-1-methylpyrrol-2-ylcarboxamido]-1-methylpyrrol-2-ylcarboxamido]-1-methylpyrrol-2-ylcarboxamido]-1-methylpyrrol-2-ylcarboxamido]ethylguanidine hydrochloride

InChI=1/C30H35BrN12O5.ClH/c1-16(31)25(44)36-17-9-22(41(3)12-17)27(46)38-19-11-24(43(5)14-19)29(48)39-20-10-23(42(4)15-20)28(47)37-18-8-21(40(2)13-18)26(45)34-6-7-35-30(32)33;/h8-15H,1,6-7H2,2-5H3,(H,34,45)(H,36,44)(H,37,47)(H,38,46)(H,39,48)(H4,32,33,35);1H

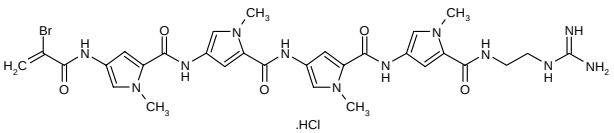

$C_{30}H_{36}BrClN_{12}O_5$
Mol wt: 760.0414

CAS: 203258-38-2

CAS: 203258-60-0 (free base)

EN: 262512

Abstract

Soft tissue sarcomas (STS) are a group of rare tumors, most of which are relatively resistant to standard chemotherapeutic agents. To date, favorable efficacy data exist for only a small number of agents in this disease. Minor groove binders (MGBs) are a new class of anticancer agents that theoretically provide a unique mechanism of antitumor activity. Brostallicin hydrochloride, a synthetic, second-generation MGB, has been shown to possess activity in STS. This article therefore aims to review the current evidence on the use of brostallicin in STS. Preclinical data have shown that brostallicin possesses certain features likely to be beneficial in the treatment of STS, such as activation in the presence of high levels of glutathione and/or glutathione *S*-transferase, as well as being unaffected by defects in DNA mismatch repair. Phase I trials established the maximum tolerated dose as 10 mg/m^2 and showed a partial response in a patient with a gastrointestinal stromal tumor. Phase II trials have shown encouraging progression-free survival figures in those with STS and further trials are ongoing to compare brostallicin with doxorubicin.

Synthesis[+]

Brostallicin can be prepared by reduction of the synthetic nitro-tripyrrole (I) with H_2 and Pd/C, followed by acylation of the resulting amine (II) with 4-(2-bromoacryloylamino)-1-methylpyrrole-2-carbonyl chloride (III) under Schotten-Baumann conditions (1, 2). Alternatively, the intermediate tripyrrolyl-amine (II) can be obtained by acidic cleavage of the Boc-protected precursors (IVa) and (IVb), which are obtained by functional group manipulation of the natural product distamycin A (3-5). In a further strategy, brostallicin is prepared by acylation of the tetrapyrrolyl-amine (V) with 2-bromoacrylic acid (VI) in the presence of EDC (6). Scheme 1.

The tripyrrolyl precursor (I) can be synthesized as follows. Protection of ethylenediamine (VII) with Boc_2O in dioxane followed by treatment of the resulting mono-protected diamine (VIII) with either *S*-methylisothiourea (IXa) (1, 7) or *O*-methylisourea (IXb) (2, 6) gives guanidine (X), which by subsequent acidic cleavage of the Boc groups yields (2-aminoethyl)guanidine (XI) (1, 2, 6, 7). This compound is then acylated with 1-methyl-4-nitropyrrole-2-carbonyl chloride (XII) using $NaHCO_3$ in aqueous dioxane to afford the nitropyrrole-carboxamide (XIII), which is reduced to the aminopyrrole analogue (XIV) by catalytic hydrogenation over Pd/C. Aminopyrrole (XIV) is then subjected to a new coupling–hydrogenation cycle with acid chloride (XII) to provide the dipyrrole derivative (XV). A further coupling of (XV) with acid chloride (XII) furnishes the nitro-tripyrrolyl precursor (I) (2, 7, 8). An analogous sequence has been applied to the synthesis of isotopically labeled brostallicin, using either deuterim-labeled ethyl-

Eitan Amir, Richard W. Griffiths, Michael G. Leahy*. Department of Medical Oncology, Christie Hospital, NHS Foundation Trust, Manchester, UK. *Correspondence: michael.leahy@christie.nhs.uk. [+]Synthesis prepared by N. Serradell, E. Rosa, J. Bolós, R. Castañer. Prous Science, Provenza 388, 08025 Barcelona, Spain.

Scheme 1: Synthesis of Brostallicin

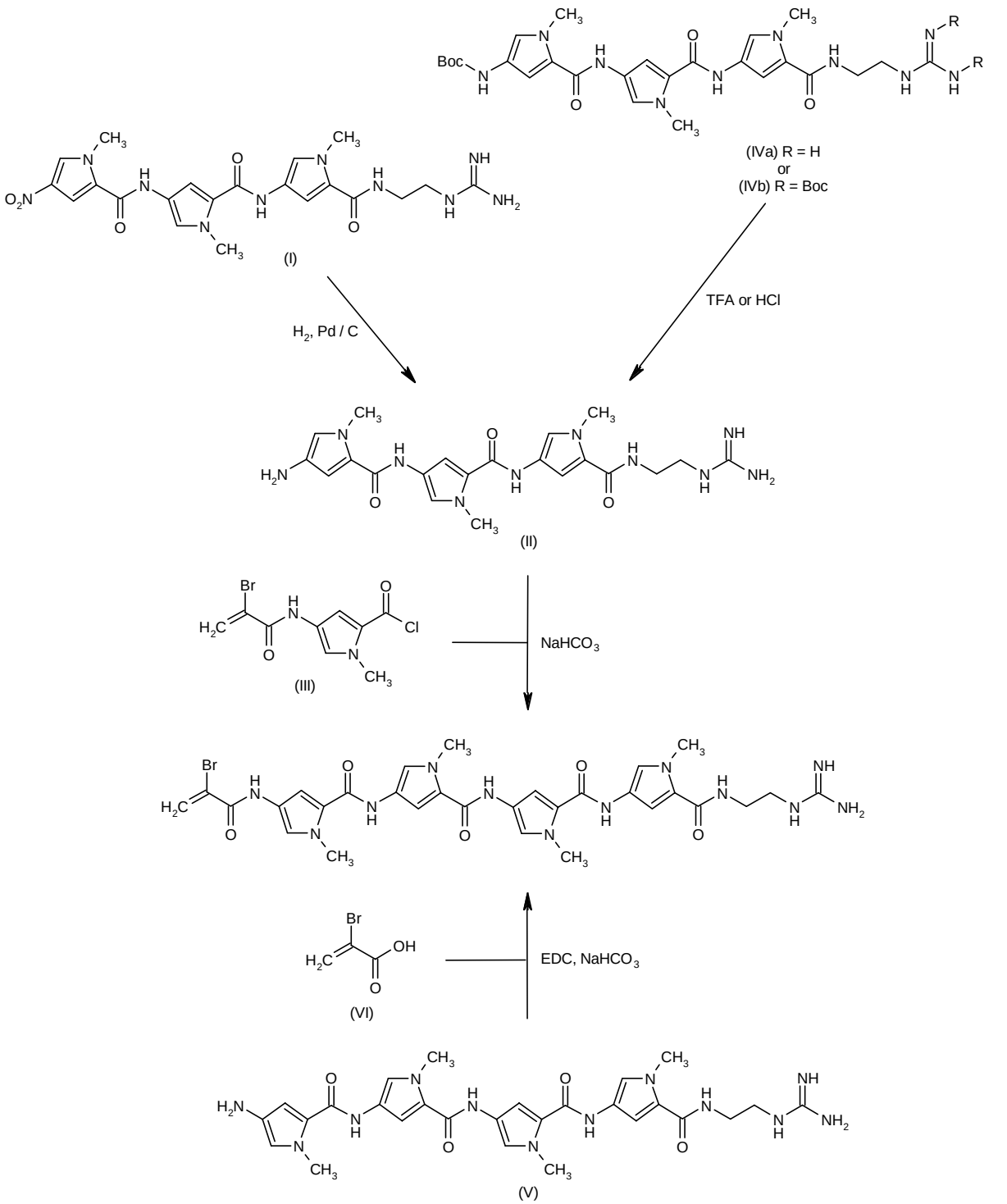

enediamine [^{2}H]-(VII) or 1-methyl-4-nitropyrrole-2-carbonyl chloride labeled with ^{14}C at the C-2 position [^{14}C]-(XII) (2). Alternatively, intermediate (I) can be prepared by coupling of aminoguanidine (XI) with the known tripyrrolyl carboxylic acid (XVI) in the presence of DCC and HOBt (1). Scheme 2.

The Boc-protected precursor (IVa) can be prepared starting from the natural antibiotic distamycin A (XVII).

Scheme 2: Synthesis of Precursor (I)

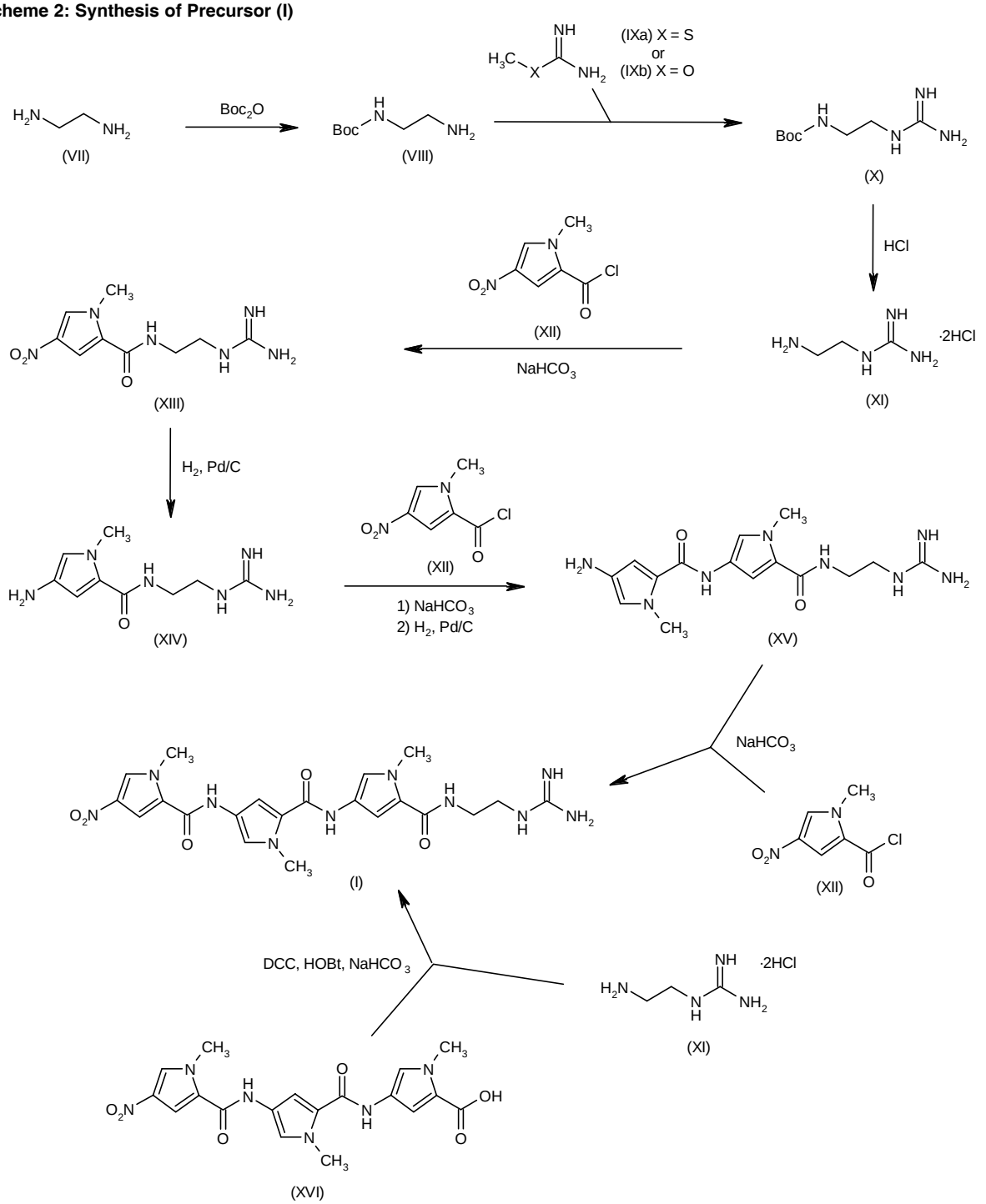

Elimination of ammonia from distamycin A (XVII) by heating with succinic anhydride and Na_2CO_3 in DMF leads to nitrile (XVIII), which by stepwise protection of its formamide NH group with Boc_2O and DMAP in CH_2Cl_2 and then the amide NH with further addition of Boc_2O in DMF affords the di-Boc compound (XIX). Subsequent hydrolysis of the formyl and cyanoethyl amide groups of (XIX) using LiOH in THF/H_2O provides the tripyrrolyl carboxylic acid (XX), which is finally coupled with (2-aminoethyl)guanidine (XI) by means of TBTU in DMF (3, 5). Scheme 3.

Scheme 3: Synthesis of Precursor (IVa)

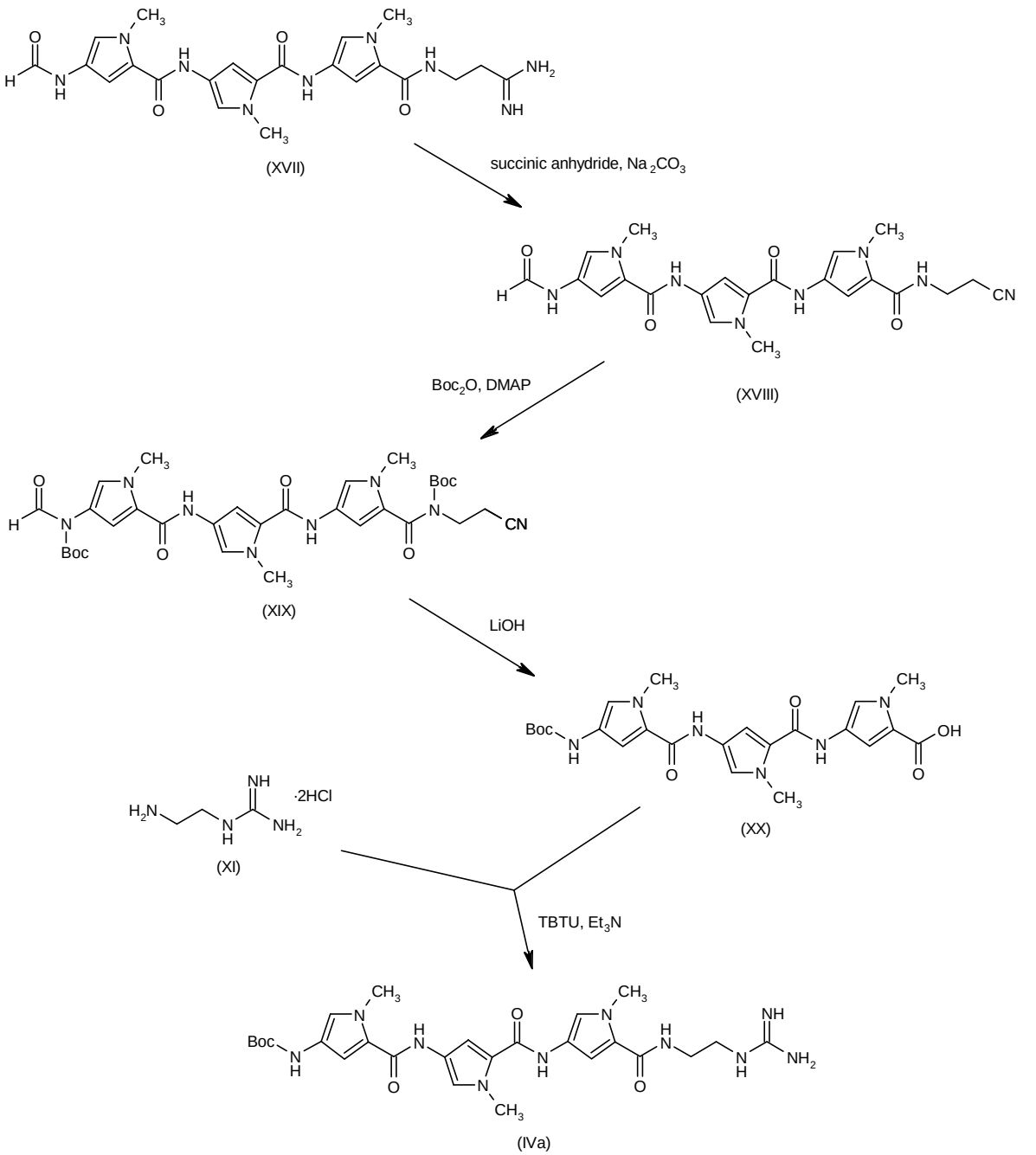

(XVII) (XVIII) (XIX) (XX) (XI) (IVa)

The tri-Boc derivative (IVb) can also be prepared from distamycin A (XVII) by the following method. Hydrolysis of (XVII) with NaOH in refluxing methanol gives the amino acid (XXI), which by subsequent protection with Boc_2O and Et_3N in DMF followed by Curtius rearrangement of the carboxy group by treatment with diphenylphosphoryl azide affords imidazolidinone (XXII). Hydrolysis of compound (XXII) with NaOH in DMF provides the aminoethyl amide (XXIII), which is converted to the Boc-protected guanidine (IVb) by reaction with *N,N*'-di-Boc-*N*''-trifluoromethylsulfonylguanidine (XXIV) in the presence of Et_3N in DMF (4). Scheme 4.

The tetrapyrrolyl-amine precursor (V) is obtained by the following procedure. 1-Methyl-4-nitropyrrole-2-car-

Scheme 4: Synthesis of Precursor (IVb)

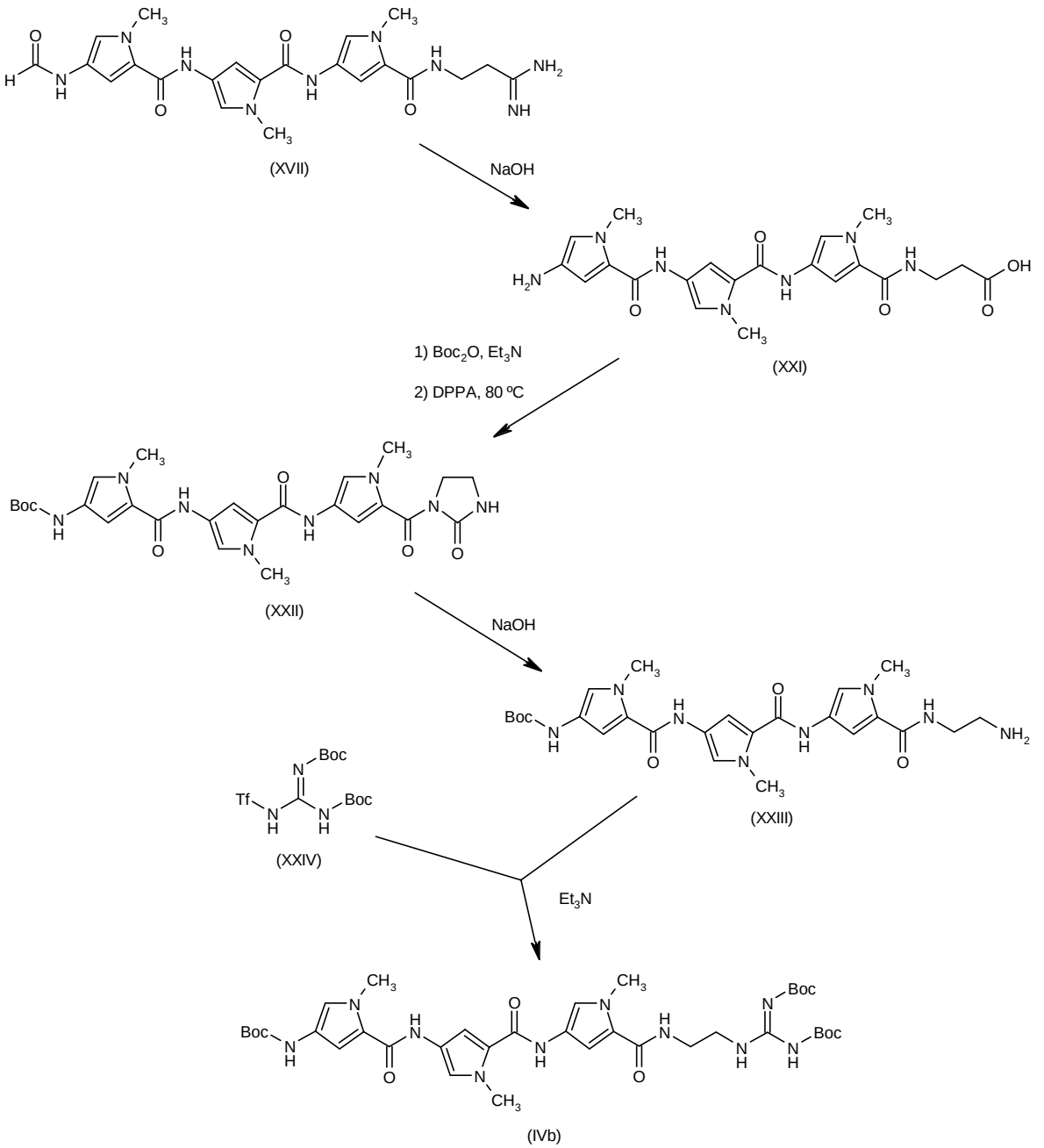

boxylic acid (XXV) is reduced to the aminopyrrole (XXVI) by catalytic hydrogenation in the presence of Pd/C. Alternatively, chlorination of acid (XXV) with $SOCl_2$ provides the pyrrolecarbonyl chloride (XII). Then, condensation between aminopyrrole (XXVI) and acid chloride (XII) using $NaHCO_3$ in aqueous dioxane gives the dipyrrolyl amide (XXVII), which is converted to the acid chloride (XXVIII) by treatment with $SOCl_2$ and a catalytic amount of DMF. Condensation of acid chloride (XXVIII) with (2-aminoethyl)guanidine (XI) yields compound (XXIX), which by reduction of the nitro group with H_2 and Pd/C leads to the aminopyrrole (XXX). This compound is then coupled with a second moiety of the dipyrrolyl-acid chloride (XXVIII) to provide the tetrapyrrolyl compound (XXXI), which is finally reduced at the nitro group by catalytic hydrogenation over Pd/C (6). Scheme 5.

Scheme 5: Synthesis of Precursor (V)

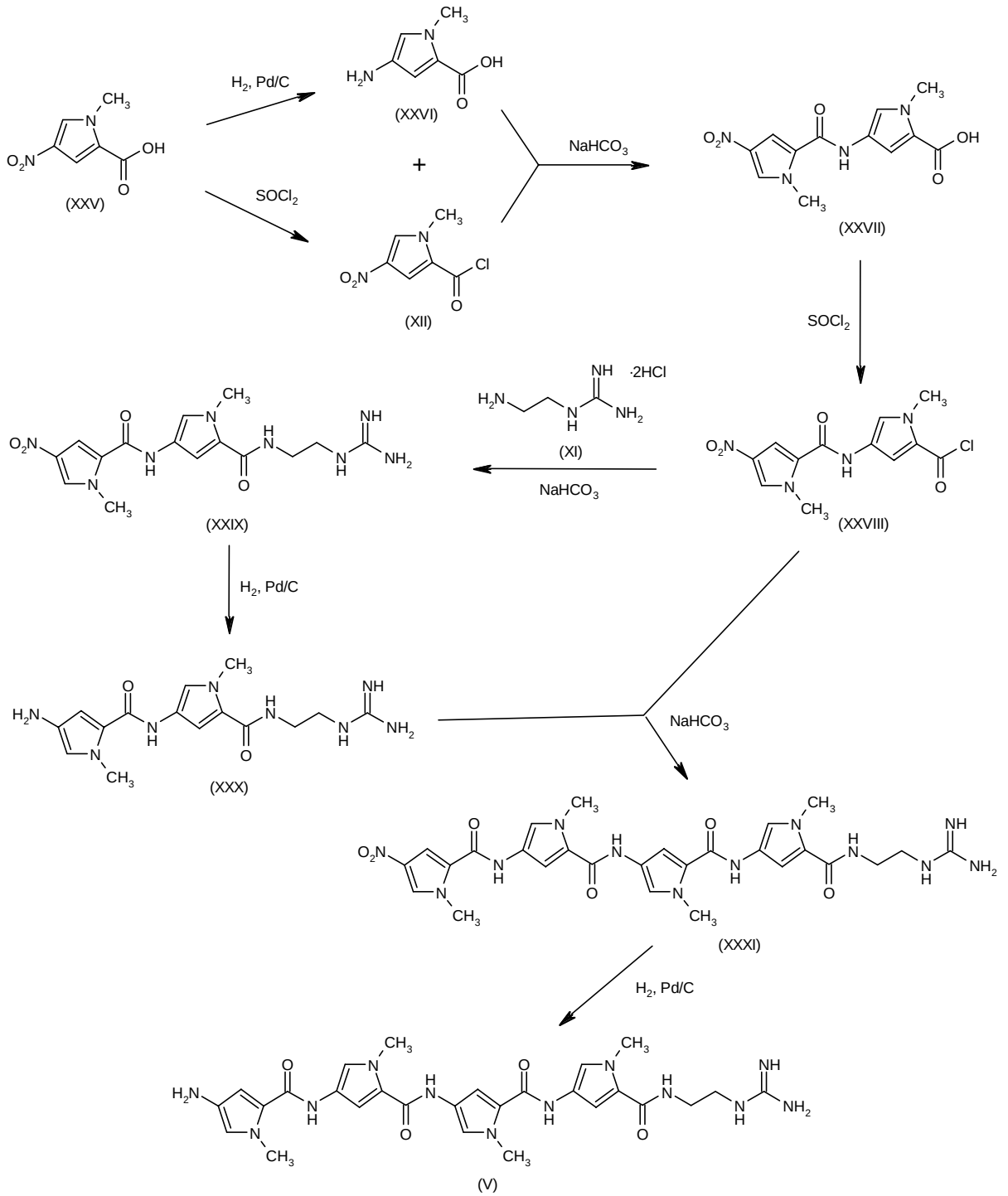

Background

Sarcomas are rare tumors with an estimated annual incidence of approximately 2-3 per 100,000 persons, and therefore account for < 1% of all solid malignancies (9, 10). These tumors usually, but not exclusively, arise from fat, muscle, nerve, nerve sheath, blood vessels, bone and other connective tissues. Although often previously

lumped together, they are a heterogeneous group of malignancies of mesenchymal cell origin with diverse clinical and pathological features. Within this group, a number of distinct clinical entities are recognized which have specific treatment protocols, including systemic therapy: osteosarcomas, the Ewing's family of tumors (including peripheral primitive neuroectodermal tumors [PNETs]), rhabdomyosarcoma and gastrointestinal stromal tumors (GISTs) (11, 12). For the remainder of histotypes (which together form the majority of cases), surgery remains the mainstay of treatment, with systemic therapy reserved for patients with advanced disease.

Soft tissue sarcomas (STSs) can occur anywhere in the body, but most originate in an extremity (59%), the trunk (19%), the retroperitoneum (15%), or the head and neck (9%) (13). There are more than 50 histological subtypes, with the most common being fibrosarcoma (18%), leiomyosarcoma (16%), liposarcoma (6%) and synovial sarcoma (1%) (10). In many tumors, it may be difficult or impossible to identify specific features of morphological differentiation, and these have been given different names over the last 50 years, causing some confusion (14).

With the exception of those tumor types mentioned above, current treatment protocols for metastatic STS are doxorubicin-based chemotherapy regimens with or without ifosfamide as front-line therapy. These drugs have been shown to have single-agent activity, with data showing response rates in the range of 10-30% (15-18). Data on dose-intense chemotherapy supported by hematopoietic growth factors or peripheral blood stem cell transplantation (PBSCT) have shown trends towards increased response rates of up to 50-60%. Unfortunately, there has been no substantial improvement in overall survival (19-23). Furthermore, dose escalation of anthracyclines is limited by nonhematological side effects, especially cardiotoxicity.

Second-line chemotherapeutic options in advanced STS after progression during or after doxorubicin are limited. Established drugs in this setting are ifosfamide (if not previously coadministered with doxorubicin as first-line therapy) and dacarbazine (24, 25). Progress in the development of other agents for use in STS has sadly been slow. Many different cytotoxic agents have been tested in phase II trials accepting all-comers with different STS subtypes, and most of these have been classed as negative trials. More recently, a number of new distinct tumor types have emerged from the pack which may respond differently to systemic agents and deserve individual treatment protocols. These include, most dramatically, the treatment of GISTs with imatinib (26), and also the treatment of Kaposi's sarcoma with liposomal doxorubicin, cutaneous angiosarcoma with paclitaxel (27) and perhaps some leiomyosarcomas with gemcitabine and docetaxel (28).

More recently, a new group of cytotoxic agents with a novel mechanism of action has attracted attention in the treatment of sarcoma. Minor groove binders (MGBs) represent a class of anticancer agents whose DNA sequence specificity leads to a highly selective mechanism of action (29-31). Unlike most cytotoxic agents, which bind the DNA major groove, MGBs fit into the space formed between the two phosphate–sugar backbones in the double helix. MGBs tend to have high selectivity for sequences rich in thymine–adenine and this theoretically provides their unique mechanism of action (32, 33). First-generation MGBs, such as agents derived from either CC-1065 (34-36) or the nitrogen mustard derivative of distamycin A tallimustine (37, 38), were found to be very active against experimental tumors unresponsive to other antineoplastic agents. Unfortunately, they did not proceed in clinical studies because of their severe dose-limiting myelotoxicity (39, 40).

The first MGB with a favorable efficacy and toxicity profile was ecteinascidin-743 (ET-743, trabectedin, Yondelis®; PharmaMar), a natural marine product derived from the tunicate *Ecteinascidia turbinata*. Phase II trials in Europe and in the U.S. have revealed that, although it was associated with low objective response rates of only 5-10% (41, 42), it had particularly high antitumor activity in liposarcoma, especially the myxoid liposarcoma subtype (43), and treatment led to disease stabilization (progression arrest) in a high proportion of patients. Retrospective analysis of the European Organisation for the Research and Treatment of Cancer (EORTC) database of clinical trials in STS has identified that progression-free survival (PFS) may be a good discriminant of active compounds and more sensitive than the traditional clinical trial endpoint of overall objective response rate (44). When the PFS of patients with STS treated with trabectedin was analyzed, it was found to segregate with the PFS seen in trials with doxorubicin and ifosfamide and was significantly different from the PFS seen in trials of agents considered inactive.

More recently, favorable data have been reported for the use of the MGB brostallicin. Brostallicin hydrochloride (PNU-166196A; Pfizer) is a synthetic, second-generation DNA MGB comprising a distamycin A backbone covalently linked to an α-bromoacryloyl group. As with trabectedin, brostallicin was selected for clinical development because of its positive antitumor activity, again based partly on significant prolongation of expected PFS, as well as its favorable toxicity profile (30, 45-47). This article will therefore review the development of brostallicin and its establishment in the treatment of STSs.

Preclinical Pharmacology

Initial laboratory work showed that brostallicin could exert antitumor activity against several murine and human tumor xenografts (40). The mechanism of action of brostallicin appears to be unique among MGB agents in that it has no DNA-alkylating activity *per se*, but is activated in the presence of high levels of glutathione (GSH) and/or glutathione *S*-transferase (GST) (48-50). Some chemotherapeutic drugs and other MGBs rely on their direct DNA-alkylating effect for cytotoxicity, and as such display little activity against tumor cell lines deficient in DNA mismatch repair enzymes (51-53). Notably, the

cytotoxicity of brostallicin is unaffected by defects in mismatch repair or other DNA repair enzymes, such as the products of the ataxia telangiectasia mutated (*ATM*) gene and DNA-dependent protein kinase (DNA-PK) (50). This is of relevance to STS, where DNA mismatch repair enzyme deficiencies have been identified and correlated with inferior survival (54).

In vitro evaluations of brostallicin have also shown potential for efficacy in refractory tumors, particularly those expressing high levels of GSH/GST, which has been associated with primary or acquired resistance to a number of anticancer drugs, including nitrogen mustards, platinum agents and anthracyclines (49, 55-59). Both *in vitro* and *in vivo* studies using isogenic cell systems differing only in the expression of the GST-π isozyme have shown that sensitivity to brostallicin occurred not only in cultured cell lines but also in tumors transplanted into nude mice (40, 49).

In vitro data from these experiments have shown that brostallicin possessed 3-fold higher activity in melphalan-resistant murine leukemia cells than in the parental cell line. These melphalan-resistant cell lines have increased levels of GSH in comparison with the parental cells. Conversely, depletion of GSH using buthionine sulfoximine in a human ovarian carcinoma cell line significantly decreased both the cytotoxic and the proapoptotic effects of brostallicin. It was postulated that GSH, as an intracellular reactive nucleophilic species, could react with the α-bromoacrylamide moiety of brostallicin, leading to the formation of a highly reactive GSH complex representing the real effective agent of brostallicin activity. Further *in vitro* work has confirmed that the α-bromoacryloyl moiety of brostallicin reacts with GSH, allowing it to covalently bind with DNA, inducing cell cycle arrest and activating proapoptotic signaling pathways via as yet uncertain mediators. The reaction between brostallicin and GSH is thought to be catalyzed by GST, with the π and μ isozymes being more effective than the α isozyme (49).

In vivo data derived from human ovarian carcinoma clones implanted into nude mice have also confirmed that the antitumor activity of brostallicin was higher in the GST-π-overexpressing tumors. In this experiment, ovarian cancer clones with different GST-π content were implanted into nude mice and the antitumor activity of brostallicin was evaluated. Results showed that brostallicin exhibited greater activity in the GST-π-overexpressing tumors than in the tumors expressing normal levels of the enzyme, without increased toxicity (40).

In an attempt to extrapolate brostallicin's enhanced activity in the presence of high GSH/GST levels, further work has evaluated the possible augmentation of the efficacy of brostallicin using thiol antioxidants. In this study, human nasopharyngeal squamous carcinoma and human hepatic carcinoma cell lines were treated with *N*-acetylcysteine and silibinin and brostallicin, either alone or in combination. Paradoxically, results showed that thiol antioxidants in fact reduced brostallicin's cytotoxicity. It was proposed that the mechanism underlying this interaction involved the inhibition of apoptosis, as an increase in Bcl-2 protein levels and a decrease in caspase-3 activity were detected with the silibinin–brostallicin combination (60). There are little further data in the literature relating to the combination of brostallicin with other agents and this is an area of research that requires further work.

Clinical Studies

The seminal phase I trial of brostallicin was reported by Ten Tije and colleagues in their study in 27 patients with a variety of solid tumors. This trial concluded that brostallicin was well tolerated, neutropenia being the principal toxicity. The maximum tolerated dose from this study was 10 mg/m^2 on a 21-day cycle. Common Terminology Criteria for Adverse Events v3.0 (CTCAE) (61) grade 4 neutropenia was the only dose-limiting toxicity at 12.5 mg/m^2, whereas grade 4 thrombocytopenia and grade 4 neutropenia were the dose-limiting toxicities at 15 mg/m^2. Of note, 1 partial response was observed in a patient with a GIST (62).

In view of the favorable response in the patient with GIST and due to the high level of GSH and GSH-related enzymes in STSs, confirmatory phase II trials were carried out to investigate the potential role of brostallicin in STS.

To date, there have been two phase II trials designed to evaluate the use of brostallicin in STS. The first of these trials was undertaken by the Soft Tissue and Bone Sarcoma Group (STBSG) of the EORTC. In this study (EORTC 62011) (63), the antitumor activity of brostallicin in patients with locally advanced or metastatic STS who had failed one prior chemotherapy treatment was explored. The patient population was stratified into two groups according to histological diagnosis, with one group comprising GIST tumors only and the other group including patients with any other type of STS (non-GIST). The primary endpoint was overall response rate. Predefined secondary endpoints included time to tumor progression, duration of objective response and the safety profile of brostallicin. Twenty-one patients with GIST and 43 patients with non-GIST were recruited. In the GIST group, there were no patients with a confirmed response and hence recruitment into this arm was discontinued subsequent to the first interim analysis. In the non-GIST group, there were 2 confirmed partial responses among the 40 patients with evaluable disease (5% of cohort). Twenty patients (50%) had stable disease. The 3- and 6-month PFS was 46% and 22%, respectively, in the non-GIST group and 33% and 21%, respectively, in the GIST group. Median survival in the non-GIST group was 231 days (range 159-421 days), while in the GIST group a figure of 298 days (range 188-?) was recorded. In general, the drug was well tolerated. Neutropenia was the most common toxicity, with CTCAE grade 3 or grade 4 toxicities observed in 22% and 48% of patients, respectively. Pyrexia associated with such neutropenic toxicity was seen in 14% of patients, while there was a single confirmed toxic death due to neutropenic septicemia. Fatigue was the most common nonhematological toxicity.

CTCAE grade 3 or grade 4 fatigue was recorded in 25% of patients. Finally, 3 patients had clinically significant allergic reactions to the 249 cycles of treatment delivered.

Evidence shows that a favorable PFS after administration of second-line agents in STS may suggest antitumor activity in the first-line setting. In a retrospective analysis of 11 agents investigated by the EORTC STBSG (64), it was shown that patients treated with either of the two agents with known clinical activity in first-line treatment (doxorubicin or ifosfamide) had improved outcome in second-line treatment. In this setting, the PFS at 3 and 6 months was significantly higher than in patients treated with agents classed as inactive. It was therefore suggested that 3-month PFS > 40% or 6-month PFS > 20% after second-line therapy might be a signal for clinically significant benefit in first-line therapy.

In view of the encouraging PFS seen in the above phase II study, the authors concluded that further investigation of brostallicin in the first-line treatment of non-GIST STS appeared to be warranted. Consequently, the EORTC has commenced a trial to evaluate the efficacy of brostallicin in the first-line setting (EORTC 62061, BRTA-0100-015) (65). In this ongoing phase II trial, patients with advanced or metastatic STS are being randomized to receive either brostallicin or doxorubicin. The predefined primary endpoint is 6-month PFS, with secondary endpoints including overall PFS, objective tumor response, toxicity, duration of response and overall survival. This study will include different strata for the main subtypes of STS. It is planned for 108 patients to be recruited into this study. Interim results are expected in the next 12 months.

Summary

Brostallicin is a novel cytotoxic agent with an interesting mechanism of action, suggesting that it may be able to overcome some chemoresistant mechanisms identified in human cancers. It is a generally well-tolerated antineoplastic agent with mild to moderate myelosuppression as the principle toxicity. In studies performed thus far, this has been a manageable and reversible side effect. Early trials have shown that, although objective tumor responses are infrequent, the drug is associated with a favorable 3-month PFS of about 40% in a group of patients with a range of STS histological subtypes. There are, however, major weaknesses in the data published on the use of brostallicin in STS. It is becoming well recognized that different histological subtypes of STS demonstrate different sensitivities to different agents and should perhaps be treated differently (44, 66). It is therefore imperative that future trials be sufficiently powered to present robust data on the efficacy of brostallicin in different subtypes of STS. The rarity of STS makes this a considerable challenge for oncologists, but it is hoped that the EORTC 62061 study will go some way to providing such information.

Source

Cell Therapeutics, Inc. (US).

References

1. Cozzi, P., Beria, I., Biasoli, G., Caldarelli, M., Capolongo, L., Franzetti, C. (Pfizer AB). *Acryloyl substituted distamycin derivatives, process for preparing them, and their use as antitumor and antiviral agents*. JP 2000515164, WO 9804524.

2. Fontana, E., Pignatti, A. *Synthesis of brostallicin (PNU-166196A) labelled with 2H and 14C*. J Label Compd Radiopharm 2002, 45(11): 899.

3. Beria, I., Nesi, M. *Syntheses of brostallicin starting from distamycin A*. Tetrahedron Lett 2002, 43(41): 7323.

4. Beria, I., Cozzi, P., Mongelli, N., Orzi, F. (Pharmacia & Upjohn SpA). *Process for preparing distamycin derivatives*. WO 0202523.

5. Beria, I., Cozzi, P. (Pharmacia & Upjohn SpA). *Process for preparing distamycin derivatives*. WO 0208184.

6. Caldarelli, F., Candiani, I., Ceriani, L. (Pfizer Italia Srl). *Process for preparing distamycin derivatives*. CA 2427177, EP 1347958, JP 2004517830, US 2004077550, US 6906199, WO 0244147.

7. Beria, I., Baraldi, P.G., Cozzi, P. et al. *Cytotoxic α-halogenoacrylic derivatives of distamycin A and congeners*. J Med Chem 2004, 47(10): 2611-23.

8. Beria, I., Caldarelli, M., Cozzi, P., Geroni, C., Mongelli, N., Pennella, G. *Cytotoxic α-bromoacrylic derivatives of distamycin analogues modified at the amidino moiety*. Bioorg Med Chem Lett 2000, 10(11): 1273-6.

9. Zahm, S.H., Tucker, M.A., Fraumeni, J.F. Jr. *Soft tissue sarcomas*. In: Cancer Epidemiology and Prevention, 2nd Ed. Schottenfeld, D., Fraumeni, J.F. Jr. (Eds.). Oxford University Press, New York, 1996, 984-99.

10. Zahm, S.H., Fraumeni, J.F. Jr. *The epidemiology of soft tissue sarcoma*. Semin Oncol 1997, 24(5): 504-14.

11. Bertuzzi, A., Castagna, L., Nozza, A. et al. *High-dose chemotherapy in poor-prognosis adult small round-cell tumors: Clinical and molecular results from a prospective study*. J Clin Oncol 2002, 20(8): 2181-8.

12. Kushner, B.H., LaQuaglia, M.P., Wollner, N. et al. *Desmoplastic small round-cell tumor: Prolonged progression-free survival with aggressive multimodality therapy*. J Clin Oncol 1996, 14(5): 1526-31.

13. Brennan, M., Singer, S., Maki, R., O'Sullivan, B. *Sarcomas of the soft tissue and bone. In: Cancer: Principles and Practice of Oncology*. Vol. 2, 7th Ed. DeVita, V.T. Jr., Hellman, S., Rosenberg, S.A. (Eds.). Lippincott Williams and Wilkins, Philadelphia, 2004, 1584.

14. Fletcher, C.D. *The evolving classification of soft tissue tumours: An update based on the new WHO classification*. Histopathology 2006, 48(1): 3-12.

15. Borden, E.C., Amato, D.A., Rosenbaum, C. et al. *Randomized comparison of three adriamycin regimens for metastatic soft tissue sarcomas*. J Clin Oncol 1987, 5(6): 840-50.

16. Lopez, M., Vici, P., Di Lauro, L., Carpano, S. *Increasing single epirubicin doses in advanced soft tissue sarcomas*. J Clin Oncol 2002, 20(5): 1329-34.

17. Cure, H., Krakowski, I., Adenis, A. et al. *Results of a phase II trial with second-line cystemustine at 60 mg/m² in advanced soft tissue sarcoma: A trial of the EORTC Early Clinical Studies Group*. Eur J Cancer 1998, 34(3): 422-3.

18. Bramwell, V.H., Anderson, D., Charette, M.L. *Doxorubicin-based chemotherapy for the palliative treatment of adult patients with locally advanced or metastatic soft tissue sarcoma*. Cochrane Database Syst Rev 2003, (3): CD003293.

19. Bokemeyer, C., Franzke, A., Hartmann, J.T. et al. *A phase I/II study of sequential, dose-escalated, high dose ifosfamide plus doxorubicin with peripheral blood stem cell support for the treatment of patients with advanced soft tissue sarcomas*. Cancer 1997, 80(7): 1221-7.

20. Frustaci, S., Buonadonna, A., Galligioni, E. et al. *Increasing 4'-epidoxorubicin and fixed ifosfamide doses plus granulocyte-macrophage colony-stimulating factor in advanced soft tissue sarcomas: A pilot study*. J Clin Oncol 1997, 15(4): 1418-26.

21. Reichardt, P., Tilgner, J., Hohenberger, P., Dorken, B. *Dose-intensive chemotherapy with ifosfamide, epirubicin, and filgrastim for adult patients with metastatic or locally advanced soft tissue sarcoma: A phase II study*. J Clin Oncol 1998, 16(4): 1438-43.

22. Steward, W.P., Verweij, J., Somers, R. et al. *Granulocyte-macrophage colony-stimulating factor allows safe escalation of dose-intensity of chemotherapy in metastatic adult soft tissue sarcomas: A study of the European Organization for Research and Treatment of Cancer Soft Tissue and Bone Sarcoma Group*. J Clin Oncol 1993, 11(1): 15-21.

23. Patel, S.R., Vadhan-Raj, S., Burgess, M.A., Plager, C., Papadopolous, N., Jenkins, J., Benjamin, R.S. *Results of two consecutive trials of dose-intensive chemotherapy with doxorubicin and ifosfamide in patients with sarcomas*. Am J Clin Oncol 1998, 21(3): 317-21.

24. Benjamin, R.S., Legha, S.S., Patel, S.R., Nicaise, C. *Single-agent ifosfamide studies in sarcomas of soft tissue and bone: The M.D. Anderson experience*. Cancer Chemother Pharmacol 1993, 31(Suppl. 2): S174-9.

25. Gottlieb, J.A., Benjamin, R.S., Baker, L.H. et al. *Role of DTIC (NSC-45388) in the chemotherapy of sarcomas*. Cancer Treat Rep 1976, 60(2): 199-203.

26. van Oosterom, A.T., Judson, I., Verweij, J. et al. *Safety and efficacy of imatinib (STI571) in metastatic gastrointestinal stromal tumours: A phase I study*. Lancet 2001, 358(9291): 1421-3.

27. Fata, F., O'Reilly, E., Ilson, D. et al. *Paclitaxel in the treatment of patients with angiosarcoma of the scalp or face*. Cancer 1999, 86(10): 2034-7.

28. Ebeling, P., Eisele, L., Schuett, P. et al. *Docetaxel and gemcitabine in the treatment of soft tissue sarcoma – A single-center experience*. Onkologie 2008, 31(1-2): 11-6.

29. D'Incalci, M., Sessa, C. *DNA minor groove binding ligands: A new class of anticancer agents*. Expert Opin Investig Drugs 1997, 6(7): 875-84.

30. D'Incalci, M. *DNA-minor-groove alkylators, a new class of anticancer agents*. Ann Oncol 1994, 5(10): 877-8.

31. Marchini, S., Broggini, S., Sessa, C., D'Incalci, M. *Development of distamycin-related DNA binding anticancer drugs*. Expert Opin Investig Drugs 2001, 10(9): 1703-14.

32. Wyatt, M.D., Lee, M., Garbiras, B.J., Souhami, R.L., Hartley, J.A. *Sequence specificity of alkylation for a series of nitrogen mustard-containing analogues of distamycin of increasing binding site size: Evidence for increased cytotoxicity with enhanced sequence specificity*. Biochemistry 1995, 34(40): 13034-41.

33. Wolff, I., Bench, K., Beijnen, J.H. et al. *Phase I clinical and pharmacokinetic study of carzelesin (U-80244) given daily for five consecutive days*. Clin Cancer Res 1996, 2(10): 1717-23.

34. Fleming, G.F., Ratain, M.J., O'Brien, S.M. et al. *Phase I study of adozelesin administered by 24-hour continuous intravenous infusion*. J Natl Cancer Inst 1994, 86(5): 368-72.

35. Schwartz, G.H., Aylesworth, C., Stephenson, J. et al. *Phase I trial of bizelesin using a single bolus infusion given every 28 days in patients with advanced cancer*. Proc Am Soc Clin Oncol (ASCO) 2000, 19: Abst 921D.

36. Broggini, M., Erba, E., Ponti, M., Ballinari, D., Geroni, C., Spreafico, F., D'Incalci, M. *Selective DNA interaction of the novel distamycin derivative FCE 24517*. Cancer Res 1991, 51(1): 199-204.

37. Baker, B.F., Dervan, P.B. *Sequence-specific cleavage of DNA by N-bromoacetyldistamycin. Product and kinetic analyses*. J Am Chem Soc 1989, 111: 2700-12.

38. Sessa, C., Pagani, O., Zurlo, M.G. et al. *Phase I study of the novel distamycin derivative tallimustine (FCE 24517)*. Ann Oncol 1994, 5(10): 901-7.

39. Abigerges, D., Armand, J.P., Da Costa, L. *Distamycin A derivative, FCE 24517: A phase I study in solid tumors*. Proc Am Assoc Cancer Res (AACR) 1993, 34: Abst 1589.

40. Cozzi, P., Beria, I., Caldarelli, M., Capolongo, L., Geroni, C., Mongelli, N. *Cytotoxic halogenoacrylic derivatives of distamycin A*. Bioorg Med Chem Lett 2000, 10(10): 1269-72.

41. Delaloge, S., Yovine, A., Taamma, A. et al. *Ecteinascidin-743: A marine-derived compound in advanced, pretreated sarcoma patients–Preliminary evidence of activity*. J Clin Oncol 2001, 19(11): 1248-55.

42. Demetri, G.D. *ET-743: The US experience in sarcomas of soft tissues*. Anticancer Drugs 2002, 13(Suppl. 1): S7-9.

43. Grosso, F., Demetri, G.D., Blay, J.Y. et al. *Patterns of tumor response to trabectedin (ET743) in myxoid liposarcomas*. J Clin Oncol [42nd Annu Meet Am Soc Clin Oncol (ASCO) (June 3-6, Atlanta) 2006] 2006, 24(18, Suppl.): Abst 9511.

44. Van Glabbeke, M., Verweij, J., Judson, I., Nielsen, O.S., *EORTC Soft Tissue and Bone Sarcoma Group. Progression-free rate as the principal end-point for phase II trials in soft-tissue sarcomas*. Eur J Cancer 2002, 38(4): 543-9.

45. Geroni, C., Pennella, G., Capolongo, L. et al. *Antitumor activity of PNU-166196, a novel DNA minor groove binder selected for clinical development*. Proc Am Assoc Cancer Res (AACR) 2000, 41: Abst 1689.

46. Hande, K.R., Roth, B.J., Vreeland, F. et al. *Phase I study of PNU-166196 given on a weekly basis*. Proc Am Soc Clin Oncol (ASCO) 2001, 20(Part 1): Abst 380.

47. Planting, A.S., De Jonge, M.J.A., Van der Gaast, A., Fiorentini, F., Fowst, C., Antonellini, A., Verweij, J. *Phase I study of PNU-166196, a novel DNA minor groove binder (MGB) with enhanced activity in tumor models expressing high glutathione*

(GSH) levels, administered to patients (pts) with advanced cancer. Proc Am Soc Clin Oncol (ASCO) 2001, 20(Part 1): Abst 379.

48. Marchini, S., Ciro, M., Gallinari, F., Cozzi, P., D'Incalci, M., Broggini, M. *Bromoacryloyl derivative of distamycin A (PNU 151807): A new non-covalent minor groove DNA binder with antineoplastic activity*. Br J Cancer 1999, 80(7): 991-7.

49. Geroni, C., Marchini, S., Cozzi, P. et al. *Brostallicin, a novel anticancer agent whose activity is enhanced upon binding to glutathione*. Cancer Res 2002, 62(8): 2332-6.

50. Fedier, A., Fowst, C., Tursi, J., Geroni, C., Haller, U., Marchini, S., Fink, D. *Brostallicin (PNU-166196) - A new DNA minor groove binder that retains sensitivity in DNA mismatch repair-deficient tumour cells*. Br J Cancer 2003, 89(8): 1559-65.

51. Ciomei, M., Pastori, W., Cozzi, P., Geroni, M.C. *Induction of apoptosis with a new distamycin derivative*. Proc Am Assoc Cancer Res (AACR) 1999, 40: Abst 1490.

52. Giusti, A.M., Moneta, D., Geroni, C., Farao, M. *In vivo induction of apoptosis with PNU-166196 in human ovarian carcinoma xenografts*. Proc Am Assoc Cancer Res (AACR) 2000, 41: Abst 5240.

53. Colella, G., Marchini, S., d'Incalci, M., Brown, R., Broggini, M. *Mismatch repair deficiency is associated with resistance to DNA minor groove alkylating agents*. Br J Cancer 1999, 80(3-4): 338-43.

54. Taubert, H.W., Bartel, F., Kappler, M. et al. *Reduced expression of hMSH2 protein is correlated to poor survival for soft tissue sarcoma patients*. Cancer 2003, 97(9): 2273-8.

55. Schecter, R.L., Alaoui-Jamali, M.A., Batist, G. *Glutathione S-transferase in chemotherapy resistance and in carcinogenesis*. Biochem Cell Biol 1992, 70(5): 349-53.

56. Shen, H., Kauvar, L., Tew, K.D. *Importance of glutathione and associated enzymes in drug response*. Oncol Res 1997, 9(6-7): 295-302.

57. Tsuchida, S., Sato, K. *Glutathione transferases and cancer*. Crit Rev Biochem Mol Biol 1992, 27(4-5): 337-84.

58. Bader, P., Fuchs, J., Wenderoth, M., von Schweinitz, D., Niethammer, D., Beck, J.F. *Altered expression of resistance associated genes in hepatoblastoma xenografts incorporated into mice following treatment with adriamycin or cisplatin*. Anticancer Res 1998, 18(4C): 3127-32.

59. Cazenave, L.A., Moscow, J.A., Myers, C.E., Cowan, K.H. *Glutathione S-transferase and drug resistance*. Cancer Treat Res 1989, 48: 171-87.

60. Pook, S.H., Toh, C.K., Mahendran, R. *Combination of thiol antioxidant silibinin with brostallicin is associated with increase in the anti-apoptotic protein Bcl-2 and decrease in caspase 3 activity*. Cancer Lett 2006, 238(1): 146-52.

61. Trotti, A., Colevas, A.D., Setser, A. et al. CTCAE v3.0: *Development of a comprehensive grading system for the adverse effects of cancer treatment*. Semin Radiat Oncol 2003, 13(3): 176-81.

62. Ten Tije, A.J., Verweij, J., Sparreboom, A. et al. *Phase I and pharmacokinetic study of brostallicin (PNU-166196), a new DNA minor groove binder, administered intravenously every 3 weeks to adult patients with metastatic cancer*. Clin Cancer Res 2003, 9(9): 2957-64.

63. Leahy, M., Ray-Coquard, I., Verweij, J. et al. *Brostallicin, an agent with potential activity in metastatic soft tissue sarcoma: A phase II study from the European Organisation for Research and Treatment of Cancer Soft Tissue and Bone Sarcoma Group*. Eur J Cancer 2007, 43(2): 308-15.

64. Clark, M.A., Fisher, C., Judson, I., Thomas, J.M. *Soft-tissue sarcomas in adults*. N Engl J Med 2005, 353(7): 701-11.

65. *Brostallicin or doxorubicin as first-line therapy in treating patients with relapsed, refractory, or metastatic soft tissue sarcoma (NCT00410462)*. ClinicalTrials.gov Web site, June 2, 2008.

66. Hogendoorn, P.C., Collin, F., Daugaard, S., Dei Tos, A.P., Fisher, C., Schneider, U., Sciot, R.; Pathology and Biology Subcommittee of the EORTC Soft Tissue and Bone Sarcoma Group. *Changing concepts in the pathological basis of soft tissue and bone sarcoma treatment*. Eur J Cancer 2004, 40(11): 1644-54.

Drugs of the Future 2007, 32(9): 771-775

CCC: 0377-8282/2007
DOI: 10.1358/dof.2007.032.09.1139032

Methylnaltrexone Bromide

Prop INN; USAN

Opioid Receptor Antagonist
Treatment of Constipation
Treatment of Postoperative Ileus

MNTX
MNTX-302
MOA-728
MRZ-2663BR

17-(Cyclopropylmethyl)-4,5α-epoxy-3,14-dihydroxy-17-methyl-6-oxomorphinanium bromide

N-Methylnaltrexone bromide

InChI=1/C21H25NO4.BrH/c1-22(11-12-2-3-12)9-8-20-17-13-4-5-14(23)18(17)26-19(20)15(24)6-7-21(20,25)16(22)10-13;/h4-5,12,16,19,25H,2-3,6-11H2,1H3;1H/t16-,19+,20+,21-,22+;/m1./s1

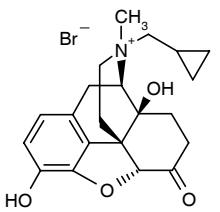

$C_{21}H_{26}BrNO_4$
Mol wt: 436.3395

CAS: 073232-52-7

EN: 284766

Abstract

Opioids are widely used in patients with moderate to severe acute and chronic pain, but gastrointestinal side effects such as nausea and constipation can often be debilitating. Opioid-induced bowel dysfunction (OBD) is mediated by mu opioid receptors in both the central nervous system and bowel wall, but the "peripheral" bowel effects may be more important. Methylnaltrexone (MNTX) is a derivative of naltrexone that does not cross the blood-brain barrier. It acts as a selective antagonist at peripheral opioid receptors without reversing central effects like analgesia. In preclinical and human volunteer studies, parenteral and oral MNTX consistently reversed OBD at doses that produced minimal side effects. Intravenous MNTX also reversed opioid inhibition of bladder function, suggesting a possible role in the treatment of opioid-induced urinary retention. Two phase III studies showed that s.c. administration of 0.15-0.3 mg/kg MNTX induced laxation in patients with advanced medical illness given chronic opioids. Additional studies of MNTX targeting postoperative ileus also show promise. An NDA submission is anticipated in early 2008.

Synthesis+

The title ammonium salt is prepared by quaternization of naltrexone (I) with bromomethane in solvents such as *N,N*-dimethylformamide, *N,N*-dimethylacetamide or *N*-methyl-2-pyrrolidinone (1, 2).

Background

Opioid analgesics are still the most widely accepted drugs for moderate to severe acute and chronic pain, but their use is accompanied by numerous unpleasant side effects. Dangerous opioid toxicity, such as respiratory depression, occurs infrequently, but large numbers of patients suffer from debilitating effects, such as constipation, urinary retention, or nausea and vomiting. Constipation is one symptom of a more general syndrome called opioid-induced bowel dysfunction (OBD) that includes inhibition of gastric emptying, decreased peristalsis, increased tone of intestinal sphincters, decreased secretions and increased fluid absorption (3). Slowed gastrointestinal (GI) transit and dessication of stools lead to constipation. Unlike opioid analgesia, little tolerance develops to OBD, and therefore it is a clinical problem in as many as 40-50% of patients receiving chronic opioids for metastatic malignancy (4, 5) or noncancer pain (6).

The GI effects of opioids are due to both central and peripheral mechanisms, although peripheral actions at mu opioid receptors in the gut wall appear to play the most important role (7-9). There have been numerous

Tong-Yan Chen, Carl E. Rosow*. Department of Anesthesia and Critical Care, Massachusetts General Hospital, Harvard Medical School, 55 Fruit St., Boston, MA 02114, USA. *Correspondence: crosow@partners.org. +Synthesis prepared by N. Serradell, J. Bolós, E. Rosa. Prous Science, P.O. Box 540, 08080 Barcelona, Spain.

Scheme 1: Synthesis of Methylnaltrexone Bromide

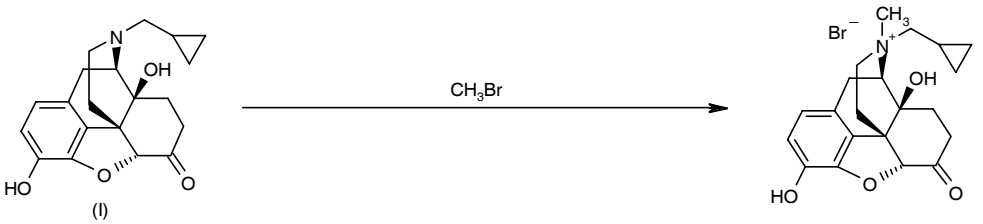

attempts to decrease peripheral opioid side effects by co-administering low doses of typical mu antagonists such as naloxone or naltrexone. Unfortunately, all clinically available opioid antagonists cross the blood-brain barrier and therefore carry the risk of reversing analgesia or precipitating withdrawal (10-12). There is thus a clinical need for an opioid antagonist that selectively inhibits peripheral opioid effects while sparing those mediated by the central nervous system.

Methylnaltrexone bromide (MNTX) is a quaternary derivative of naltrexone. It is a white, odorless, water-soluble powder that has been formulated as a sterile solution for injection and as tablets for oral administration. The addition of a methyl group on the piperidine nitrogen creates a permanently charged, polar compound that does not cross the blood-brain barrier (13, 14).

Preclinical Pharmacology

MNTX is a competitive mu opioid antagonist with no intrinsic opioid-agonist properties (15). In the guinea pig ileum and rat brain, it is 25-42 times less potent than naltrexone. The IC_{50} to displace etorphine from rat brain mu opioid receptors is 305 nM *versus* 7.2 nM for naltrexone (16). MNTX has about 18 times greater affinity for mu than for kappa opioid receptors, and it does not bind appreciably to delta opioid or other receptor populations. In an isolated gastric-brainstem preparation from neonatal rats, MNTX competitively antagonized the GI-inhibitory effects of mu agonists (17). In a human small intestine preparation, administration of MNTX alone increased smooth muscle contraction by 30%, suggesting the reversal of endogenous opioid activity (18). Some forms of GI hypomotility, such as postoperative ileus, are thought to be partially mediated by endogenous opioids, suggesting a therapeutic role for MNTX in these conditions.

In vivo, MNTX antagonizes the GI but not the central effects of morphine. Morphine prolonged the intestinal transit time of a charcoal meal in rats and this effect was completely prevented by s.c. administration of MNTX. Morphine-induced analgesia can be antagonized by MNTX following intracerebroventricular but not s.c. injection (15). MNTX doses as high as 50 mg/kg do not precipitate abstinence in morphine-dependent dogs (14).

Pharmacokinetics and Metabolism

Peak plasma concentrations (C_{max}) and area under the concentration-time curve (AUC) in human subjects were proportional to dose after i.v., s.c. or oral administration. Time to peak (t_{max}) was 16-20 min after s.c. and 30 min after oral dosing. The C_{max} after 0.3 mg/kg s.c. was 287 ng/ml (750 nM), a concentration twice as high as the IC_{50} needed to prevent opioid binding *in vitro* (16). Extremely low plasma concentrations were observed after oral ingestion, and enteric coating reduced them even further. This suggests that a small amount may be absorbed in the upper GI tract. No correlation exists between drug effects and plasma concentrations after 3.2 or 6.4 mg/kg of enteric-coated MNTX (19).

MNTX undergoes rapid distribution ($t_{1/2}$ = 6-9 min) followed by slower elimination ($t_{1/2}$ = 2 h in volunteers) (20). Elimination half-lives of 7 h or longer have been reported in some cancer patients (21). Administration of 0.3 mg/kg every 6 h for 12 doses showed no evidence of accumulation or toxicity in healthy subjects (22). Clearance is primarily by renal excretion of the unchanged drug. About 50% of an MNTX dose appears in the urine within 6 h after injection, while < 0.1% appears after oral dosing (19, 20). Unlike rats and mice, humans do not demethylate MNTX to the centrally active compound naltrexone (23).

Clinical Studies

A volunteer study demonstrated that MNTX prevents the effect of morphine on gastric emptying. Eleven healthy volunteers were given placebo, 0.09 mg/kg morphine or 0.09 mg/kg morphine plus 0.3 mg/kg MNTX, and the rate of gastric emptying was measured by bioimpedance and acetaminophen absorption. The times for 50% emptying were 5.5, 21 and 7.4 min, respectively, after placebo, morphine and morphine/MNTX. Morphine induced a delay in acetaminophen transfer from stomach to proximal jejunum which decreased the acetaminophen C_{max}, and this effect was also prevented by MNTX (24).

The effects on oral-cecal transit time and analgesia were assessed in 12 subjects given i.v. placebo, morphine 0.5 mg/kg or MNTX 0.45 mg/kg plus morphine 0.5 mg/kg. Transit times (measured by the lactulose-hydrogen breath test) were 105, 163 and 106 min, respective-

ly, for placebo, morphine and morphine/MNTX. Experimental pain (cold pressor test) was reduced by morphine and this effect was unchanged by the addition of MNTX. This confirms that MNTX reverses only the peripheral effects and spares the central effects such as analgesia (25). A separate volunteer study showed that MNTX does not reverse opioid-induced ventilatory depression (26).

Patients who have advanced medical illness (AMI) such as cancer or AIDS often receive large doses of opioids in a home or hospice setting. For this reason, there has been a particular effort to develop convenient s.c. and oral dosage forms of MNTX. A volunteer trial showed that s.c. administration of 0.1 or 0.3 mg/kg MNTX completely reversed the delay in intestinal transit induced by 0.05 mg/kg morphine (27). Oral MNTX was also effective, but doses as high as 19.2 mg/kg were required to produce complete reversal (28). An enteric-coated oral preparation was subsequently developed that reduces gastric absorption and releases MNTX only in the small and large intestine. Complete reversal occurred after only 3.2 mg/kg, suggesting that enteric-coated drug is about 6-fold more potent than uncoated MNTX. Greater potency was associated with lower bioavailability, suggesting that more of the enteric-coated preparation reaches opioid receptors in the colonic lumen (19).

Opioid abusers receiving chronic methadone maintenance treatment are also prone to severe OBD, and MNTX has been investigated in three relevant protocols. A pilot trial showed that i.v. MNTX produces immediate and marked laxation in these individuals, and the data suggested that lower doses might be needed. The results of a second study in 22 subjects receiving 30-100 mg/day of methadone are shown in Figure 1. Placebo was ineffective, but 0.1 mg/kg MNTX administered i.v. produced immediate laxation, decreased the intestinal transit time and caused mild to moderate cramping. Other than signs of increased GI motility, there was no indication of opioid withdrawal (29). A third trial of oral MNTX showed a dose-dependent laxation response 18, 12 and 5 h after doses of 0.3, 1.0 and 3.0 mg/kg, respectively (30).

Two pivotal phase III trials of s.c. MNTX have now been completed in patients with AMI and opioid-induced constipation. The first multicenter trial in 154 cancer patients evaluated single doses of s.c. MNTX (0.15 or 0.3 mg/kg) and found that it induced laxation within 4 h (31). The second trial examined the effect of 0.15 mg/kg given every other day for a week, with the option to double the dose as needed during a second week. A total of 48.4% of patients had laxation responses within 4 h of the initial dose, and 38.7% had responses after at least 4 of the 7 doses ($p < 0.0001$ *vs.* placebo). Other than abdominal cramping and flatulence, there were few adverse effects and no reports of opioid withdrawal (32).

Opioid-induced urinary retention is due to inhibition of bladder detrusor tone, suppression of the micturition reflex and decreases in awareness of bladder distension. The clinical problem has not been as well studied as OBD, but some reports suggest a significant incidence in the perioperative period. Certain patient populations are likely to be at greater risk; for example, one study reported an incidence of 18.1% in older patients who used patient-controlled analgesia with morphine after lower limb joint replacements (33). The occurrence of complete urinary retention can be painful and distressing for the patient, and the usual treatment is immediate insertion of a bladder catheter to relieve symptoms.

Opioid actions on the brain and spinal cord undoubtedly play a significant role in the bladder effect, but until recently, the involvement of peripheral opiate receptors had not been demonstrated. We recently compared MNTX, naloxone and placebo for reversal of bladder dys-

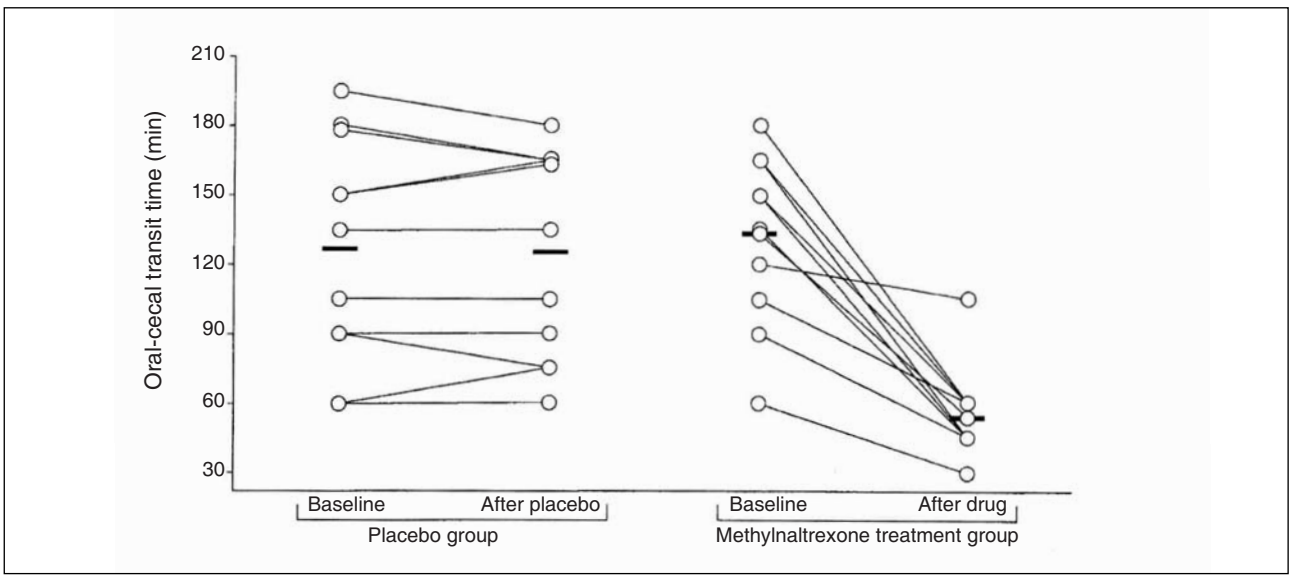

Fig. 1. Changes in individual oral-cecal transit times of subjects undergoing long-term methadone treatment. The average change in the methylnaltrexone group was significantly greater that the average change in the placebo group. Reprinted with permission from Ref. 29.

function induced by the opioid agonist remifentanil (34). Detrusor pressure was measured in 13 male volunteers using bladder and rectal catheters, and pupil constriction (a central opioid effect) was measured by infrared pupillometry. Remifentanil decreased detrusor pressure in 21 of 25 sessions and caused complete urinary retention in 18 of 25. Voiding was possible after naloxone, MNTX and placebo in 7 of 7, 5 of 12 and 0 of 6 sessions, respectively (Fig. 2). Pupil constriction was reversed only by naloxone, indicating once again that MNTX is working peripherally. To our knowledge, this is the first demonstration of a peripheral opioid effect on bladder function. It suggests that MNTX should be evaluated as a potential treatment for opioid-induced urinary retention.

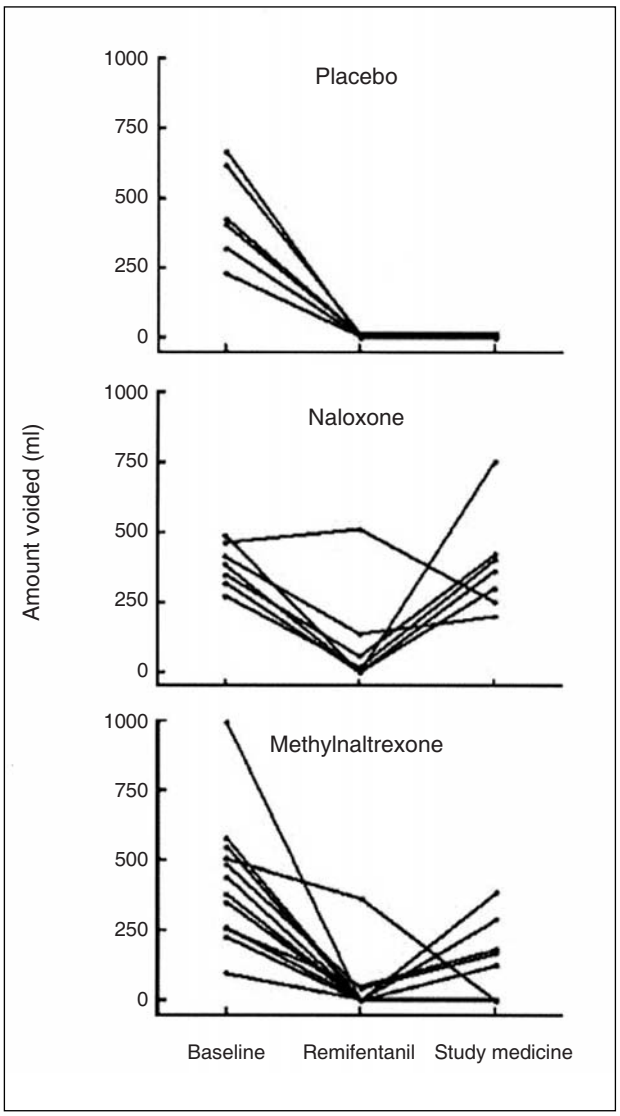

Fig. 2. Amount voided at baseline, after remifentanil and after study medicine (placebo, naloxone or methylnaltrexone). In almost every session, remifentanil prevented voiding or greatly reduced the amount voided, and this effect was fully or partially reversed by naltrexone and methylnaltrexone, but not placebo (see text). Reprinted with permission from Ref. 34.

Conclusions

MNTX is a unique peripheral opioid receptor antagonist. Animal and clinical studies demonstrate that it can reverse or prevent opioid-induced GI effects without antagonizing analgesia. Thus far, there have been remarkably few reports of adverse events, and the therapeutic dose range is likely to be quite large. The most commonly reported side effects, *i.e.*, cramping and abdominal discomfort, appear to be expected GI consequences of drug action. The drug is a hydrophilic small molecule that undergoes mainly first-order renal elimination, so more information will need to be obtained on dosing in patients with renal insufficiency. MNTX has been studied in i.v., s.c. and oral formulations, and the likely availability of all these dosage forms will afford clinicians great flexibility in its clinical application. The drug is being developed jointly by Progenics and Wyeth, and submission of an NDA with the FDA is anticipated in early 2008. A wide variety of opioid-treated patients may eventually benefit from MNTX, although the pivotal phase III studies have specifically targeted s.c. administration in cancer patients and others with AMI. Results from initial studies of postoperative ileus also appear promising (earlier laxation, earlier hospital discharge), and additional trials for this indication are being organized. The human volunteer data on bladder dysfunction are provocative, but further clinical studies will be needed to confirm them. Although not included here, there have been evaluations of MNTX action on many other opioid effects, such as cough suppression, itch and nausea (35), as well as laboratory investigations of immune modulation and endothelial barrier function. These may or may not lead to new therapeutic opportunities, but they do illustrate the value of this new drug as a tool for investigating opioid biology.

Acknowledgements

Dr. Rosow has received research support from Progenics Pharmaceuticals.

Sources

Progenics Pharmaceuticals, Inc. (US); co-developed by Wyeth Pharmaceuticals (US).

References

1. Goldberg, L.I., Stockhaus, K., Merz, H. (Boehringer Ingelheim Pharma GmbH & Co., KG). *Quaternary derivatives of noroxymorphone which relieve intestinal immobility*. US 4176186.

2. Cantrell, G., Halvachs, R.E. (Mallinckrodt, Inc.). *Process for the preparation of quaternary N-alkyl morphinan alkaloid salts*. WO 2004043964.

3. Kurz, A., Sessler, D. *Opioid induced bowel dysfunction. Pathophysiology and potential new therapies*. Drugs 2000, 63: 649-71.

4. Walsh, T.D. *Oral morphine in chronic cancer pain*. Pain 1984, 18(1): 1-11.

5. Vanegas, G., Ripamonti, C., Sbanotto, A., De Conno, F. *Side effects of morphine administration in cancer patients*. Cancer Nurs 1998, 21(4): 289-97.

6. Pappagallo, M. *Incidence, prevalence, and management of opioid bowel dysfunction*. Am J Surg 2001, 182(5A, Suppl.): 11S-8S.

7. Manara, L., Bianchetti, A. *The central and peripheral influences of opioids on gastrointestinal propulsion*. Annu Rev Pharmacol Toxicol 1985, 25: 249-73.

8. Manara, L., Bianchi, G., Ferretti, P., Tavani, A. *Inhibition of gastrointestinal transit by morphine in rats results primarily from direct drug action on gut opioid sites*. J Pharmacol Exp Ther 1986, 237(3): 945-9.

9. Shook, J.E., Pelton, J.T., Hruby, J., Burks, T.F. *Peptide opioid antagonist separates peripheral and central opioid antitransit effects*. J Pharmacol Exp Ther 1987, 243(2): 492-500.

10. Culpepper-Morgan, J.A., Inturrisi, C.E., Portenoy, R.K., Foley, K., Houde, R.W., Marsh, F., Kreek, M.J. *Treatment of opioid-induced constipation with oral naltrexone: A pilot study*. Clin Pharmacol Ther 1992, 52(1): 90-5.

11. Sykes, N.P. *Oral naltrexone in opioid-associated constipation*. Lancet 1991, 337(8755): 1475.

12. Cheskin, L.J., Chami, T.N., Johnson, R.E., Jaffe, J.H. *Assessment of nalmefene glucuronide as a selective gut opioid antagonist*. Drug Alcohol Depend 1995, 39(2): 151-4.

13. Brown, D.R., Goldberg, L.I. *The use of quaternary narcotic antagonists in opiate research*. Neuropharmacology 1985, 24(3): 181-91.

14. Russell, J., Bass, P., Goldberg, L.I., Schuster, C.R., Merz, H. *Antagonism of gut, but not central effects of morphine with quaternary narcotic antagonists*. Eur J Pharmacol 1982, 78(3): 255-61.

15. Gmerek, D.E., Cowan, A., Woods, J.H. *Independent central and peripheral mediation of morphine-induced inhibition of gastrointestinal transit in rats*. J Pharmacol Exp Ther 1986, 236(1): 8-13.

16. Valentino, R.J., Katz, J.L., Medzihradsky, F., Woods, J.H. *Receptor binding, antagonist, and withdrawal precipitating properties of opiate antagonists*. Life Sci 1983, 32(25): 2887-96.

17. Yuan, C.S., Foss, J.F. *Gastric effects of methylnaltrexone on mu, kappa, and delta opioid agonists induced brainstem unitary responses*. Neuropharmacology 1999, 38(3): 425-32.

18. Yuan, C.S., Foss, J.F., Moss, J. *Effects of methylnaltrexone on morphine-induced inhibition of contraction in isolated guinea pig ileum and human intestine*. Eur J Pharmacol 1995, 276(1-2): 107-11.

19. Yuan, C.S., Foss, J.F., O'Connor, M., Karrison, T., Osinski, J., Roizen, M.F., Moss, J. *Effects of enteric-coated methylnaltrexone in preventing opioid-induced delay in oral-cecal transit*. Clin Pharmacol Ther 2000, 67(4): 398-404.

20. Foss, J.F., O'Connor, M.F., Yuan, C.S., Murphy, M., Moss, J., Roizen, M.F. *Safety and tolerance of methylnaltrexone in healthy humans: A randomized, placebo-controlled, intravenous, ascending-dose, pharmacokinetic study*. J Clin Pharmacol 1997, 37(1): 25-30.

21. Yuan, C.S., Foss, J.F. *Methylnaltrexone: Investigation of clinical applications*. Drug Develop Res 2000, 50(2): 133-41.

22. Yuan, C.S., Doshan, H., Charney, M.R. et al. *Tolerability, gut effects, and pharmacokinetics of methylnaltrexone following repeated intravenous administration in humans*. J Clin Pharmacol 2005, 45(5): 538-46.

23. Kotake, A.N., Kuwahara, S.K., Burton, E., McCoy, C.E., Goldberg, L.I. *Variations in demethylation of N-methylnaltrexone in mice, rats, dogs, and humans*. Xenobiotica 1989, 19(11): 1247-54.

24. Murphy, D.B., Sutton, J.A., Prescott, L.F., Murphy, M.B. *Opioid-induced delay in gastric emptying: A peripheral mechanism in humans*. Anesthesiology 1997, 87(4): 765-70.

25. Yuan, C.S., Foss, J.F., O'Connor, M., Toledano, A., Roizen, M.F., Moss, J. *Methylnaltrexone prevents morphine-induced delay in oral-cecal transit time without affecting analgesia: A double-blind randomized placebo-controlled trial*. Clin Pharmacol Ther 1996, 59(4): 469-75.

26. Amin, H.M., Sopchak, A.M., Foss, J.F., Esposito, B.F., Roizen, M.F., Camporesi, E.M. *Efficacy of methylnaltrexone versus naloxone for reversal of morphine-induced depression of hypoxic ventilatory response*. Anesth Analg 1994, 78(4): 701-5.

27. Yuan, C.S., Wei, G., Foss, J.F., O'Connor, M., Karrison, T., Osinski, J. *Effects of subcutaneous methylnaltrexone on morphine-induced peripherally mediated side effects: A double-blind randomized placebo-controlled trial*. J Pharmacol Exp Ther 2002, 300(1): 118-23.

28. Yuan, C.S., Foss, J.F., Osinski, J., Toledano, A., Roizen, M.F., Moss, J. *The safety and efficacy of oral methylnaltrexone in preventing morphine-induced delay in oral-cecal transit time*. Clin Pharmacol Ther 1997, 61(4): 467-75.

29. Yuan, C.S., Foss, J.F., O'Connor, M., Osinski, J., Karrison, T., Moss, J., Roizen, M.F. *Methylnaltrexone for reversal of constipation due to chronic methadone use*. JAMA – J Am Med Assoc 2000, 283(3): 367-72.

30. Yuan, C.S., Foss, J.F. *Oral methylnaltrexone for opioid-induced constipation [research letter]*. JAMA – J Am Med Assoc 2000, 284(11): 1383-4.

31. Thomas, J., Lipman, A., Slakin, N. et al. *A phase III double-blind placebo-controlled trial of methylnaltrexone (MNTX) for opioid-induced constipation (OIC) in advanced medical illness (AMI)*. 41st Annu Meet Am Soc Clin Oncol (ASCO) (May 13-17, Orlando) 2005, Abst LBA8003.

32. Slatkin, N., Karver, S., Thomas, J. et al. *A phase III double-blind, placebo-controlled trial of methylnaltrexone for opioid-induced constipation in advanced illness (MNTX 302)*. Digest Dis Week (May 20-25, Los Angeles) 2006, Abst 686e.

33. O'Riordan, J.A., Hopkins, P.M., Ravenscroft, A., Stevens, J.D. *Patient-controlled analgesia and urinary retention following lower limb joint replacement: Prospective audit and logistic regression analysis*. Eur J Anaesthesiol 2000, 17(7): 431-5.

34. Rosow, C.E., Gomery, P., Chen, T.Y., Stefanovich, P., Stambler, N., Israel, R. *Reversal of opioid-induced bladder dysfunction by intravenous naltrexone and methylnaltrexone*. Clin Pharmacol Ther 2007, 82(1): 48-53.

35. Yuan, C.S., Foss, J.F., Osinski, J.P., Roizen, M.F., Moss, J. *Efficacy of orally administered methylnaltrexone in decreasing subjective effects after intravenous morphine*. Drug Alcohol Depend 1998, 52(2): 161-5.

Drugs of the Future 2004, 29(11): 1088-1095

CCC: 0377-8282/2004

Olcegepant

Prop INN

Antimigraine Drug
CGRP Antagonist

BIBN-4096BS

N-[2-[5-Amino-1(*S*)-[4-(4-pyridinyl)piperazin-1-ylcarbonyl]pentylamino]-1(*R*)-(3,5-dibromo-4-hydroxybenzyl)-2-oxoethyl]-4-(2-oxo-1,2,3,4-tetrahydroquinazolin-3-yl)piperidine-1-carboxamide

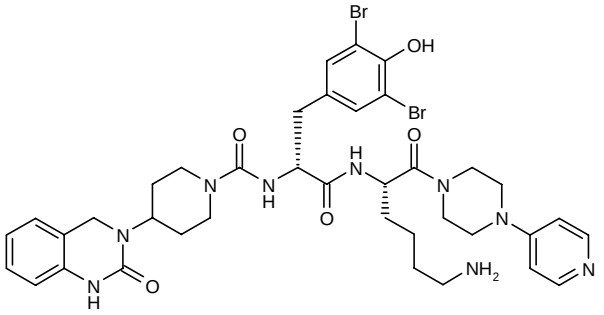

C38 H47 Br2 N9 O5
Mol wt: 869.6553
CAS: 204697-65-4
EN: 285741

Abstract

Migraine involves dysfunction of brainstem pathways that normally modulate sensory input. The involvement of calcitonin gene-related peptide (CGRP) in migraine pathology is supported by both clinical and experimental evidence. The release of CGRP and other neuropeptides from trigeminal nerves is thought to mediate neurogenic inflammation within the meninges, which contributes to the generation of severe cerebral pain experienced during migraine attacks. Hence, structure-activity relationship studies have been conducted in an attempt to develop small molecules that behave as CGRP antagonists. Recently, the development of a potent, nonpeptide CGRP antagonist, BIBN-4096BS (olcegepant), represented a major breakthrough. BIBN-4096BS demonstrates very high affinity for the human CGRP receptor expressed in SK-N-MC cells and may be useful in the treatment of migraine, as well as providing new information on CGRP receptor subtypes.

Introduction

Migraine is defined as benign recurring headache and/or neurological dysfunction, usually accompanied by pain-free interludes and often provoked by stereotyped stimuli (1). It is more prevalent in females than in males. Although considerable progress has been made, the pathophysiology of migraine is still far from clear. As depicted in Figure 1, current theories propose that migraine-specific triggers (cause unknown) evoke changes in meningeal blood vessels causing dilatation and activation of perivascular trigeminal nerves (2-6). These nerves provide sensory information from the major blood vessels, such as cerebral arteries, that are responsible for regulating cerebral blood flow and from smaller blood vessels located within the pain-sensitive meninges (7, 8). Activated trigeminal nerve terminals release vasoactive neuropeptides such as calcitonin gene-related peptide (CGRP) within the meninges, mediating neurogenic inflammation that is characterized by vasodilatation, plasma extravasation and mast cell degranulation, releasing mediators such as histamine (8). Additionally, neuropeptides relay nociceptive transmission to the central nervous system (thalamus, hypothalamus, chemoreceptor trigger zone) via second-order neurons, leading to severe migraine pain, photophobia/phonophobia, nausea and vomiting, respectively.

Calcitonin gene-related peptide is one of several neuropeptides found in human trigeminal sensory neurons (2, 9-19). Present in both the pericranial vascular nerves and the trigeminal ganglion, it is a potent dilator of cerebral and dural vessels (20, 21) and is involved in meningeal dural vasodilatation (22). Cranial CGRP levels are elevated in patients with migraine (23, 24) and an infusion

Kapil Kapoor[1,2]*, Pramod Saxena[1]. [1]Department of Pharmacology, Cardiovascular Research Institute COEUR, Erasmus MC, University Medical Center Rotterdam, P.O. Box 1738, 3000 DR Rotterdam, The Netherlands; [2]Cardiovascular Pharmacology Unit, Pharmacology Division, Central Drug Research Institute, Chattar Manzil Palace, P.O. Box 173, Lucknow-226001, U.P. India. *Correspondence: e-mail: kapoorcdri@yahoo.co.uk

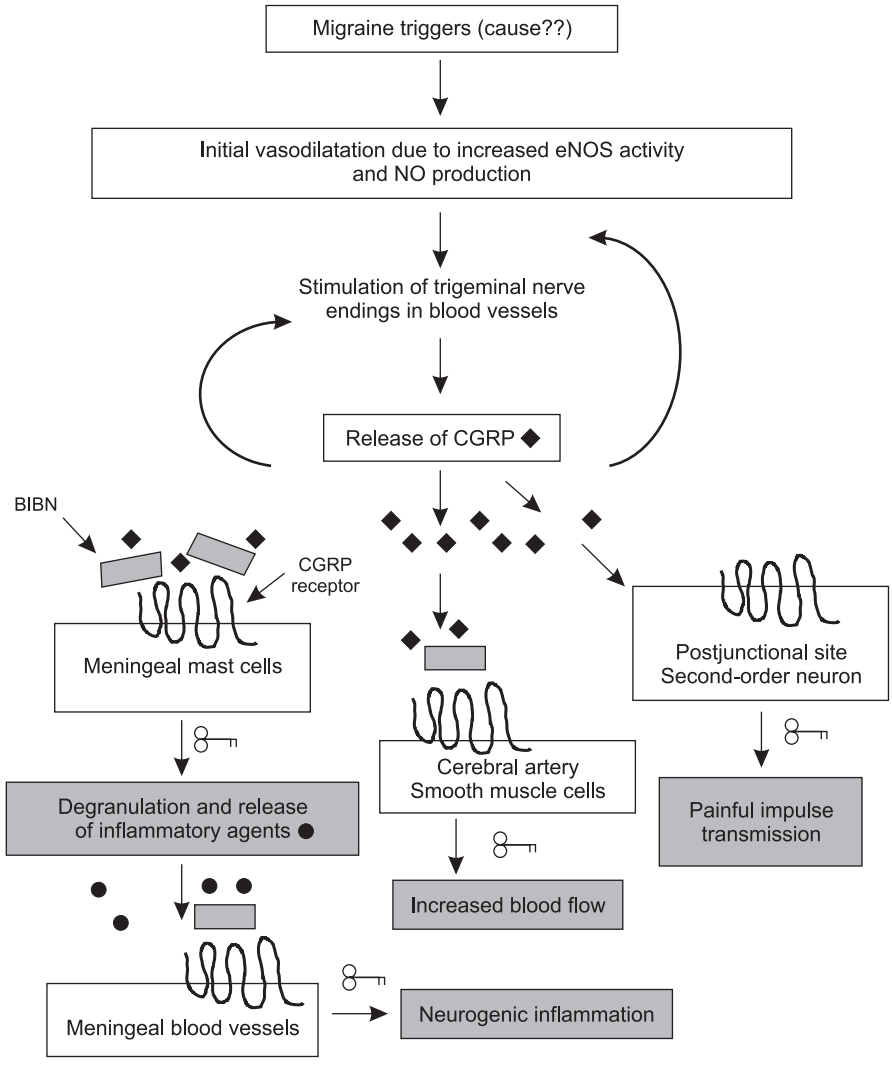

Fig. 1. Schematic representation of migraine pathophysiology and possible sites of action of BIBN-4096BS (●inflammatory products such as histamine; ◆ CGRP; ⊖inhibited).

of CGRP can trigger a migraine attack (25). It has therefore been hypothesized that CGRP antagonists might be effective in the treatment of acute migraine.

Calcitonin gene-related peptide is a 37-amino-acid peptide that is expressed by neurons and endocrine cells in various tissues. Two discrete isoforms have been described: αCGRP, which is produced by alternative splicing of a calcitonin gene transcript, and βCGRP, the product of a separate gene (1, 2). The two transcripts are highly similar, differing by 3 and 1 amino acids in humans and rats, respectively (9). For both CGRP isoforms, potent vasodilating activity has been demonstrated both *in vitro* and *in vivo* (10). The vasodilating activity of CGRP has recently gained importance in the pathogenesis of migraine (11).

At least two receptor types, $CGRP_1$ and $CGRP_2$, have been proposed from functional pharmacological experiments. The family of CGRP receptors that has been characterized molecularly consists of the 7-transmembrane G-protein-coupled calcitonin receptor-like receptor (CRLR) linked to one of three single membrane-spanning receptor activity-modifying proteins (RAMPs). RAMPs are required for both receptor trafficking and ligand binding. The association of CRLR with RAMP1 leads to a CGRP receptor that is antagonized by the CGRP fragment $CGRP_{8-37}$, whereas CRLR associated with RAMP2 produces an adrenomedullin receptor that is antagonized by $adrenomedullin_{22-52}$, and CRLR associated with RAMP3 gives a CGRP/adrenomedullin receptor.

Physiological studies have demonstrated that CGRP is a potent dilator of cerebral and dural vessels (15, 18, 26, 27), and therefore has an important function in regulating blood flow to the brain and pain-sensitive meninges, suggesting that CGRP receptor antagonists might be effective in treating migraine by blocking the

Table I: pA_2 values of BIBN-4096BS as compared to $CGRP_{8-37}$ (antagonists) in different cell lines expressing corresponding receptors, as measured by human αCGRP (agonist)-induced cAMP production.

Cell line	Receptor	pA_2 BIBN-4096BS	pA_2 $CGRP_{8-37}$	Ref.
Rat L6	CRLR + RAMP1 ($CGRP_1$)	9.25	7.81	31, 55
Human SK-N-MC		9.95	8.35	31, 55
	CRLR + RAMP1 ($CGRP_1$)	11	-	56
		11.2	-	37
Human colony Col-29	CRLR + RAMP2 ($hCGRP_2$)	9.98	7.34	31, 55
Rat2	CRLR + RAMP2 (ADM)	Unable to antagonize	6.72	31, 55

ADM, adrenomedullin; CGRP, calcitonin gene-related peptide; CRLR, calcitonin receptor-like receptor; RAMP, receptor-associated membrane protein.

actions of CGRP. Agents acting as CGRP receptor antagonists are likely to inhibit the dilatation of major cerebral vessels, diminish neurogenic inflammation within the meninges, and block the activation of nociceptive neural pathways. Thus, the ability of both triptans and CGRP receptor antagonists to alleviate migraine pain may be mediated by the same molecular targets activated following CGRP receptor activation.

Boehringer Ingelheim's BIBN-4096BS (olcegepant) is the first CGRP receptor antagonist for which significant efficacy has been demonstrated in the treatment of migraine, which in turn provides further evidence for the critical role of CGRP in the pathology of migraine. A non-peptide CGRP antagonist, BIBN-4096BS (28), has undergone clinical investigation (29) to assess the importance of CGRP in migraine headache and to ascertain whether the concept of CGRP antagonism may offer advantages, *e.g.*, higher efficacy, lower recurrence rate or improved side effect profile, compared to currently used antimigraine drugs.

Pharmacological Actions

Based on its antagonist properties, BIBN-4096BS has been used as a pharmacological tool to characterize cell lines endogenously expressing receptors of known composition. The pA_2 values of BIBN-4096BS and $CGRP_{8-37}$ for antagonism of hCGRP-induced cAMP production are shown in Table I. These studies describe the ability of BIBN-4096BS to interact with cell lines expressing human and rat $CGRP_1$ (CRLR/RAMP1) receptors (*i.e.*, SK-N-MC and L6 cells), rat adrenomedullin receptors (CRLR/RAMP2; *i.e.*, Rat2 cells) and a potential human $CGRP_2$-like receptor (Col-29 cells). The results clearly demonstrate that BIBN-4096BS shows preferential binding to the human CRLR/RAMP1 complex in functional assays and that the differences in affinity for CGRP receptors reported previously are due to species differences within the same receptor subtype. In another study, BIBN-4096BS was more potent than $CGRP_{8-37}$ in antagonizing agonist-induced cAMP production in smooth muscle cells, endothelial cells and astrocytes, with pIC_{50} values of 9.4, 10.9 and 13.8, respectively (30).

Surprisingly, BIBN-4096BS also acts as an antagonist at adrenomedullin receptors in rat vas deferens, suggesting an unlikely CRLR/RAMP2 receptor pharmacology (31). Additionally, characterization of CGRP receptor subtypes in rat left atrium and vas deferens employing CGRP as agonist demonstrated 10-fold higher affinity for BIBN-4096BS for rat atrium over rat vas deferens. BIBN-4096BS also exhibited 10-fold greater potency in antagonizing $(Cys(Et)^{2,7}$-human αCGRP- and human adrenomedullin-induced responses compared to CGRP-induced responses in rat vas deferens, indicating receptor heterogeneity in rat vas deferens (32). The selectivity of BIBN-4096BS for human over rat receptors is due to binding to residue 74 of human RAMP1 (33). The greater selectivity of BIBN-4096BS for CRLR/RAMP1 over CRLR/RAMP2 compared to $CGRP_{8-37}$ suggests that the latter compound undergoes greater interactions with CRLR (31). Recently, the affinity of BIBN-4096BS and $CGRP_{8-37}$ was compared on CRLR/RAMP2 and CRLR/RAMP3 complexes. BIBN-4096BS did not antagonize adrenomedullin at any of these receptors (34).

The isolated perfused murine mesenteric bed provides a model for direct measurement of microvascular vasodilatation. The vessels are preconstricted with noradrenaline prior to application of a vasodilator, and a decrease in perfusion pressure correlates with vasodilatation. BIBN-4096BS was found to be an effective antagonist of CGRP and adrenomedullin responses in the murine mesenteric and cutaneous microvasculature, and of CGRP in the murine aorta. Additionally, after local application, BIBN-4096BS selectively inhibited the potentiation of microvascular permeability in the cutaneous microvasculature by CGRP and adrenomedullin, with no effect on responses induced by other microvascular vasodilators. BIBN-4096BS reversed both newly developed and established vasoactive responses induced by CGRP (35).

It is unlikely that BIBN-4096BS is interacting with the CRLR/RAMP2 (AM1 receptor) or CRLR/RAMP3 (AM2 receptor) complexes, as it has a very low affinity for these receptors (34), but rather its effects appear to be

mediated via the CGRP receptor (35). This observation was initially confirmed in pig coronary and basilar arteries (36), where BIBN-4096BS was used as a pharmacological tool to determine the different CGRP receptors. It was evident from this study that αCGRP receptors are present in these arteries, which are potently blocked by BIBN-4096BS. In another study in bovine middle cerebral artery segments, BIBN-4096BS and $\alpha CGRP_{8-37}$ both blocked αCGRP-induced dilatation with respective pK_B values of 6.3 and 7.8.

BIBN-4096BS has been shown to possess potent competitive antagonist activity at human cerebral and coronary artery $CGRP_1$ receptors (37). The pA_2 values are similar to those obtained in the SK-N-MC cell line (see Table I), suggesting the involvement of a common receptor mechanism mediating the vasodilating effects of CGRP, *i.e.*, CRLR/RAMP1. Interestingly, CGRP was approximately 10-fold less potent on coronary than cerebral arteries (pEC_{50} values of 8.3 and 9.4, respectively), which was probably related to differences in receptor density in the two arteries (37, 38).

Antidromic stimulation of the trigeminal ganglion in marmosets is a model suggested to measure facial blood flow to evaluate drugs that target the trigemino-vascular system during migraine headache (39). Antidromic stimulation of this ganglion results in the release of neuropeptides, including CGRP, leading to an increase in the skin blood flow innervated by sensory nerves. BIBN-4096BS completely inhibited this response, demonstrating that CGRP plays a major role in the vasodilatation observed following stimulation of the trigeminal nerve in marmosets. Triptans such as sumatriptan and zolmitriptan partially inhibited the increase in facial blood flow due to trigeminal ganglion stimulation (28).

We have carried out different sets of experiments in a porcine model of migraine (5, 40) to study the hemodynamic effects of CGRP after endogenous release through capsaicin administration or exogenous administration of human αCGRP. Hemodynamic effects of exogenous intracarotid infusion of human αCGRP and the cardiovascular safety of BIBN-4096BS in pigs were initially assessed. Activation of CGRP receptors elicits dilatation in different vascular beds in several species (41-43). Consistent with these studies, our experiments show that intracarotid infusions of αCGRP produced a marked vasodilatation in the porcine carotid circulation, with an accompanying fall in systemic arterial blood pressure (Fig. 2). The fact that the animals were systematically vagosympathectomized may explain why the hypotension was not accompanied by a baroreflex-mediated tachycardia, as reported earlier (41-43). Interestingly, the ipsilateral skin redness, together with the marked decrease in arteriovenous oxygen saturation difference (A-V SO_2) induced by CGRP, indicate that porcine carotid arteriovenous anastomoses dilated in response to αCGRP (44). In this experimental study in anesthetized pigs, BIBN-4096BS proved to be an effective antagonist at the CGRP receptors mediating the systemic (hypotension), as well as the carotid (increased carotid conductance, pulsations and skin redness) hemodynamic responses to αCGRP.

The fact that BIBN-4096BS also abolished αCGRP-induced decreases in the A-V SO_2 difference suggests an action on carotid arteriovenous anastomoses (for further considerations, see 45). Chemical substances, such as capsaicin, release endogenously stored CGRP (3, 46), which in turn dilates the carotid vasculature, including carotid arteriovenous anastomoses (43). In our study, intracarotid administration of capsaicin dilated carotid arteriovenous anastomoses and arterioles, together with an increase in carotid pulsations (Fig. 3) and a narrowing of arteriovenous oxygen saturation difference (A-V SO_2), as well as an elevation in jugular vein plasma CGRP concentration (Figs. 4 and 5). These effects were dose-dependently antagonized by BIBN-4096BS, except jugular venous plasma CGRP concentrations which increased (47). We concluded that blockade of prejunctional 'inhibitory' CGRP autoreceptors by BIBN-4096BS led to increased release of CGRP by capsaicin, similar to the modulation of sympathetic neurotransmission by presynaptic α-adrenoceptors (48).

Although the exact nature of CGRP receptors that mediate porcine carotid vascular responses is not certain, cardiac inotropic and vasodilator responses are mediated predominantly by $CGRP_1$ receptors (49), for which BIBN-4096BS has very high affinity (28, 50). Although we cannot rule out the involvement of CGRP in certain other conditions, for example, in cardiac preconditioning or coronary artery disease (51-53), the present results suggest cardiovascular safety for BIBN-4096BS. Nevertheless, the role of CGRP in cardiovascular pathophysiology needs to be elucidated before it can be established whether or not CGRP receptor antagonists like BIBN-4096BS are completely safe in patients with cardiovascular disorders.

Pharmacokinetics

The safety, tolerability and pharmacokinetics of BIBN-4096BS have been evaluated in healthy young male and female volunteers in a double-blind, placebo-controlled, randomized first-in-human study using single rising doses (54). BIBN-4096BS was infused i.v. for 10 min at doses ranging from 0.1 to 10 mg. Blood and urine samples were collected at different time periods. More adverse effects were observed with the higher doses of 5 and 10 mg of BIBN-4096BS, while lower doses had incidence rates similar to placebo. Mild to moderate adverse effects included reactions at the injection site, fatigue, headache, diarrhea, flatulence, paresthesia, rhinitis, flushing and abdominal pain. BIBN-4096BS exhibited multicompartmental disposition characteristics following i.v. administration. The apparent volume of distribution at steady state (V_{ss}) was 20 l and the terminal half-life was 2.5 h. The total plasma clearance of BIBN-4096BS was 12 l/h and the mean renal clearance was 2 l/h, suggesting that elimination is mainly via nonrenal pathways.

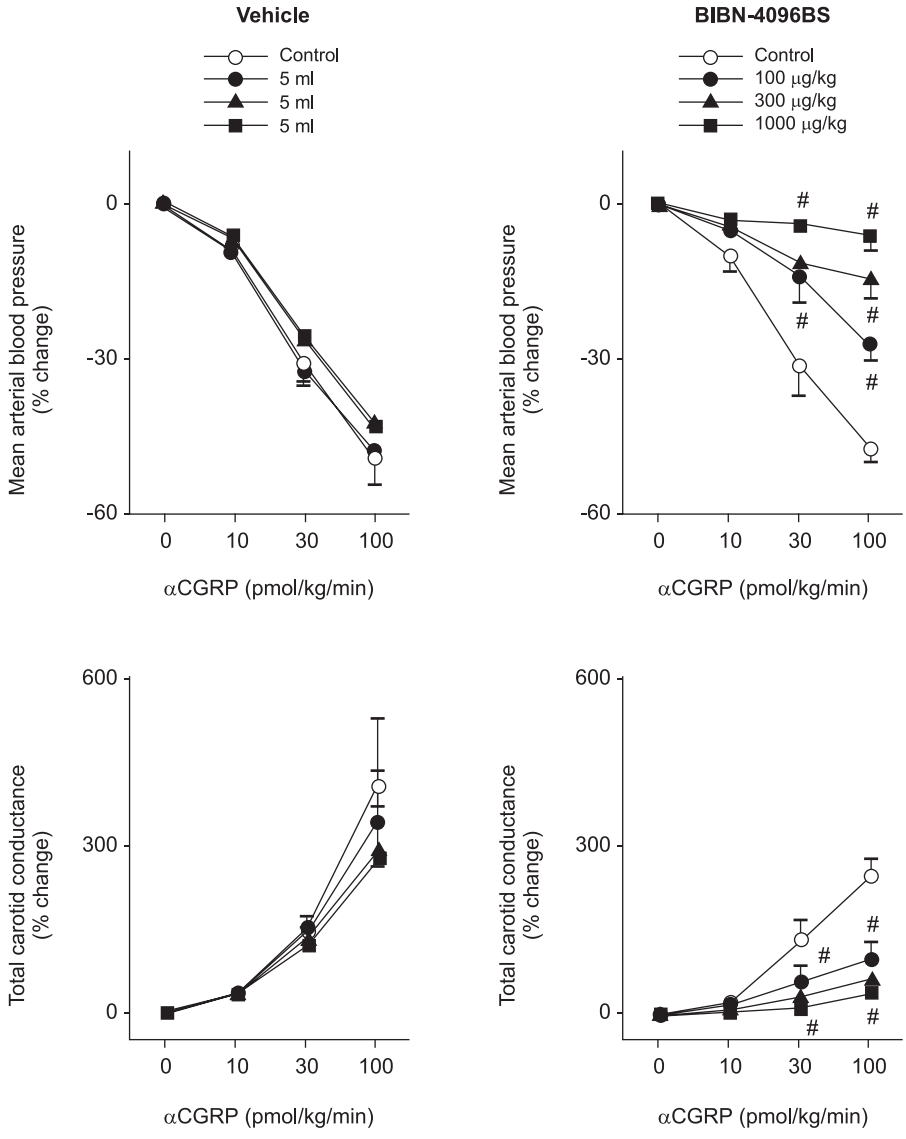

Fig. 2. Changes in mean arterial blood pressure and total carotid vascular conductance from baseline following intracarotid infusion of αCGRP in anesthetized pigs before (control) and after i.v. treatment with vehicle (n=6) or BIBN-4096BS (100, 300 and 1000 μg/kg; n=7). All values are expressed as mean ± s.e.m. The two highest doses of αCGRP significantly decreased mean arterial blood pressure and increased total carotid conductance (significance not shown for the sake of clarity). These effects of αCGRP were dose-dependently antagonized by BIBN-4096BS. #$p < 0.05$ *vs.* response after the corresponding volume of vehicle.

Clinical Studies

A multicenter, double-blind, randomized clinical trial of BIBN-4096BS was performed in patients with migraine receiving either placebo or 0.25, 0.5, 1, 2.5, 5 or 10 mg of BIBN-4096BS intravenously over a period of 10 min (29). BIBN-4096BS was effective in treating migraine headaches up to 6 h after onset. It had no vasoconstrictor effect, with paresthesia as the only adverse event. This confirmed the favorable safety and tolerability results reported earlier in the phase I study (54). Additionally, the rate of response to pain 2 h after treatment, the primary endpoint of the study, was significantly higher after infusion of BIBN-4096BS than after placebo.

Although these clinical findings are very encouraging, future research will be required to compare the safety and tolerability of BIBN-4096BS with the triptans and to develop more convenient formulations for the administration of nonpeptide CGRP receptor antagonists.

Acknowledgements

This article has a CDRI communication no. 6553.

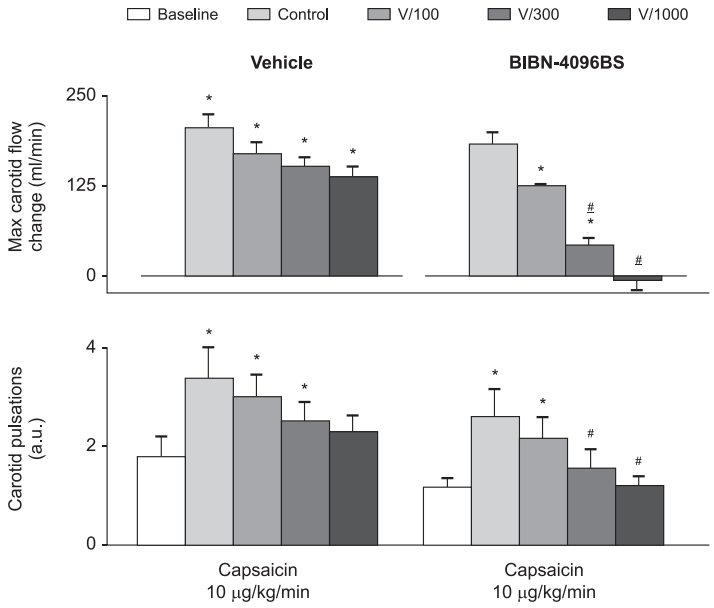

Fig. 3. Maximum changes in absolute carotid blood flow and carotid blood flow pulsations measured at baseline and following intracarotid infusions of capsaicin (10 μg/kg/min) in anesthetized pigs before (control) and after i.v. administration of vehicle (V; n=11) or BIBN-4096BS (100, 300 and 1000 μg/kg; n=11). All values are expressed as mean ± s.e.m. *$p < 0.05$ *vs.* baseline values; #$p < 0.05$ *vs.* response after the corresponding volume of vehicle. a.u., Arbitrary units.

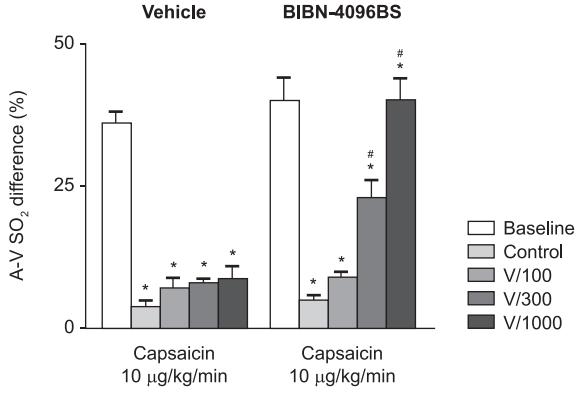

Fig. 4. Difference between arterial and jugular venous oxygen saturations (A-V SO_2 difference) measured at baseline and following intracarotid infusions of capsaicin (10 μg/kg/min) in anesthetized pigs before (control) and after i.v. administration of vehicle (V; n=11) or BIBN-4096BS (100, 399 and 1000 μg/kg; n=11). All values are expressed as mean ± s.e.m. *$p < 0.05$ *vs.* baseline values; #$p < 0.05$ *vs.* response after the corresponding volume of vehicle.

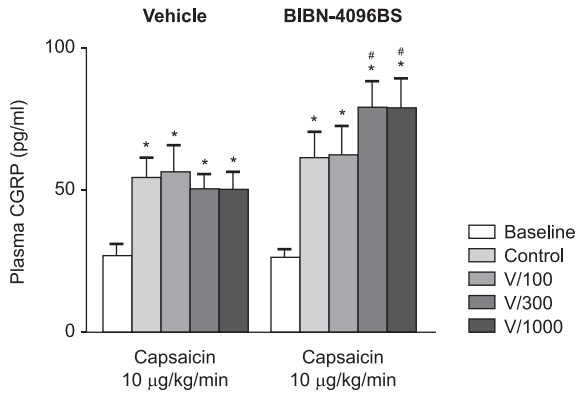

Fig. 5. Jugular vein plasma CGRP concentrations measured at baseline and after intracarotid infusions of capsaicin (10 μg/kg/min) in anesthetized pigs before (control) and after i.v. administration of vehicle (V; n=7) or BIBN-4096BS (100, 300 and 1000 μg/kg; n=6). All values are expressed as mean ± s.e.m. *$p < 0.05$ *vs.* baseline values; #$p < 0.05$ *vs.* response after the corresponding volume of vehicle.

Source

Boehringer Ingelheim Pharma GmbH & Co. KG (DE).

References

1. Raskin, N.H. *Diseases of the central nervous system.* In: Harrison's Principles of Internal Medicine. McGraw Hill, 1998, 2307-11.

2. Goadsby, P.J., Edvinsson, L. *The trigeminovascular system and migraine: Studies characterizing cerebrovascular and neuropeptide changes seen in humans and cats.* Ann Neurol 1993, 33: 48-56.

3. Buzzi, M.G., Bonamini, M., Moskowitz, M.A. *Neurogenic model of migraine.* Cephalalgia 1995, 15: 277-80.

4. Doggrell, S.A. *Migraine and beyond: Cardiovascular therapeutic potential for CGRP modulators.* Expert Opin Invest Drugs 2001, 10: 1131-8.

5. De Vries, P., Villalon, C.M., Saxena, P.R. *Pharmacological aspects of experimental headache models in relation to acute antimigraine therapy.* Eur J Pharmacol 1999, 375: 61-74.

6. Goadsby, P.J. *New directions in migraine research.* J Clin Neurosci 2002, 9: 368-73.

7. Kapoor, K. *Novel potential antimigraine compounds: Carotid and systemic haemodynamic effects in a porcine model of migraine.* In: Thesis Pharmacology. Rotterdam: Erasmus MC, 2003, 1-163.

8. Durham, P.L. *CGRP-receptor antagonists - A fresh approach to migraine therapy?* New Engl J Med 2004, 350: 1073-5.

9. Goadsby, P.J., Edvinsson, L. *Human in vivo evidence for trigeminovascular activation in cluster headache. Neuropeptide changes and effects of acute attacks therapies.* Brain 1994, 117: 427-34.

10. Goadsby, P.J. *Current concepts of the pathophysiology of migraine.* Neurol Clin 1997, 15: 27-42.

11. Hargreaves, R.J., Shepheard, S.L. *Pathophysiology of migraine - New insights.* Can J Neurol Sci 1999, 26: S12-9.

12. Poyner, D.R. *Calcitonin gene-related peptide: Multiple actions, multiple receptors.* Pharmacol Ther 1992, 56: 23-51.

13. Poyner, D. *Pharmacology of receptors for calcitonin gene-related peptide and amylin.* Trends Pharmacol Sci 1995, 16: 424-8.

14. Sams, A., Knyihar-Csillik, E., Engberg, J., Szok, D., Tatji, J., Bodi, I., Edvinsson, L., Vecsei, L., Jansen-Olesen, I. *CGRP and adrenomedullin receptor populations in human cerebral arteries: In vitro pharmacological and molecular investigations in different artery sizes.* Eur J Pharmacol 2000, 408: 183-93.

15. van Rossum, D., Hanisch, U.K., Quirion, R. *Neuroanatomical localization, pharmacological characterization and functions of CGRP, related peptides and their receptors.* Neurosci Biobehav Rev 1997, 21: 649-78.

16. Smith, D., Hill, R.G., Edvinsson, L., Longmore, J. *An immunocytochemical investigation of human trigeminal nucleus caudalis: CGRP, substance P and 5-HT_{1D}-receptor immunoreactivities are expressed by trigeminal sensory fibres.* Cephalalgia 2002, 22: 424-31.

17. Welch, K.M., Barkley, G.L., Tepley, N., Ramadan, N.M. *Central neurogenic mechanisms of migraine.* Neurology 1993, 43: S21-5.

18. Wimalawansa, S.J. *Calcitonin gene-related peptide and its receptors: Molecular genetics, physiology, pathophysiology, and therapeutic potentials.* Endocr Rev 1996, 17: 533-85.

19. Juaneda, C., Dumont, Y., Quirion, R. *The molecular pharmacology of CGRP and related peptide receptor subtypes.* Trends Pharmacol Sci 2000, 21: 432-8.

20. Goadsby, P.J., Duckworth, J.W. *Effect of stimulation of trigeminal ganglion on regional cerebral blood flow in cats.* Am J Physiol 1987, 253: R270-4.

21. Olesen, J.I., Mortensen, A., Edvinsson, L. *Calcitonin gene-related peptide is released from capsaicin-sensitive nerve fibres and induces vasodilatation of human cerebral arteries concomitant with activation of adenylyl cyclase.* Cephalalgia 1996, 16: 310-6.

22. Williamson, D.J., Hargreaves, R.J. *Neurogenic inflammation in the context of migraine.* Microsc Res Tech 2001, 53: 167-78.

23. Goadsby, P.J., Edvinsson, L., Ekman, R. *Release of vasoactive peptides in the extracerebral circulation of humans and the cat during activation of the trigeminovascular system.* Ann Neurol 1988, 23: 193-6.

24. Goadsby, P.J., Edvinsson, L., Ekman, R. *Vasoactive peptide release in the extracerebral circulation of humans during migraine headache.* Ann Neurol 1990, 28: 183-7.

25. Lassen, L.H., Haderslev, P.A., Jacobsen, V.B., Iversen, H.K., Sperling, B., Olesen, J. *CGRP may play a causative role in migraine.* Cephalalgia 2002, 22: 54-61.

26. Wisskirchen, F.M., Burt, R.P., Marshall, I. *Pharmacological characterization of CGRP receptors mediating relaxation of the rat pulmonary artery and inhibition of twitch responses of the rat vas deferens.* Br J Pharmacol 1998, 123: 1673-83.

27. Brain, S.D., Williams, T.J., Tippins, J.R., Morris, H.R., MacIntyre, I. *Calcitonin gene-related peptide is a potent vasodilator.* Nature 1985, 313: 54-6.

28. Doods, H., Hallermayer, G., Wu, D., Entzeroth, M., Rudolf, K., Engel, W., Eberlein, W. *Pharmacological profile of BIBN4096BS, the first selective small molecule CGRP antagonist.* Br J Pharmacol 2000, 129: 420-3.

29. Olesen, J., Diener, H.C., Husstedt, I.W. et al. *Calcitonin gene-related peptide receptor antagonist BIBN 4096 BS for the acute treatment of migraine.* New Engl J Med 2004, 350: 1104-10.

30. Moreno, M.J., Terrón, J.A., Stanimirovic, D.B., Doods, H., Hamel, E. *Characterization of calcitonin gene-related peptide (CGRP) receptors and their receptor-activity-modifying proteins (RAMPs) in human brain microvascular and astroglial cells in culture.* Neuropharmacology 2002, 42: 270-80.

31. Hay, D.L., Howitt, S.G., Conner, A.C., Doods, H., Schindler, M., Poyner, D.R. *A comparison of the actions of BIBN4096BS and $CGRP_{8-37}$ on CGRP and adrenomedullin receptors expressed on SK-N-MC, L6, Col 29 and Rat 2 cells.* Br J Pharmacol 2002, 137: 80-6.

32. Wu, D., Eberlein, W., Rudolf, K., Engel, W., Hallermayer, G., Doods, H. *Characterisation of calcitonin gene-related peptide receptors in rat atrium and vas deferens: Evidence for a (Cys(Et)(2,7))hCGRP-preferring receptor.* Eur J Pharmacol 2000, 400: 313-9.

33. Mallee, J.J., Salvatore, C.A., LeBourdelles, B., Oliver, K.R., Longmore, J., Koblan, K.S., Kane, S.A. *Receptor activity-modifying protein 1 determines the species selectivity of non-peptide CGRP receptor antagonists.* J Biol Chem 2002, 277: 14294-8.

34. Hay, D.L., Howitt, S.G., Conner, A.C., Schindler, M., Smith, D.M., Poyner, D.R. *CL/RAMP2 and CL/RAMP3 produce pharmacologically distinct adrenomedullin receptors: A comparison of effects of $adrenomedullin_{22-52}$, $CGRP_{8-37}$ and BIBN4096BS.* Br J Pharmacol 2003, 140: 477-86.

35. Grant, A.D., Tam, C.W., Lazar, Z., Shih, M.K., Brain, S.D. *The calcitonin gene-related peptide (CGRP) receptor antagonist BIBN4096BS blocks CGRP and adrenomedullin vasoactive responses in the microvasculature.* Br J Pharmacol 2004, 142: 1091-8.

36. Wu, D., Doods, H., Arndt, K., Schindler, M. *Development and potential of non-peptide antagonists for calcitonin-generelated peptide (CGRP) receptors: Evidence for CGRP receptor heterogeneity.* Biochem Soc Trans 2002, 30: 468-73.

37. Edvinsson, L., Alm, R., Shaw, D., Rutledge, R.Z., Koblan, K.S., Longmore, J., Kane, S.A. *Effect of the CGRP receptor*

antagonist BIBN4096BS in human cerebral, coronary and omental arteries and in SK-N-MC cells. Eur J Pharmacol 2002, 434: 49-53.

38. Moreno, M.J., Abounader, R., Hebert, E., Doods, H., Hamel, E. *Efficacy of the non-peptide CGRP receptor antagonist BIBN4096BS in blocking CGRP-induced dilations in human and bovine cerebral arteries: Potential implication in acute migraine treatment.* Neuropharmacology 2002, 42: 568-76.

39. Escott, K.J., Beattie, D.T., Connor, H.E., Brain, S.D. *Trigeminal ganglion stimulation increases facial skin blood flow in the rat: A major role for calcitonin gene-related peptide.* Brain Res 1995, 669: 93-9.

40. Saxena, P.R. *Cranial arteriovenous shunting, an in vivo animal model for migraine.* In: Experimental Headache Models. J. Olesen and M.A. Moskowitz (Eds), Lippincott-Raven Publishers, Philadelphia, 1995, 189-98.

41. Gardiner, S.M., Compton, A.M., Kemp, P.A., Bennett, T., Bose, C., Foulkes, R., Hughes, B. *Antagonistic effect of human α-CGRP$_{8-37}$ on the in vivo regional haemodynamic actions of human α-CGRP.* Biochem Biophys Res Commun 1990, 171: 938-43.

42. Shen, Y.-T., Pittman, T.J., Buie, P.S., Bolduc, D.L., Kane, S.A., Koblan, K.S., Gould, R.J., Lynch, J.J. Jr. *Functional role of α-calcitonin gene-related peptide in the regulation of the cardiovascular system.* J Pharmacol Exp Ther 2001, 298: 551-8.

43. Van Gelderen, E.M., Du, X.Y., Schoemaker, R.G., Saxena, P.R. *Carotid blood flow distribution, haemodynamics and inotropic responses following calcitonin gene-related peptide in the pig.* Eur J Pharmacol 1995, 284: 51-60.

44. Kapoor, K., Arulmani, U., Heiligers, J.P.C., Willems, E.W., Doods, H., Villalón, C.M., Saxena, P.R. *Effects of BIBN4096BS on cardiac output distribution and on CGRP induced carotid haemodynamic responses in the pig.* Eur J Pharmacol 2003, 475: 69-77.

45. Saxena, P.R. *Arteriovenous anastomoses and veins in migraine research.* In: Migraine, Clinical, Therapeutic, Conceptual and Research Aspects. J.N. Blau (Ed.), Chapman and Hall Medicine, London, 1987.

46. Eltorp, C.T., Olesen, J.I., Hansen, A.J. *Release of calcitonin gene-related peptide (CGRP) from guinea pig dura mater in vitro is inhibited by sumatriptan but unaffected by nitric oxide.* Cephalalgia 2000, 20: 838-44.

47. Kapoor, K., Arulmani, U., Heiligers, J.P.C., Garrelds, I.M., Willems, E.W., Doods, H., Villalón, C.M., Saxena, P.R. *Effects of the CGRP receptor antagonist BIBN4096BS on capsaicin-induced carotid haemodynamic changes in anaesthetised pigs.* Br J Pharmacol 2003, 140: 329-38.

48. Langer, S.Z. *Presynaptic regulation of catecholamine release.* Biochem Pharmacol 1974, 23: 1793-800.

49. Saetrum Opgaard, O., Hasbak, P., de Vries, R., Saxena, P.R., Edvinsson, L. *Positive inotropy mediated via CGRP receptors in isolated human myocardial trabeculae.* Eur J Pharmacol 2000, 397: 373-82.

50. Poyner, D., Marshall, I. *CGRP receptors: Beyond the CGRP1-CGRP2 subdivision?* Trends Pharmacol Sci 2001, 22: 223.

51. Lu, R., Li, Y.J., Deng, H.W. *Evidence for calcitonin gene-related peptide-mediated ischaemic preconditioning in the rat heart.* Regul Pept 1999, 82: 53-7.

52. Peng, J., Xiao, J., Ye, F., Deng, H.-W., Li, Y.-J. *Inhibition of cardiac tumor necrosis factor-α production by calcitonin gene-related peptide-mediated ischaemic preconditioning in isolated rat hearts.* Eur J Pharmacol 2000, 407: 303-8.

53. Wu, D.-M., van Zwieten, P.A., Doods, H.N. *Effects of calcitonin gene-related peptide and BIBN4096BS on myocardial ischaemia in anaesthetized rats.* Acta Pharmacol Sin 2001, 22: 588-94.

54. Iovino, M., Feifel, U., Yong, C.-L., Wolters, J.-M., Wallenstein, G. *Safety, tolerability and pharmacokinetics of BIBN 4096 BS, the first selective small molecule calcitonin gene-related peptide receptor antagonist, following single intravenous administration in healthy volunteers.* Cephalalgia 2004, 24: 645-56.

55. Choksi, T., Hay, D.L., Legon, L., Poyner, D.R., Hagner, S., Bloom, S.R., Smith, D.M. *Comparison of the expression of calcitonin receptor-like receptor (CRLR) and receptor activity modifying proteins (RAMPs) with CGRP and adrenomedullin binding in cell lines.* Br J Pharmacol 2002, 136: 784-92.

56. Doods, H. *Development of CGRP antagonists for the treatment of migraine.* Curr Opin Invest Drugs 2001, 2: 1261-8.

Drugs of the Future 2005, 30(5): 462-468

CCC: 0377-8282/2005
DOI: 10.1358/dof.2005.030.05.903432

Etravirine

Prop INN; USAN

Anti-HIV Agent
Reverse Transcriptase Inhibitor

R-165335
TMC-125

4-[6-Amino-5-bromo-2-(4-cyanophenylamino)pyrimidin-4-yloxy]-3,5-dimethylbenzonitrile

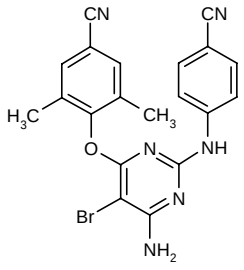

$C_{20}H_{15}BrN_6O$

Mol wt: 435.2769

CAS: 269055-15-4

EN: 290137

Abstract

The success of antiretroviral agents such as non-nucleoside reverse transcriptase inhibitors (NNRTIs) is compromised by the rapid emergence of resistant HIV-1 viral strains. A new-generation NNRTI, etravirine (TMC-125), has demonstrated potent activity against wild-type HIV-1 *in vitro*, with significantly greater efficacy and delayed emergence of resistance against HIV-1 strains carrying mutations when compared to other clinically approved NNRTIs. The compound is well tolerated and possesses a good oral pharmacokinetic profile in HIV-1-infected patients. Clinical studies have revealed significant antiviral activity in antiretroviral-naïve patients, with comparable if not higher potency than a 5-drug antiretroviral regimen, as well as in treatment-experienced patients, with rapid and long-term efficacy. Etravirine therefore shows immense promise as a new NNRTI.

Synthesis

Etravirine can be prepared by two different ways:

1) Reaction of 5-bromo-2,4,6-trichloropyrimidine (I) with 4-aminobenzonitrile (II) by means of DIEA in refluxing dioxane gives the diarylamine (III), which is condensed with 4-hydroxy-3,5-dimethylbenzonitrile (IV) by means of NaH in NMP to yield the corresponding adduct (V). Finally, this compound is treated with ammonia in dioxane at 150 °C in a pressure vessel (1). Scheme 1.

2) Cyclization of 4-guanidinobenzonitrile (VI) with diethyl malonate (VII) by means of NaOEt in ethanol gives 4-(4,6-dihydroxypyrimidin-2-ylamino)benzonitrile (VIII), which is treated with $POCl_3$ to yield the corresponding dichloro derivative (IX). Bromination of compound (IX) with Br_2 and $NaHCO_3$ in methanol/water affords 4-(5-bromo-4,6-dichloropyrimidin-2-ylamino)-benzonitrile (III), which is condensed with sodium 4-cyano-2,6-dimethylphenolate (X) and NMP in dioxane to provide the chloro precursor (V). Finally, this compound is treated with ammonia in isopropanol (2). Scheme 2.

Introduction

The human immunodeficiency virus (HIV), a retrovirus belonging to the Retroviridae family, *Lentivirus* genus, causes acquired immune deficiency syndrome, or AIDS, a gradual deterioration of the immune system leading to opportunistic infections and ultimately death. According to UNAIDS, there are currently 39.4 million people living with HIV/AIDS worldwide: 37.2 million adults and 2.2 million children under the age of 15 (figures current as of December 2004) (3).

Highly active antiretroviral therapies (HAARTs) include protease inhibitors (PIs), nucleoside reverse transcriptase inhibitors (NRTIs), non-nucleoside reverse transcriptase inhibitors (NNRTIs) and the more novel entry inhibitors and integrase inhibitors. A unique characteristic of retroviruses is the retrotranscription of viral RNA into DNA by the enzyme reverse transcriptase (RT), which is then integrated into the host cell genome. NNRTIs bind directly to the RT enzyme, at the pocket proximal to the polymerase active site, thereby deactivat-

S.L. Davies, J. Castañer, J.S. Silvestre, M. Bayés. Prous Science, P.O. Box 540, 08080, Barcelona, Spain.

Scheme 1: Synthesis of Etravirine

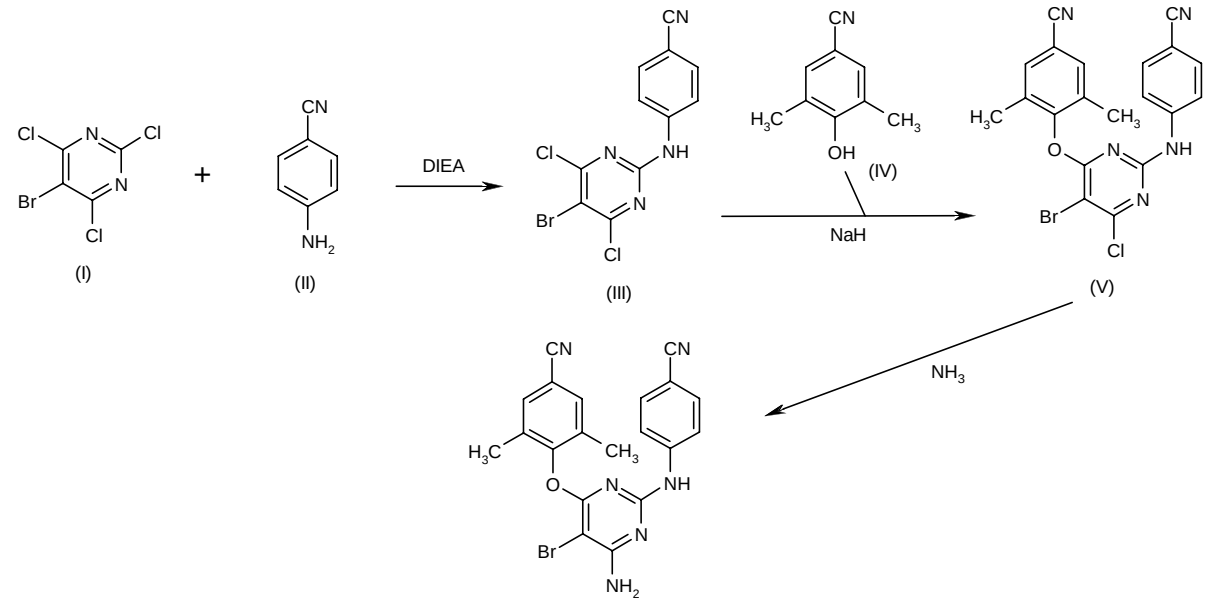

Scheme 2: Synthesis of Etravirine

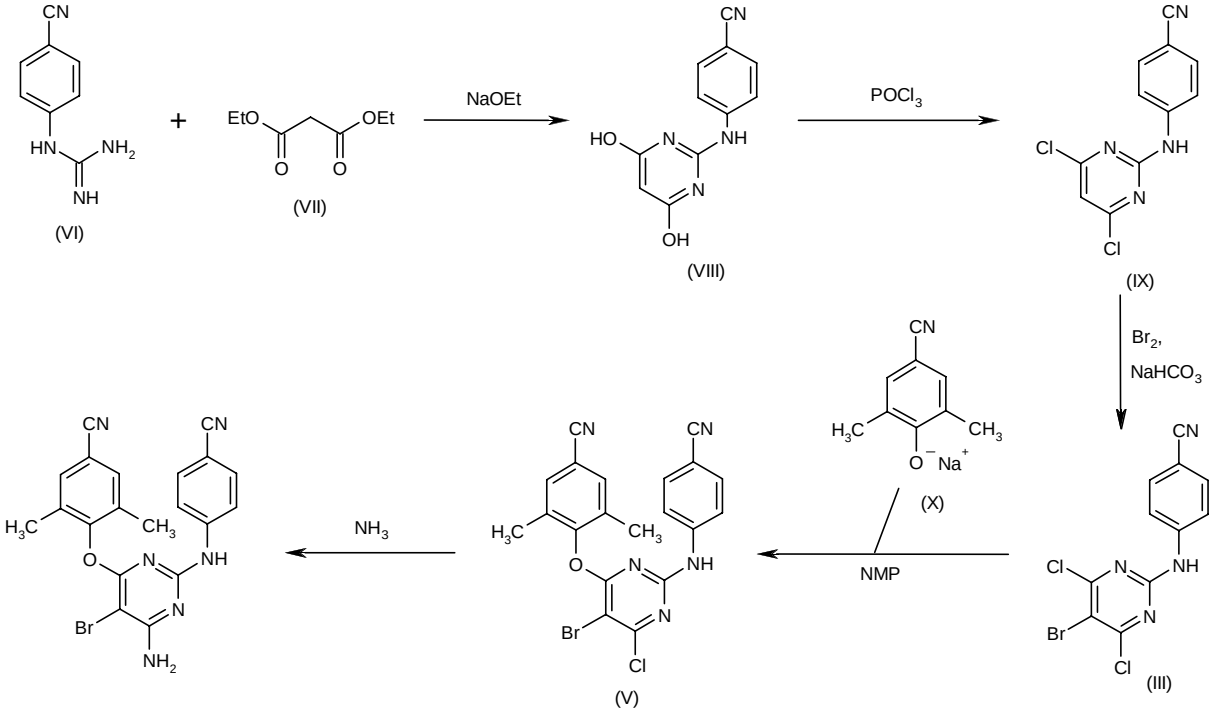

ing it. Several NNRTIs are now available as clinical treatments for HIV-1 infection (3) (Table I).

However, the success of NNRTI therapy is compromised by the rapid emergence of resistant viral strains carrying mutations at residues that surround the NNRTI binding pocket. Combination therapy, introduced because of the issue of drug resistance, has also led to the development of adherence problems, reduced antiretroviral

Table I: Non-nucleoside reverse transcriptatse inhibitors (NNRTIs) marketed for the treatment of HIV/AIDS.

Drug	Source	Phase
1. Nevirapine (Viramune)	Boehringer Ingelheim	L-1996
2. Delavirdine mesilate (Rescriptor)	Pfizer	L-1997
3. Efavirenz (Sustiva, Stocrin)	Bristol-Myers Squibb; Merck & Co.	L-1998

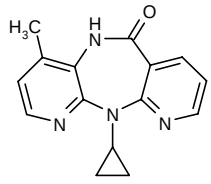

(1)

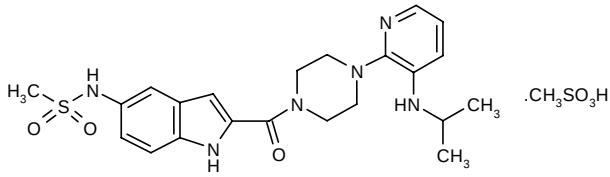

(2)

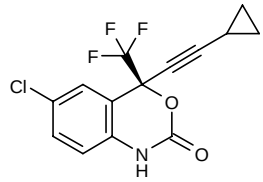

(3)

activity and drug toxicity. As a result, there is a need for new antiretroviral agents that can improve treatment with convenience, reduced toxicity and improved antiretroviral activity against both wild-type and drug-resistant HIV. Furthermore, extensive crossresistance among the available NNRTIs has been documented (4-7). Therefore, next-generation NNRTIs that show promise against 'signature' mutations are in development. One such new drug is etravirine (TMC-125, R-165335), a potent diarylpyrimidine derivative discovered during a screening involving comprehensive profiling of antiviral activity against wild-type and mutant NNRTI-resistant HIV-1 strains (2, 8-13) and currently under phase II development at Tibotec (14).

Pharmacological Actions

In vitro, etravirine demonstrated potent activity against wild-type HIV-1 (EC_{50} = 1.4-4.8 nM), comparable to efavirenz, with some activity against HIV-2 (EC_{50} = 3.5 μM) and very low cytotoxicity (CC_{50} > 100 μM in MT-4 cells). It was also significantly more effective than other clinically approved NNRTIs against HIV-1 strains carrying mutations, with EC_{50} values of 1-19 nM against a panel of viruses carrying 1 or 2 amino acid substitutions. Human serum albumin or α_1-acid glycoprotein did not significantly affect its antiviral activity. Etravirine also inhibited 98% of over 2,000 clinical isolates and 97% of approximately 1,000 NNRTI-resistant strains, compared to 77% and 54% of strains, respectively, with efavirenz (2, 8-12). Its inhibitory activity against RT and HIV-1, including NNRTI-resistant strains, and its cytotoxicity in comparison to other RT inhibitors are shown in Table II.

In further studies, etravirine exhibited antiviral activity against 91% of 5,610 clinical samples, with an EC_{50} of < 10 nM, while efavirenz inhibited 67% at 10 nM. In those samples showing resistance to the currently available NNRTIs, etravirine inhibited 76% at 10 nM (15).

Rates of emergence of resistance were monitored in MT-4 cells infected with wild-type HIV-1 at high multiplicities of infection (MOIs). Resistance to the first-generation NNRTIs nevirapine and efavirenz developed rapidly in viruses harboring single mutations in Y181C and G190E, respectively. In contrast, the emergence of HIV-1 resistance to etravirine was delayed, requiring the presence of 2 mutations (L100I + Y181C after 21 days), and in some cases did not occur at all (16-18). Furthermore, etravirine exhibited an EC_{50} of < 10 nM against 63% of recombinant clinical isolates harboring 4 NNRTI resistance mutations. For comparison, an EC_{50} of < 10 nM was recorded for efavirenz against 70% of the samples with only 2 mutations (15).

The sensitivity to etravirine of specific single and multiple mutations observed *in vitro* or associated with decreased susceptibility in clinical isolates was also examined. The drug exhibited potent antiviral activity against the majority of site-directed mutants and decreased susceptibility was only associated with the less prevalent triple mutants (19, 20).

Computer modeling and structural analysis of etravirine has enabled characterization of its interaction with the RT binding pocket, and the effects of pocket mutations on this binding profile. These experiments demonstrated that etravirine benefits from a shape that potentially enables the molecule to bend or flex and reposition, and this may help it retain RT binding despite mutations, which normally push other NNRTIs out of their site of action. These characteristics appear to be crucial for the drug's potency against wild-type and a wide range of drug-resistant mutant HIV-1 RTs (21-23).

Pharmacokinetics and Metabolism

Incubation of etravirine with human liver microsomal fractions suggested good metabolic stability, with 15% drug degradation and a 7% decrease in antiviral activity after 120 min (8-10).

A phase I study was carried out to examine the drug interaction profile of etravirine. As the agent induces the cytochrome P-450 (CYP) isozyme CYP3A4, its metabo-

Table II: Pharmacological profile of etravirine compared to other selected RT inibitors launched or currently under active development (from Prous Science Integrity®).

Compound	HIV-1 RT inhibition (IC_{50}, nM)	HIV-1 antiviral activity (IC_{50}, nM)	HIV-1 (NNRTI-resistant) antiviral activity (IC_{50}, nM)	Cytotoxicity (CC_{50}, μM)
Etravirine	38.0	1.56 (1.4-2.0)	1.1 (1.0-1.2)	> 100
Abacavir		865.5 (321-1410)		136
Amdoxobir		3827 (540-10,000)		> 100
BCH-10618		21,075 (2800-43,000)		> 500
BCH-13520		140		> 250
Calanolide A	472.5 (25-1600)	186.7 (53-400)		9.1 (7.0-14.8)
Capravirine	227.7 (5.3-450)	0.70		
Dapivirine	24.0	0.98 (0.9-1.0)	1.0	2.3 (2.2-2.5)
D-D4FC	371.8 (67-1000)			> 206
Delavirdine	254.0 (230-260)	69.4 (14.4-200)	38.0	73
Didanosine	650.0 (620-680)	8500 (530-32,000)	8083 (7150-9800)	368 (59->2000)
Efavirenz	18.2 (0.7-48)	5.9 (0.9-50)	34,616 (2.0-207,000)	57.5 (42-> 100)
Emtricitabine		515 (500-530)		> 100
Foscarnet	200.0	24,533 (16,300-41,000)		223
GW-5634	13.4 (5.7-21)	49.0		
GW-8248	2.80 (1.8-4.7)	1.0		
Lamivudine	284.8 (4.0-600)	1331 (56-4400)		2667
Nevirapine	3774 (0.75-23,000)	1154 (20-38,000)	9617 (638-> 100,000)	329 (75-743)
Rilpivirine		0.40		10
SP-1093V		1000		> 100
Stavudine	545 (80-1010)	1313 (240-2800)		268 (47-564)
Tenofovir	K_i = 22	75,218 (630-500,000)		737 (197-1250)
Tenofovir disoproxil fumarate		5.0 (3.0-7.0)		31.3 (22-50)
UC-781	23.0	10.4		
Zalcitabine	399 (1.0-1440)	716.1 (9.8-3020)	170 (60-280)	335 (4.0-3000)
Zidovudine	79.7 (3.0-480)	63.5 (0.5-2100)	11.6 (1.0-100)	65.5 (0.09-> 500)

HIV-1 antiviral activity and cytotoxicity evaluated in infected and noninfected MT-4 or MT-2 human T-lymphoblastoid cells, respectively. Range in parentheses.

lism can be moderately reduced by pure CYP3A4 inhibitors, such as the PI indinavir, and increased by other CYP3A4 inducers, such as the first-generation NNRTI nevirapine. Ritonavir, which is associated with both inhibition and induction of CYP3A4 and induction of glucuronidation, reduced etravirine exposure (24).

New tablet formulations of etravirine were compared to the reference formulation in an open-label, randomized, crossover study in 45 healthy volunteers. The subjects received single 400-mg doses of each formulation with a standard meal, separated by a washout period of 2 weeks. Rapid absorption was observed after all formulations, but the relative oral bioavailability, as measured by C_{max} and AUC, was significantly greater after administration of the new tablet formulations and intersubject variability was lower (25).

Table III: Clinical studies of etravirine (from Prous Science Integrity®).

Indication	Design	Treatments	n	Conclusions	Ref.
HIV infection	Randomized Double-blind	Etravirine, 900 mg p.o. b.i.d. x 7 d (n=12) Placebo (n=7)	19	Etravirine was well tolerated and effective in decreasing the viral load of treatment-naïve patients with HIV-1 infection after only 7 days of treatment	21-23
HIV infection	Pooled/meta-analysis	Etravirine, 900 mg b.i.d. x 7 d (n=12) Zidovudine + Lamivudine + Abacavir + Indinavir + Nevirapine x 7 d (n=13)	25	Etravirine monotherapy given for 7 days was as effective as a combination of 5 antiretroviral drugs in reducing plasma viral levels in patients with HIV-1 infection	24, 25
HIV infection	Open	Etravirine, 900 mg p.o. b.i.d. x 7 d	16	Patients with HIV-1 infection and resistance to current NNRTIs showed a median HIV-1 viral load reduction of 0.89 $\log_{10}$ copies/ml after receiving etravirine for 7 days. Only mild to moderate adverse events were found	26, 27
HIV infection	Open	Etravirine, 800 mg b.i.d. + 3-4 Antiretroviral agents x 48 wks	7	Long-term treatment of patients with HIV infection with etravirine in addition to other antiretroviral therapies was well tolerated and effective	28

Another study in healthy subjects examined the pharmacokinetic interaction between etravirine and didanosine. In this open-label, randomized, crossover study, the volunteers received etravirine 800 mg b.i.d. for 7 days followed by a single dose on day 8. After a 14-day washout period, they were administered didanosine 400 mg/day for 16 days and etravirine 800 mg b.i.d. on either days 1-8 or days 9-16. No significant pharmacokinetic interaction was seen between etravirine and didanosine, and therefore no dose adjustment should be necessary when they are used in combination (26).

Clinical Studies

Etravirine advanced to clinical studies within 1 year of its identification. The first study in HIV-1-infected patients was a double-blind, randomized, placebo-controlled trial conducted in Russia to evaluate the antiviral activity of etravirine as monotherapy in antiretroviral-naïve male patients. Twelve patients received etravirine (900 mg b.i.d.) for 7 days and 6 received matching placebo. Baseline characteristics included median $CD4^+$ cell counts of 650 cells/mm^3 and a median viral load of 57,619 copies/ml. Viral load was reduced by a mean of 1.99 $\log_{10}$ copies/ml and 0.06 $\log_{10}$ copies/ml, respectively, after 7 days in the etravirine and placebo groups. Daily plasma viral decline rates of 0.33 $\log_{10}$ copies/ml and 0.02 $\log_{10}$ copies/ml, respectively, were observed in the etravirine and placebo groups. Of 12 etravirine-treated patients, plasma viral load decreased to < 50 copies/ml in 2 and to < 400 copies/ml in 8. No viral rebound was seen and there was no evidence of resistance development. Adverse events were mild, the most common being somnolence (reported in 3 etravirine patients and 1 placebo patient). Steady state was reached in 4-5 days, with mean trough plasma levels (246 ng/ml) well exceeding the *in vitro* EC_{50} (27-29). The results from this and the following clinical studies are summarized in Table III.

The rate of viral decline achieved with etravirine monotherapy (900 mg b.i.d. for 1 week) was compared to a 5-drug antiretroviral regimen (zidovudine, lamivudine, abacavir, indinavir, nevirapine) in 25 antiretroviral-naïve patients. A similar initial rate of decline in plasma HIV-1 RNA was observed, with a median decrease in HIV-1 RNA of 1.92 and 1.55 $\log_{10}$ copies/ml, respectively, and a median increase in $CD4^+$ T-cells of 119 and 60 cells/mm^3, respectively, measured on etravirine and the 5-drug regimen (30, 31).

Etravirine also demonstrated high potency in treatment-experienced patients. The drug was examined for its efficacy in HIV-1-infected patients failing NNRTI (efavirenz or nevirapine) therapy and with confirmed resistance to efavirenz in an open-label phase IIa trial. Sixteen patients receiving an NNRTI-containing antiretroviral regimen with an HIV-1 RNA viral load of > 2,000 copies/ml and phenotypic resistance to NNRTIs received etravirine for 7 days as a substitute for their current NNRTI. Viral loads after treatment showed a median decrease of 0.9 $\log_{10}$ copies/ml from baseline, which continued to decrease following treatment on day 8. Seven patients showed a decrease of > 1 $\log_{10}$ copies/ml. Steady-state drug levels were achieved by day 6, with mean peak plasma concentrations reached at 4 h and a

mean elimination half-life of 36 h. The most significant adverse events were grade 1 diarrhea (31%) and mild headache (25%) (32, 33).

Long-term treatment of patients with HIV-1 infection with etravirine was evaluated in an open phase II trial including 7 patients continuing other antiretroviral therapies. In addition to 3 or 4 other antiretroviral agents, patients received etravirine 800 mg b.i.d. Results were assessed at 48 weeks and all but 2 patients had a viral load below 50 copies/ml; the remaining 2 patients had a viral load below 500 copies/ml. In an exploratory cohort of patients (n=77) with matched treatment history who began a new antiretroviral therapy, the probability of achieving such reductions in viral load was greatly reduced. Etravirine was well tolerated and in treated patients the median decrease from baseline in viral load was 1.4 $\log_{10}$ copies/ml (34).

A long-term phase IIb dose-finding study in treatment-experienced HIV-1-infected patients is currently recruiting subjects in a number of countries in Europe and in Canada (14).

Source

Tibotec (BE, US) (a subsidiary of Johnson & Johnson).

References

1. De Cort, B., De Jonge, M.R., Heeres, J., Ho, C.Y., Kavash, R.W., Koymans, L.M.H., Kukla, M.J., Ludovici, D.W., Van Aken, K.J.A. (Janssen Pharmaceutica NV). *HIV replication inhibiting pyrimidines.* EP 1002795, EP 1270560, JP 2002529456, US 2003114472, US 6878717, WO 0027825.

2. Ludovici, D.W., De Corte, B.L., Kukla, M.J. et al. *Evolution of anti-HIV drug candidates. Part 3: Diarylpyrimidine (DAPY) analogues.* Bioorg Med Chem Lett 2001, 11: 2235-9.

3. Prous Science Drug R&D Backgrounders: *HIV and AIDS (online publication).* Updated May 23, 2005.

4. Van Laethem, K., Witvrouw, M., Pannecouque, C. et al. *Mutations in the non-nucleoside binding-pocket interfere with the multi-nucleoside resistance phenotype.* AIDS 2001, 15: 553-61.

5. St. Clair, M.H., Martin, J.L., Tudor-Williams, G., Bach, M.C., Vavro, C.L., King, D.M., Kellam, P., Kemp, S.D., Larder, B.A. *Resistance to ddI and sensitivity to AZT induced by a mutation in HIV-1 reverse transcriptase.* Science 1991, 253: 1557-9.

6. Casado, J.L., Hertogs, K., Ruiz, L. et al. *Non-nucleoside reverse transcriptase inhibitor resistance among patients failing a nevirapine plus protease inhibitor-containing regimen.* AIDS 2000, 14: F1-7.

7. Antinori, A., Zaccarelli, M., Cingolani, A. et al. *Cross-resistance among nonnucleoside reverse transcriptase inhibitors limits recycling efavirenz after nevirapine failure.* AIDS Res Hum Retroviruses 2002, 18: 835-8.

8. Andries, K., De Bethune, M.P., Kukla, M.J., Azun, H., Lewi, P.J., Janssen, P.A.J., Pauwels, R. *R165335-TMC125, a novel non nucleoside reverse transcriptase inhibitor (NNRTI) with nanomolar activity against NNRTI resistant HIV strains.* 40th Intersci Conf Antimicrob Agents Chemother (Sept 17-20, Toronto) 2000, Abst F-1840.

9. Andries, K., de Béthune, M.-P., Ludovici, D.W., Kukla, M.J., Azijn, H., Lewi, P., Janssen, P.A.J., Pauwels, R. *R165335-TMC125, a novel non nucleoside reverse transcriptase inhibitor (NNRTI) with nanomolar activity against NNRTI resistant HIV strains.* AIDS 2000, 14(Suppl. 4): Abst PL4.5.

10. Andries, K., Azijn, H., Thielemans, T. et al. *TMC125, a novel next-generation nonnucleoside reverse transcriptase inhibitor active against nonnucleoside reverse transcriptase inhibitor-resistant human immunodeficiency virus type 1.* Antimicrob Agents Chemother 2004, 48: 4680-6.

11. De Bethune, M.P. et al. *R165335-TMC125, a third generation non nucleoside reverse transcriptase inhibitor (NNRTI), inhibits 98% of more than 2,000 recombinant HIV clinical isolates at 100 nM.* 40th Intersci Conf Antimicrob Agents Chemother (ICAAC) (Sept 17-20, Toronto) 2000, Abst F-1841

12. de Béthune, M.-P., Hertogs, K., Azijn, H., Larder, B., Andries, K., Janssen, P.A.J., Pauwels, R. *R165335-TMC125, a third generation nonnucleoside reverse transcriptase inhibitor (NNRTI), inhibits 97% of more than 1000 recombinant NNRTI resistant HIV clinical isolates with an IC_{50} below 100 nM.* AIDS 2000, 14(Suppl. 4): Abst P2.

13. De Corte, B.L. *From 4,5,6,7-tetrahydro-5-methylimidazo[4,5,1-jk](1,4)benzodiazepin-2(1H)-one (TIBO) to etravirine (TMC125): Fifteen years of research on non-nucleoside inhibitors of HIV-1 reverse transcriptase.* J Med Chem 2005, 48(6): 1689-96.

14. *TMC125.* Tibotec Web Site, April 18, 2005.

15. Vingerhoets, J., Van Marck, H., Veldeman, J., Peeters, M., McKenna, P., Pauwels, R., de Béthune, M.-P. *Antiviral activity of TMC125, a potent next-generation non-nucleoside reverse transcriptase inhibitor (NNRTI), against > 5000 recombinant clinical isolates exhibiting a wide range of NNRTI resistance.* Antivir Ther 2003, 8(3): Abst 8.

16. De Bethune, M., Azijn, H., Janssen, P., Pauwels, R. *In vitro selection experiments demonstrate reduced resistance with TMC120 and TMC125 compared with first generation NNRTIs.* 41st Intersci Conf Antimicrob Agents Chemother (Dec 16-19, Chicago) 2001, Abst F-1681.

17. de Béthune, M.-P., Azijn, H., Andries, K., Janssen, P., Pauwels, R. *In vitro selection experiments demonstrate reduced development of resistance with TMC120 and TMC125 compared with first generation non-nucleoside reverse transcriptase inhibitors.* Antivir Ther 2001, 6(Suppl. 1): Abst 7.

18. Vingerhoets, J., Azijn, H., Fransen, E., Andries, K., Pauwels, R., de Béthune, M.-P. *TMC125 can suppress the selection of resistant HIV from a virus population carrying the K103N or the Y181C mutation.* Antivir Ther 2002, 7(2, Suppl. 1): Abst 9.

19. Vingerhoets, J., De Baere, I., Azijn, H., Van den Bulcke, T., McKenna, P., Pattery, T., Pauwels, R., de Béthune, M.-P. *Antiviral activity of TMC125 against a panel of site-directed mutants encompassing mutations observed in vitro and in vivo.* 11th Conf Retroviruses Opportunistic Infect (Feb 8-11, San Fransisco) 2004, Abst 621.

20. Vingerhoets, J., De Baere, I., Azijn, H., Van den Bulcke, T., Mc Kenna, P., Pattery, T., Pauwels, R., de Bethune, M.P. *Antiviral activity of the next generation NNRTI TMC125 against a panel of site-directed mutants encompassing mutations observed in vitro and in vivo.* 15th Int AIDS Conf (July 11-16, Bangkok) 2004, Abst WeOrA1271.

21. De Kerpel, J.O.A., Kukla, M.J., Azijn, H., de Béthune, M.-P., Vingerhoets, J., Pauwels, R. *Structural characteristics of the binding of TMC125, a potent, next generation NNRTI, to wild type, single and double HIV mutants.* 224th ACS Natl Meet (Aug 18-22, Boston) 2002, Abst MEDI 29.

22. Udier-Blagovic, M., Tirado-Rives, J., Jorgensen, W.L. *Validation of a model for the complex of HIV-1 reverse transcriptase with nonnucleoside inhibitor TMC125.* J Am Chem Soc 2003, 125: 6016-7.

23. Das, K., Clark, A.D. Jr., Lewi, P.J. et al. *Roles of conformational and positional adaptability in structure-based design of TMC125-R165335 (etravirine) and related non-nucleoside reverse transcriptase inhibitors that are highly potent and effective against wild-type and drug-resistant HIV-1 variants.* J Med Chem 2004, 47: 2550-60.

24. Baede, P., Piscitelli, S., Graham, N., Van't Klooster, G. *Drug interactions with TMC125, a potent next generation NNRTI.* 42nd Intersci Conf Antimicrob Agents Chemother (Sept 27-30, San Diego) 2002, Abst A-1827.

25. Scholler, M., Hoetelmans, R., Beets, G., Vandermeulen, K., Peeters, M., Bastiaanse, L., Leemans, R., Debroye, C., Woodfall, B. *Substantial improvement of oral biovailability of TMC125 using new tablet formulations in healthy volunteers.* 6th Int Workshop Clin Pharmacol HIV Ther (April 28-30, Québec) 2005, Abst 82.

26. Scholler, M., Hoetelmans, R., Bollen, S., Vandermeulen, K., Peeters, M., Bastiaanse, L., Debroye, C., Woodfall, B. *No significant interaction between TMC125 and didanosine (ddI) in healthy volunteers.* 6th Int Workshop Clin Pharmacol HIV Ther (April 28-30, Québec) 2005, Abst 29.

27. Gruzdev, B., Rakhmanova, A., van't Klooster, G., De Dier, K., Comhaire, S., Baede-Van Dijk, P., de Béthune, M.P., Pauwels, R. *One week of monotherapy with TMC125, a novel highly potent NNRTI, produces a mean 2-log reduction in viral load in antiretroviral-naïve, HIV-1 infected volunteers.* 8th Eur Conf Clin Aspects Treat HIV Infect (Oct 28-31, Athens) 2001, Abst O9.

28. Gruzdev, B., Rakhmanova, A., De Dier, K., Comhaire, S., Baede-Van Dijk, P., Van't Klooster, G. *TMC125 is a highly potent non-nucleoside reverse transcriptase inhibitor (NNRTI) in antiretroviral therapy (ART)-naïve, HIV-1 infected subjects.* 41st Intersci Conf Antimicrob Agents Chemother (Dec 16-19, Chicago) 2001, Abst I-668.

29. Gruzdev, B., Rakhmanova, A., Doubovskaya, E., Yakovlev, A., Peeters, M., Rinehart, A., de Dier, K., Baede-Van Dijk, P., Parys, W., van 't Klooster, G. *A randomized, double-blind, placebo-controlled trial of TMC125 as 7-day monotherapy in antiretroviral naive, HIV-1 infected subjects.* AIDS 2003, 17: 2487-94.

30. Sankatsing, S., Weverling, G., van't Klooster, G., Prins, J., Lange, J. *TMC125 monotherapy for 1 week results in a similar initial rate of decline of HIV-1 RNA as therapy with a 5-drug regimen.* 9th Conf Retroviruses Opportunistic Infect (Feb 24-28, Seattle) 2002, Abst 5.

31. Sankatsing, S.U.C., Weverling, G.J., Peeters, M., van't Klooster, G., Gruzdev, B., Rakhmanova, A., Danner, S.A., Jurriaans, S., Prins, J.M., Lange, J.M. *TMC125 exerts similar initial antiviral potency as a five-drug, triple class antiretroviral regimen.* AIDS. 2003, 17: 2623-7.

32. Gazzard, B.G., Pozniak, A.L., Rosenbaum, W. et al. *An open-label assessment of TMC 125 - A new, next-generation NNRTI, for 7 days in HIV-1 infected individuals with NNRTI resistance.* AIDS 2003, 17: F49-54.

33. Gazzard, B.G., Pozniak, A., Arasteh, K., Staszewski, S., Rozenbaum, W., Yeni, P., van't Klooster, G., De Dier, K., Peeters, M., de Béthune, M.P., Graham, N., Pauwels, R. *One-week therapy with TMC125, a next generation NNRTI, demonstrates high potency in treatment-experienced HIV-1-infected individuals with phenotypic NNRTI-resistance.* 14th Int AIDS Conf (July 7-12, Barcelona) 2002, Abst TuPeB4438.

34. Montaner, J., Lazzarin, A., Arribas, J., Pozniak, A., Peeters, M., Woodfall, B., Simonts, M., Hogg, B., Bonner, S. *Sustained antiviral activity of TMC125 plus optimised antiretroviral therapy in highly treatment-experienced patients.* 7th Int Congr Drug Ther HIV Infect (Nov 14-18, Glasgow) 2004, Abst P316.

Additional References

Raoof, A., Lachau-Durand, S., Willems, B., De Zwart, L., Mouche, M., Steemans, K., Verbeeck, J., Van Cauteren, H. *The pharmacokinetics of TMC125 in different mouse strains: Impact on carcinogenicity testing strategy.* 11th Annu FDA Sci Forum (April 27-28) 2005, Abst C-21.

Drugs of the Future 2013, 38(9): 625-630

CCC: 0377-8282/2013
DOI: 10.1358/dof.2013.38.9.1990154

MONOGRAPH

REMIMAZOLAM

Prop INN

$GABA_A$ Benzodiazepine Site Receptor Agonist
Anesthetic/Sedative

CNS-7056
ONO-2745

3-[8-Bromo-1-methyl-6-(2-pyridyl)-4*H*-imidazo[1,2-*a*][1,4]benzodiazepin-4(*S*)-yl]propionic acid methyl ester

InChI: 1S/C21H19BrN4O2/c1-13-12-24-21-17(7-9-19(27)28-2)25-20(16-5-3-4-10-23-16)15-11-14(22)6-8-18(15)26(13)21/h3-6,8,10-12,17H,7,9H2,1-2H3/t17-/m0/s1

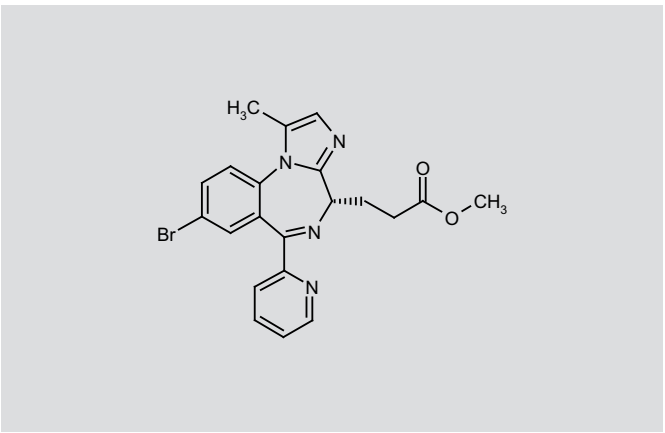

$C_{21}H_{19}BrN_4O_2$
Mol wt: 439.305
CAS: 308242-62-8
EN: 297752

SUMMARY

Remimazolam, also known as CNS-7056, is a novel, ultra-short-acting benzodiazepine. It has a faster onset and shorter duration of action than midazolam, with reliable metabolism to an inactive metabolite, CNS-7054, by plasma esterases. The sedative effects appear typical of benzodiazepines and are dependent on dose, with a wide therapeutic range.

Key words: Anesthetic – Benzodiazepine – Sedation – Remimazolam – CNS-7056

Estee Piehl, M.D., Department of Anesthesiology, University of Colorado Denver, 12631 E 17th Ave., AO-1 building, R2007, MS 8202, Aurora, Colorado 80045, USA. E-mail: Estee.Piehl@ucdenver.edu.
*Synthesis prepared by J. Bolòs, R. Castañer. Thomson Reuters, Provença 398, 08025 Barcelona, Spain.

SYNTHESIS*

Condensation of 5-bromoanthranilic acid (I) with the lithium derivative of 2-bromopyridine (II) in cold THF/ethyl ether gives the diaryl ketone (III). *N*-Fmoc-L-glutamic acid 5-methyl ester (IV) is chlorinated with oxalyl chloride and catalytic DMF to produce the acid chloride (V), which is then coupled with the amino ketone (III) in boiling chloroform to afford amide (VI). Base-mediated deprotection of amine (VI), followed by cyclization by treatment with AcOH in dichloroethane leads to the benzodiazepinone (VII). Subsequent treatment of lactam (VII) with *bis*-morpholinophosphorochloridate and NaH affords the imino phosphate (VIII), which is then condensed with 1-amino-2-propanol (IX) producing amidine (X). Finally, remimazolam is obtained by Swern oxidation of the secondary alcohol of (X), followed by cyclization under acidic conditions (1). Scheme 1.

BACKGROUND

All benzodiazepines act as agonists at a specific site on the γ-aminobutyric acid type A ($GABA_A$) receptor to enhance inhibitory activity of the neurotransmitter, GABA (2). $GABA_A$ receptors are present throughout the CNS and their activation causes sedation, anxiolysis and amnesia. Older benzodiazepines, such as diazepam, were limited in their anesthetic use due to slow onset, long half-lives and insolubility in water. Midazolam was introduced to the market in the early 1980s (3). It was a breakthrough at the time because, unlike diazepam, it had a fast onset, did not cause pain with injection and had a relatively short half-life. Thus, midazolam use has become widespread in critical care and surgical settings. However, midazolam metabolites, such as 1'-hydroxymidazolam, activate the $GABA_A$ receptor and can cause prolonged sedation (4). Midazolam also relies on cytochrome P450 3A4 for metabolism, levels of which can be influenced by liver failure and concomitant drug administration (5).

In August 2012, the results of a phase I trial of remimazolam in human subjects were published as two parts in Anesthesia & Analgesia (6, 7). These showed that remimazolam produced sedation, with a rapid onset and reliable, fast offset in human subjects with minimal side effects or complications. Phase Ib, IIa and IIb trials have been conducted but not published in the literature (www.paion.de).

Scheme 1. Synthesis of Remimazolam

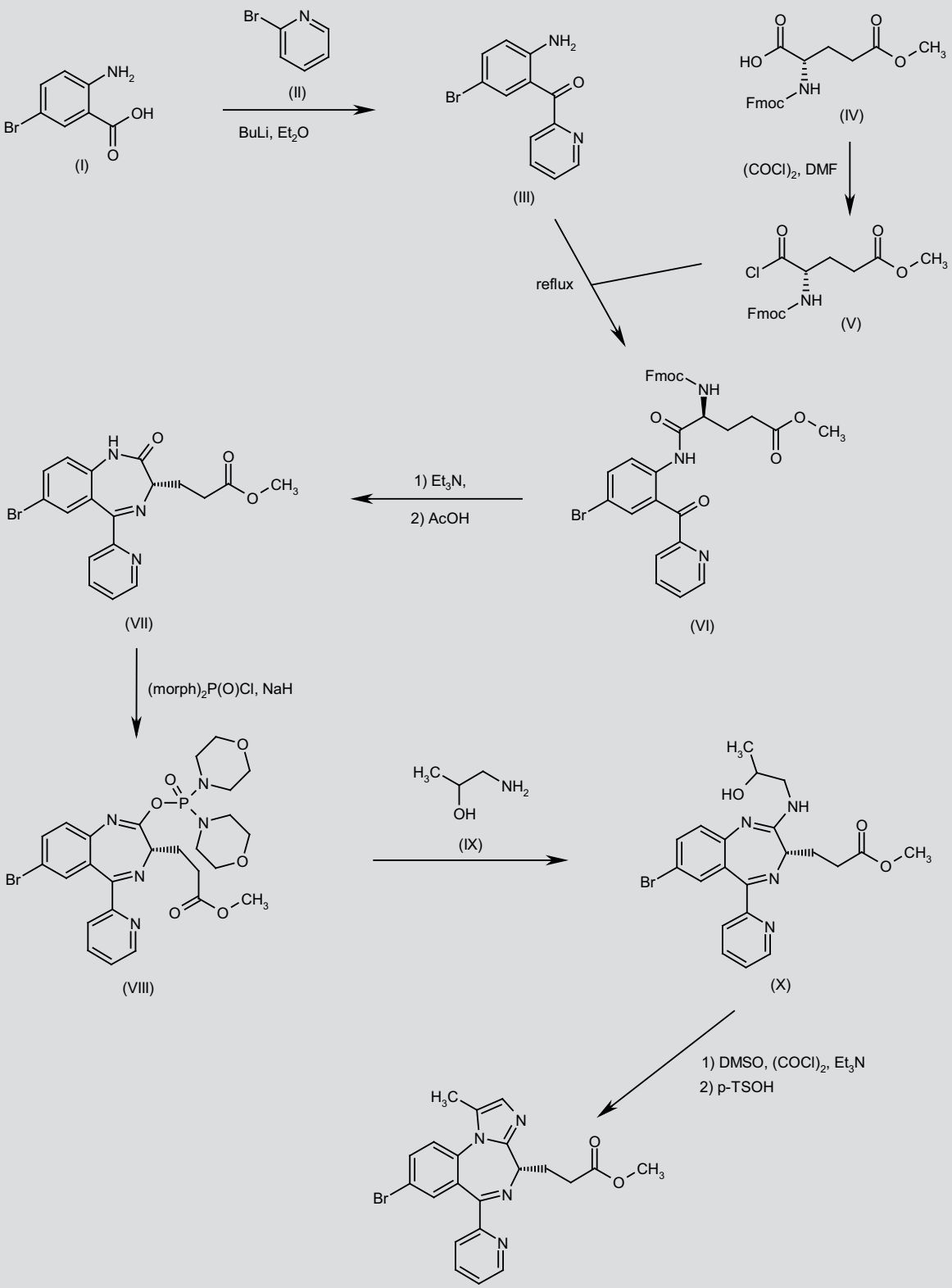

PHARMACOLOGY

Remimazolam is a carboxylic acid ester, much like remifentanil, that is metabolized by tissue esterases to a largely inactive compound, CNS-7054 (Fig. 1) (8).

Using radioligand binding, remimazolam was found to have more affinity for the human, rat and pig brain than [^{3}H]-flunitrazepam. It also had 410-fold more affinity for the human brain and 320-fold more affinity for the rat brain than CNS-7054 (8).Neither remimazolam nor its metabolite showed any detectable binding to other sites tested, including adenosine, adrenergic, cholecystokinin, dopamine, endothelin, glutamate, muscarinic, nicotinic, opiate and serotonin receptors, and Ca^{2+}, K^+ and Na^+ ion channels. To illustrate that the ligand was in fact binding to the $GABA_A$ receptor, currents were recorded from Ltk cells stably transfected with the rat $GABA_A$ subtypes α1, α2, α3 and α5. Midazolam and remimazolam both enhanced GABA (2 µM) currents in these cells at all subtypes.

Additionally, neuronal firing rates in the substantia nigra pars reticulata (an area with significant GABAergic input) were measured in rats during remimazolam infusion. Remimazolam caused dose-related decreases in neuronal firing rates. Higher doses were able to suppress firing to around 20% of baseline. The ED_{95} for this experiment in rats was 0.83 mg/kg (8).

The preclinical studies of remimazolam were conducted in rats, mice and sheep. In vitro studies were first performed with remimazolam, which determined the affinity and specificity of remimazolam binding to the $GABA_A$receptor using radioligand binding, whole cell patch clamping and inhibition of substantia nigra firing in situ (8). Remimazolam was also found to cause rapid sedation in rats and mice, as evidenced by loss of righting reflex (LRR). Rats treated with 25 mg/kg of either midazolam or remimazolam had a faster recovery from remimazolam. This study also established that CNS-7054 had little affinity for the $GABA_A$ receptor or any other binding site tested. To further explore dose–response, in the same study, mice were treated with escalating doses of remimazolam (15-30 mg/kg) or midazolam (20-50 mg/kg). Both agents had dose-related sedative responses. These were of a much shorter duration for remimazolam (1.1-3.6 minutes) than for midazolam (49-65 minutes). CNS-7054, the metabolite of remimazolam (30-100 mg/kg), caused no LRR in any animal tested. Flumazenil significantly reduced the LRR caused by remimazolam (30 mg/kg) in mice (0.7 ± 0.7 vs. 8.4 ± 2.6 minutes; P = 0.013).

A more extensive dose-escalation study (0.037-8.82 mg/kg) was performed to evaluate sedation, cardiovascular and respiratory effects in sheep (9). EEG parameters (SE/RE and alpha power) and observer analysis of the sheep (head drop and lift) were used to determine loss of consciousness (LOC) and recovery of consciousness (ROC) times. The measurements of ROC among the three methods correlated well when averaged across sheep. Sheep became drowsy at the lowest doses (0.037 and 0.074 mg/kg) and had profound LOC for over 30 minutes at the highest dose (8.82 mg/kg).

Respiratory effects, measured as a percentage change in baseline, were significant (20-30%) for all doses except 8.82 mg/kg. The decreases in respiratory rate were associated with increases in arterial carbon dioxide tension and decreases in arterial oxygen tension, arterial hemoglobin desaturation and acidosis, as expected. Remimazolam also caused dose-related decreases in mean arterial pressure (MAP; except the dose of 8.82 mg/kg) and slight reductions in central venous pressure and increased heart rate. None of these physiological changes were sufficient to endanger the animals.

In the same study, other parameters measured in response to remimazolam included cardiac output and cerebral blood flow. Cardiac output was unaffected by remimazolam. Cerebral blood flow was reduced by a maximum of 20% for the highest doses of remimazolam.

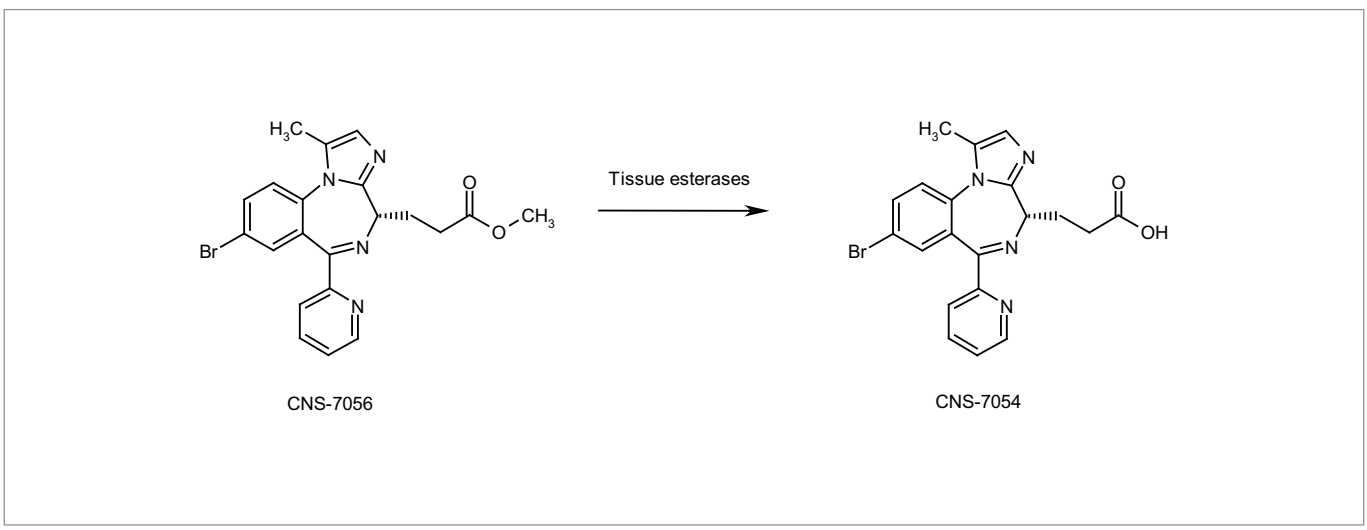

Figure 1. CNS-7056, also known as remimazolam and its inactive metabolite, CNS-7054, after metabolism by tissue esterases (8).

A lower magnitude increase in saggital sinus oxygen tension was noted, suggesting coupling of cerebral blood flow and oxygen consumption in sheep.

In a study published in 2009, the researchers compared low, medium and high doses of remimazolam, midazolam and propofol in sheep (10). They again used EEG parameters (RE/SE and alpha power) with observation of head drop and lift to determine LOC and ROC. Remimazolam showed a rapid onset and offset of sedation. With increasing doses, duration of sedation increased, whereas anesthetic depth remained consistent. Midazolam sedation, in comparison, was of poorer quality at all doses, with slower onset and offset. Medium- and high-dose propofol was more similar to remimazolam with regard to sedation depth and rapid recovery time. However, unlike remimazolam, the depth of propofol was dose-dependent and onset was slow (for the 2-minute infusions performed in the study). All three drugs caused expected decreases in respiratory rate, blood pressure and central venous pressure, and increases in heart rate. Notably, in this study, only remimazolam caused a statistically significant decrease in cardiac output in sheep. Again, none of the physiological derangements were of sufficient degree to harm or endanger the animals.

PHARMACOKINETICS

In human subjects, the consistent systemic clearance values of remimazolam illustrated linear pharmacokinetic values in the dose range studied (0.01-0.30 mg/kg) (6). The clearance of remimazolam was rapid (overall mean = 70.3 ± 13.9 L/h) and it showed moderate distribution (mean steady state volume of distribution = 34.8 ± 9.4 L). The mean residence time of remimazolam (0.5 hours) was seven times shorter than that of midazolam (3.56 hours), due to the lower systemic clearance and higher volume of distribution of midazolam. The terminal half-life of remimazolam was 0.75 ± 0.15 hours. Remimazolam exhibited no changes in systemic clearance relative to body weight in the dose and weight ranges (60-100 kg) studied.

Population pharmacokinetic models and simulations were performed using Bispectral Index (BIS) and Modified Observer's Assessment of Alertness/Sedation (MOAA/S) scores as markers of awareness after single and multiple doses of remimazolam (7). Using a recirculation pharmacokinetic model, the authors obtained similar values for population clearance, volume of distribution, terminal half-life and mean residence time as those obtained for the individual subject data in the companion paper. The simulated mean population context-sensitive half-times of remimazolam and midazolam (7-8 and 60 minutes, respectively) predicted a much more rapid recovery from sedation with remimazolam.

In human subjects, remimazolam was given as a 1-minute i.v. injection in the dose range of 0.01 to 0.30 mg/kg. In this range, the degree and duration of sedation was dose-dependent (7). Peak sedation was achieved 1-4 minutes after the start of the infusion. Onset of sedation was rapid for doses 0.05 mg/kg and above. The median duration of sedation increased with increasing remimazolam dose from 5.5 minutes (0.075 mg/kg) to 34 minutes (0.25 mg/kg). At higher doses, remimazolam (0.1-0.2 mg/kg; 10-20 minutes) achieved deeper sedation with faster recovery times than midazolam (0.075 mg/kg; 40 minutes).

Monte-Carlo simulations of remimazolam multiple-dose regimens have been performed (7). These predicted that a single 1-minute 6-mg infusion followed by a 3-mg dose 2 minutes later, if necessary, would produce rapid sedation within 3 minutes for > 80% of patients. This dose would produce loss of consciousness in a small percentage of patients (7%). The simulations also predicted that 3 mg of remimazolam given in intervals of 2 minutes or longer would be sufficient to maintain sedation.

Pharmacokinetic and pharmacodynamic parameters were modeled in sheep, but due to the more clinically informative human pharmacokinetic studies published recently, these data do not merit review here (11).

Currently, remimazolam is the subject of several clinical trials investigating single- and multiple-dose regimens. The ideal remimazolam doses and interval timing for procedural sedation, prolonged sedation and induction of general anesthesia have not yet been determined (12-14).

SAFETY

In the single human trial published, remimazolam was found to be safe across a wide range of doses (6). Small percentages of subjects treated with remimazolam and midazolam reported headache and somnolence. Hemoglobin desaturation was infrequent, mild and related to depth of sedation. Changes in heart rate, blood pressure, laboratory values, temperature and respiratory rate were not considered clinically significant in the study.

CLINICAL STUDIES

In Anesthesia & Analgesia (6, 7), the only published clinical trial data appear as two separate manuscripts evaluating safety, efficacy and basic pharmacokinetics in part 1 and population pharmacokinetic and pharmacodynamic modeling in part 2. In this phase I trial, 81 subjects were enrolled in a single-center, randomized, double-blind, placebo- and active-controlled trial. The study was a single-dose escalation study in which clinically effective midazolam doses and placebo were used as controls for the doses of remimazolam. Fifty-four subjects received remimazolam, 18 midazolam and 9 placebo. The initial remimazolam doses were 0.01 mg/kg and the stop criterion of LOC > 5 minutes in > 50% of subjects was reached at 0.3 mg/kg of remimazolam.

As expected from the animal studies, remimazolam produced dose-related sedative effects in human subjects. Very little or no sedation was observed in the smaller dose ranges (0.01-0.05 mg/kg), while doses above 0.075 mg/kg resulted in deeper sedation. Increasing doses also increased the duration of sedation. As the dose increased from 0.075 mg/kg to 0.2 mg/kg, the duration of sedation increased from 5.5 to 20 minutes as shown by BIS and MOAA/S scores. Higher doses of remimazolam (0.25-0.3 mg/kg) produced prolonged sedation of up to 34 minutes. In comparison, midazolam produced variable, moderate sedation (MOAA/S scores of 3 to 4) with a duration of 40 minutes for the 0.075 mg/kg dose.

Treatment-related adverse events (AEs) were reported by 17-33% of subjects in all treatment groups within 3 days following infusion. The AEs reported with remimazolam were composed mainly of complaints of headache (7%) and somnolence (6%). Patients treated with midazolam had similar complaints, with 6% complaining of headache and

6% somnolence. Both remimazolam and midazolam caused some mild and transient nausea.

Four episodes of hemoglobin desaturation (one with midazolam and three with remimazolam) were reported in the subjects during the trial. One episode of hemoglobin desaturation, at the highest remimazolam dose (0.3 mg/kg), required a chin lift to resolve. This was the only instance of airway management in the study and no supplemental oxygen was used in the subjects.

Mean heart rate was increased significantly in both the remimazolam and midazolam treatment groups of 0.075 mg/kg and above. These heart rate changes were not considered clinically significant. Changes in blood pressure, laboratory values, temperature or respiratory rate were not considered significant with the administration of either drug.

This clinical trial analyzed arterial samples for time points from 1 minute to 4 hours after the start of the remimazolam infusion and venous samples for 2 hours to 12 hours post-dose. The plasma levels of remimazolam in the venous samples were higher than the arterial values at the same time points studied (2, 3 and 4 hours). Due to this unexpected result, the traditional multicompartmental mammillary pharmacokinetic model of analysis was replaced with a recirculation model to better fit the data (Fig. 2). Multicompartment models assume that a drug given intravenously is instantaneously mixed into the central circulation at the time of administration. These models are appropriate for drugs that have slow distribution and clearance times when compared with blood flow. The recirculatory model divides the central compartment into arterial, venous and cardiac/lung compartments to provide a more detailed description of early uptake and distribution of the drug (15). This is clearly important with drugs that are quickly metabolized, such as remimazolam. The lack of both arterial samples within the first 2 hours and of venous samples after 4 hours renders the determination of the most correct pharmacokinetic model difficult. However, the population simulations (data presented above) were the basis for the Monte-Carlo multiple dosing simulations. The Monte-Carlo simulation data appear to have merit when applied to actual human volunteers, as presented below.

In addition to the phase I trial published in Anesthesia & Analgesia, Paion, the parent company of remimazolam, has performed a phase IIa single-dose study in subjects undergoing upper gastrointestinal endoscopy (12) and a phase IIb multiple-dose study in volunteers undergoing colonoscopy (13). Neither of these studies have been published in the literature, but results can be found on the company's website: www.paion.de.

The latest reported phase IIb trial employed initial doses of remimazolam of 5-8 mg, with "top-up" doses of 2-3 mg, compared to initial doses of 2.5 mg of midazolam, with "top-up" doses of 1 mg. The website abstract states that successful sedation was achieved in 92.5-97.5% of remimazolam patients and only 75% of midazolam patients. However, remimazolam showed only modest decreases in recovery times vs. midazolam (11.3-13.6 minutes vs. 15.2 minutes). The authors site the concomitant use of propofol with midazolam as the cause of shortened midazolam recovery times.

The ClinicalTrials.gov website states that recruitment has begun for "An Open-label, Single-dose, Intravenous Administration Study of ONO-2745/CNS 7056 in Subjects With Chronic Hepatic Impairment" (NCT01790607) (14).

Also, the Paion website includes many press releases detailing ongoing studies in Japan (performed by Ono Pharmaceuticals), the U.S. and Europe. These include a phase II/III general anesthesia trial and phase II ICU sedation trial in Japan. A phase II general anesthesia trial is to begin in the second half of 2013 in Europe.

CONCLUSIONS

As one of the new rapidly metabolized anesthetic drugs entering the market, remimazolam could have a large clinical impact if the clinical trials bear out the predictions of initial studies. Unlike its parent compound, midazolam, remimazolam is considered a "soft" drug, i.e., one that has a wide therapeutic index and rapid, predictable metabolism with no active metabolites (16). It produces consistent depth of sedation in volunteers with a duration of sedation that directly corre-

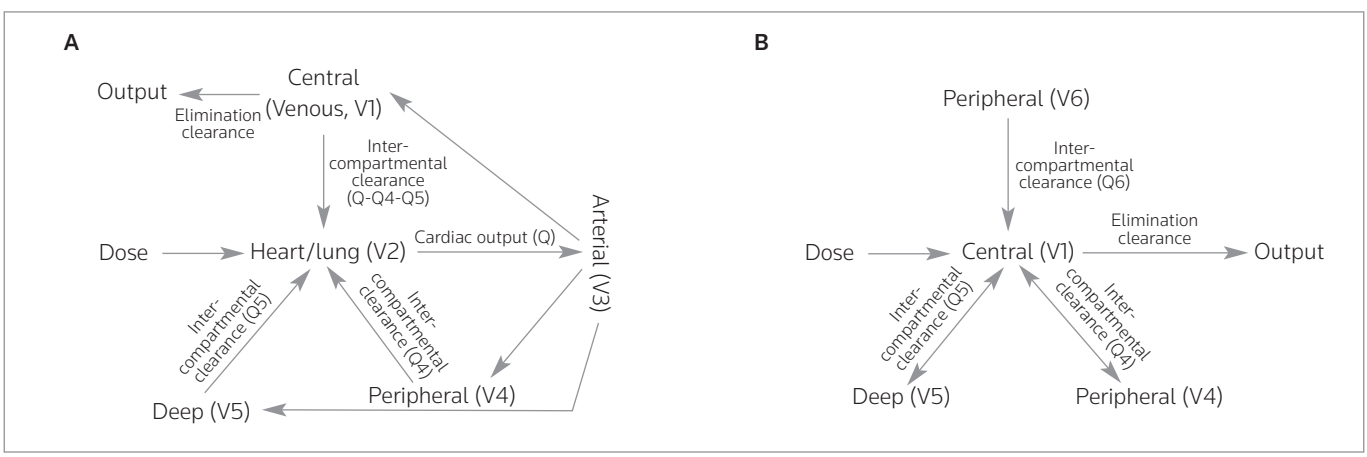

Figure 2. Representation of population recirculation model: **A**) that fits pharmacokinetic data obtained by Wiltshire et al. (7) and a conventional mammalian model, **B**) that simplifies the early phases of drug distribution (19).

lates with dose. In initial, albeit unpublished, studies, multiple dosing regimens appear to be uncomplicated and clinically possible. In this age of constant and varied anesthesia drug shortages, remimazolam could possibly prove to be an alternative to propofol as an induction agent and as a sedative (17). It could also replace drugs commonly used in procedural sedation, such as midazolam, if the reliability and rapidity of remimazolam metabolism actually conferred a cost-savings advantage in outpatient settings (18).

Remimazolam is an innovative, short-acting benzodiazepine that is being developed by PAION for use in the U.S. and Europe, and by PAION's licensing partners for use in Japan and China. It has been shown to produce reliable deep sedation of with a rapid recovery in humans. Metabolism of the drug is independent of body weight in healthy individuals. In published clinical studies, it is well tolerated by volunteers, with minimal side effects in a wide range of doses. Whether this drug proves to be more useful than midazolam or propofol as a sedative for outpatient procedures, induction of general anesthesia and critical care sedation has yet to be proven. The acceptance and usage of remimazolam on large scale will depend, in part, on the price point selected by the manufacturer if this drug gains approval from the FDA in the U.S.

SOURCES

GlaxoSmithKline (UK); licensed to PAION AG (DE), Ono Pharmaceutical Co., Ltd. (JP) and Yichang Humanwell Pharmaceutical (CN).

DISCLOSURES

The author states no conflicts of interest.

REFERENCES

1. Jung, D.K., Pacofsky, G.J., Stafford, J.A., Feldman, P.L., Kaldor, I., Tidwell, J.H. (GlaxoSmithKline plc). *Short-acting benzodiazepines*. EP 1183243, JP 2002544266, JP 2006151984, JP 2007197468, JP 2007197469, US 7160880, US 2007093475,US 2007135419, US 2007135420, US 2007135421, US 7435730, US 7528127, US 7473689, US 7485635, WO 2000069836.
2. Sigel, E., Buhr, A. *The benzodiazepine binding site of GABAA receptors.* Trends Pharmacol Sci 1997, 18(11): 425-9.
3. Kanto, J.H. *Midazolam: The first water-soluble benzodiazepine: Pharmacology, pharmacokinetics and efficacy in insomnia and anesthesia.* Pharmacotherapy 1985, 5(3): 138-55.
4. Dundee, J.W., Halliday, N.J., Harper, K.W., Brogden, R.N. *Midazolam. A review of its pharmacological properties and therapeutic use.* Drugs 1984, 28(6): 519-43.
5. Yuan, R., Flockhard, D.A., Balian, J.D. *Pharmacokinetic and pharmacodynamic consequences of metabolism-based drug interactions with alprazolam, midazolam and triazolam.* J Clin Pharmacol 1999, 39(11): 1109-25.
6. Antonik, L.J., Goldwater, D.R., Kilpatrick, G.J., Tilbrook, G.S., Borkett, K.M. *A placebo- and midazolam-controlled phase I single ascending-dose study evaluating the safety, pharmacokinetics, and pharmacodynamics of remimazolam (CNS 7056): Part I. Safety, efficacy, and basic pharmacokinetics.* Anesth Analg 2012, 115(2): 274-83.
7. Wiltshire, H.R., Kilpatrick, G.J., Tilbrook, G.S., Borkett, K.M. *A placebo- and midazolam-controlled phase I single ascending-dose study evaluating the safety, pharmacokinetics, and pharmacodynamics of remimazolam (CNS 7056): Part II. Population pharmacokinetic and pharmacodynamic modeling and simulation.* Anesth Analg 2012, 115(2): 284-96.
8. Kilpatrick, G.J., McIntyre, M.S., Cox, R.F. et al. *CNS 7056: A novel ultra-short-acting benzodiazepine.* Anesthesiology 2007, 107(1): 60-6.
9. Upton, R.N., Martinez, A. Grant, C. *A dose escalation study in sheep of the effects of the benzodiazepine CNS 7056 on sedation, the EEG and the respiratory and cardiovascular systems.* Br J Pharmacol 2008, 155(1): 52-61.
10. Upton, R.N., Martinez, A.M., Grant, C. *Comparison of the sedative properties of CNS 7056, midazolam, and propofol in sheep.* Br J Anaesth 2009, 103(6): 848-57.
11. Upton, R.N., Somogyi, A.A., Martinez, M.M., Colvill, J., Grant, C. *Pharmacokinetics and pharmacodynamics of the short-acting sedative CNS 7056 in sheep.* Br J Anaesth 2010, 105(6): 798-809.
12. *Dose-finding safety study evaluating CNS 7056 in patients undergoing diagnostic upper GI endoscopy (NCT00869440).* ClinicalTrials.gov Web site, August 19, 2013.
13. *Multiple dose safety and efficacy study evaluating CNS 7056 versus midazolam in patients undergoing colonoscopy.* ClinicalTrials.gov Web site, August 19, 2013.
14. *An open-label, single-dose, intravenous administration study of ONO-2745/CNS 7056 in subjects with chronic hepatic impairment.* Clinical Trials.gov Web site, August 19, 2013.
15. Upton, R.N. *The two-compartment recirculatory pharmacokinetic model—An introduction to recirculatory pharmacokinetic concepts.* Br J Anaesth 2004, 92(4): 475-84.
16. Johnson, K.B. *New horizons in sedative hypnotic drug development: Fast, clean, and soft.* Anesth Analg 2012, 115(2): 220-2.
17. Jensen, V., Rappaport, B.A. *The reality of drug shortages—The case of the injectable agent propofol.* N Engl J Med 2010, 363(9): 806-7.
18. Sneyd, J.R. *Remimazolam: New beginnings or just a me-too?* Anesth Analg 2012, 115(2): 217-9.
19. Krejcie, T.C., Avram, M.J. *Recirculatory pharmacokinetic modeling: What goes around, comes around.* Anesth Analg 2012, 115(2): 223-6.

Drugs of the Future 2005, 30(2): 138-145

CCC: 0377-8282/2005
DOI: 10.1358/dof.2005.030.02.879289

Vandetanib

Prop INN

Angiogenesis Inhibitor
VEGFR Inhibitor

AZD-6474
ZD-6474

N-(4-Bromo-2-fluorophenyl)-6-methoxy-7-(1-methylpiperidin-4-ylmethoxy)quinazolin-4-amine

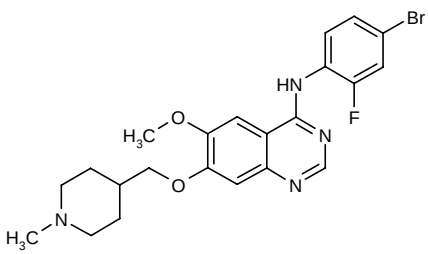

$C_{22}H_{24}BrFN_4O_2$
Mol wt: 475.3596
CAS: 338992-00-0
CAS: 338992-48-6 (as hydrochloride)
CAS: 338992-53-3 (as monotrifluoroacetate)
EN: 304792

Abstract

Tumor angiogenesis, or the formation of blood vessels within a tumor, plays a key role in cancer cell survival, local tumor growth and the development of distant metastases. Vascular endothelial growth factor (VEGF) is a potent and specific mitogen for endothelial cells that activates angiogenesis and enhances vascular permeability. Vandetanib (ZD-6474) is a potent, orally active, low-molecular-weight inhibitor of KDR/VEGFR2 tyrosine kinase activity and also displays inhibitory activity towards epidermal growth factor receptor (EGFR) tyrosine kinase and oncogenic RET kinase. Chronic oral dosing of mice bearing human tumor xenografts of diverse tissue origin with vandetanib results in dose-dependent inhibition of tumor growth. Vandetanib also enhanced the antitumor effects of radiation in several tumor models. In phase I trials, vandetanib was well tolerated and was associated with only mild adverse events (skin rash and diarrhea). It is currently in phase II clinical development for a range of solid tumors, both as monotherapy and in combination with certain anticancer agents.

Synthesis

Vandetanib can be prepared by two related ways:

1) Reaction of 2-amino-4-benzyloxy-5-methoxybenzamide (I) and Gold's reagent in dioxane at reflux gives 7-benzyloxy-6-methoxy-3,4-dihydroquinazolin-4-one (II), which is treated with thionyl chloride in DMF at reflux to yield 7-benzyloxy-4-chloro-6-methoxyquinazoline (III) (1, 2). Nucleophilic substitution of the chloroquinazoline (III) with 4-bromo-2-fluoroaniline (IV) in refluxing isopropanol provides the anilino quinazoline (V), which is submitted to cleavage of the benzyl ether group by treatment with hot trifluoroacetic acid to afford alcohol (VI). Condensation of compound (VI) with tosylate (VII) in DMF furnishes the ether adduct (VIII), which by acid deprotection of the *N*-Boc group gives the piperidine derivative (IX). Finally, this compound is subjected to reductive methylation using formaldehyde and sodium cyanoborohydride in THF/MeOH (3). Scheme 1.

Intermediate (VII) is obtained by protection of ethyl isonipecotate (X) with di-*tert*-butyl dicarbonate in ethyl acetate to give the *N*-Boc derivative (XI), which is reduced to alcohol (XII) using $LiAlH_4$ in THF. Finally, alcohol (XII) is treated with *p*-toluenesulfonyl chloride in the presence of DBU (3). Scheme 1.

2) Treatment of 7-benzyloxy-6-methoxy-3,4-dihydroquinazolin-4-one (II) with NaH in DMF and subsequent condensation with chloromethyl pivalate gives 7-benzyloxy-6-methoxy-3-(pivaloyloxymethyl)-3,4-dihydroquinazolin-4-one (XIII), which is deprotected to alcohol (XIV) by hydrogenation over Pd/C (2). Reaction of alcohol (XIV) with *N*-(*tert*-butoxycarbonyl)piperidine-4-methanol (XII) by means of DEAD and PPh_3 in dichloromethane or K_2CO_3 in DMF provides the aryl ether (XV), which is deprotected with TFA to yield the free piperidine (XVI). Reductive methylation of compound (XVI) with HCHO and $NaBH_3CN$ in methanol/THF affords the methylated piperidine (XVII), which is submitted to cleavage of the pivaloyloxymethyl group with NH_3 in methanol to provide

G. Zareba, J. Castañer, J. Bozzo. Prous Science, P.O. Box 540, 08080 Barcelona, Spain.

Scheme 1: Synthesis of Vandetanib

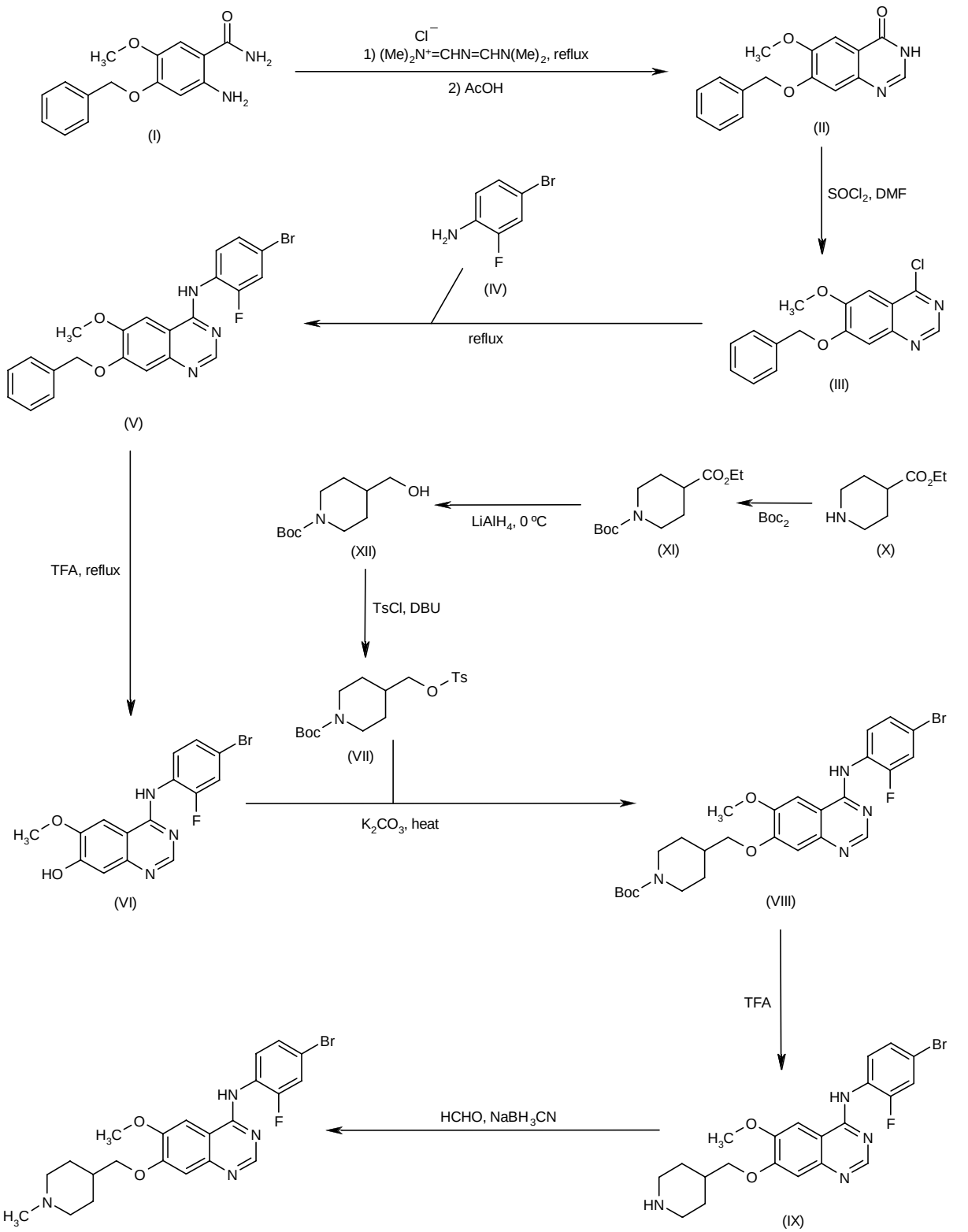

Scheme 2: Synthesis of Vandetanib

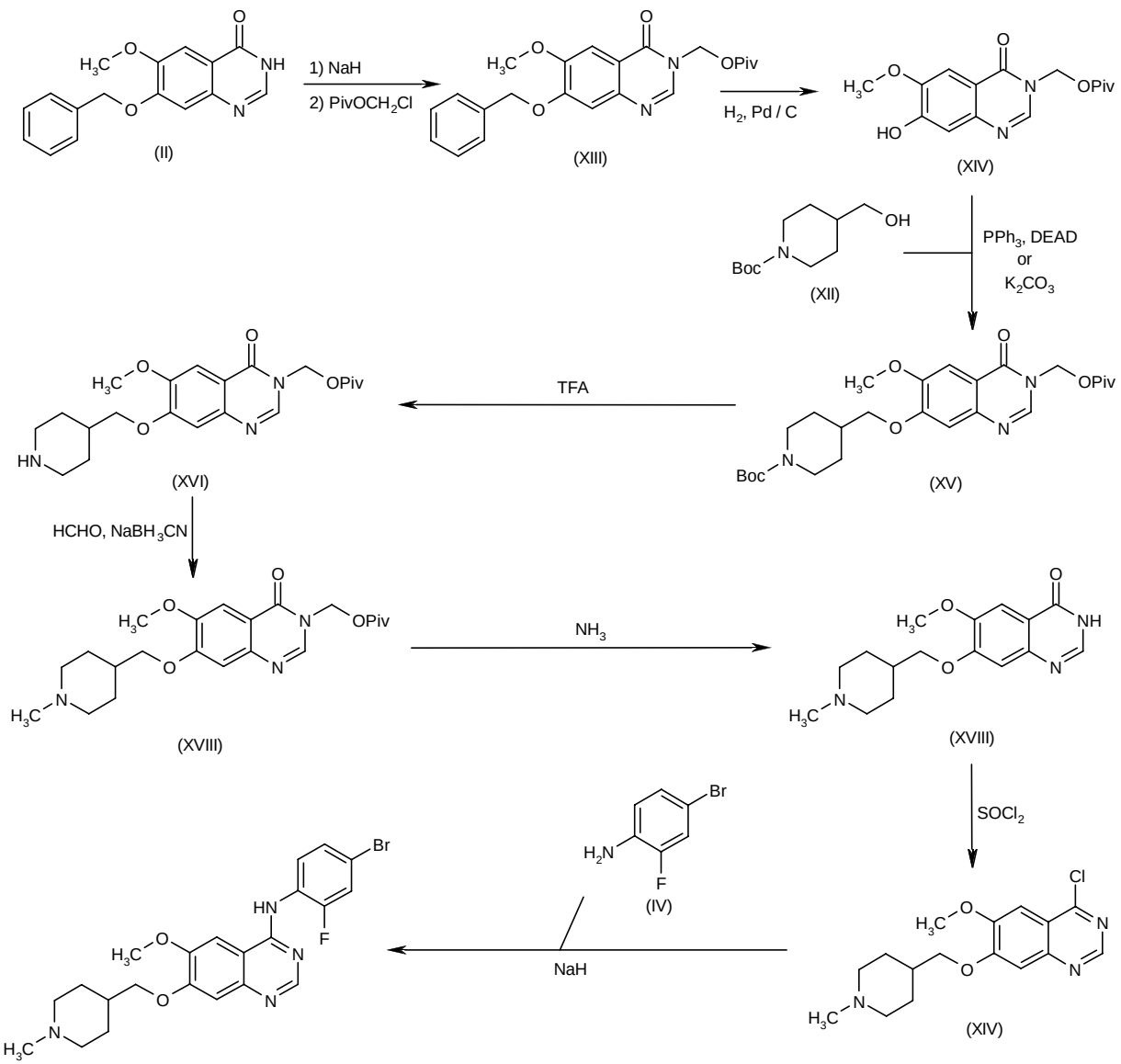

the quinazolinone (XVIII). Reaction of compound (XVIII) with $SOCl_2$ in DMF gives the 4-chloroquinazoline (XIX), which is finally condensed with 4-bromo-2-fluoroaniline (IV) by means of NaH in DMF (4). Scheme 2.

Introduction

Tumor angiogenesis, or the formation of blood vessels within a tumor, plays a key role in cancer cell survival, local tumor growth and the development of distant metastases (5). New blood vessels provide an adequate oxygen and nutrient supply to the growing tumor and initiate invasion and metastatic spread. The continued growth of a tumor requires a series of sequential and interrelated steps that include transformation, growth, invasion of adjacent tissue (parenchyma, lymphatics and small blood vessels), dissemination, arrest in distant sites, extravasation and proliferation. Without small blood vessels to supply the needed nutrients to the neoplastic cells, tumors cannot grow more than 2-3 mm^3. The synthesis and secretion of angiogenic growth factors is thought to play a central role in tumor growth and spread. Some of the major endogenous proangiogenic factors upregulated in tumors include vascular endothelial growth

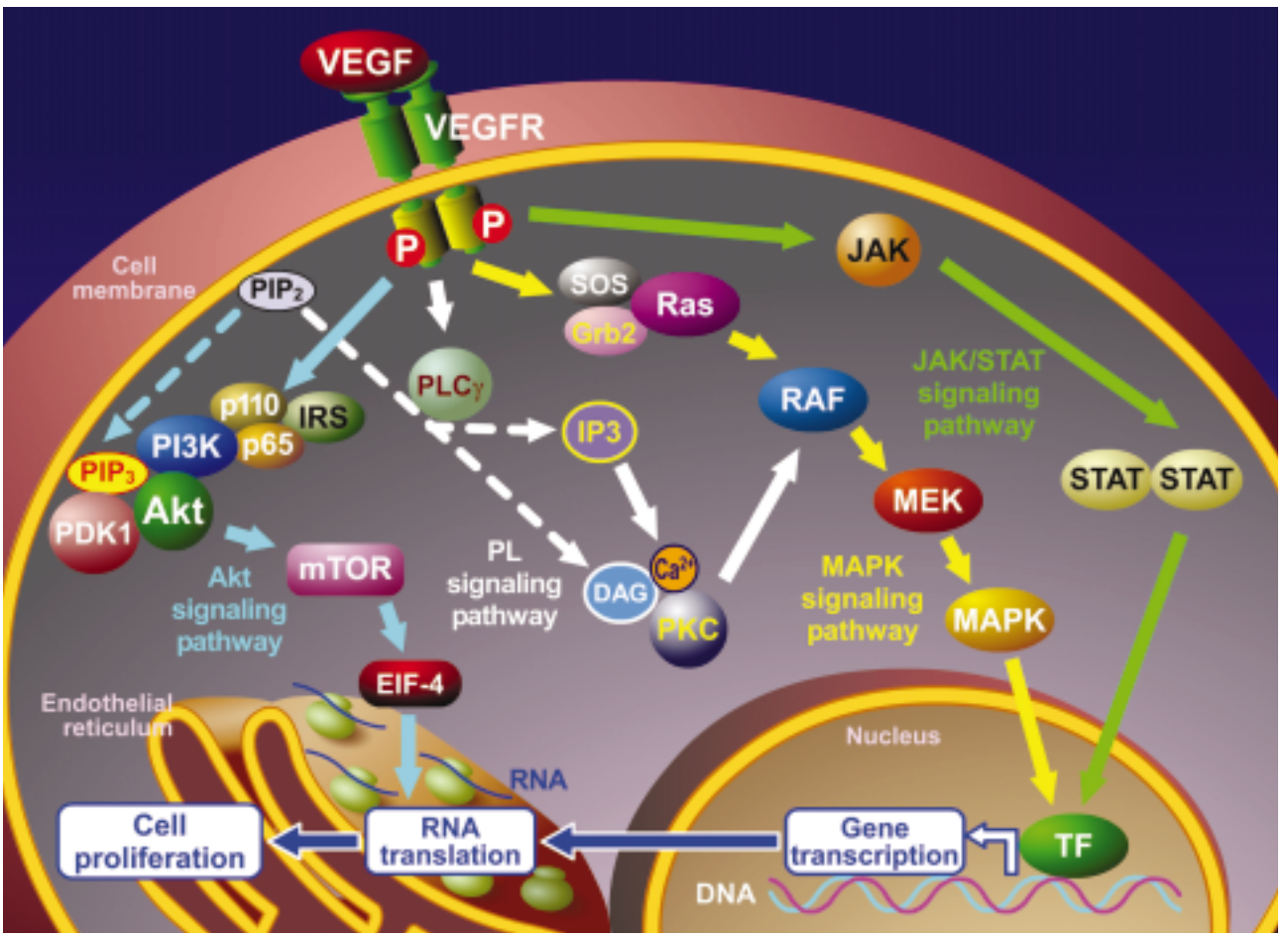

Fig. 1. VEGF signaling pathways.

factor (VEGF), basic fibroblast growth factor (bFGF) and platelet-derived endothelial cell growth factor (PDGF) (6).

Inhibition of VEGF signal transduction (VEGF signaling pathways depicted in Figure 1) may represent a particularly attractive therapeutic approach given its pivotal role in pathological angiogenesis. VEGF is a potent and specific mitogen for endothelial cells and promotes both vasculogenesis and angiogenesis. Several members of this growth factor family have been identified, including placental growth factor, VEGF-B, VEGF-C and VEGF-D. Three transmembrane receptors for VEGF family ligands on endothelium have also been identified –Flt-1 (VEGFR1), KDR (VEGFR2) and Flt-4 (VEGFR3)–, although activation of KDR alone appears to be sufficient to promote all of the major phenotypic responses to VEGF, *e.g.*, endothelial cell proliferation, migration and survival, and the induction of vascular permeability (7-14).

EGFR and other receptor tyrosine kinases have been validated as suitable pharmacological targets for anticancer therapy and several small-molecule drugs have been developed, including the potent and selective EGFR tyrosine kinase inhibitor gefitinib (ZD-1839, Iressa; AstraZeneca) and the potent and selective Abl tyrosine kinase inhibitor imatinib (STI-571, Glivec, Gleevec; Novartis). One of the most promising new angiogenesis inhibitors is vandetanib (ZD-6474; AstraZeneca), an orally available KDR/VEGFR2 tyrosine kinase inhibitor which has entered phase II clinical trials (4, 15).

Pharmacological Actions

Vandetanib is a potent, orally active, low-molecular-weight inhibitor of KDR/VEGFR2 tyrosine kinase activity (IC_{50} = 40 nM), with additional inhibitory activity against VEGFR3 (IC_{50} = 110 nM) and weaker activity against EGFR tyrosine kinase (IC_{50} = 500 nM), but selectivity over a range of other tyrosine and serine/threonine kinases (16). Vandetanib also displays strong inhibitory activity (IC_{50} = 100 nM or less) towards oncogenic RET kinases (17). It produces potent inhibition of VEGF-stimulated proliferation of human umbilical vein endothelial cells (HUVEC; IC_{50} = 60 nM). Oral administration of vandetanib to athymic mice bearing established, histologically distinct (lung, prostate, breast, ovarian, colon or vulval) human tumor xenografts, or after implantation of aggressive

syngeneic rodent tumors (lung, melanoma) in immunocompetent mice, produced dose-dependent inhibition of tumor growth in all cases at doses of 25 mg/kg once daily and above, even against large, well-established tumors (16, 18).

In vitro and *in vivo* studies demonstrated that vandetanib can target not only tumors that use VEGF signaling for the promotion of angiogenesis, but also EGFR-dependent tumors, thus potentially expanding possible future indications for the drug. Vandetanib even inhibited the growth of several EGFR-expressing human cancer cell lines that lack VEGFR2 expression (19). Moreover, using the non-small cell lung cancer (NSCLC) PC-9 cell line, vandetanib was shown to inhibit the phosphorylation of mutant EGFR 10-fold more potently as compared to wild-type EGFR (20).

Vandetanib therapy targeting two distinct aspects of tumor growth –angiogenesis and tumor cell proliferation– was studied in the TMK-1 human gastric adenocarcinoma model in nude mice. Vandetanib inhibited orthotopic growth and angiogenesis of gastric cancer. Doses of 50 and 100 mg/kg/day reduced tumor cell proliferation by 48% and 65%, respectively, and increased tumor cell apoptosis *in vivo*. Although microvessel density was decreased by vandetanib, the remaining vessels showed a relatively higher percentage of pericyte coverage, reflecting probable selective loss of uncovered vessels after vandetanib treatment (21).

The effects of vandetanib were assessed on malignant glioma growth, neovascularization, proliferation and apoptosis in the intracerebral rat glioma BT4C model. The results deemonstrated that the compound (50 and 100 mg/kg/day via gavage) significantly decreased tumor volume. Microvascular density increased after treatment with vandetanib and the tumor cell proliferation index was reduced. An increase in tumor cell apoptosis was also observed (22).

In mice bearing brain metastases from the highly angiogenic human melanoma cell line Mel57-VEGF-A, the effect of different doses of vandetanib was evaluated using contrast-enhanced magnetic resonance imaging (CE-MRI) and immunomorphological analysis. After prophylactic or therapeutic treatment with vandetanib (100 mg/kg), CE-MRI failed to detect tumors. Immunohistological analysis revealed the presence of numerous small, nonangiogenic lesions. Treatment with 25 mg/kg vandetanib also resulted in blockade of vessel formation, although it did not fully inhibit vascular leakage (23).

The effects of vandetanib were studied at very early stages of the carcinogenic process in the rat 7,12-dimethylbenz[*a*]anthracene (DMBA) model after administration of a dose of 30 mg/kg/day for 6 weeks. Marked inhibition of the formation of atypical ductal hyperplasia and carcinoma *in situ* (> 95%) was observed in treated animals, and no invasive disease was seen (24).

The antitumor effect of the drug (12.5-50 mg/kg/day p.o. for 21 days) against gefitinib-sensitive lung adenocarcinoma PC-9 and gefitinib-resistant PC-9/ZD tumor xenografts in athymic mice was investigated. The greatest effect was seen in gefitinib-sensitive PC-9 tumors, where vandetanib treatment (> 12.5 mg/kg/day) resulted in tumor regression. Dose-dependent growth inhibition, but no tumor regression, was seen in vandetanib-treated PC-9/ZD tumors (25). In other experiments, both vandetanib and gefitinib significantly reduced tumor growth in the gefitinib-sensitive NSCLC line NCI-H322, and vandetanib also significantly inhibited the growth of the gefitinib-resistant NSCLC line NCI-H520 (26).

Combined androgen ablation and inhibition of VEGF signaling in an androgen-sensitive human prostate cancer xenograft model (LNCaP) known to develop androgen-independent growth after androgen ablation was examined using vandetanib. Tumors from mice receiving combined treatment (castration and vandetanib 50 mg/kg/day p.o.) were found to be more necrotic than tumors from mice receiving either androgen ablation or vandetanib alone (27).

Vandetanib has been demonstrated to be a successful adjuvant to radiotherapy in different tumor models. *In vivo* studies in a mouse NSCLC Calu-6 tumor model responsive to treatment with selective VEGFR tyrosine kinase inhibitors demonstrated schedule-dependent efficacy for combination of vandetanib and radiotherapy. Vandetanib (50 mg/kg p.o.) was administered with or without radiotherapy in 2 combination schedules: before each dose of radiation (concurrent schedule) and 30 min after the last dose of radiotherapy (sequential schedule). When administered sequentially, tumor growth delay was markedly enhanced as compared to radiation alone or the concurrent schedule. Impaired reoxygenation between fractions in the concurrent protocol was suggested to be responsible for the schedule dependency of the radiopotentiation observed (28). In the mouse UMSCC2 head and neck tumor model, concurrent radiotherapy and vandetanib treatment demonstrated the greatest therapeutic benefit in terms of tumor growth delay (29). Vandetanib also enhanced the antitumor effect of radiation therapy in the human colorectal cancer HT-29 xenograft model, independent of the sequencing of the therapies (30).

The efficacy of combined antiangiogenic and vascular-disrupting agents in the treatment of solid tumors was also recently studied. ZD-6126 (vascular-targeting agent) therapy consisted of 3 doses of 100 mg/kg administered 1, 3 and 5 days after the tumor reached the starting size. Vandetanib was administered daily (25 mg/kg) on days 1-5. In the combination studies, vandetanib treatment began immediately after the first dose of ZD-6126. Significant tumor growth delays were observed in human renal cell carcinoma and Kaposi's sarcoma tumor models with either agent with the treatment regimen used. Vandetanib produced a tumor growth delay of 24.5 and 14.5 days, respectively, in the Caki-1 and KSY-1 models. When ZD-6126 and vandetanib were combined, respective tumor growth delays increased to 55 and 86 days. Combination therapy also gave 3 of 8 long-term tumor-free survivors in the KSY-1 model (31).

Dynamic CE-MRI was used to monitor the acute effects on tumor vascular permeability following inhibition

of VEGF-A signal transduction with vandetanib. Mice bearing human prostate adenocarcinoma PC-3 xenografts were imaged immediately before and following acute treatment with vandetanib (12.5-100 mg/kg orally). A dose-dependent reduction in K_{trans} values, which reflects vascular permeability and perfusion, was observed and correlated with the growth-inhibitory effect of vandetanib following chronic treatment. Vandetanib appeared to induce a reduction in K_{trans} in both the most enhancing rim and the core of the tumors (32).

Recently, results using a mouse model of intestinal cancer demonstrated that vandetanib significantly reduced the number and size of polyps when administered at either an early or late stage of polyp development (33). Other studies demonstrated that hypoxia is not a limiting factor in the effectiveness of vandetanib in inhibiting EGFR activation (34).

Pharmacokinetics

The effect of food on the intrasubject variability of the pharmacokinetics of vandetanib was evaluated in 16 healthy subjects. There was no clinically significant difference in C_{max} or AUC of vandetanib when it was given with food as compared with the fasted state. In addition, the overall intrasubject variability of vandetanib was small (coefficients of variation [CV] of 8% and 11% for AUC and C_{max}, respectively), and appeared to decrease when the drug was taken with food (CV for AUC = 5% and 10%, respectively, and CV for C_{max} = 10% and 13%, respectively, for fed and fasted states). The results of this study indicate that the day-to-day variability in exposure to vandetanib will not increase if it is taken with or without food (35).

Clinical Studies

In a dose-escalating phase I study on the safety, tolerability, pharmacokinetics and clinical biology of vandetanib, patients (at least 8 per group) with different solid tumors (mesothelioma, breast carcinoma, melanoma and others) were given a single dose of vandetanib followed by a 7-day observation period. Thereafter, patients received daily oral doses for continuous 28-day cycles. Drug-related toxicity was minimal, with facial flushing, facial rash and fatigue reported. C_{max} and AUC for the dose of 50 mg were 21.8 ng/ml and 3343 ng·h/ml, respectively, and for 100 mg the respective values were 84.6 ng/ml and 13,240 ng·h/ml. The estimated half-life was 130 h (82-206 h). After 56 days, stable disease was obtained in 2 patients (gastrointestinal stromal tumor, melanoma) (36).

Clinical evaluation of vandetanib was performed in 49 patients with malignant solid tumors refractory to standard therapy, or for whom no standard therapy exists. Each patient received a single oral dose of vandetanib (50, 100, 200, 300, 500 or 600 mg), followed by a 7-day observation period to evaluate single-dose pharmacokinetics. Thereafter, patients commenced daily oral dosing until disease progression or dose-limiting toxicity emerged. Adverse events were mild, with only diarrhea and rash increasing with the dose. Rash occurred in single patients at 300 and 500 mg, and diarrhea developed in 1 patient at 500 mg and 2 patients at 600 mg. An additional patient at 600 mg had thrombocytopenia and this dose was considered to exceed the maximum tolerated dose. Asymptomatic Q-T_c prolongation was observed in 7 patients at different dose levels. Vandetanib exposure in terms of C_{max} and AUC increased with dose. The terminal half-life was approximately 120 h, with no evidence of change with increasing dose (37).

A phase I study of vandetanib was conducted in 18 Japanese patients (31-72 years old) with solid tumors refractory to standard therapy. Patients received a single oral dose of drug (100, 200, 300 or 400 mg; n=3, 6, 6 and 3, respectively) followed by a 7-day observation period, and then received daily dosing at the same dose for a total of 28 days. Further 28-day treatment cycles were administered without interruption. After Q-T_c prolongation was observed, ECG was monitored 3 times a week for 3 weeks and then weekly. Vandetanib therapy was well tolerated at doses of up to 300 mg/day. Common adverse events in all groups were rash (n=14), asymptomatic Q-T_c prolongation (n=11), diarrhea (n=10), proteinuria (n=10) and hypertension (n=7). C_{max} and AUC increased linearly with dose. The terminal half-life was long, ranging from 72 to 167 (median = 96) h. $AUC_{(0\text{-}24)}$ was increased by 6-14 times following daily dosing for 28 days. The dose level of 100-300 mg/day yielded protein-unbound trough concentrations of 0.08-0.31 μmol/l (n=10), which exceeded the IC_{50} of vandetanib against KDR tyrosine kinase (IC_{50} = 0.04 μmol/l). Tumor regressions were seen in 4 patients with NSCLC at 200 and 300 mg/day (maintained even after dose modification from 200 to 100 mg/day in 2 responders and from 300 to 200 mg/day in 1 responder). Doses of 100-300 mg/day of vandetanib were well tolerated and this was considered to be an appropriate dose range in terms of efficacy for use in phase II studies in patients with NSCLC (38).

In the run-in phase of a 2-part randomized phase II study of vandetanib and docetaxel, the safety, efficacy and possible pharmacokinetic interaction of the combination were assessed. Patient eligibility criteria included locally advanced or metastatic NSCLC after failure of first-line platinum-based chemotherapy, WHO status of 0 or 1, and no significant hematological or cardiac abnormalities. In the open-label part 1 phase, patients received docetaxel (75 mg/m^2 i.v. every 21 days) and vandetanib (100 mg p.o. once daily). If no dose-limiting toxicity occurred by week 4, the next cohort received a higher dose of vandetanib (300 mg). Preliminary evaluation in patients who continued to receive vandetanib and docetaxel for at least 3 cycles revealed rash as the most common adverse effect (CTC grade 3 in 6 of 9 patients), classified as acneiform or desquamation, with a photosensitivity component in all affected patients. The rash

was reversible, and could be managed by dose interruption followed by dose reduction. Other adverse events included gastrointestinal complaints (nausea/vomiting) and laboratory abnormalities (CTC grade 1 or 2). Seven patients experienced CTC grade 3 or 4 myelosuppression, probably related to docetaxel treatment. The study confirmed that the combination of vandetanib and docetaxel is not associated with significant changes in exposure to either drug and that toxicities are manageable (39).

Source

AstraZeneca plc (GB).

References

1. Lohmann, J.-J.M., Hennequin, L.F.A., Thomas, A.P. (AstraZeneca plc; AstraZeneca SA). *Quinazoline derivs.* EP 0873319, JP 2000515114, US 5962458, US 6071921, WO 9722596.

2. Hennequin, L.F., Thomas, A.P., Johnstone, C. et al. *Design and structure-activity relationship of a new class of potent VEGF receptor tyrosine kinase inhibitors.* J Med Chem 1999, 42: 5369-89.

3. Hennequin, L.F.A., Stokes, E.S.E., Thomas, A.P. (AstraZeneca AB; AstraZeneca plc). *Quinazoline derivs. as VEGF inhibitors.* CA 2389767, EP 1244647, JP 2003513089, WO 0132651.

4. Hennequin, L.F., Stokes, E.S., Thomas, A.P., Johnstone, C., Plé, P.A., Ogilvie, D.J., Dukes, M., Wedge, S.R., Kendrew, J., Curwen, J.O. *Related novel 4-anilinoquinazolines with C-7 basic side chains: Design and structure activity relationship of a series of potent, orally active, VEGF receptor tyrosine kinase inhibitors.* J Med Chem 2002, 45: 1300-12.

5. Folkman, J. *Tumor angiogenesis: Therapeutic implications.* New Engl J Med 1971, 285: 1182-6.

6. Rosen, L.S. *Inhibitors of the vascular endothelial growth factor receptor.* Hematol Oncol Clin North Am 2002, 16: 1173-87.

7. Keck, P.J., Hauser, S.D., Krivi, G., Sanzo, K., Warren, T., Feder, J., Connolly, D.T. *Vascular permeability factor, an endothelial cell mitogen related to PDGF.* Science 1989, 246: 1309-12.

8. Dvorak, H.F., Detmar, M., Claffey, K.P., Nagy, J.A., van de Water, L., Senger, D.R. *Vascular permeability factor/vascular endothelial growth factor: An important mediator of angiogenesis in malignancy and inflammation.* Int Arch Allergy Immunol 1995, 107: 233-5.

9. Ferrara, N., Houck, K., Jakeman, L., Leung, D.W. *Molecular and biological properties of the vascular endothelial growth factor family of proteins.* Endocr Rev 1992, 13: 18-32.

10. Ferrara, N. *The role of vascular endothelial growth factor in pathological angiogenesis.* Breast Cancer Res Treat 1995, 36: 127-37.

11. Robinson, D.R., Wu, Y.-M., Lin, S.-F. *The protein tyrosine kinase family of the human genome.* Oncogene 2000, 19: 5548-57.

12. Petrova, T.V., Makinen, T., Alitalo, K. *Signaling via vascular endothelial growth factor receptors.* Exp Cell Res 1999, 253: 117-30.

13. Zeng, H., Sanyal, S., Mukhopadhyay, D. *Tyrosine residues 951 and 1059 of vascular endothelial growth factor receptor-2 (KDR) are essential for vascular permeability factor/vascular endothelial growth factor-induced endothelium migration and proliferation, respectively.* J Biol Chem 2001, 276: 32714-9.

14. Gille, H., Kowalski, J., Li, B., LeCouter, J., Moffat, B., Zioncheck, T.F., Pelletier, N., Ferrara, N. *Analysis of biological effects and signaling properties of Flt-1 (VEGFR-1) and KDR (VEGFR-2). A reassessment using novel receptor-specific vascular endothelial growth factor mutants.* J Biol Chem 2001, 276: 3222-30.

15. Gschwind, A., Fisher, O.M., Ullrich, A. *The discovery of receptor tyrosine kinases: Targets for cancer therapy.* Nat Rev Cancer 2004, 4: 361-70.

16. Wedge, S.R., Ogilvie, D.J., Dukes, M. et al. *ZD-6474 inhibits vascular endothelial growth factor signaling, angiogenesis, and tumor growth following oral administration.* Cancer Res 2002, 62: 4645-55.

17. Carlomagno, F., Vitagliano, D., Guida, T., Ciardiello, F., Tortora, G., Vecchio, G., Ryan, A.J., Fontanini, G., Fusco, A., Santoro, M. *ZD-6474, an orally available inhibitor of KDR tyrosine kinase activity, efficiently blocks oncogenic RET kinases.* Cancer Res 2002, 62: 7284-90.

18. Wedge, S.R., Oglivie, D.J., Dukes, M., Kendrew, J., Hennequin, L.F., Stokes, E.S.E., Curry, B. *Chronic and acute effects of ZD-6474, a VEGF receptor trosine kinase inhibitor, on established human tumor xenografts.* Clin Cancer Res 2000, 6(Suppl.): Abst 268.

19. Ciardiello, F., Caputo, R., Damiano, V. et al. *Antitumor effects of ZD-6474, a small molecule vascular endothelial growth factor receptor tyrosine kinase inhibitor, with additional activity against epidermal growth factor receptor tyrosine kinase.* Clin Cancer Res 2003, 9: 1546-56.

20. Arao, T., Fukumoto, H., Takeda, M., Tamura, T., Saijo, N., Nishio, K. *Small in-frame deletion in the epidermal growth factor receptor as a target for ZD-6474.* Cancer Res 2004, 64: 9101-4.

21. McCarty, M.F., Wey, J., Stoeltzing, O., Liu, W., Fan, F., Bucana, C., Mansfield, P.F., Ryan, A.J., Ellis, L.M. *ZD-6474, a vascular endothelial growth factor receptor tyrosine kinase inhibitor with additional activity against epidermal growth factor receptor tyrosine kinase, inhibits orthotopic growth and angiogenesis of gastric cancer.* Mol Cancer Ther 2004, 3: 1041-8.

22. Sandström, M., Johansson, M., Andersson, U., Bergh, A., Bergenheim, A.T., Henriksson, R. *The tyrosine kinase inhibitor ZD-6474 inhibits tumour growth in an intracerebral rat glioma model.* Br J Cancer 2004, 91: 1174-80.

23. Leenders, W.P., Küsters, B., Verrijp, K., Maass, C., Wesseling, P., Heerschap, A., Ruiter, D., Ryan, A., de Waal, R. *Antiangiogenic therapy of cerebral melanoma metastases results in sustained tumor progression via vessel co-option.* Clin Cancer Res 2004, 10: 6222-30.

24. Heffelfinger, S.C., Yan, M., Gear, R.B., Schneider, J., LaDow, K., Warshawsky, D. *Inhibition of VEGFR2 prevents DMBA-induced mammary tumor formation.* Lab Invest 2004, 84: 989-98.

25. Taguchi, F., Koh, Y., Koizumi, F., Tamura, T., Saijo, N., Nishio, K. *Anticancer effects of ZD-6474, a VEGF receptor tyrosine kinase inhibitor, in gefitinib ("Iressa")-sensitive and resistant xenograft models.* Cancer Sci 2004, 95: 984-9.

26. Helfrich, B., Troiani, T., Raben, D., Frederick, B., Gustafson, D., Merz, A., Weed, S., Bunn, P. *Anticancer effects of ZD-6474 in gefitinib (Iressa™)-resistant lung cancer cell lines in vitro.* Eur J Cancer - Suppl 2004, 2(8): Abst 161.

27. Nicholson, B., Gulding, K., Conaway, M., Wedge, S.R., Theodorescu, D. *Combination antiangiogenic and androgen deprivation therapy for prostate cancer: A promising therapeutic approach.* Clin Cancer Res 2004, 10: 8728-34.

28. Williams, K.J., Telfer, B.A., Brave, S., Kendrew, J., Whittaker, L., Stratford, I.J., Wedge, S.R. *ZD-6474, a potent inhibitor of vascular endothelial growth factor signaling, combined with radiotherapy. Schedule-dependent enhancement of antitumor activity.* Clin Cancer Res 2004, 10: 8587-93.

29. Gustafson, D.L., Merz, A.L., Zirrolli, J.A., Connaghan-Jones, K.D., Raben, D. *Impact of scheduling on combined ZD-6474 and radiotherapy in head and neck tumor xenografts.* Eur J Cancer - Suppl 2004, 2(8): Abst 142.

30. Siemann, D., Shi, W. *The VEGFR-2 tyrosine kinase inhibitor, ZD-6474, enhances the antitumor effect of radiation.* Eur J Cancer - Suppl 2004, 2(8): Abst 154.

31. Siemann, D.W., Shi, W. *Efficacy of combined antiangiogenic and vascular disrupting agents in treatment of solid tumors.* Int J Radiat Oncol Biol Phys 2004, 60: 1233-40.

32. Checkley, D., Tessier, J.J., Kendrew, J., Waterton, J.C., Wedge, S.R. *Use of dynamic contrast-enhanced MRI to evaluate acute treatment with ZD-6474, a VEGF signalling inhibitor, in PC-3 prostate tumours.* Br J Cancer 2003, 89: 1889-95.

33. Goodlad, R.A., Ryan, A., Watson, J., Wedge, S.R., Pyrah, I.T., Mandir, N., Wilkinson, R.W. *Antitumor therapy with VEGF receptor tyrosine kinase inhibitor ZD-6474 in a mouse model of intestinal cancer.* Eur J Cancer - Suppl 2004, 2(8): Abst 160.

34. Frederick, B., Helfrich, B., Raben, D. *Is hypoxia relevant in modulating the effects of the novel antiangiogenic agent, ZD-6474, in head and neck cancer?* Eur J Cancer - Suppl 2004, 2(8): Abst 187.

35. Smith, R.P., Kennedy, S., Roberton, J., Sandall, D., Oliver, R. *The effect of food on the intra-subject variability of the pharmacokinetics of ZD-6474, a novel antiangiogenic agent, in healthy subjects.* 40th Annu Meet Am Soc Clin Oncol (June 5-8, New Orleans) 2004, Abst 3167.

36. Basser, R., Hurwitz, H., Barge, A. *Phase 1 pharmacokinetic and biological study of the angiogenesis inhibitor, ZD-6474, in patients with solid tumors.* Proc Am Soc Clin Oncol 2001, 20(Part 1): Abst 396.

37. Hurwitz, H., Holden, S.N., Eckhardt, S.G., Rosenthal, M., de Boer, R., Rischin, D., Green, M., Basser, R. *Clinical evaluation of ZD-6474, an orally active inhibitor of VEGF signaling, in patients with solid tumors.* Proc Am Soc Clin Oncol 2002, 21(Part 1): Abst 325.

38. Minami, H., Ebi, H., Tahara, M., Sasaki, Y., Yamamoto, N., Yamada, Y., Tamura, T., Saijo, N. *A phase I study of an oral VEGF receptor tyrosine kinase inhibitor ZD-6474, in Japanese patients with solid tumors.* Proc Am Soc Clin Oncol 2003, 22: Abst 778.

39. Heymach, J.V, Dong, R.-P., Dimery, I., Wheeler, C., Fidias, P., Lu, C., Johnson, B., Herbst, R. *ZD-6474, a novel antiangiogenic agent, in combination with docetaxel in patients with NSCLC. Results of the run-in phase of two-part, randomized phase II study.* 40th Annu Meet Am Soc Clin Oncol (June 5-8, New Orleans) 2004, Abst 3051.

Additional References

Carlomagno, F., Guida, T., Anaganti, S., Vecchio, G., Fusco, A., Ryan, A.J., Billaud, M., Santoro, M. *Disease associated mutations at valine 804 in the RET receptor tyrosine kinase confer resistance to selective kinase inhibitors.* Oncogene 2004, 23: 6056-63.

Vitagliano, D., Carlomagno, F., Motti, M.L. et al. *Regulation of p27Kip1 protein levels contributes to mitogenic effects of the RET/PTC kinase in thyroid carcinoma cells.* Cancer Res 2004, 64: 3823-9.

Drugs of the Future 2015, 40(3): 157-165

CCC: 0377-8282/2015
DOI: 10.1358/dof.2015.40.3.2297483

MONOGRAPH

BINIMETINIB

Prop INN; USAN

MEK 1/2 inhibitor
Treatment of NRAS-mutated melanoma
Treatment of ovarian cancer

J. Gras

Barcelona, Spain

CONTENTS

SUMMARY

Mutations in BRAF and in NRAS are present in 40-60%, and 15-25% of melanomas, respectively, and no approved targeted therapy exists yet for patients with NRAS-mutated melanoma. Binimetinib is a potent, orally active dual specificity mitogen-activated protein kinase kinase 1 and 2 (MEK 1/2) inhibitor in phase III clinical trials for the treatment of metastatic melanoma with NRAS mutations; in combination with encorafenib (a serine/threonine-protein kinase B-raf inhibitor) in patients with BRAF V600-mutant melanoma; and for the treatment of low-grade serous carcinomas of the ovary, fallopian tube or primary peritoneum. In a phase II clinical trial (N = 117), binimetinib administered orally at 45 mg b.i.d. to patients with NRAS-mutated melanoma showed a disease control rate of 56% and a median overall survival of 12.2 months. The most common adverse events were gastrointestinal and skin disorders, and grade 3-4 adverse events were diarrhea and elevated creatinine phosphokinase. Binimetinib is the first targeted therapy active in patients with NRAS-mutated melanoma.

Key words: Binimetinib – MEK-162 – MEK 1/2 inhibitor – NRAS mutation

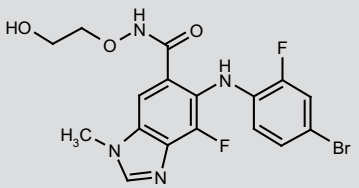

ARRY-162
ARRY-438162
MEK-162

5-(4-Bromo-2-fluorophenylamino)-4-fluoro-1-methyl-1*H*-benzimidazole-6-carbohydroxamic acid 2-hydroxyethyl ester

InChI = 1S/C17H15BrF2N4O3/c1-24-8-21-16-13(24)7-10(17(26)23-27-5-4-25)15(14(16)20)22-12-3-2-9(18)6-11(12)19/h2-3,6-8,22,25H,4-5H2,1H3,(H,23,26)

$C_{17}H_{15}BrF_2N_4O_3$; Mol wt: 441.227
CAS RN®: 606143-89-9
Thomson Reuters Integrity℠ Entry Number: 349927

SYNTHESIS*

Binimetinib can be obtained as follows:

a) Nitration of 2,3,4-trifluorobenzoic acid (I) using HNO_3 and H_2SO_4 gives 2,3,4-trifluoro-5-nitrobenzoic acid (II), which by displacement with NH_4OH in H_2O at 0 °C yields 4-amino-2,3-difluoro-5-nitrobenzoic acid (III). Fisher esterification of acid (III) with Me_3SiCHN_2 in THF/MeOH at 0 °C affords 4-amino-2,3-difluoro-5-nitrobezoic acid methyl ester (IV), which is condensed with 2-fluoroaniline (V) in xylene at 140 °C to provide methyl 4-amino-3-fluoro-2-(2-fluorophenylamino)-5-nitrobenzoic acid methyl ester (VI). Reduction and cyclization of intermediate (VI) using formic acid and $Pd(OH)_2/C$ in EtOH at 95 °C generates methyl 4-fluoro-5-(2-fluorophenylamino)-benzimidazole-6-carboxylate (VII), which by bromination with NBS and *p*-TsOH in DMF produces the bromo derivative (VIII). *N*-Methylation of compound (VIII) with methyl iodide by means of K_2CO_3 in DMF at 75 °C gives compound (IX), which is hydrolyzed with NaOH in THF/H_2O to yield the free carboxylic acid (X). Condensation of carboxylic acid (X) with *O*-[2-(vinyloxy)ethyl]hydroxylamine (XI) using HOBt, Et_3N and EDC in DMF affords amide (XII), which is finally treated with HCl in EtOH (1). Scheme 1.

Intermediate *O*-[2-(vinyloxy)ethyl]hydroxylamine (XI) is prepared by Mitsnoubu reaction of 2-(vinyloxy)ethanol (XIII) with *N*-hydroxy-

Correspondence: Jordi Gras, PhD (Pharmacol), Freelance Medical Writer, Barcelona, Spain. E-mail: scientific.prousjournals@thomsonreuters.com.

*Synthesis prepared by J. Bolòs, R. Castañer, Thomson Reuters, Barcelona, Spain.

Scheme 1. Synthesis of Binimetinib

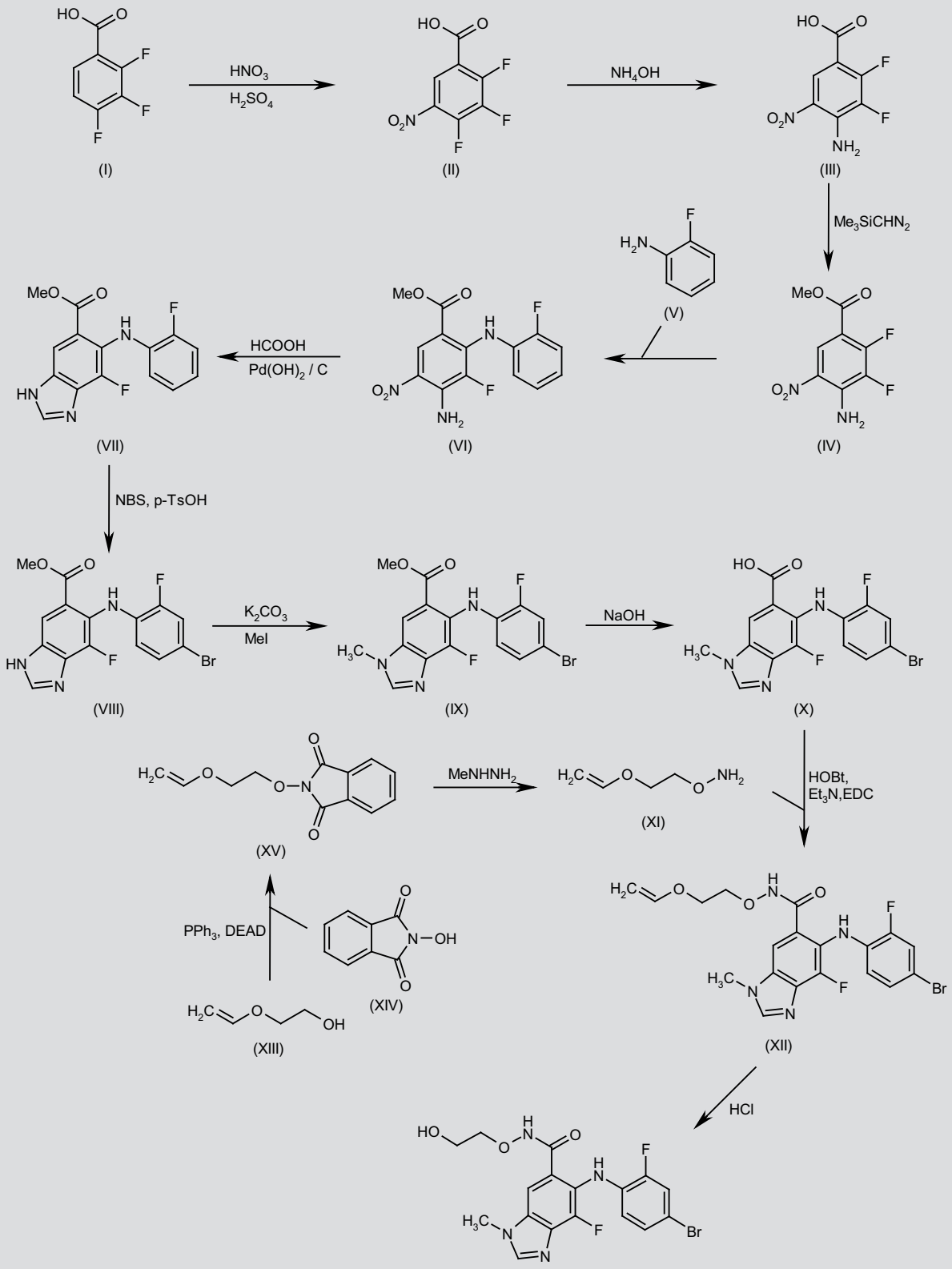

phthalimide (XIV) using PPh_3 and DEAD in THF at 0 °C to give 2-[2-(vinyloxy)ethoxy]-1*H*-isoindole-1,3(2*H*)-dione (XV), which is finally treated with $MeNHNH_2$ in CH_2Cl_2 (2). Scheme 1.

b) Condensation of methyl 5-amino-4-fluoro-1-methylbenzimidazole-6-carboxylate (XVI) with 4-bromo-2-fluoro-1-iodobenzene (XVII) by means of Pd_2dba_3, Cs_2CO_3 and xantphos in toluene/dioxane gives the 5-phenylamino-benzimidazole derivative (IX), which is hydrolyzed with $KOSiMe_3$ in DMF/THF to provide the potassium salt (XVIII). Compound (XVIII) is activated as its imidazolide (XIX) by treatment with carbonyl diimidazole (XX) in the presence of imidazole hydrochloride in THF/optionally DMF at 50 °C. Alternatively, hydrolysis of methyl ester (IX) by means of NaOH in H_2O affords carboxylic acid (X), which is further activated as its imidazolide (XIX) under the same conditions mentioned above. Condensation of intermediate (XIX) with *O*-(2-*tert*-butoxyethyl)hydroxylamine (XXI) in H_2O provides amide (XXII), which is finally *O*-deprotected by means of H_3PO_4 in acetonitrile (3). Scheme 2.

Scheme 2. Synthesis of Binimetinib

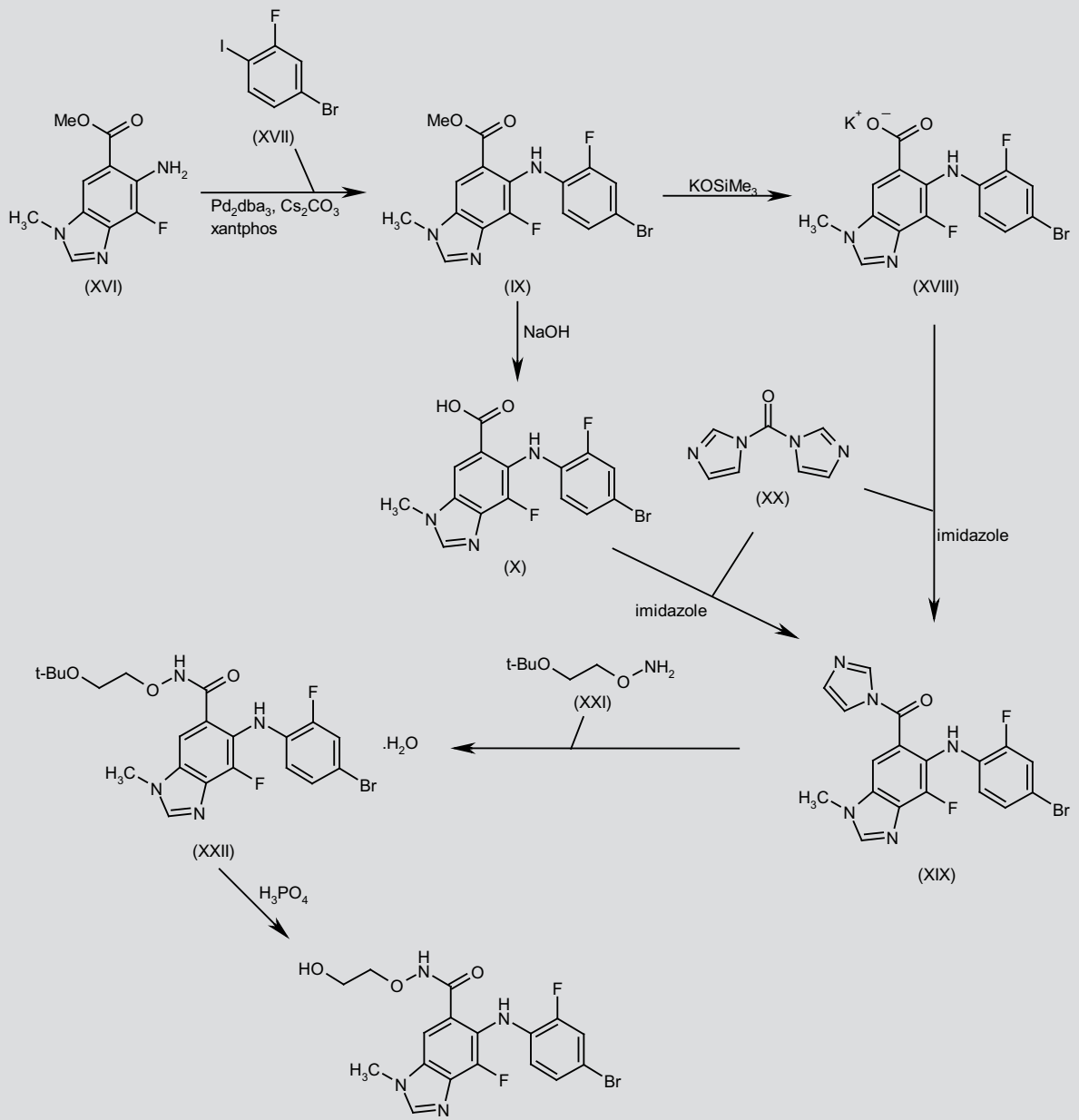

BACKGROUND

In recent years, a variety of molecular and genetic alterations in several cancers have been unveiled, providing a deeper insight into the complexity of tumorigenesis and the opportunity to target specific markers to improve patient outcomes (4). For instance, RAS-encoding genes (primarily *KRAS*, *NRAS* and *HRAS*) are some of the most often mutated genes in human cancers, while *BRAF* mutations have been detected in a relatively narrow range of malignancies (5). Mutations in *BRAF* and in *NRAS* are present in 40-60%, and 15-25% of melanomas, respectively, and unlike for patients with *BRAF* mutations, no approved targeted therapy exists for patients with *NRAS*-mutated melanoma (6). Low-grade serous ovarian cancers, which have a high frequency of mutations (i.e., 35% in KRAS and 33% in BRAF), are also chemoresistant (7).

The RAS and RAF families of protein kinases are steps of the mitogen-activated protein kinase (MAPK) cascade (also named RAS-RAF-MEK 1/2-ERK-1/2 pathway) that control multiple key physiological processes, by linking extracellular stimuli to intracellular gene expression pathways. When dysregulated this cascade has been implicated in human malignancies, accounting for abnormal cellular proliferation, impaired apoptosis, enhanced angiogenesis, and the development of drug resistance (7-10).

Dual specificity mitogen-activated protein kinase kinase 1 and 2 (MEK 1/2) are an attractive target for different reasons, i.e., it is a potential bottleneck in the activation of diverse cellular responses because extracellular signal-regulated kinase 1 and 2 (ERK-1/2) are the only known physiological substrates of MEK 1/2, and MEK molecules possess a unique hydrophobic allosteric pocket structure adjacent to, but separate from, the ATP-binding site. Thus, MEK inhibitors bind to this unique binding site eliciting a selective noncompetitive inhibition, and avoiding cross inhibition of other serine/threonine protein kinases (5, 7-11).

The PI3K/AKT/mTOR pathway shares common activators with the MAPK pathway, and there exists a considerable degree of cross-talk between both pathways such that when one is inhibited the other is upregulated to sustain growth and survival signaling. In fact, PI3K/AKT/mTOR pathway activation has been related to MEK resistance, and synergistic antitumoral effects have been detected when both pathways are inhibited concomitantly. Treatment strategies by simultaneously using multiple medications with different targets are likely to become the standard-of-care in most metastatic malignancies (12).

Binimetinib (MEK-162, ARRY-438162, ARRY-162) is a potent, orally active MEK 1/2 inhibitor in phase III clinical trials at Array BioPharma for the treatment of metastatic or unresectable cutaneous melanoma with *NRAS* mutations and in combination with encorafenib (a serine/threonine-protein kinase B-raf inhibitor) in adult patients with *BRAF* V600. Phase III studies are also under way at Array BioPharma for the treatment of low-grade serous carcinomas of the ovary, fallopian tube or primary peritoneum following at least one prior platinum-based chemotherapy regimen and no more than three lines of prior chemotherapy regimens (13).

PRECLINICAL PHARMACOLOGY

Binimetinib showed a potent and selective activity against MEK enzyme in vitro with an IC_{50} of 12 nM. When tested against 220 serine/threonine and tyrosine kinases, it showed no inhibitory activity at concentrations up to 20 μM. In addition, both basal and induced levels of ERK phosphorylation were inhibited by binimetinib in several cancer cell lines with IC_{50} values in the low nanomolar range. Of note, binimetinib potently inhibited cell proliferation of mutant B-Raf and Ras cell lines such as HT29, Malme-3M, SK-MEL-2, COLO 205, SK-MEL-28, and A375, with IC_{50} values between 30 and 250 nM. In vivo, binimetinib has showed antitumoral efficacy in various xenograft murine models, encompassing colonic (HT29, LoVo, COLO 205), pancreatic (BxPC3, MIA PaCa2), pulmonary (A549, Calu6), and prostatic (DU145) cancer models. In the HT29 and COLO 205 colonic cancer models, oral binimetinib displayed a dose-dependent inhibition, with up to 75% of tumor growth inhibition (TGI); even significant tumor regressions were observed in the COLO 205 model, with 13% having complete responses, and 50% partial responses. In the BxPC3 pancreatic carcinoma model, binimetinib showed approximately 70% TGI and 13% partial responses. Consistently, decreased pERK levels in tumor xenografts correlated with TGI (14).

In various tumor xenograft models, the activity of binimetinib in combination with inhibitors of mTOR and the ErbB receptor family, as well as standard-of-care chemotherapeutics were tested. In an A549 (KRAS mutant) model, binimetinib and an mTOR inhibitor, administered alone, inhibited tumor growth (TGI of 71 and 82%, respectively), whereas an enhanced activity (TGI 89%) was seen when the two drugs were administered in combination. In the NCI-H460 (KRAS mutant and constitutively active PI3K) lung carcinoma model, binimetinib was inactive and an mTOR inhibitor showed moderate activity (TGI of 64%), but when administered in combination TGI was enhanced and a significant tumor growth delay was observed. In the LoVo CRC (KRAS mutant and pEGFR overexpression) model, binimetinib and a pan-ErbB kinase inhibitor, when administered alone, showed modest TGI (50 and 57%, respectively), and no tumor regressions. In contrast, when administered in combination, it produced an 83% TGI and more than 50% tumor regression. In MIA PaCa2 and COLO 205 models, binimetinib administered alone showed TGI of 40 and 79%, respectively, whereas gemcitabine or paclitaxel (standard-of-care chemotherapy) showed TGI of 16 and 43%, respectively. When binimetinib was dosed in combination, TGI was enhanced and regressions were reached in both models. In summary, binimetinib showed significant activity as a single agent, and promising additivity with anticancer agents (15).

To target both the RAS/RAF/MEK/ERK and PI3K signaling pathways, a MEK inhibitor and a TORC1 inhibitor were administered concomitantly. Thus, the growth inhibitory activities of binimetinib and everolimus (a TORC1 inhibitor) were gauged as a single agent and in combination in 26 different human cancer cell lines with mutations in *KRAS*, *PTEN*, *PI3K* and *BRAF* genes. This study allowed the identification of key genotypes associated with antagonistic, additive and synergistic responses to the combination. For instance, binimetinib and everolimus as single agents showed a modest growth inhibition against the NCI-H460 NSCLC line [KRASG12D/PI3KCA], but in combination significantly inhibited the growth in a synergistic way. These data were confirmed in vivo using NCI-H460 xenografts in nude mice. Indeed, everolimus alone showed no TGI and binimetinib produced only dose-related modest inhibition (up to 50%), whereas the combination enhanced the effects of all doses of binimetinib without altering the exposure of either agent (16).

Although tumors harboring mutated forms of Ras and Raf are considered to be highly sensitive to MEK inhibition, binimetinib, in a survey of 15 xenograft models, showed the greatest efficacy, including partial and complete regressions, in models not harboring these mutations, i.e., BxPC-3 pancreatic carcinoma, CRC13B2 colon carcinoma, HT1080 fibrosarcoma, and NCI-H1975 NSCL carcinoma (EGFR T790M). In order to elucidate whether this antitumoral effect was due to the antiangiogenic activity reported for MEK inhibitors, binimetinib was studied in an in vivo vascular endothelial cell growth factor (VEGF)- and basic fibroblast growth factor (bFGF)-induced matrigel invasion assay. Nevertheless, while binimetinib showed high potency as an inhibitor of the neoangiogenesis in this assay, an investigation of angiogenesis endpoints (VEGF and microvessel density) in xenografts did not support a role for angiogenesis in the antitumoral activity of binimetinib, suggesting that stimulation of proapoptotic pathways may be a major contributor to the potent antitumor activity seen in vivo (17).

Biliary cancer is characterized by deregulated PI3K/Akt signaling, upregulated MAPK pathway, and an autocrine interleukin-6/signal transducer and activator of transcription 3 (IL-6/STAT3) feedback loop, which can also drive immunosuppression. Binimetinib studied in a panel of human biliary cancer cell lines, namely HuCCT1, HuH28 and MzCha1, showed significant inhibition of cell growth and induction of apoptosis in all three cell lines. In addition, in HuCCT1 cells a decreased ERK phosphorylation was confirmed, and clinically relevant immunomodulatory effects were detected. Indeed, culture supernatants displayed significant reductions in IL-6 protein after binimetinib treatment, and in peripheral blood mononuclear cells cultured with IL-6 and granulocyte-macrophase colony-stimulating factor (GM-CSF), binimetinib inhibited the generation of human myeloid-derived suppressor cells. In vivo, in athymic mice bearing HuCCT1 xenografts, oral binimetinib showed significant growth inhibition, and tumor immunohistochemical analysis revealed significant reductions in both Ki67 and pERK. To conclude, MEK inhibition can be a promising therapeutic approach in biliary cancer (18).

The major mechanism of oncogenesis in pancreatic cancer is thought to be activating mutations in the KRAS oncogene. Thus, the antitumor activity of binimetinib was assessed in a panel of 29 pancreatic cancer cell lines, most of them KRAS-mutant cell lines. The sensitivity of these cell lines to binimetinib was not uniform. In fact, 15 cell lines were sensitive showing IC_{50} values lower than 500 nM, 14 cell lines were resistant with IC_{50} values greater than 500 nM, and one cell line, PATU8988T, did not reach IC_{50} even at 10 μM. When researchers assessed genomic copy number variation (CNV) on each cell line, sensitivity to binimetinib appeared related to KRAS CNV, i.e., in the 15 sensitive cell lines only 2 had KRAS copy number gains and 13 had normal KRAS copy number, whereas in the 14 resistant cell lines, 10 had KRAS CNVs and 4 had normal KRAS copy number. In addition, although the IC_{50} of wild-type KRAS cell lines (n = 4) did not differ from those from cell lines with mutant KRAS (n = 25), cell lines with KRAS(V12) mutation were more resistant to binimetinib than those with wild-type or KRAS(D12) mutations. In conclusion, in pancreatic cancer cell lines, sensitivity to binimetinib is associated with KRAS CNV and mutational subtype. Clinical validation is needed (19).

After investigation of the growth inhibitory effect of binimetinib in 328 cancer cell lines, encompassing melanoma, head and neck, colon, pancreas, lung, ovarian, liver, kidney, breast and endometrial cell lines, the most sensitive turned out to be melanoma cell lines. Out of 47 melanoma cell lines, 83% were sensitive to binimetinib based on an IC_{50} lower than 500 nM or a greater than 70% inhibition at 1 μM, and sensitivity was independent of BRAF V600E and NRAS Q61 mutation status. In most of the sensitive melanoma cell lines, regardless of their origin and oncogenic driver mutations, binimetinib led to a G_1 arrest and apoptosis. When the effects elicited for binimetinib in the MAPK and PI3K/mTOR pathways were assessed, a decrease in pERK was observed in all the cell lines tested, no matter their mutational status or their sensitivity. In NRAS and BRAF mutant cell lines, binimetinib decreased phosphorylated AKT (pAKT) and pS6, suggesting that the inhibition of the PI3K/mTOR pathway may be crucial for the sensitivity to binimetinib (20).

In a systematic evaluation of over 11,000 different compound combinations using the human cancer cell line encyclopedia in order to combat the resistance of tumors to chemotherapy, binimetinib combined with docetaxel was deemed as synergistic in KRAS-mutant NSCLC murine models in vivo (21).

Although the activity of the MAPK pathway is thought to be critical for the survival of, among others, chronic lymphocytic leukemia (CLL) cells, to date, MEK inhibitors in preclinical studies have demonstrated little efficacy against CLL cells. An in vitro study using recombinant stromal cell-derived factor CXCL12 or media conditioned by the HS5 stromal cell line (HS5-CM) to mimic the microenvironment of primary CLL cells, showed a significant increase of MAPK pathway activity; and binimetinib, under these conditions, blocked the ERK-1/2 activation and induced apoptosis in CLL cells. Moreover, binimetinib nullifies the survival advantage due to HS5-CM and reduced cell migration. These data suggest that MEK inhibition may be a useful strategy to treat CLL (22).

The BRAF inhibitor vemurafenib induced apoptosis in BRAF V600-mutant melanoma cells through a mechanism involving induction of endoplasmic reticulum (ER) stress. Another BRAF inhibitor, encorafenib, that induces morphological features of ER stress in NRAS-mutant metastatic melanoma cell lines, significantly enhanced growth inhibition and apoptosis induced by binimetinib in these cell lines, and induced the expression of the ER stress-related factors p8, ATF4, ATF3, CHOP and TRB3. These data suggest that the antitumor activity of MEK inhibitors in NRAS-mutant melanoma may be potentiated by ER stress (23).

The IC_{50}s, the effects on MAPK and PI3K/AKT signaling, and on cell-cycle progression of binimetinib alone or in combination with the PI3Kα inhibitor alpelisib (BYL-719), were studied in 40 human NSCLC and 30 squamous cell carcinoma of the head and neck (SCCHN) cell lines. Fifty percent of NSCLC were sensitive to binimetinib (IC_{50} equal to or less than 500 nM), 22.5% were intermediately sensitive (IC_{50} from 500 nM to 1 μM), and 27.5% were resistant (IC_{50} greater than 1 μM). Among SCCHN, 80% were sensitive, 7% were intermediately sensitive and 13% were resistant, based on the same cut-offs. Binimetinib exposure increased cells in G_0/G_1 and decreased cells in S-phase, it decreased phosphorylated ERK (pERK) and increased pAKT probably to offset MAPK pathway inhibition. Binimetinib combined with alpelisib caused a synergistic growth inhibition and decreased levels of both pERK and pAKT for all cell lines, suggesting that synergism can be mediated by the simultaneous blockade of MAPK and

PI3K/AKT pathways. These data provide a rationale for the clinical evaluation of binimetinib alone or combined with a PI3K inhibitor in metastatic NSCLC and SCCHN patients (24).

In seven colorectal cancer (CRC) cell lines (two of them resistant to irinotecan), binimetinib was tested in combination with buparlisib (BKM-120, a PI3K inhibitor) or SN-38 (the active metabolite of irinotecan). The results displayed a pronounced synergism between binimetinib and BKM-120, a moderate synergism between binimetinib and SN-38, and a mainly additive effect with the combination of BKM-120 and SN-38 (25).

PHARMACOKINETICS AND METABOLISM

In preliminary pharmacokinetic studies, binimetinib displayed good physico-chemical characteristics, low clearance, medium-to-high Caco-2 permeability, and a minimal proclivity for drug–drug interactions (14).

The pharmacokinetics of binimetinib was studied in a phase I dose-escalation study in patients with advanced solid tumors that received binimetinib orally at 30, 45, 60 or 80 mg b.i.d. Systemic exposure increased in a dose-related manner, with good inter-patient variability, and a modest accumulation. The mean elimination half-life was approximately 5 hours, and the mean steady-state plasma levels were above the in vitro IC_{50} value for cell proliferation at all doses tested (26).

Japanese patients with advanced solid tumors treated with oral binimetinib showed a rapid absorption, with a t_{max} value less than 2 hours and dose-dependent systemic exposure similar to that observed in Caucasian patients (27).

Pharmacokinetics after repeated dosing of binimetinib (45 mg b.i.d.) was assessed in patients with advanced melanoma harboring NRAS or V600 BRAF mutations. Data from 22 patients showed a rapid oral absorption of binimetinib (t_{max} = 1.48 h) with moderate variability between patients (6).

CLINICAL STUDIES

To determine the maximum tolerated dose (MTD), safety profile, pharmacodynamics and preliminary efficacy of binimetinib, a phase I dose-escalation study was developed in patients with advanced solid tumors (NCT00959127). A total of 19 patients were enrolled in 4 dose cohorts (30, 45, 60 and 80 mg orally b.i.d.), of whom 17 patients were evaluable for MTD and efficacy. The most frequent treatment-related adverse events (AEs), generally grade 1-2, were rash, diarrhea, nausea, vomiting and peripheral edema. Grade 3-4 treatment-related AEs included rash, palmar-plantar syndrome, central serous-like retinopathy and creatine phosphokinase (CPK) elevation. Dose-limiting toxicities were observed at 80 mg, and consequently MTD was 60 mg b.i.d. Concerning efficacy, one patient with NRAS-mutant cholangiocarcinoma showed partial response (PR), and nine patients showed stable disease (SD). The remaining evaluable patients with known mutational status included two wild-type in all locus tested, five KRAS, one NRAS, one BRAF, one PIK3Ca and one dual KRAS/PIK3Ca mutants. From the 60-mg cohort, skin biopsies displayed decreases in pERK and in Ki67 (a cellular marker for proliferation) (26). An expansion phase of this study was performed to assess safety, pharmacodynamics and preliminary efficacy in patients with unresectable, locally advanced or metastatic biliary tract cancer. The 28 patients enrolled received oral binimetinib at 60 mg b.i.d. The most common treatment-related AEs were rash, nausea, vomiting, diarrhea, peripheral edema, fatigue and central serous-like retinopathy, generally of grade 1-2, while grade 3-4 AEs included anasarca, hypokalemia, hyponatremia, upper/lower gastrointestinal hemorrhage and mucositis. Three patients withdrew from the study due to AEs. Efficacy assessed in 26 evaluable patients showed 1 complete response (CR), 1 PR and 11 SD. It deserves to be mentioned that both responders were wild-type on all loci tested and had extrahepatic cholangiocarcinoma (28).

Clinical studies indicate that binimetinib can be safely combined with encorafenib with promising clinical amelioration in patients with BRAF V600-mutant advanced cancers (NCT01543698) (29).

A multicenter phase I trial to determine the MTD and/or the recommended phase II dose of binimetinib was performed in Japanese patients with advanced solid tumors (NCT01469130). This study includes an expansion part in patients with BRAF/RAS-mutant tumors. As of January 7, 2013, 6 patients received binimetinib at 30 mg b.i.d., and 11 at 45 mg b.i.d. The most common treatment-related AEs of any grade were central serous-like retinopathy (88% of patients), increased CPK (71%), diarrhea (59%), increased aspartate transaminase (AST, 53%), rash (47%), increased lipase (41%), acneiform dermatitis (36%), decreased appetite (36%) and stomatitis (36%). The only grade 3-4 AEs reported in more than one patient was increased CPK. Four patients discontinued treatment due to an AE, and MTD, which was determined to be 45 mg b.i.d., was the dose selected for the ongoing expansion part of the study in Japanese patients with BRAF/RAS-mutant tumors (27).

Advanced melanoma

The efficacy and AEs of binimetinib at 45 mg b.i.d. in the treatment of advanced melanoma harboring NRAS or V600 BRAF mutations were assessed in an open-label, nonrandomized, phase II study (NCT01320085). Of note, patients with NRAS mutations have a poor overall survival and a higher incidence of CNS metastases. As of February 29, 2012, 71 patients were enrolled in this ongoing study, of whom 30 harbor NRAS and 41 BRAF mutations. Objective responses were assessed according to RECIST version 1.0 criteria. No patients showed a CR. In the NRAS arm, 6 (20%) patients showed PR (3 confirmed) and 13 (43%) patients showed SD, thus disease control rate (CR, PR or SD) was seen in 19 (63%) patients. Median time to response was 7.9 weeks, median duration of response was 7.6 weeks, and PFS was 3.7 months. In the BRAF arm, 8 (20%) patients showed PR (2 confirmed) and 13 (32%) patients showed SD, therefore, in this case, disease control rate was 21 (51%) patients. Of note, patients previously treated with a BRAF inhibitor showed no response. In the BRAF arm, median time to response was 8.5 weeks, median duration of response was 9.2 weeks, and PFS was 3.6 months. Concerning safety, the most common treatment-related AEs were acneic dermatitis (60% of patients in the NRAS arm and 37% in the BRAF arm), rash (20 and 39%, respectively), peripheral edema (33 and 34%), facial edema (30 and 17%), diarrhea (27 and 37%), CPK increases (37 and 22%), and retinal events (27 and 12%). The most common grade 3-4 AE was CPK increase. Overall, the most common AEs (gastrointestinal and skin disorders) were manageable with standard treatments,

and most retinal events were transient, resolving without treatment discontinuation, after dose reduction or after interruption of the treatment. Due to AEs, 4 (13%) patients in NRAS arm and 11 (27%) in the BRAF arm discontinued treatment. No deaths related to treatment occurred. In summary, binimetinib is the first targeted therapy active in patients with NRAS-mutated melanoma (6). Based on these data, the protocol of this trial (NCT01320085) was amended to enroll an additional 70 NRAS-mutated melanoma patients. Recently, updated efficacy, safety and biomarker analysis of a larger NRAS-mutant group were reported. Binimetinib administered at 45 mg orally b.i.d. to 117 patients showed an objective response rate (ORR) of 14.5% (1 CR, 16 PRs), disease control rate of 56%, median PFS of 3.6 months, and median overall survival (OS) of 12.2 months. Concerning safety, the most common treatment-related AEs were dermatitis acneiform (54%), increased CPK (51%) and peripheral edema (42%); and the most common grade 3-4 AE was increased CPK (25%). MAPK inhibition elicited by binimetinib was corroborated by the decreased expression of pERK and DUSP6 (30).

Currently, a two-arm, open-label, 2:1 randomized, phase III trial to compare the efficacy of binimetinib (45 mg b.i.d. orally) versus dacarbazine (1000 mg/m^2 i.v.) in patients with metastatic NRAS-mutant melanoma is ongoing (NEMO, NCT01763164). This study is designed to enroll 393 patients and is recruiting patients at more than 150 centers worldwide (31).

A study in patients with advanced melanoma harboring a BRAF mutation compared the duration of disease control (time from the start of treatment to discontinuation due to disease progression or toxicity) in a cohort treated initially with a BRAF inhibitor (vemurafenib or encorafenib) followed by a MEK inhibitor (AZD-6244, trametinib or binimetinib) versus a cohort that first received a MEK inhibitor and later a BRAF inhibitor. In the 16 patients evaluated the mean duration of disease control was similar in both groups. The sum of duration of disease control of both groups (9.3 and 8.6 months) is similar to the combination therapy of a BRAF inhibitor plus a MEK inhibitor (median PFS 9.4 months). The authors concluded that in addition to the sequenced administration analyzed here, an intermittent administration deserves to be studied (32).

The efficacy and safety of the combination of binimetinib plus encorafenib versus vemurafenib and encorafenib monotherapy is being compared in an ongoing phase III, randomized, open-label, multicenter, parallel group trial in patients with unresectable or metastatic BRAF V600 mutant melanoma (COLUMBUS, NCT01909453) (33).

Clinical studies indicate that binimetinib can be combined with the cyclin-dependent kinase (CDK) 4/6 inhibitor ribociclib (LEE-011), with promising preliminary antitumor activity in patients with NRAS-mutant melanoma (NCT01781572) (34).

Other currently ongoing clinical trials of binimetinib for the indication of melanoma include the following: A phase II study assessing the efficacy of the intermittent administration of binimetinib and encorafenib to patients with metastatic melanoma and BRAF V600 mutations (NCT02263898); a phase II study of single-agent encorafenib followed by a rational combination with agents (including binimetinib) after progression on encorafenib, to assess the antitumor activity in adult patients with locally advanced or metastatic BRAF V600 melanoma (LOGIC, NCT01820364); a phase II study of sequential binimetinib/encorafenib combination followed by a rational combination with targeted agents after progression, to assess the antitumor activity in adult patients with locally advanced or metastatic BRAF V600 melanoma (LOGIC-2, NCT02159066); and a phase Ib/II study of the combination of binimetinib and sotrastaurin (AEB-071, a protein kinase C inhibitor) to assess the safety and efficacy in adult patients with metastatic uveal melanoma (NCT01801358) (33).

Carcinomas of the ovary, fallopian tube or primary peritoneum

On the basis of preclinical studies that showed synergistic effects of the dual inhibition of MAPK and PI3K pathways, a phase Ib, open-label study in patients with RAS- or BRAF-mutant advanced solid malignancies (including ovarian cancer) treated with the combination of binimetinib with alpelisib was performed (NCT01449058). The main objective of this dose-escalation study was to determine the MTD and/or the recommended dose for expansion, and also preliminary efficacy was assessed. As of September 2, 2013, 58 patients were enrolled which were treated orally with the combination of binimetinib (30 or 45 mg b.i.d.) and alpelisib (from 80 to 270 mg q.d.) in 28-day cycles. The most common AEs were gastrointestinal and skin disorders, and the most common grade 3-4 AEs were diarrhea (12%) and elevated CPK (10%). The MTD was established as binimetinib 45 mg b.i.d. plus alpelisib 200 mg q.d. Concerning efficacy, 3 out of 4 patients with ovarian cancer with KRAS-mutant status showed PR (confirmed). In addition, PR was observed in one patient with NRAS-mutant melanoma (confirmed), and in one patient with KRAS-mutant endometrial cancer (unconfirmed). Moreover, lasting (more than 6 weeks) SD was reported for 31% of patients. In conclusion, further exploration in RAS-mutant ovarian cancer patients is fully justified (35, 36).

Currently, a 2-arm, open-label, 2:1 randomized, phase III trial to compare the efficacy of binimetinib versus physician's choice (doxorubicin, paclitaxel or topotecan) in patients with recurrent or persistent low-grade serous carcinomas of the ovary, fallopian tube or primary peritoneum is ongoing (MILO, NCT01849874). This study is designed to enroll 300 patients and the primary endpoint is PFS (37).

Another currently ongoing clinical trial of binimetinib for patients with gynecologic malignancies is a phase I safety/efficacy trial (NCT01649336) gauging binimetinib combined with paclitaxel in patients with platinum-resistant epithelial ovarian, fallopian tube, or primary peritoneal cancers (33).

Other oncologic studies

A phase II, multiple arm, open-label study will assess the efficacy and safety as a single agent of binimetinib, luminespib (AUY-922, an HSP90 inhibitor), alpelisib, ceritinib (LDK-378, an ALK inhibitor), or capmatinib (INC-280, a MET inhibitor) administered to Chinese patients with advanced NSCLC (NCT02276027). The primary endpoint is overall response rate, and PFS, disease control rate, duration of response, safety and pharmacokinetics will also be assessed (33, 38).

Other oncologic trials with binimetinib in earlier phases include indications as myeloid leukemia, colorectal cancer, biliary tract carcinoma, gastrointestinal stromal tumors, and gliomas (33).

CONCLUSIONS

Binimetinib is a potent, orally active MEK 1/2 inhibitor in phase III clinical trials for, among others, the treatment of metastatic melanoma with NRAS mutations; in combination with encorafenib in BRAF V600 mutant melanoma; and for the treatment of low-grade serous carcinomas of the ovary, fallopian tube or primary peritoneum.

Binimetinib showed a potent and selective activity against MEK enzyme in vitro with an IC_{50} value in the low nanomolar range. In cancer cell lines in vitro, and in various tumor xenografts models in vivo, binimetinib alone showed significant activity, and often when combined with other anticancer agents showed synergism.

In a phase II clinical trial (N = 117), binimetinib in patients with NRAS-mutated melanoma showed a disease control rate of 56%, and a median overall survival of 12.2 months, thus becoming the first targeted therapy active in patients with NRAS-mutated melanoma. The most common AEs were gastrointestinal and skin disorders, and grade 3-4 AEs were diarrhea and elevated CPK.

DISCLOSURES

The author states no conflicts of interest.

Submitted: February 13, 2015. Revised: March 30, 2015. Accepted: March 31, 2015.

REFERENCES

1. Wallace, E.M., Marlow, A.L., Hurley, B.T., Lyssikatos, J.P. (Array BioPharma, Inc.). *N3 Alkylated benzimidazole derivatives as MEK inhibitors*. WO 2003077914.
2. Barrett, S.D., Biwersi, C., Warmus, J.S., Tecle, H., Kaufman, M. (Pfizer, Inc.). *Oxygenated esters of 4-iodo phenylamino benzhydroxamic acids*. WO 2002006213; EP 1301472; CA 2416685; US 2004054172; US 6960614.
3. Krell, C.M., Misun, M., Niederer, D.A. et al. (Array BioPharma, Inc., Novartis AG). *Preparation of and formulation comprising a MEK inhibitor*. WO 2014063024; US 2014128442.
4. McDermott, U., Settleman, J. *Personalized cancer therapy with selective kinase inhibitors: an emerging paradigm in medical oncology*. J Clin Oncol 2009, 27(33): 5650-9.
5. Zhao, Y., Adjei, A.A. *The clinical development of MEK inhibitors*. Nat Rev Clin Oncol 2014, 11(7): 385-400.
6. Ascierto, P.A., Schadendorf, D., Berking, C. et al. *MEK162 for patients with advanced melanoma harbouring NRAS or Val600 BRAF mutations: A non-randomised, open-label phase 2 study*. Lancet Oncol 2013, 14(3): 249-56.
7. Miller, C.R., Oliver, K.E., Farley, J.H. *MEK1/2 inhibitors in the treatment of gynecologic malignancies*. Gynecol Oncol 2014, 133(1): 128-37.
8. Akinleye, A., Furqan, M., Mukhi, N., Ravella, P., Liu, D. *MEK and the inhibitors: from bench to bedside*. J Hematol Oncol 2013, 6: 27.
9. Cheng, Y., Zhang, G., Li, G. *Targeting MAPK payhway in melanoma therapy*. Cancer Metastasis Rev 2013, 32(3-4): 567-84.
10. McCubrey, J.A., Steelman, L.S., Chappell, W.H. et al. *Ras/Raf/MEK/ERK and PI3K/PTEN/Akt/mTOR cascade inhibitors: how mutations can result in therapy resistance and how to overcome resistance*. Oncotarget 2012, 3(10): 1068-111.
11. Roskoski, R. Jr. *ERK1/2 MAP kinases:structure, function, and regulation*. Pharmacol Res 2012, 66(2): 105-43.
12. Griewank, K.G., Scolyer, R.A., Thompson, J.F., Flaherty, K.T., Schadendorf, D., Murali, R. *Genetic alterations and personalized medicine in melanoma: Progress and future prospects*. J Natl Cancer Inst 2014, 106(2): djt435.
13. Array BioPharma Web site. http://www.arraybiopharma.com/. Accessed February 11, 2015.
14. Lee, P.A., Wallace, E., Marlow, A. et al. *Preclinical development of ARRY-162, a potent and selective MEK 1/2 inhibitor*. Cancer Res [101st Annu Meet Am Assoc Cancer Res (AACR) (April 17-21, Washington, D.C.) 2010] 2010, 70 (8, Suppl.): Abst 2515.
15. Woessner, R., Winski, S., Rana, S., Anderson, D., Winkler, J.D., Lee, P.A. *Arry-162, a potent and selective MEK 1/2 inhibitor, shows enhanced efficacy in combination with other targeted kinase inhibitors and with chemotherapy*. Cancer Res [101st Annu Meet Am Assoc Cancer Res (AACR) (April 17-21, Washington, D.C.) 2010] 2010, 70 (8, Suppl.): Abst 2514.
16. Tunquist, B., Risom, T., Anderson, D. et al. *Investigation of the growth inhibitory activity of the MEK inhibitor ARRY-438162 in combination with everolimus in a variety of KRas and PI3K pathway mutant cancers*. Cancer Res [101st Annu Meet Am Assoc Cancer Res (AACR) (April 17-21, Washington, D.C.) 2010] 2010, 70 (8, Suppl.): Abst 3855.
17. Winski, S., Anderson, D., Bouhana, K. et al. *MEK162 (ARRY-162), a novel MEK 1/2 inhibitor, inhibits tumor growth regardless of KRas/Raf pathway mutations*. 22nd EORTC-NCI-AACR Symp Mol Targets Cancer Ther (November 16-19, Berlin) 2010, Abst 162.
18. Yang, J., Mace, T.A., Young, G.S. et al. *MEK162, an allosteric MEK inhibitor promotes apoptosis and in vivo antitumor activity against human biliary cancer cell lines*. Cancer Res [104th Annu Meet Am Assoc Cancer Res (AACR) (April 6-10, Washington, D.C.) 2013] 2013, 73(8, Suppl.): Abst 934.
19. Hamidi, H.R., Finn, R., Anderson, L. et al. *KRAS mutational subtypes and copy number variations are predictive of response of human pancreatic cancer cell lines to MEK162 in vitro*. Cancer Res [104th Annu Meet Am Assoc Cancer Res (AACR) (April 6-10, Washington, D.C.) 2013] 2013, 73(8, Suppl.): Abst 936.
20. Von Euw, E.M., Rong, H.- M., O'Brien, N. et al. *MEK162 (ARRY438162), a MEK1/2 inhibitor, has activity in melanoma cells independent of BRAF and NRAS mutation status*. Cancer Res [104th Annu Meet Am Assoc Cancer Res (AACR) (April 6-10, Washington, D.C.) 2013] 2013, 73(8, Suppl.): Abst 2437.
21. Mcsheehy, P.M.J., Cao, A., Caponigro, G. et al. *Evaluation of prediction of in vivo activity from in vitro combinations: Examples using a MEK1/2 inhibitor combined with docetaxel in NSCLC models*. Mol Cancer Ther [25th AACR-NCI-EORTC Symp Mol Targets Cancer Ther (October 19-23, Boston) 2013] 2013, 12 (11, Suppl.): Abst A140.
22. Best, O.G., Crassini, K., Stevenson, W.S., Mulligan, S.P. *MAPK-Erk1/2 pathway activation and survival of chronic lymphocytic leukemia (CLL) cells is induced by in vitro modeling of the tumor microenvironment and can be effectively inhibited using the mek1 inhibitor MEK162*. Blood [55th Annu Meet Am Soc Hematol (December 7-10, New Orleans) 2013] 2013, 122 (21): Abst 4192.
23. Meier, F.E., Garbe, C., Smalley, K. et al. *Effect of the BRAF inhibitor LGX818 on endoplasmic reticulum stress and sensitivity of NRASmutant melanoma cells to the MEK inhibitor binimetinib*. J Clin Oncol [50th Annu Meet Am Soc Clin Oncol (ASCO) (May 30-June 3, Chicago) 2014] 2014, 32 (15, Suppl.): Abst 9062.
24. Wong, D.J.L., Garon, E.B., Silveira, D.D. et al. *Potent anti-tumor activity of the MEK1/2 inhibitor MEK162 inhuman non-small cell lung cancer (NSCLC) and squamous cell carcinoma of the head and neck (SCCHN) cell lines*. Cancer Res [105th Annu Meet Am Assoc Cancer Res (AACR) (April 5-9, San Diego) 2014] 2014, 74(19, Suppl.): Abst 743.

25. Tosi, D., Atis, S., Mollevi, C., Martineau, P., Gongora, C. *Synergism analysis of dose matrices for combinations of BKM120 (a PI3K inhibitor), MEK162 (a MEK1/2 inhibitor) and chemotherapy in colorectal cancer (CRC) cell lines*. Cancer Res [105th Annu Meet Am Assoc Cancer Res (AACR) (April 5-9, San Diego) 2014] 2014, 74(19, Suppl.): Abst 3681.

26. Bendell, J.C., Papadopoulos, K., Jones, S.F. et al. *A phase I dose-escalation study of MEK inhibitor MEK162 (ARRY-438162) in patients with advanced solid tumors*. Mol Cancer Ther [AACR-NCI-EORTC Int Conf Mol Targets Cancer Ther (November 12-16, San Francisco) 2011] 2011, 10(11, Suppl.): Abst B243.

27. Shimokata, T., Watanabe, K., Shibata, T. et al. *Results of a phase 1 study of MEK162, an oral MEK inhibitor, in Japanese patients with advanced solid tumors*. Eur J Cancer [Eur Cancer Congr (September 27-October 1, Amsterdam) 2013] 2013, 49 (Suppl. 2): Abst 3746.

28. Finn, R.S., Javle, M.M., Tan, B.R. et al. *A phase I study of MEK inhibitor MEK162 (ARRY-438162) in patients with biliary tract cancer*. J Clin Oncol [Gastrointest Cancers Symp (January 19-21, San Francisco) 2012] 2012, 30(4, Suppl.): Abst 220.

29. Kefford,R., Miller, W.H., Tan, D.S.-W. et al. *Preliminary results from a phase Ib/II, open-label, dose-escalation study of the oral BRAF inhibitor LGX818 in combination with the oral MEK1/2 inhibitor MEK162 in BRAF V600-dependent advanced solid tumors*. J Clin Oncol [49th Annu Meet Am Soc Clin Oncol (ASCO) (May 31-June 4, Chicago) 2013] 2013, 31 (15, Suppl.): Abst 9029.

30. Van Herpen, C., Agarwala, S., Hauschild, A. et al. *Overall survival and biomarker results from a phase 2 study of MEK1/2 inhibitor binimetinib (MEK162) in patients with advanced NRAS-mutant melanoma*. Ann Oncol [39th Eur Soc Med Oncol (ESMO) Congr (September 26-30, Madrid) 2014] 2014, 25 (Suppl. 5): Abst LBA35.

31. Dummer, R., Arenberger, P., Ascierto, P. et al. *NEMO: A phase 3 trial of binimetinib (MEK162) versus dacarbazine in patients with advanced NRAS-mutant melanoma who are untreated or have progressed after any number of immunotherapy regimens*. Ann Oncol [39th Eur Soc Med Oncol (ESMO) Congr (September 26-30, Madrid) 2014] 2014, 25 (Suppl. 4): Abst 1130TiP.

32. Goldinger, S.M., Murer, C., Stieger, P., Dummer, R. *Upstream MAPK pathway inhibition: MEK inhibitor followed by a BRAF inhibitor in advanced melanoma patients*. J Clin Oncol [49th Annu Meet Am Soc Clin Oncol (ASCO) (May 31-June 4, Chicago) 2013] 2013, 31(15, Suppl.): Abst 9071.

33. ClinicalTrials.gov web site. *Binimetinib, MK162, ARRY162*. Accessed February 8, 2015.

34. Sosman, J.A., Kittaneh, M., Lolkema, M.P. et al. *A phase 1b/2 study of LEE011 in combination with binimetinib (MEK162) in patients with advanced NRAS-mutant melanoma: early encouraging clinical activity*. J Clin Oncol [50th Annu Meet Am Soc Clin Oncol (ASCO) (May 30-June 3, Chicago) 2014] 2014, 32 (15, Suppl.): Abst 9009.

35. Juric, D., Soria, J.-C., Sharma, S. et al. *A phase 1b dose-escalation study of BYL719 plus binimetinib (MEK162) in patients with selected advanced solid tumors*. J Clin Oncol [50th Annu Meet Am Soc Clin Oncol (ASCO) (May 30-June 3, Chicago) 2014] 2014, 32 (15, Suppl.): Abst 9051.

36. Banerji, U., Smith, A.D., Zivi, A. et al. *Dual targeting of RAF-MEK-ERK and PI3K-AKT-mTOR pathways in RAS-mutant cancers: Preclinical insights and institutional experience from a clinical trial of binimetinib (MEK162) plus BYL719*. J Clin Oncol [50th Annu Meet Am Soc Clin Oncol (ASCO) (May 30-June 3, Chicago) 2014] 2014, 32 (15, Suppl.): Abst e13559.

37. Monk, B.J., Grisham, R.N., Marth, C. et al. *The MEK inhibitor in low-grade serous ovarian cancer (MILO)/ENGOT-ov11 study: A multinational, randomized, open-label phase 3 study of binimetinib (MEK162) versus physicians choice chemotherapy in patients with recurrent or persistent low-grade serous carcinomas of the ovary, fallopian tube, or primary peritoneum*. J Clin Oncol [50th Annu Meet Am Soc Clin Oncol (ASCO) (May 30-June 3, Chicago) 2014] 2014, 32 (15, Suppl.): Abst TPS5618.

38. Zhou, Q., Zhang, X.-C., Peng, B., Yu, X., Akimov, M., Weber, B.L., Wu, Y.-L. *A phase II cluster study of single agent AUY922, BYL719, INC280, LDK378, and MEK162 in Chinese patients with advanced non-small cell lung cancer (NSCLC)*. J Clin Oncol [50th Annu Meet Am Soc Clin Oncol (ASCO) (May 30-June 3, Chicago) 2014] 2014, 32 (15, Suppl.): Abst TPS8122.

Drugs of the Future 2006, 31(10): 854-858

CCC: 0377-8282/2006
DOI: 10.1358/dof.2006.031.10.1040269

AZD-6244

MEK1/2 Inhibitor
Oncolytic

ARRY-142886

5-(4-Bromo-2-chlorophenylamino)-4-fluoro-1-methyl-1*H*-benzimidazole-6-carbohydroxamic acid 2-hydroxyethyl ester

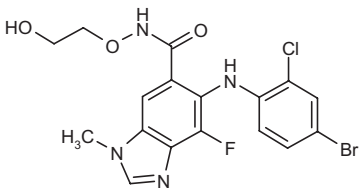

$C_{17}H_{15}BrClFN_4O_3$
Mol wt: 457.6813

CAS: 606143-52-6

EN: 355417

Abstract

The MEK/ERK-dependent mitogen-activated protein (MAP) kinase pathway mediates cellular responses to growth signals, and aberrant regulation of the pathway has been implicated in many human cancers. Because of its key position as the only known activator of ERK, and its location downstream of the oncogenes *ras* and *raf*, MEK offers an attractive target for chemotherapeutic intervention. AZD-6244 (ARRY-142886) is an orally active, highly specific inhibitor of MEK that has shown tumor-suppressive activity in a wide range of preclinical models of human cancer. AZD-6244 is currently in phase II development for the treatment of melanoma, non-small cell lung and pancreatic cancer.

Synthesis

AZD-6244 is synthesized as follows:

Nitration of 2,3,4-trifluorobenzoic acid (I), followed by selective displacement with aqueous ammonia of the 4-fluoride in the resulting nitrobenzoic acid (II) gives 4-amino-2,3-difluoro-5-nitrobenzoic acid (III), which is further esterified to (IV) upon treatment with trimethylsilyldiazomethane. Subsequent condensation of (IV) with aniline (V) in hot xylene yields the diaminobenzoate (VI). The reduction of the nitroamine (VI) in the presence of formic acid and Pearlman's catalyst under transfer hydrogenation conditions proceeds with concomitant cyclization to produce the benzimidazole (VII). The anilino moiety in (VII) is stepwise brominated to (VIII) with *N*-bromosuccinimide (NBS) and then chlorinated with NCS to afford the 4-bromo-2-chlorophenylamino derivative (IX). Alternatively, the intermediate (IX) is obtained by condensation of difluorobenzoate (IV) with 2-chloroaniline (X), followed by reduction of the resulting diaminonitrobenzoate (XI) with Zn dust in AcOH, cyclization of the *ortho*-diamine (XII) to the benzimidazole (XIII) by means of formamidine acetate, and bromination with NBS. After methylation of the benzimidazole (IX) with iodomethane and K_2CO_3, the methyl ester (XIV) is hydrolyzed to the benzimidazolecarboxylic acid (XV) under alkaline conditions. Coupling of acid (XV) with *O*-(2-vinyloxyethyl)hydroxylamine (XVI) in the presence of EDC/HOBt gives the vinyl-protected hydroxamate (XVII), which is finally deprotected by hydrolysis with HCl in aqueous ethanol (1). Scheme 1.

Background

Under normal circumstances, the regulation of cell growth and development is mediated by growth factors (*e.g.*, epidermal growth factor [EGF], erbB-2, vascular endothelial growth factor [VEGF], platelet-derived growth factor [PDGF]) that interact with their respective cell-surface receptor tyrosine kinases. The activated receptors coordinate the activation of mitogen-activated protein (MAP) kinase signal pathways (Fig. 1), leading to the appropriate changes in the cell (2).

One of the best understood MAP kinase pathways is the Ras/Raf/MEK/ERK cascade, and its constitutive activation has been implicated in aberrant cell growth and the development of many tumors (3-5). The cascade initiates with receptor tyrosine kinase-mediated activation of the G-protein Ras. GTP-Ras then phosphorylates Raf, which phosphorylates MEK1/2, which phosphorylates ERK1/2.

P. Revill, N. Serradell, J. Bolós, J. Bozzo. Prous Science, P.O. Box 540, 08080 Barcelona, Spain.

Scheme 1: Synthesis of AZD-6244

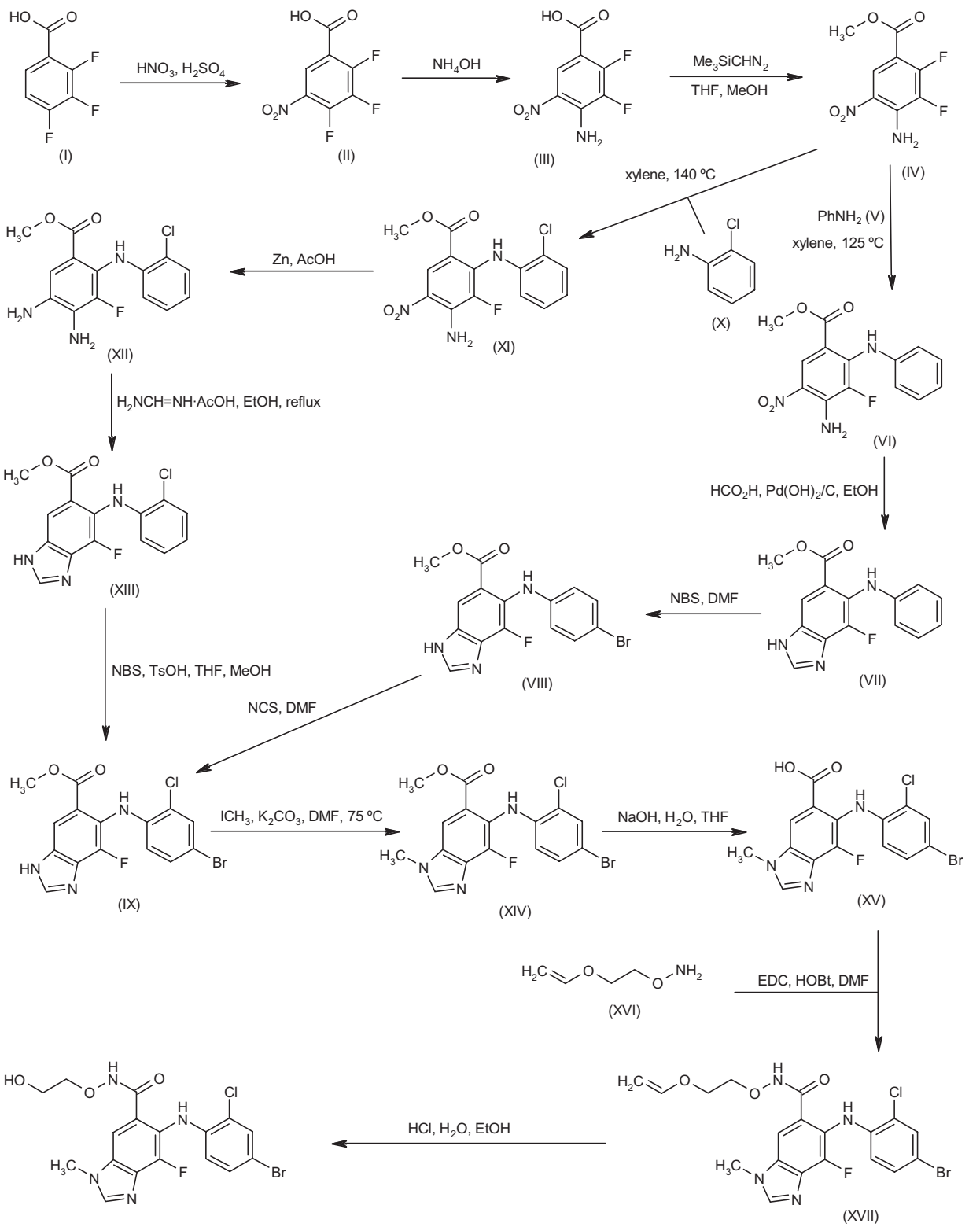

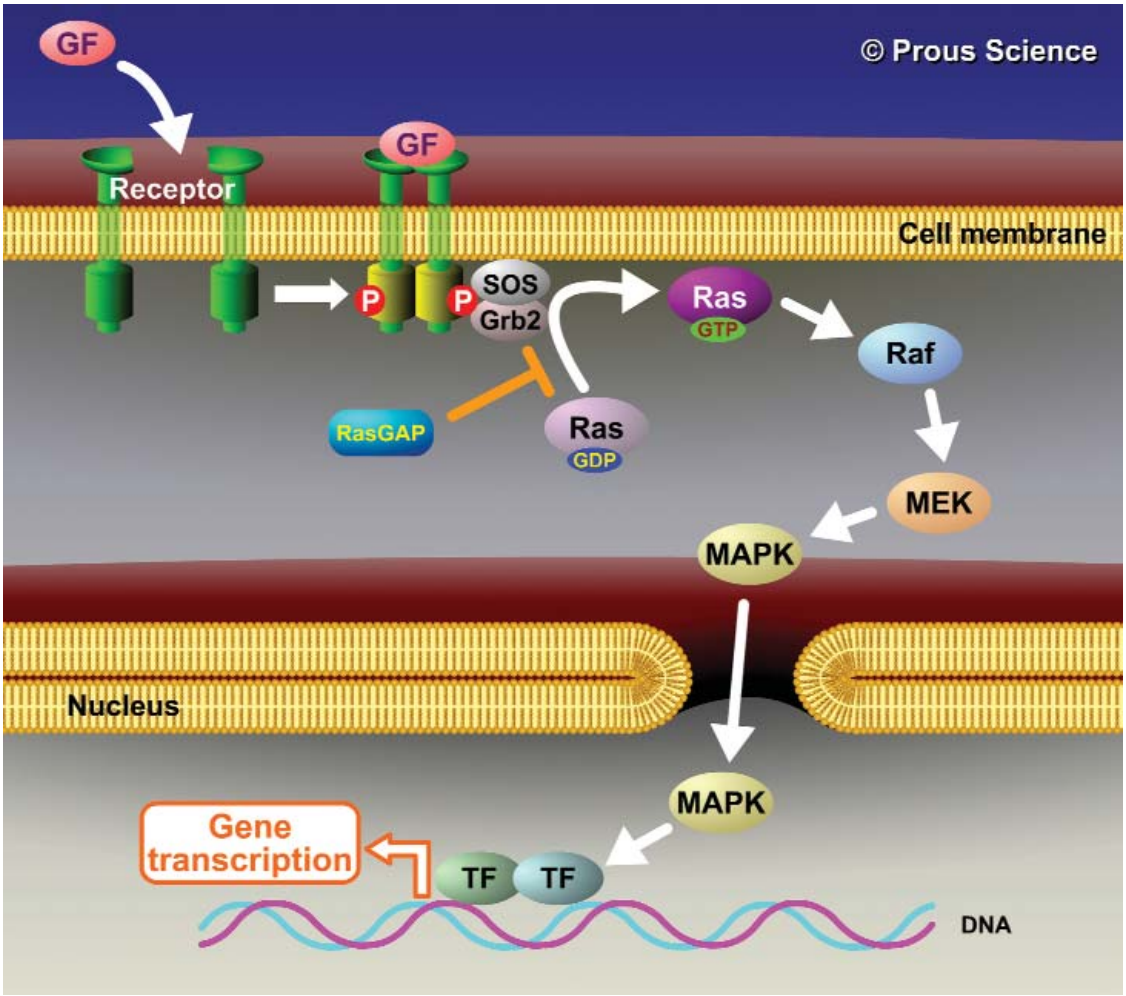

Fig. 1. Mitogen-activated protein kinase (MAPK) signaling pathway. Cell signaling is triggered when an inducer molecule such as a growth factor (GF) binds to its enzyme-linked receptor. This leads to receptor dimerization and phosphorylation of the cytoplasmic domain. The phosphorylated receptor activates and recruits the small adaptor protein Grb2, which induces the binding of the guanylnucleotide exchange factor SOS. The small G-protein Ras is then recruited to the plasma membrane by the Grb2-SOS complex. Ras becomes activated through the release of bound GDP, allowing a GTP molecule to bind in its place. The GTP-bound form of Ras can be negatively regulated by interacting directly with RasGAP. Activated Ras phosphorylates and activates Raf protein. Activated Raf phosphorylates and activates MEK, which in turn phosphorylates and activates MAPK. Activated MAPK migrates to the nucleus, where it phosphorylates gene transcription factors (TF).

Phosphorylated ERK1 and ERK2 dimerize and translocate to the nucleus, where they in turn phosphorylate a number of proteins that regulate cytoskeletal proteins, metabolism, chromatin remodeling and numerous transcription factors (2, 6, 7).

MEK offers two advantages as a potential target for therapeutic intervention in the treatment of cancer: 1) it is the only known activator of ERK1/2; and 2) it is downstream of both Raf and Ras. AZD-6244 (ARRY-142886) is an orally active inhibitor of MEK with high specificity for this enzyme. AZD-6244 has shown tumor-suppressive activity in a wide range of preclinical models of human cancer with aberrant expression of the ERK pathway, including melanoma, pancreatic, colon, lung and breast cancers, and is undergoing clinical development for the treatment of cancer (8-11).

Preclinical Pharmacology

AZD-6244 inhibits purified MEK1 with an IC_{50} of 12 nM, and is noncompetitive with respect to ATP. The agent is highly selective for MEK, and at 10 μM it did not inhibit any of over 40 purified tyrosine and serine/threonine kinases, including the cyclin-dependent kinase CDK2, c-Raf, IκB kinase β (IKKβ), c-Src, c-Jun *N*-terminal kinase (JNK), protein kinase C (PKC), EGFR, insulin-like growth factor-1 receptor (IGF-1R) and Lyn. In cell-based assays, it also potently and selectively inhibited the MEK pathway (IC_{50} = 10 nM), but not the phosphatidylinositol 3-kinase (PI3K), p38 or JNK pathways at up to 10 μM, and its selectivity for the MEK1/2/ERK1/2 pathway *versus* the MEK5/ERK5 pathway was also demonstrated in tumor cell lines (8-10).

AZD-6244 was shown to inhibit basal and stimulated ERK phosphorylation in cancer ell lines, with IC_{50} values as low as 8 nM (9, 10, 12). It was also found to be active against numerous cancer cell lines with Ras and B-Raf mutations, including the human colon carcinoma cell line HT-29, the melanoma cell lines Malme-3M, SK-MEL-28 and SK-MEL-2, and the pancreatic cancer cell line MIA PaCa-2 (IC_{50} = 50-270 nM). The cells were arrested at the G1/S phase of the cell cycle, and apoptosis was induced in the Malme-3M and SK-MEL-2 cell lines. The proliferation of Malme-3 cells (the normal counterpart of Malme-3M) was not inhibited, indicating that AZD-6244 specifically targets cells with activated MEK (9, 12).

Experiments using the human breast cancer MCF7 cell line (estrogen receptor-positive/HER2-negative, tamoxifen-sensitive) and the estrogen receptor/HER2-positive, tamoxifen-resistant MCF7/HER2 line indicated that AZD-6244 may be able to enhance the endocrine responsiveness of estrogen receptor-positive breast cancer, especially in cancers with activated MEK1/2 and increased ERK phosphorylation (13).

AZD-6244 was active in several murine human tumor xenograft models, including the HT-29 (tumor growth inhibition at 10 mg/kg p.o. b.i.d. and above), COLO 205 (tumor regression at < 25 mg/kg/day), HCT 116 (tumor growth inhibition at < 20 mg/kg/day) and SW620 (tumor growth inhibition at < 25 mg/kg/day) colorectal carcinoma models, the NSCLC A549 (tumor growth inhibition at 15 mg/kg/day) and Calu-6 (tumor growth inhibition at < 20 mg/kg/day) carcinoma models, the pancreatic BxPC-3 (tumor regression at 10-50 mg/kg p.o. b.i.d.), PANC-1 (tumor growth inhibition at 20-40 mg/kg/day) and MIA PaCa-2 (tumor regression at 40 mg/kg/day) carcinoma models, the breast MDA-MB-231 (tumor growth inhibition at < 20 mg/kg/day) and ZR-75-1 (tumor growth inhibition at 22 mg/kg/day) carcinoma models, and the LOX melanoma model (tumor regression at < 20 mg/kg/day) (9, 10, 14, 15).

Consistent with its proposed mechanism of action, tumor growth inhibition was correlated with a reduction in phosphorylated ERK in tumors (10, 14, 15).

Upon withdrawal of the drug in the BxPC-3 mouse model, tumor regrowth was seen, but when treatment was resumed, the tumors again regressed, indicating that they remained sensitive to the drug (9, 10, 15).

Oral administration of AZD-6244 in mouse models of primary human hepatocellular carcinoma resulted in dose-dependent inhibition of tumor growth, which was associated with inactivation of ERK1/2 and p90RSK, and upregulation of cleaved caspase-3, cleaved caspase-7, cleaved poly(ADP-ribose) polymerase (PARP) and phosphorylated MEK1/2 (16).

In a nude mouse model of BxPC-3 human pancreatic tumor xenografts, AZD-6244 caused tumor growth inhibition at 1 mg/kg p.o. b.i.d. and tumor regression at 3 and 10 mg/kg p.o. b.i.d. Inhibition of phosphorylated ERK in tumors was sustained at all time points after the two higher doses, but not at the low dose. Mean trough plasma levels of > 0.3 μg/ml were associated with activity (17).

In an analysis of four different murine human tumor xenograft models with varying sensitivity to AZD-6244, ERK1/2 phosphorylation was rapidly inhibited in all models after a single oral dose of 25 mg/kg. The two most sensitive models, COLO 205 and Calu-6, showed signs of apoptosis, whereas in the less responsive SW620 model, AZD-6244 appeared to inhibit proliferation and induce differentiation. PC-3 tumors were insensitive to AZD-6244 and showed no change in biomarkers of cell proliferation or apoptosis (10, 18).

The combination of AZD-6244 with gefitinib, an ATP-competitive inhibitor of EGFR, showed enhanced activity compared to either agent alone against human colorectal tumor LoVo xenografts (10, 19). Enhanced activity was also seen in combination with docetaxel in the SW620 xenograft model (10).

AZD-6244 exhibits other favorable characteristics, including minimal inhibition of cytochrome P-450 enzymes (> 10 μM), low hepatic clearance, no cytotoxic effects in normal cells and no changes in blood chemistry parameters. Moreover, it is negative in the Ames test and shows no activity at hERG channels (10).

Findings from cynomolgus monkeys, healthy volunteers and cancer patients treated with AZD-6244 indicated a strong correlation between drug plasma levels and inhibition of ERK phosphorylation in whole blood, suggesting the utility of pERK as a potential pharmacodynamic marker for MEK inhibition (10, 20).

Clinical Studies

In an open-label, multiple-dose phase I study, 23 patients with refractory solid tumors were administered oral doses of AZD-6244 of up to 300 mg b.i.d. The maximum tolerated dose (MTD) was found to be 200 mg b.i.d. The most common treatment-related adverse events were rash, diarrhea, nausea and fatigue, with dose-limiting toxicity (DLT) consisting of 1 case of hypoxia (200 mg b.i.d.), 1 case of diarrhea and 2 cases of rash (300 mg b.i.d.). After a single dose, t_{max} was reached in 1.3-2.6 h and the $t_{1/2}$ was 7-12 h. C_{max} and exposure were dose-dependent, and the mean C_{min} (12 h) at the 200 mg b.i.d. dose was 590 nM, well above the IC_{50} for inhibition of TPA-induced phosphorylation of ERK1/2. Stable disease was the best clinical response in this first part of the study, with Part B analyzing biomarkers (10, 21).

Based on findings from the phase I study demonstrating inhibition of MEK and downstream markers in tumors at well-tolerated doses, a phase II study of AZD-6244 *versus* temozolomide was initiated in stage III/IV melanoma patients (22, 23). An open, randomized phase II trial is also in progress comparing AZD-6244 to pemetrexed in patients with NSCLC who have failed 1 or 2 prior chemotherapy regimens (24), and another study is comparing AZD-6244 and capecitabine in patients with advanced metastatic pancreatic cancer who have failed first-line gemcitabine therapy (25).

Sources

Array BioPharma, Inc (US); licensed to AstraZeneca (GB).

References

1. Wallace, E.M., Lyssikatos, J.P., Hurley, B.T., Marlow, A.L. (Array BioPharma, Inc.). *N3 alkylated benzimidazole derivatives as MEK inhibitors*. EP 1482932, EP 1663210, JP 2005530709, US 2004116710, WO 03077914, WO 2005023251.

2. Pearson, G., Robinson, F., Beers Gibson, T., Xu, B.E., Karandikar, M., Berman, K, Cobb, M.H. *Mitogen-activated protein (MAP) kinase pathways: Regulation and physiological functions*. Endocr Rev 2001, 22(2): 153-83.

3. Herrera, R., Sebolt-Leopold, J.S. *Unraveling the complexities of the Raf/MAP kinase pathway for pharmacological intervention*. Trends Mol Med 2002, 8(4, Suppl.): S27-31.

4. Kohno, M., Pouyssegur, J. *Targeting the ERK signaling pathway in cancer therapy*. Ann Med 2006, 38(3): 200-11.

5. Staehler, M., Rohrmann, K., Haseke, N., Stief, C.G., Siebels, M. *Targeted agents for the treatment of advanced renal cell carcinoma*. Curr Drug Targets 2005, 6(7): 835-46.

6. Imajo, M., Tsuchiya, Y., Nishida, E. *Regulatory mechanisms and functions of MAP kinase signaling pathways*. IUBMB Life 2006, 58(5-6): 312-7.

7. Lewis, T.S., Hunt, J.B., Aveline, L.D. et al. *Identification of novel MAP kinase pathway signaling targets by functional proteomics and mass spectrometry*. Mol Cell 2000, 6(6): 1343-54.

8. Lyssikatos, J., Yeh, T., Wallace, E. et al. *ARRY-142886, a potent and selective MEK inhibitor: I) ATP-independent inhibition results in high enzymatic and cellular selectivity*. Proc Am Assoc Cancer Res (AACR) 2004, 45: Abst 3888.

9. Wallace, E., Yeh, T., Lyssikatos, J. et al. *Preclinical development of ARRY-142886, a potent and selective MEK inhibitor*. Proc Am Assoc Cancer Res (AACR) 2004, 45: Abst 3891.

10. Lyssikatos, J. *ARRY-142886 (AZD6244): Preclinical and early clinical development of a potent, selective MEK inhibitor*. Proc Am Assoc Cancer Res (AACR) 2006, 47: Presentation April 3.

11. Koch, K. *ARRY-142886, a novel and highly selective MEK inhibitor in clinical trials*. Proc Am Assoc Cancer Res (AACR) 2004, 45: 1309.

12. Yeh, T., Wallace, E., Lyssikatos, J., Winkler, J. *ARRY-142886, a potent and selective MEK inhibitor: II) Potency against cellular MEK leads to inhibition of cellular proliferation and induction of apoptosis in cell lines with mutant Ras or B-Raf*. Proc Am Assoc Cancer Res (AACR) 2004, 45: Abst 3889.

13. Zhou, Y., Benz, C. *AZD6244 (ARRY-142886), a potent and selective MEK1/2 inhibitor, enhances tamoxifen sensitivity in resistant ER-positive/HER2-positive breast cancer cells with constitutively elevated MEK1/2*. Proc Am Assoc Cancer Res (AACR) 2006, 47: Abst 1344.

14. Lee, P., Wallace, E., Yeh, T. et al. *Demonstration of broad in vivo anti-tumor activity of ARRY142886 (AZD6244), a potent and selective MEK inhibitor*. Eur J Cancer - Suppl 2004, 2(8): Abst 368.

15. Lee, P., Wallace, E., Yeh, T. et al. *ARRY-142886, a potent and selective MEK inhibitor: III) Efficacy in murine xenograft models correlates with decreased ERK phosphorylation*. Proc Am Assoc Cancer Res (AACR) 2004, 45: Abst 3890.

16. Tran, E., Chee Soo, K., Chow, P., Huynh, H. *Targeted inhibition of the MEK-ERK signaling cascade by the selective MEK1/2 inhibitor AZD6244 (ARRAY-142886) for the treatment of hepatocellular carcinoma*. Proc Am Assoc Cancer Res (AACR) 2006, 47: Abst 5470.

17. Winkler, J., Lee, P., Wallace, E. et al. *Anti-tumor activity, pharmacokinetic and pharmacodynamic effects of the MEK inhibitor ARRY-142886 (AZD6244) in a BxPC3 pancreatic tumor xenograft model*. Eur J Cancer - Suppl 2004, 2(8): Abst 342.

18. Logie, A., Cockerill, M., Moore, S. et al. *In vivo evaluation of pharmacodynamic biomarkers and mode of action of AZD6244 (ARRY142886)*. 17th AACR-NCI-EORTC Int Conf Mol Targets Cancer Ther 2005, Abst A240.

19. Cockerill, M., Logie, A., Speake, G. et al. *Combination studies in vitro and in vivo with gefitinib (Iressa) and the MEK1/2 inhibitor AZD6244 (ARRY142886)*. 17th AACR-NCI-EORTC Int Conf Mol Targets Cancer Ther 2005, Abst A110.

20. Doyle, M., Yeh, T., Suzy, B. et al. *Validation and use of a biomarker for clinical development of the MEK1/2 inhibitor ARRY-142886 (AZD6244)*. 41st Annu Meet Am Soc Clin Oncol (ASCO) (May 13-17, Orlando) 2005, Abst 3075.

21. Chow, L., Eckhardt, S., Reid, J. et al. *A first in human dose-ranging study to assess the pharmacokinetics, pharmacodynamics, and toxicities of the MEK inhibitor, ARRY-142886 (AZD6244), in patients with advanced solid malignancies*. 17th AACR-NCI-EORTC Int Conf Mol Targets Cancer Ther 2005, Abst C162.

22. *Array BioPharma receives phase 2 milestone payment from AstraZeneca*. Array BioPharma Press Release September 14, 2006.

23. *Randomised study to compare the efficacy of AZD6244 vs TMZ (NCT00338130)*. ClinicalTrials.gov Web site 2006.

24. *AZD6244 versus pemetrexed (Alimta®) in patients with non-small cell lung cancer, who have failed one or two prior chemotherapy regimen (NCT00372788)*. ClinicalTrials.gov Web site 2006.

25. *AZD6244 vs. capecitabine (Xeloda®) in patients with advanced or metastatic pancreatic cancer, who have failed first line gemcitabine therapy (NCT00372944)*. ClinicalTrials.gov Web site 2006.

Additional Reference

Friday, B., Yu, C., Smith, P., Adjei, A. *A potential role for modulation of a negative feedback loop between Erk and Raf in mediating sensitivity to the MEK inhibitor AZD6244 (ARRY-142886) in human lung cancer cell lines*. Proc Am Assoc Cancer Res (AACR) 2006, 47: Abst 4868.

Drugs of the Future 2008, 33(12): 1018-1024

CCC: 0377-8282/2008
DOI: 10.1358/dof.2008.033.12.1291333

TMC-207

Mycobacterial ATP Synthase Inhibitor
Treatment of Tuberculosis

R-207910

(αS,βR)-6-Bromo-α-[2-(dimethylamino)ethyl]-2-methoxy-α-(1-naphthalenyl)-β-phenyl-3-quinolineethanol

1(*R*)-(6-Bromo-2-methoxyquinolin-3-yl)-4-(dimethylamino)-2(*S*)-(1-naphthyl)-1-phenylbutan-2-ol

InChI=1/C32H31BrN2O2/c1-35(2)19-18-32(36,28-15-9-13-22-10-7-8-14-26(22)28)30(23-11-5-4-6-12-23)27-21-24-20-25(33)16-17-29(24)34-31(27)37-3/h4-17,20-21,30,36H,18-19H2,1-3H3/t30-,32-/m1/s1

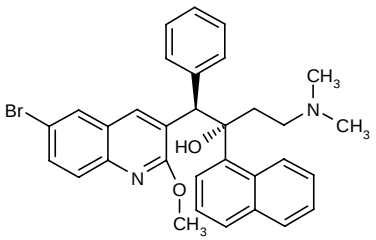

$C_{32}H_{31}BrN_2O_2$
Mol wt: 555.505

CAS: 843663-66-1

CAS: 654653-93-7 (racemate)

CAS: 654655-80-8 (no stereochemistry)

EN: 386239

Abstract

The tuberculosis (TB) epidemic constitutes a major global health threat. The steady emergence of *Mycobacterium tuberculosis* strains resistant to current anti-TB drugs, the therapeutic obstacles posited by coinfection with HIV and the cumbersome implementation of current treatment protocols all demand the development of new, fast-acting, effective compounds that shorten and simplify the treatment of TB. TMC-207 (R-207910) is a novel diarylquinoline with a unique biological target: the F0 subunit of mycobacterial ATP synthase. TMC-207 exhibits high in vitro activity against a wide range of mycobacterial strains, both susceptible or resistant to all of the first-line and many of the second-line anti-TB drugs available. It has also shown remarkable in vivo efficacy against *M. tuberculosis* and other mycobacterial species in several animal models. Preliminary pharmacokinetic, safety and efficacy analyses in humans have reasserted the potential of this compound for treating TB. TMC-207 is currently undergoing phase II clinical evaluation.

Synthesis*

Condensation of 4-bromoaniline (I) with 3-phenylpropionyl chloride (II) by means of triethylamine in dichloromethane gives the propionamide (III), which is cyclized with dimethylformamide by means of $POCl_3$ in hot DMF to yield 3-benzyl-6-bromo-2-chloroquinoline (IV). Reaction of compound (IV) with NaOMe in refluxing methanol affords the 2-methoxyquinoline derivative (V), which is condensed with 3-(dimethylamino)-1-(1-naphthyl)propanone (VI) by means of BuLi in THF to provide a mixture of two diastereomeric racemates (*R**,*R**/*R**,*S**) (VII) that are separated by column chromatography. Finally, the desired (*R**,*S**)-racemic mixture is submitted to chiral chromatography (1). Scheme 1.

In an improved process, 3-benzyl-6-bromo-2-methoxyquinoline (V) is condensed with 3-(dimethylamino)-1-(1-naphthyl)propanone (VI) by means of LDA in THF and then treated with AcOH to afford the tertiary alcohol (VII). Finally, alcohol (VII) is submitted to optical resolution by crystallization with chiral 4-hydroxydinaphtho[2,1-*d*:1',2'-*f*][1,3,2]dioxaphosphepin 4-oxide (2). Scheme 1.

Background

Tuberculosis (TB), one of the leading causes of death worldwide by an identifiable pathogenic microorganism (3), is an infectious disease caused by *Mycobacterium tuberculosis* bacilli. The common route of transmission is the inhalation of airborne particles carrying viable microorganisms that are phagocytosed by alveolar macrophages. In immunocompetent adults, primary infection is generally asymptomatic and results in small

A. Arjona. Howard Hughes Medical Institute & Department of Internal Medicine, Yale School of Medicine, P.O. Box 208022, New Haven, CT 06520, USA. *Synthesis prepared by R. Castañer. Prous Science, Provenza 388, 08025 Barcelona, Spain.

Scheme 1: Synthesis of TMC-207

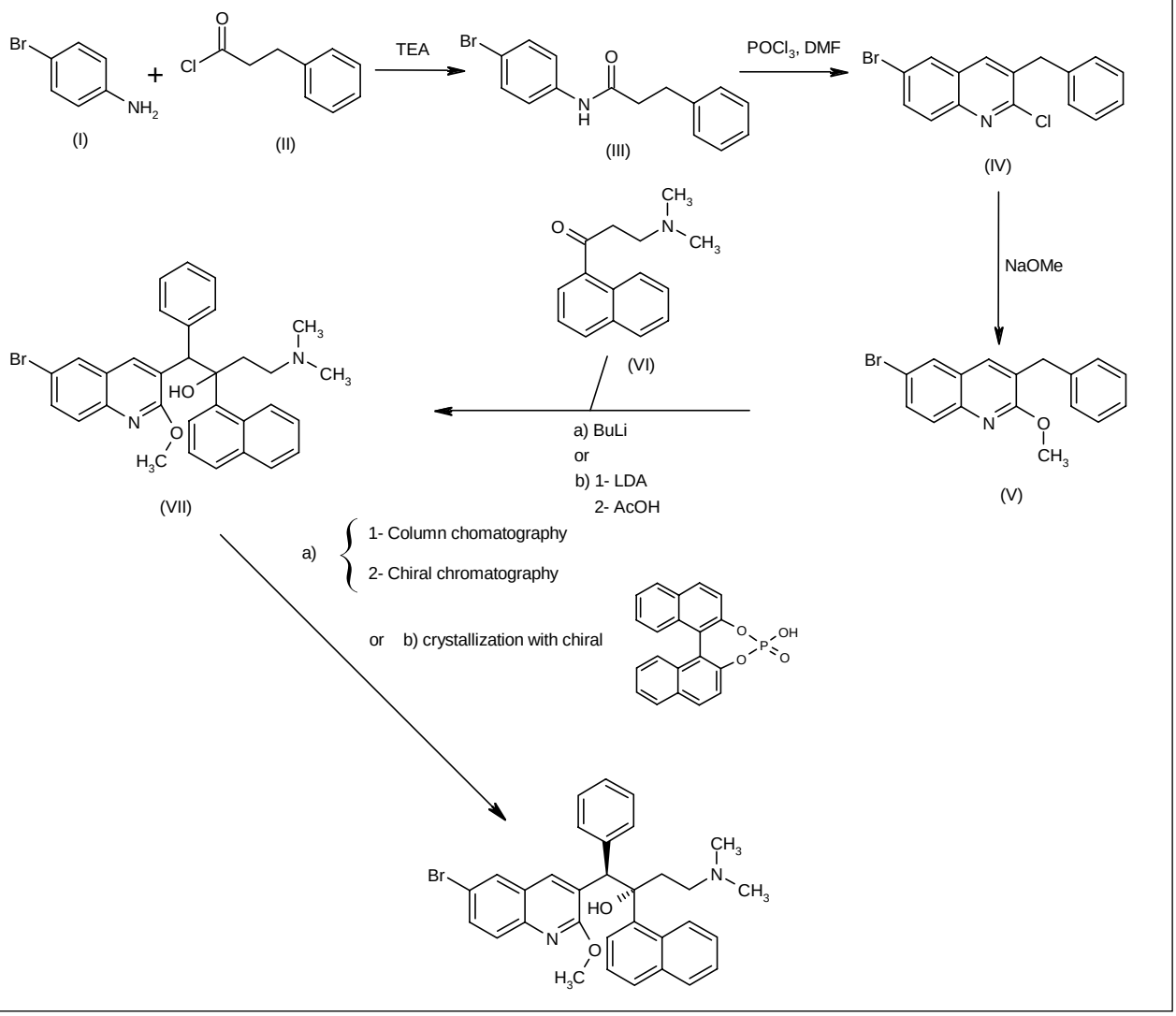

lesions containing low numbers of dormant bacilli. This latent infection may be reactivated years to decades later, producing either local disease (usually affecting the lungs) or disseminated infection (4). Recent estimates indicate that there are 9 million new TB cases per year. Also, one-third of the world's population carries TB bacilli and approximately 10% of these will develop active disease, leading to 1.6 million deaths annually (5). The risk of developing TB is greatly increased by immunosuppression (including HIV infection), repeated exposure to bacilli-spreading individuals and chronic malnutrition. Indeed, 95% of all TB cases and 98% of all deaths caused by TB occur in developing countries (4).

The HIV epidemic, which greatly expanded the TB-susceptible population, together with the common appearance of drug-resistant strains due predominantly to the inadequate therapeutic management of latent and persistent infections, have placed TB as one of the greatest current global public health emergencies (6). The standard multidrug regimen for the treatment of TB has been modified minimally in the last few decades, it takes many months to complete, and it is in many circumstances difficult to implement (7). Not surprisingly, the Global Alliance for TB Drug Development has indicated that new compounds shortening and simplifying TB treatment would substantially improve TB control programs (8). The emergence of multiple and extensively drug-resistant strains, as well as *M. tuberculosis*/HIV coinfection (which precludes the use of anti-TB agents that interact with antiretroviral agents), further stress the need for new anti-TB drugs (9). There is a consensus among health professionals that the available drug repertoire is not sufficient to control the TB epidemic, and that the treatment of both active disease and latent TB infection

needs to be reevaluated. The devastating association between TB and HIV requires new drug regimens that do not interfere with antiretroviral agents, and markedly improved therapy is needed for the treatment of multiple and extensively drug-resistant TB. In this sense, fast-acting compounds with novel mechanisms of action would be extremely useful not only to fight the emergence of resistant strains but also to reduce toxicity (10). Moreover, shortening the length of the treatment will facilitate the monitoring of patient compliance.

Here we review the current data on the pharmacology, metabolism, efficacy and safety of TMC-207, a promising investigational diarylquinoline with a novel mechanism of action and potent preclinical activity against both drug-susceptible and -resistant *M. tuberculosis* isolates.

Preclinical Pharmacology

Initial in vitro studies showed the potent activity of TMC-207 against *M. tuberculosis*. The minimal inhibitory concentration (MIC) range for the international reference *M. tuberculosis* strain H37Rv and six fully antibiotic-susceptible isolates was 0.030-0.120 μg/ml (11). The growth of an additional 10 fully antibiotic-susceptible *M. tuberculosis* strains was inhibited at similar concentrations. TMC-207 also exhibited in vitro efficacy against *M. tuberculosis* clinical isolates resistant to the first-line anti-TB drugs isoniazid, rifampicin, streptomycin, ethambutol, pyrazinamide and moxifloxacin. Moreover, TMC-207 was effective against multidrug-resistant (MDR) TB strains (0.010-0.1 μg/ml). Low MICs were also found for other mycobacterial species, including *Mycobacterium bovis*, *Mycobacterium kansasii* and *Mycobacterium ulcerans*, as well as species naturally resistant to many other anti-TB agents and involved in opportunistic infections, such as *Mycobacterium abscessus*, *Mycobacterium fortuitum*, *Mycobacterium marinum* and *Mycobacterium avium* (12). A recent mouse study, however, has shown that the in vivo efficacy of TMC-207 against *M. avium* does not match the efficacy shown by clarithromycin or amikacin treatment (13).

The activity of TMC-207 appears to be specific for mycobacteria, as it had a much higher MIC for *Corynebacterium* and *Helicobacter pylori* (4.0 μg/ml), as well as for other organisms such as Gram-positive *Nocardia*, *Streptococcus pneumoniae*, *Staphylococcus aureus* and *Enterococcus faecalis*, or Gram-negative *Escherichia coli* and *Haemophilus influenzae*. Exposure of *M. tuberculosis* in log-phase growth to concentrations of TMC-207 at 10 times the MIC resulted in a reduction in bacterial load of 3 log units after 12 days, supporting the in vitro bactericidal activity of TMC-207. Additional in vitro analyses have expanded the antimycobacterial activity range of TMC-207 to 41 drug-susceptible and 44 multidrug-resistant *M. tuberculosis* clinical isolates (MIC_{50} = 0.032 μg/ml) (12). In another study, of 20 additional mycobacterial species, only 3 were found to be naturally resistant to TMC-207 and were shown to exhibit a polymorphism in the *atpE* gene (14). Collectively, these results provide strong evidence for the unique-spectrum, potent and selective antimycobacterial activity of TMC-207.

Mutant selection experiments have revealed that, in the case of *M. tuberculosis*, the proportion of resistant mutants that emerged under TMC-207 treatment was comparable to that resulting from rifampicin treatment. Genetic analyses demonstrated that the only gene commonly affected in all mutants encodes the atpE protein, a component of the F0 subunit of ATP synthase. This finding led investigators to postulate that TMC-207 inhibits the proton pump of *M. tuberculosis* ATP synthase, which was demonstrated by complementation studies (12). Later experiments assessing the genetic diversity of the *atpE* gene in 13 mycobacterial species revealed that the region involved in resistance to TMC-207 is highly conserved among mycobacteria. Of note, in *Mycobacterium xenopi* atpE, the highly conserved residue Ala63 is replaced by Met, a substitution that likely underlies the natural resistance of *M. xenopi* to TMC-207 (15). De Jonge et al. have recently created a homology model of the putative TMC-207 binding site, which would be located on the contact area of the a-subunit (gene *atpB*) and c-subunit (gene *atpE*) of *M. tuberculosis* ATPase. The model suggests that the activity of TMC-207 against *M. tuberculosis* relies on the interference of the compound with the escapement geometry of the proton transfer chain. Upon binding, the compound would mimic the conserved Arg186 residue of the a-subunit and would therefore interact with the conserved acidic residue Glu61 of the c-subunit. The concordance between the computed interaction energies and the observed pattern of stereospecificity in the model of the binding region further supported the proposed mechanism of action (16).

The in vivo efficacy of TMC-207 was first evaluated in a nonestablished murine TB infection model (12). A single dose of TMC-207 (50 mg/kg p.o.) resulted in a bacteriostatic effect (decrease of 0.5 log units in lung bacterial load) that lasted for 8 days and was similar to the effect of rifapentine (10 mg/kg), a second-line anti-TB drug. A single 100 mg/kg dose of TMC-207 had a bactericidal effect (decrease of up to 2.5 log units in lung bacterial load) that lasted for 8 days. The extended effect of a single TMC-207 dose provided support for a dosing regimen less frequent than 5 times per week. In mouse studies using oral administration of TMC-207 5 days per week for 4 weeks, the minimal dose that prevented mortality in a nonestablished infection model was 1.5 mg/kg, and the minimal effective dose preventing gross lung lesions was 6.5 mg/kg. In mice receiving doses of 12.5 mg/kg, the bacterial load per organ was reduced by 3 log units. At 25 mg/kg, the activity of TMC-207 improved significantly. Remarkably, at 12.5 and 25 mg/kg, TMC-207 was significantly more active than isoniazid (25 mg/kg), a drug known for its strong, early bactericidal activity. Moreover, at 12.5 mg/kg, a once-weekly dose of TMC-207 was as effective as a dose of 6.5 mg/kg given 5 times per week, which is likely a consequence of the long half-life of TMC-207 (12, 17).

When evaluated in an established murine TB infection model (treatment beginning 12-14 days after inoculation, when bacterial load was 5.94 log units), TMC-207 (25 mg/kg) alone was at least as active as the triple combination therapy rifampicin/isoniazid/pyrazinamide and more active than rifampicin alone. When added to the first-line triple TB therapy, TMC-207 (25 mg/kg) yielded a significantly larger decrease in lung bacterial load relative to the standard triple treatment regimen (2 log units after 1 month and an additional 1 log unit after 2 months of therapy). When substituting each first-line drug of the triple combination therapy with TMC-207 (25 mg/kg), the activity of each combination containing the investigational diarylquinoline was significantly improved, achieving lung culture negativity after 2 months of treatment. Of note, the bactericidal activity obtained by the standard triple-drug cocktail after 2 months of therapy was matched by TMC-207 combinations after just 1 month of therapy, indicating that the inclusion of TMC-207 in anti-TB regimens may effectively reduce the duration of treatment (12, 17).

An animal study conducted subsequently aimed to identify the optimal TMC-207-containing regimen to administer to patients who cannot be administered rifampicin and isoniazid because of MDR, the concomitant use of antiretroviral drugs or toxicity. Mice were infected i.v. with 5×10^6 colony-forming units (cfu) of the *M. tuberculosis* H37Rv strain and treated 5 times per week with TMC-207 alone or combined with second-line drugs such as amikacin. After 1 month of therapy, all regimens containing TMC-207 were significantly more active than those without TMC-207. When given for 2 months, TMC-207 alone was more active than the standard first-line regimen. When the investigational diarylquinoline was combined with second-line drugs, the combinations were more active than the currently recommended regimen for MDR TB, and culture negativity of lung and spleen was achieved after 2 months of treatment in almost every case (18). These findings were confirmed in a later study assessing the sterilizing activity of TMC-207 combined with second-line drugs in mice infected with *M. tuberculosis* H37Rv. Adding TMC-207 to amikacin/ethionamide/moxifloxacin/pyrazinamide improved the efficacy of the second-line therapeutic regimen, further supporting the theory that the addition of TMC-207 to current drug combinations containing pyrazinamide plus rifampicin or moxifloxacin may shorten the duration of MDR TB treatment (19).

Another study employing the proportional bactericidal technique in mouse footpads found that the bactericidal activity of TMC-207 against *Mycobacterium leprae* was equal to that of rifapentine, rifampicin or moxifloxacin, and significantly greater than that of minocycline, PA-824 and linezolid. These data suggest that TMC-207 could also be useful for the treatment of leprosy (20). In addition, when compared in vitro to 7 antimicrobials against 29 clinical isolates of *M. ulcerans*, TMC-207 demonstrated the lowest MIC_{50} and MIC_{90} values. Although TMC-207 also demonstrated some degree of in vivo bactericidal activity against *M. ulcerans* when administered as monotherapy to mice, it failed to outperform the efficacy of currently available drug regimens (21).

As described above, TMC-207 exhibited high bactericidal activity against *M. tuberculosis* when combined with first- or second-line anti-TB drugs. Ibrahim et al. extended the evaluation of TMC-207 in the curative model of murine tuberculosis by assessing the activities of one-, two- and three-drug combinations containing TMC-207 and isoniazid, rifampicin, pyrazinamide or moxifloxacin in the setting of a high initial bacillary load (7.2 log cfu). The research team found that 2 months of treatment with TMC-207 combined with pyrazinamide, pyrazinamide/isoniazid, pyrazinamide/rifampicin or pyrazinamide/moxifloxacin resulted in culture-negative lung homogenates in 70-100% of the mice, while mice treated with the standard regimen (isoniazid/rifampicin/pyrazinamide) or rifampicin/moxifloxacin/pyrazinamide remained culture-positive. Combinations including TMC-207 without pyrazinamide were less active than TMC-207/pyrazinamide-containing regimens administered either alone or combined with isoniazid, rifampicin or moxifloxacin, revealing a synergistic interaction between TMC-207 and pyrazinamide (22). These results provided further evidence supporting the notion that three-drug combinations containing TMC-207 and pyrazinamide (plus isoniazid, rifampicin or moxifloxacin) have the potential to significantly shorten the treatment duration in TB patients.

TMC-207 has also proven effective in a guinea pig model in which lung lesions produced by *M. tuberculosis* resemble those caused by natural infections in humans. After aerosol inoculation, guinea pigs develop necrotic primary lesions that are morphologically different from the secondary lesions resulting from hematogenous dissemination. Conventional 6-week anti-TB therapy reduced the bacterial load by 1.7 log in the lungs, and although it completely reversed lung inflammation associated with secondary lesions, the primary granulomas remained largely unaffected. On the other hand, when animals were treated with TMC-207 for 6 weeks, the investigators found an almost complete eradication of the bacteria in both the primary and secondary lesions (23).

The impact of reducing the dose of TMC-207 on its efficacy when combined with a background regimen of isoniazid, rifampin and pyrazinamide has been assessed in mice. Addition of TMC-207 (12.5-25 mg/kg) to the background regimen resulted in faster bacterial clearance and culture negativity. The minimal bactericidal dose of TMC-207 in combination with the mentioned drugs was identical to that obtained when it was administered as monotherapy (24). Importantly, these data showed that TMC-207 retains significant activity when its exposure is reduced and when it is added to a strong background regimen of isoniazid, rifampicin and pyrazinamide.

The long half-life for TMC-207 seen in pharmacokinetic analyses prompted investigators to evaluate the activity of once-weekly TMC-207 monotherapy and its combinations with other anti-TB agents (isoniazid, rifapentine, moxifloxacin and pyrazinamide) in an estab-

lished murine TB infection model. Veziris et al. found that 8 weeks of rifapentine monotherapy reduced the lung bacillary load by 3-4 log units, while 8 weeks of TMC-207 monotherapy reduced the lung bacillary load by 5-6 log units. The addition of rifapentine and isoniazid/moxifloxacin did not improve the bactericidal activity of TMC-207 monotherapy. In contrast, the triple combination TMC-207/rifapentine/pyrazinamide given once a week during 2 months (8 administrations) was significantly more active than TMC-207 alone or in other combinations. This triple TMC-207-containing combination led to lung culture negativity in 9 of 10 mice, while all lungs remained culture-positive in the groups treated with other drug combinations. Moreover, TMC-207/rifapentine/pyrazinamide given once a week was more active than the current standard regimen (rifampicin/isoniazid/pyrazinamide) given 5 times a week. The striking efficacy of the triple combination TMC-207/rifapentine/pyrazinamide pointed towards the feasibility of developing a fully intermittent once-a-week regimen (25).

Of special consideration are the recent findings demonstrating that TMC-207 kills dormant *M. tuberculosis* bacilli as effectively as aerobically grown bacilli with the same target specificity. In vitro experiments have shown that the residual ATP synthase enzymatic activity in dormant mycobacteria is blocked by nanomolar concentrations of TMC-207, further reducing ATP levels and ultimately causing a pronounced bactericidal effect. The authors interpreted that this residual ATP synthase activity is indispensable for the survival of dormant mycobacteria. Thus, the unique mechanism of action of TMC-207 not only distinguishes this investigational diarylquinoline from currently available anti-TB drugs, but also makes TMC-207 a promising treatment option to fight latent TB infections (26). Along this line, TMC-207 late bactericidal activity was recently evaluated in mice by assessing its ability to kill *M. tuberculosis* H37Rv bacilli persisting after initial intensive 1-month therapy with the standard regimen (rifampicin/isoniazid/pyrazinamide, treatment beginning 14 days after infection). This initial treatment phase was followed by 2 months of monotherapy with isoniazid, rifampicin, moxifloxacin or TMC-207. The study showed that 2 months of TMC-207 monotherapy was able to achieve 100% culture negativity, compared to 50% for rifampicin, 38% for moxifloxacin and 12% for isoniazid. These data demonstrated that during the continuation phase of treatment, TMC-207 has bactericidal activity superior to that of existing anti-TB drugs (27).

Finally, the activity of TMC-207 has been studied jointly with another investigational anti-TB drug (SQ-109) that inhibits mycobacterial cell wall synthesis. Similarly to TMC-207, SQ-109 has potent activity against susceptible and MDR TB bacilli in vitro and is active in *M. tuberculosis*-infected mice. In vitro experiments indicated that the combination SQ-109/TMC-207 is synergistic, while the combination TMC-207/rifampicin is additive (28). In time-to-kill studies, the combination SQ-109/TMC-207 was superior to TMC-207/rifampicin and SQ-109/rifampicin. The SQ-109/TMC-207 combination also showed superior intracellular killing activity compared to TMC-207/rifampicin and SQ-109/rifampicin. The MIC of SQ-109 in the presence of TMC-207 was 50% less than that of SQ-109 alone, and the MIC of TMC-207 in the presence of SQ-109 was 75% less than that of TMC-207 alone. Hence, SQ-109 and TMC-207 in combination synergistically enhance their individual activities against *M. tuberculosis*. It is worth remarking that in three-drug combinations that included rifampicin at 0.1-0.5 x MIC, the synergy displayed by SQ-109/TMC-207 was unaltered.

Pharmacokinetics and Metabolism

The first pharmacokinetic study of TMC-207 in mice showed that it is rapidly absorbed after either single or multiple oral doses. For example, after a single dose of 6.25 mg/kg, a C_{max} of 0.40-0.54 μg/ml was reached within 1 h. After a dose of 25 mg/kg, a C_{max} of 1.1-1.3 μg/ml was reached within 2-4 h. AUCs were 5.0-5.9 and 18.5-19.4 μg.h/ml, respectively, following doses of 6.25 and 25 mg/kg. TMC-207 was well distributed to tissues, including lung and spleen. Half-lives ranged from 43.7 to 64 h in plasma and from 28.1 to 92 h in tissues. No accumulation of TMC-207 was observed after five daily oral doses, indicating that slow redistribution from tissues contributed to its relatively long half-life in plasma (12). It was concluded that the long half-life and resulting prolonged exposure of TMC-207 were important factors determining the duration of its activity in vivo, warranting the assessment of less frequent dosing regimens.

The combination of data from in vivo efficacy and separate pharmacokinetic studies in mice has shed light on the dose–response and exposure–response relationships between TMC-207 and TB infection. A single-dose pharmacokinetic study comparing C_{max} values and AUCs after doses of 6.25, 25 and 100 mg/kg confirmed that AUC showed a better dose correlation than C_{max} values. This phenomenon would be indicative of limitations in the rate of absorption at higher doses. Dose linearity was improved in tissues in terms of both C_{max} and AUC. The results from these comparative analyses led to the conclusion that maintaining average plasma levels of 0.3 μg/ml throughout a dosing interval of 24 h (which is obtained with a dose of 100 mg/kg/week) is necessary to achieve the optimal effect of monotherapy in mice infected with *M. tuberculosis* strain H37Rv (12).

As part of the first TMC-207 clinical study, investigators explored the pharmacokinetics in healthy male subjects receiving escalating oral doses (10-700 mg). The results from this single-ascending-dose study showed that the drug was well absorbed after a single oral dose, with peak concentrations reached at 5 h (median value) after the dose. The pharmacokinetic profile of TMC-207 was linear even at the highest dose tested, with both C_{max} and AUC increasing proportionally with the dose. There was no dose-dependent change in the terminal half-life. Data from a parallel multiple-ascending-dose study (once-daily doses of TMC-207 at 50, 150 and 400 mg) indicated a 2-fold increase in the AUC_{0-24} between day 1

and day 14, with no substantial variation among subjects. These findings suggest an effective half-life of 24 h, which is significantly higher than the half-life of available anti-TB drugs. The mean AUC_{0-24} values were 7.91, 24 and 52 μg.h/ml, respectively, at steady state (corresponding to average concentrations of 0.33, 1.0 and 2.2 μg/ml, respectively, across the dosing interval) with 50, 150 and 400 mg/day doses. Of note, these average concentrations were greater than those associated with optimal activity in established infection models in mice (12).

Safety

Preclinical safety studies that included 28-day toxicology assays in rats and dogs, genetic toxicology and safety pharmacology indicated that the evaluation of TMC-207 in humans was warranted. In the first single-dose clinical study in healthy patients, adverse events were mild to moderate and were experienced by 56% of the subjects receiving TMC-207 and by 39% of those receiving placebo. The majority of adverse events reported were considered unrelated to the study interventions. In a second safety assessment, good tolerability was maintained and only 1 subject withdrew from the study due to an unrelated urinary tract infection. The study team also reported that there were no significant changes in vital signs, electrocardiogram or laboratory tests in any of the cohorts (12).

Clinical Studies

In an open-label phase II trial assessing the early bactericidal activity of TMC-207 (29), 75 treatment-naïve patients with smear-positive pulmonary TB were randomized to once-daily oral TMC-207 (25, 100 or 400 mg), 600 mg rifampicin or 300 mg isoniazid for 7 days. The mean decreases in log cfu counts in sputum from baseline to day 7 were 0.04 ± 0.46 for 25 mg TMC-207, 0.26 ± 0.64 for 100 mg TMC-207, 0.77 ± 0.58 for 400 mg TMC-207, 1.88 ± 0.74 for isoniazid and 1.70 ± 0.71 for rifampicin. Significant bactericidal activity for the highest dose of TMC-207 was observed from day 4 onward and was similar in magnitude to that of isoniazid and rifampicin over the same period. The pharmacokinetic profile of TMC-207, as assessed up to 24 h on day 7 of administration, was linear across the dose range. In conclusion, TMC-207 demonstrated bactericidal activity with a delayed onset and was well tolerated, with no serious adverse events reported.

Tibotec, a Johnson & Johnson subsidiary, is currently conducting a second placebo-controlled, double-blind, randomized phase II trial to evaluate the antimycobacterial activity, safety and tolerability of TMC-207 in subjects with newly diagnosed sputum smear-positive pulmonary infection with MDR TB (30). An interim analysis on the first stage of this trial was recently released, and comprised patients who were randomized to receive a five-drug MDR regimen plus either placebo (n = 24) or TMC-207 (n = 23) for 8 weeks (31). There were no differences in biometrics, adherence or resistance to second-line agents. This initial assessment showed that TMC-207 administered for 8 weeks with a standardized five-drug MDR regimen was generally well tolerated and significantly increased the proportion of subjects who became culture-negative (47.5%) compared to placebo (8.7%). These data serve as an early clinical validation of mycobacterial ATP synthase as a promising new target for TB treatment and confirm the results obtained with TMC-207 in animal models.

Source

Tibotec Pharmaceuticals (a subsidiary of Johnson & Johnson).

References

1. Van Gestel, J.F.E., Venet, M.G., Vernier, D.F.J., Decrane, L.F.B., Poignet, H.J.J. (Janssen Pharmaceutica NV). *Quinoline derivatives and their use as mycobacterial inhibitors.* CA 2493225, EP 1527050, JP 2006504658, WO 2004011436.

2. Porstmann, F.R., Horns, S., Bader, T. (Janssen Pharmaceutica NV). *Process for preparing (alphaS,betaR)-6-bromo-alpha-[2-(dimethylamino)ethyl]-2-methoxy-alpha-1-naphthalenyl-beta-phenyl-3-quinolineethanol.* CA 2606675, EP 1888604, US 2008200683, WO 2006125769.

3. Global Alliance for TB Drug Development. www.tballiance.org.

4. Wallis, R.S., Johnson, J.L. *Adult tuberculosis in the 21st century: Pathogenesis, clinical features, and management*. Curr Opin Pulm Med 2001, 7(3): 124-32.

5. World Health Organization Fact Sheet 104, Tuberculosis. www.who.int/mediacentre/factsheets/fs104/en.

6. Maartens, G., Wilkinson R.J. *Tuberculosis*. Lancet 2007, 370(9064): 2030-43.

7. Sacchettini, J.C., Rubin E.J., Freundlich, J.S. *Drugs versus bugs: In pursuit of the persistent predator Mycobacterium tuberculosis*. Nat Rev Microbiol 2008, 6(1): 41-52.

8. Claxton, A.J., Cramer, J., Pierce, C. *A systematic review of the associations between dose regimens and medication compliance.* Clin Ther 2001, 23(8): 1296-310.

9. Rivers, E.C., Mancera, R.L. *New anti-tuberculosis drugs with novel mechanisms of action*. Curr Med Chem 2008, 15(19): 1956-67.

10. Spigelman, M.K. *New tuberculosis therapeutics: A growing pipeline*. J Infect Dis 2007, 196(Suppl. 1): S28-34.

11. Andries, K., Gullemont, J., Bush, K., Williams, P., Cambau, E., Truffot-Pernot, C., Jarlier, V. *Diarylquinolines (DARQ), a novel class of anti-tuberculosis agents*. 44th Intersci Conf Antimicrob Agents Chemother (ICAAC) (Dec 16-19, Washington, D.C.) 2004, Abst F-1113.

12. Andries, K., Verhasselt, P., Guillemont, J. et al. *A diarylquinoline drug active on the ATP synthase of Mycobacterium tuberculosis*. Science 2005, 307(5707): 223-7.

13. Lounis, N., Gevers, T., Van der Berg, J. et al. *Activity of TMC207 against Mycobacterium avium in vitro and in the mouse*

model. 48th Annu Intersci Conf Antimicrob Agents Chemother (ICAAC) (Oct 25-28, Washington, D.C.) 2008, Abst B-877.

14. Huitric, E., Verhasselt, P., Andries, K., Hoffner, S.E. *In vitro antimycobacterial spectrum of a diarylquinoline ATP synthase inhibitor.* Antimicrob Agents Chemother 2007, 51(11): 4202-4.

15. Petrella, S., Cambau, E., Chauffour, A., Andries, K., Jarlier, V., Sougakoff, W. *Genetic basis for natural and acquired resistance to the diarylquinoline R207910 in mycobacteria*. Antimicrob Agents Chemother 2006, 50(8): 2853-6.

16. de Jonge, M.R., Koymans, L.H., Guillemont, J.E., Koul, A., Andries, K. *A computational model of the inhibition of Mycobacterium tuberculosis ATPase by a new drug candidate R207910*. Proteins 2007, 67(4): 971-80.

17. Jarlier, V., Lounis, N., Veziris, N., Truffot-Pernot, C., Ji, B., Guillemont, J., Andries, K. *Potent activity of a novel diarylquinoline (DARQ) in murine tuberculosis*. 44th Intersci Conf Antimicrob Agents Chemother (ICAAC) (Dec 16-19, Washington, D.C.) 2004, Abst F-1114.

18. Lounis, N., Veziris, N., Chauffour, A., Truffot-Pernot, C., Andries, K., Jarlier, V. *Combinations of R207910 with drugs used to treat multidrug-resistant tuberculosis have the potential to shorten treatment duration*. Antimicrob Agents Chemother 2006, 50(11): 3543-7.

19. Ibrahim, M., Truffot-Pernot, C., Andries, K. et al. *Sterilizing activity of a second line regimen including R207910 (TMC207) in murine tuberculosis*. 48th Annu Intersci Conf Antimicrob Agents Chemother (ICAAC) (Oct 25-28, Washington, D.C.) 2008, Abst B-876.

20. Ji, B., Chauffour, A., Andries, K., Jarlier, V. *Bactericidal activities of R207910 and other newer antimicrobial agents against Mycobacterium leprae in mice.* Antimicrob Agents Chemother 2006, 50(4): 1558-60.

21. Ji, B., Lefrancois, S., Robert, J., Chauffour, A., Truffot, C., Jarlier, V. *In vitro and in vivo activities of rifampin, streptomycin, amikacin, moxifloxacin, R207910, linezolid, and PA-824 against Mycobacterium ulcerans*. Antimicrob Agents Chemother 2006, 50(6): 1921-6.

22. Ibrahim, M., Andries, K., Lounis, N., Chauffour, A., Truffot-Pernot, C., Jarlier, V., Veziris, N. *Synergistic activity of R207910 combined with pyrazinamide against murine tuberculosis*. Antimicrob Agents Chemother 2007, 51(3): 1011-5.

23. Lenaerts, A.J., Hoff, D., Aly, S. et al. *Location of persisting mycobacteria in a guinea pig model of tuberculosis revealed by R207910*. Antimicrob Agents Chemother 2007, 51(9): 3338-45.

24. Lounis, N., Gevers, T., Van Den Berg, J., Andries, K. *Impact of the interaction of R207910 with rifampin on the treatment of tuberculosis studied in the mouse model.* Antimicrob Agents Chemother 2008, 52(10): 3568-72.

25. Veziris, N., Ibrahim, M., Lounis, N., Chauffour, A., Truffot-Pernot, C., Andries, K., Jarlier, V. *A once-weekly R207910-containing regimen exceeds activity of the standard daily regimen in murine tuberculosis*. Am J Respir Crit Care Med 2008, Epub ahead of print.

26. Koul, A., Vranckx, L., Dendouga, N. et al. *Diarylquinolines are bactericidal for dormant mycobacteria as a result of disturbed ATP homeostasis*. J Biol Chem 2008, 283(37): 25273-80.

27. Ibrahim, M., Truffot-Pernot, C., Andries, K. et al. *Early and late bactericidal activity of R207910 (TMC207) in murine tuberculosis*. 48th Annu Intersci Conf Antimicrob Agents Chemother (ICAAC) (Oct 25-28, Washington, D.C.) 2008, Abst B-062.

28. Reddy, V.M., Einck, L., Andries, K. et al. *The new antitubercular drugs SQ109 and TMC207 act synergistically in vitro to kill M. tuberculosis*. 48th Annu Intersci Conf Antimicrob Agents Chemother (ICAAC) (Oct 25-28, Washington, D.C.) 2008, Abst C1-3848.

29. Rustomjee, R., Diacon, A.H., Allen, J. et al. *Early bactericidal activity and pharmacokinetics of the diarylquinoline TMC207 in treatment of pulmonary tuberculosis*. Antimicrob Agents Chemother 2008, 52(8): 2831-5.

30. *TMC207-TiDP13-C-208: Anti-bacterial activity, safety, and tolerability of TMC207 in patients with multi-drug resistant Mycobacterium tuberculosis (MDR-TB) (NCT00449644).* ClinicalTrials.gov Web site, December 15, 2008.

31. Diacon, A.H., Pym, A., Grobusch, M. et al. *Interim analysis of a double-blind, placebo-controlled study with TMC207 in patients with multi-drug resistant (MDR) tuberculosis*. 48th Annu Intersci Conf Antimicrob Agents Chemother (ICAAC) (Oct 25-28, Washington, D.C.) 2008, Abst B-881b.

Drugs of the Future 2007, 32(10): 879-882

CCC: 0377-8282/2007
DOI: 10.1358/dof.2007.032.10.1145702

YM-155

Apoptosis Inducer
Survivin Expression Inhibitor
Oncolytic

3-(2-Methoxyethyl)-2-methyl-4,9-dioxo-1-(pyrazin-2-ylmethyl)-4,9-dihydro-3*H*-naphtho[2,3-*d*]imidazol-1-ium bromide

InChI=1/C20H19N4O3.BrH/c1-13-23(9-10-27-2)17-18(24(13)12-14-11-21-7-8-22-14)20(26)16-6-4-3-5-15(16)19(17)25;/h3-8,11H,9-10,12H2,1-2H3;1H/q+1;/p-1

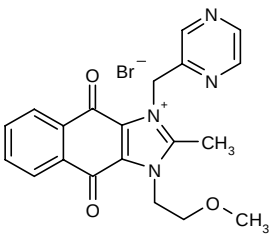

$C_{20}H_{19}BrN_4O_3$
Mol wt: 445.3099

CAS: 781661-94-7

CAS: 753440-91-4 (free base)

EN: 413279

Abstract

YM-155, a small-molecule survivin suppressant, has demonstrated potent antiproliferative activity against a wide spectrum of human tumor cell lines. Preclinical studies indicated that the antitumor activity of YM-155 in various human tumor xenograft models, including prostate cancer, lung cancer and melanoma, was more potent compared to available anticancer agents (equipotent to paclitaxel) without causing loss of body weight or hematological toxicity. Three-day continuous infusion of YM-155 completely inhibited tumor growth and induced marked tumor regression in mice bearing human prostate tumor xenografts. Continuous infusion of YM-155 was associated with greater efficacy and less toxicity than bolus injection. YM-155 as monotherapy demonstrated promising anticancer activity and an acceptable toxicity profile in patients with various types of cancer and is currently undergoing phase II clinical trials.

Synthesis

YM-155 can be synthesized as follows:

3-Chloro-2-[*N*-(2-methoxyethyl)acetamido]naphthoquinone (I) is condensed with 2-(aminomethyl)pyrazine (II) in benzene to afford the diaminonaphthoquinone derivative (III) (1), which is cyclized to the title naphthoimidazolium bromide by treatment with HBr in hot EtOH or MeOH (1, 2). Scheme 1.

Background

Survivin, a key member of the inhibitor of apoptosis (IAP) family, is overexpressed in many human tumors but not in normal tissues, and its overexpression in tumors is associated with a poor prognosis and shorter survival times (3, 4). By using a cell-based high-throughput screening and lead optimization, scientists at Astellas Pharma identified YM-155 as a highly potent, first-in-class survivin suppressant with potent antiproliferative activity against various human tumor cell lines (5). Phase II clinical trials in various types of cancer are currently in progress.

Preclinical Pharmacology

In vitro studies revealed that YM-155 selectively suppressed survivin expression in a gene promoter assay (IC_{50} = 0.54 nM), while having no effect on the expression of other IAP or Bcl-2 family proteins. YM-155 inhibited tumor cell viability and induced tumor cell apoptosis in a concentration-dependent manner in human hormone-refractory prostate cancer (HRPC) PC-3 cells at concentrations of 10-100 nM, while having no effect on the viability of human umbilical vein endothelial cells (HUVEC). The agent demonstrated promising antiproliferative activity against a panel of human tumor cell lines derived from HRPC, with GI_{50} values of 2.3-11 nM. *In vivo*, long-term continuous infusion of YM-155 was associated with greater efficacy and less systemic toxicity than i.v. bolus administration. Hematological and systemic toxicities of YM-155 were also milder compared to conventional chemotherapeutic agents (cisplatin, paclitaxel) at the corresponding

Y. Wang. IBC, 8106 Runnymeade Dr., Frederick, MD 21702, USA. N. Serradell, J. Bolós, E. Rosa. Prous Science, P.O. Box 540, 08080 Barcelona, Spain.

Scheme 1: Synthesis of YM-155

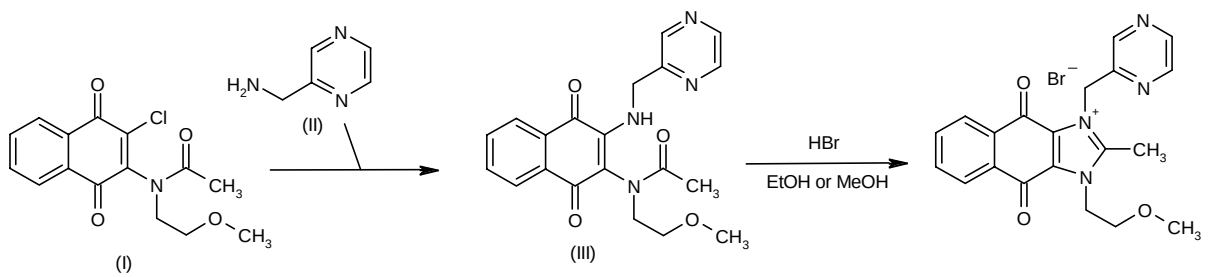

maximum tolerated dose (MTD). Three-day continuous infusion of YM-155 showed potent antitumor activity in an s.c.-xenografted PC-3 tumor model and reduced intratumoral survivin expression. In an orthotopic model of human prostate cancer, PC-3 tumor growth was almost completely inhibited by 3-day continuous infusion of YM-155 at 5 mg/kg. Analysis of YM-155 tissue distribution during a 3-day continuous infusion indicated higher distribution in tumor tissue (351-489 ng/g) than plasma (steady-state concentration of YM-155 = 18.4-23.7 ng/ml) (5-7).

The effect of infusion schedule on the antitumor activity of YM-155 was studied in mice bearing s.c. PC-3 xenografts. The mice received a fixed total dose of YM-155 as an i.v. bolus once or 3 times daily or as a continuous infusion. YM-155 administered by infusion showed significantly more potent antitumor activity, with > 100% tumor growth inhibition compared to 64% with bolus injections. Moreover, YM-155 infusion demonstrated significant and dose-dependent antitumor activity even at doses below the MTD, whereas conventional chemotherapeutic agents such as cisplatin and doxorubicin were only active at the MTD. Paclitaxel was almost as effective as YM-155 at the MTD in this study, but it was associated with a significant decrease in body weight (8).

The preclinical efficacy of YM-155 in experimental human lung tumor models was further evaluated both *in vitro* and *in vivo*. The agent suppressed the expression of survivin in human lung tumor cells and inhibited the growth of the cells with GI_{50} values of 1.5-540 nM. In human non-small cell lung cancer (NSCLC) Calu-6 and NCI-H358 xenograft models in mice, 168-h continuous infusion of YM-155 at doses of 3 and 10 mg/kg induced significant tumor regression without causing a decrease in body weight. Survivin suppression, induction of apoptosis in tumors and tumor regression caused by YM-155 occurred almost simultaneously (9).

Similar experiments were performed in murine models of diffuse large B-cell lymphoma (DLBCL, RL) and Burkitt's lymphoma (Ramos). A single administration of YM-155 as a 168-h continuous s.c. infusion at a dose of 1 or 3 mg/kg was repeated every 3 weeks. In mice bearing RL and Ramos lymphoma xenografts, YM-155 produced statistically significant tumor regression without body weight loss by day 21; the agent also suppressed survivin expression and induced cell death in the tumors. Four of 6 animals bearing RL tumors and 5 of 6 animals bearing Ramos tumors experienced complete tumor regression after treatment with YM-155. The antitumor efficacy of vincristine (0.5 mg/kg i.v.) and rituximab (50 mg/kg i.p.) was also evaluated in this study, but the two agents did not show greater antitumor activity or a survival benefit compared to YM-155 (10).

Using a panel of 127 human tumor cell lines, YM-155 demonstrated antiproliferative activity against 123 cell lines, with a mean log GI_{50} value of –7.85 (14 nM). The agent demonstrated marked activity against HRPC, melanoma, NSCLC, breast cancer, ovarian cancer, sarcoma, lymphoma and leukemia cell lines. The antiproliferative activity of YM-155 was not correlated with survivin expression or p53 status, and it showed similar activity against cell lines with normal, mutated or truncated p53. Drug resistance was observed in small cell lung cancer SHP-77, resistant breast cancer MCF7/ADR and MCF7/mdr1, and resistant human lung carcinoma A549 cell lines. Tumor regression at doses ranging from 1 to 10 mg/kg was observed in A-375 and SK-MEL-5 human malignant melanoma xenograft models, without a decrease in body weight (11).

Pharmacokinetics and Metabolism

The pharmacokinetics of YM-155 were evaluated in a phase I study conducted in 41 patients with advanced solid tumors. At the MTD (4.8 mg/m^2/day), the median clearance of YM-155 was 45.6 l/h, the median steady-state plasma concentration was 7.7 ng/ml and the median terminal half-life was 24 h (12-14).

The pharmacokinetics of YM-155 were further evaluated in a similar phase I study conducted in Japan. At the MTD (8.0 mg/m^2/day), the median clearance was 39 l/h, the median steady-state plasma concentration was 13 ng/ml and the median terminal half-life was 20 h (15).

Safety

YM-155 was well tolerated in both phase I studies. In the first study (12-14), the most frequent adverse events (AEs) included grade 1-2 pyrexia, arthralgia, nausea, fatigue and diarrhea and grade 3 or 4 drug-related AEs were mucosal inflammation (n=2), renal tubular necrosis (n=1) and transient neutropenia (n=1). Dose-limiting toxicity (DLT) consisted of 1 case each of reversible renal tubular necrosis with grade 3 mucositis and increased serum creatinine at 6 mg/m^2/day. In the Japanese study (15), 2 of 5 patients in the 10.6 mg/m^2/day dose group experienced DLT of increased blood creatinine during cycle 1, although both patients recovered to grade 1 or below in 2 weeks without plasma dialysis. The most frequent AEs included fatigue (39%), microalbuminuria (39%), pyrexia (33%) and anemia/decrease in hemoglobin (30%).

Generally good tolerance was also observed in a phase II study conducted in chemotherapy-naïve patients with unresectable stage III or IV melanoma (see Clinical Studies for further details). Four of 31 evaluable patients experienced serious AEs possibly or probably related to treatment, consisting of sepsis, headache and acute renal failure. The most frequent adverse events included fatigue (30.8%), nausea (30.8%), pyrexia (15.4%) and back pain (15.4%) (16, 17).

The safety and toxicity of YM-155 were evaluated in another phase II study conducted in patients with HRPC who previously received taxane chemotherapy. YM-155 showed an acceptable toxicity profile in this study. The most frequent AEs included fatigue (47%), nausea (31%) and anorexia (22%). Two patients discontinued the study because of AEs. Five patients experienced grade 3-5 drug-related AEs, including coagulopathy (grade 3) followed by intracranial hemorrhage (grade 5), fatigue (grade 3), upper respiratory tract infection (grade 3), decreased hemoglobin (grade 3) and thrombocytopenia (grade 3) (18, 19).

Preliminary data from a phase II study in 37 patients with advanced stage IIIB or IV NSCLC showed that 7 patients discontinued the study because of AEs, 4 of whom experienced elevated creatine kinase, fatigue, nausea, vomiting and allergic reactions which were considered to be related to YM-155. Another patient experienced grade 3 or 4 AEs, including cardiac arrhythmia, allergic reaction and fatigue, which were also considered to be drug-related, and the other 3 patients had procedure-related severe AEs. Fourteen patients discontinued the study because of progressive disease. Five patients died during the study, but none of the deaths was related to YM-155 treatment (20).

Clinical Studies

In addition to pharmacokinetics and safety, the phase I study in 41 patients with advanced solid tumors also examined the efficacy of YM-155 (1.8-6.0 mg/m^2/day by continuous i.v. infusion every 3 weeks). The most common tumor types evaluated in the study included prostate cancer (n=9), non-Hodgkin's lymphoma (NHL; n=5) and colorectal cancer (n=5). Three patients with NHL experienced partial responses (PRs), 1 of whom achieved a near-complete response (CR) and subsequently underwent bone marrow transplantation (BMT); the patient was back in remission for more than 14 months at the time of publication. The other 2 patients with NHL remained on treatment with YM-155 with sustained PRs. Two HRPC patients achieved a prostate-specific antigen (PSA) response (> 50% reduction), and 1 patient with NSCLC experienced a minor response (12-14).

In the Japanese phase I study (YM-155 1.8-10.6 mg/m^2/day), 9 patients experienced stable disease, 5 of whom achieved minor tumor shrinkage (15).

To evaluate the objective tumor response rate, including complete and partial responses defined by RECIST, progression-free survival and toxicity of YM-155 in the treatment of melanoma, a phase II study was conducted in 34 chemotherapy-naïve patients with unresectable stage III or IV melanoma (see above). YM-155 was administered as a 168-h continuous infusion every 3 weeks (1 cycle) at a dose of 4.8 mg/m^2/day. Clinical data from 31 evaluable patients demonstrated that YM-155 monotherapy was associated with an encouraging response rate. One patient achieved a CR at cycle 2 but progressed at cycle 8, another patient had a PR at cycle 12 and 7 patients had stable disease, for an overall disease control rate of 27% (16, 17).

As described above, another phase II study evaluated the PSA response (decline of > 50% from baseline) and objective response by RECIST in patients with HRPC who had previously received taxane chemotherapy. Patients received a 168-h continuous infusion every 3 weeks (1 cycle) at a dose of 4.8 mg/m^2/day. Preliminary data from 32 patients indicated that YM-155 was effective in the treatment of HRPC. At the time of reporting, 2 of the 32 patients were PSA responders: 1 achieved response at cycle 2 and the other at cycle 6 (18, 19).

The anticancer efficacy of YM-155 was also evaluated in the phase II study in patients with advanced stage IIIB or IV NSCLC who had failed previous therapy. The primary endpoint of the study was objective tumor response rate measured by RECIST and the secondary endpoints of the study were the progression-free survival rate and safety (see above). Patients received a 168-h continuous i.v. infusion every 3 weeks (1 cycle) at a dose of 4.8 mg/m^2/day for up to 6 cycles. Data on 37 patients with ECOG performance status of 0-2 were presented at the 5th International Symposium on Targeted Anticancer Therapies. One patient had a confirmed PR but subsequently progressed, and 15 patients experienced stable disease after 2 cycles (20).

Phase II clinical studies are in progress in patients with refractory DLBCL, NSCLC and unresectable stage III or metastatic stage IV melanoma (21-23).

Source

Astellas Pharma, Inc. (JP).

References

1. Matsuhisa, A., Kinoyama, I., Okada, M., Nakahara, T., Takeuchi, M., Toyoshima, A. (Astellas Pharma, Inc.). *Fused imidazolium derivatives*. EP 1256576, US 2003114508.

2. Noyama, I., Sakamoto, K., Matsuhisa, A., Hamada, N., Okui, H. (Astellas Pharma, Inc.). *Bromide and its crystal*. EP 1614686.

3. Kawasaki, H., Altieri, D.C., Lu, C-D., Toyoda, M., Tenjo, T., Tanigawa, N. *Inhibition of apoptosis by survivin predicts shorter survival rates in colorectal cancer*. Cancer Res 1998, 58(22): 5071-4.

4. Ambrosini, G., Adida, C., Altieri, D.C. *A novel anti-apoptosis gene, survivin, expressed in cancer and lymphoma*. Nat Med 1997, 3(8): 917-21.

5. Kinoyama, I., Matsuhisa, A., Nakahara, T. et al. *Discovery of YM155, a novel survivin suppressant for the treatment of cancer*. 234th ACS Natl Meet (Aug 19-23, Boston) 2007, Abst MEDI 312.

6. Nakahara, T., Takeuchi, M., Kinoyama, I. et al. *YM155, a novel survivin suppressant, induced downregulation of survivin and potent antitumor activities in experimental human prostate tumor xenograft models*. 17th AACR-NCI-EORTC Int Conf Mol Targets Cancer Ther (Nov 14-18, Philadelphia) 2005, Abst B203.

7. Nakahara, T., Takeuchi, M., Kinoyama, I. et al. *Schedule-dependent antitumor activity of YM155, a novel small molecule survivin suppressant, in experimental human hormone refractory prostate carcinoma xenograft model*. 4th Int Symp Target Anticancer Ther (March 16-18, Amsterdam) 2006, Abst P.205.

8. Nakahara, T., Takeuchi, M., Kinoyama, I. et al. *YM155, a novel small-molecule survivin suppressant, induces regression of established human hormone-refractory prostate tumor xenografts*. Cancer Res 2007, 67(17): 8014-21.

9. Nakahara, T., Takeuchi, M., Kinoyama, I., Kita, A., Yamanaka, K., Matsuhisa, A., Sasamata, M. *Tumor regression induced by YM155, a novel, small molecule survivin suppressant, in experimental human lung tumor models*. Proc Am Assoc Cancer Res (AACR) 2006, 47: Abst 5671.

10. Kita, A., Nakahara, T., Yamanaka, K. et al. *YM155, a novel small molecule survivin suppressant, exhibits curative antitumor activities in experimental human malignant lymphoma models in vivo*. Eur J Cancer - Suppl [18th EORTC-NCI-AACR Symp Mol Targets Cancer Ther (Nov 7-10, Prague) 2006] 2006, 4(12): Abst 377.

11. Nakahara, T., Takeuchi, M., Kita, A. et al. *Broad spectrum and potent antitumor activity of YM155, a novel small molecule survivin suppressant, against a large scale panel of human tumor cell lines*. Eur J Cancer - Suppl [18th EORTC-NCI-AACR Symp Mol Targets Cancer Ther (Nov 7-10, Prague) 2006] 2006, 4(12): Abst 396.

12. Tolcher, A.W., Antonia, S., Lewis, L.D. et al. *A phase I study of YM155, a novel survivin suppressant, administered by 168 hour continuous infusion to patients with advanced solid tumors*. J Clin Oncol [42nd Annu Meet Am Soc Clin Oncol (ASCO) (June 3-6, Atlanta) 2006] 2006, 24(18, Suppl.): Abst 3014.

13. Mita, A., Antonia, S., Lewis, L.D. et al. *Final safety, pharmacokinetic and antitumor activity results of a phase I study of YM155, a novel survivin inhibitor, when administered by 168 hour continuous infusion*. Eur J Cancer - Suppl [18th EORTC-NCI-AACR Symp Mol Targets Cancer Ther (Nov 7-10, Prague) 2006] 2006, 4(12): Abst 29LB1.

14. Tolcher, A.W., Antonia, S., Lewis, L.D. et al. *YM155, a novel survivin suppressant, demonstrated anti-tumor activity in patients with advanced solid tumors and non-Hodgkin's lymphoma*. 4th Int Symp Target Anticancer Ther (March 16-18, Amsterdam) 2006, Abst O.403.

15. Nakagawa, K., Satoh, T., Okamoto, I. et al. *Phase I study of YM155, a first-in-class survivin suppressant, in patients with advanced solid tumors in Japan*. J Clin Oncol [43rd Annu Meet Am Soc Clin Oncol (ASCO) (June 1-5, Chicago) 2007] 2007, 25(18, Suppl.): Abst 3536.

16. Gonzalez, R., Lewis, K., Samlowski, W. et al. *A phase II study of YM155, a novel survivin suppressant, administered by 168 hour continuous infusion in patients with unresectable stage III or stage IV melanoma*. J Clin Oncol [43rd Annu Meet Am Soc Clin Oncol (ASCO) (June 1-5, Chicago) 2007] 2007, 25(18, Suppl.): Abst 8538.

17. Gonzalez, R., Samlowski, W., Cranmer, L. et al. *YM155, a novel survivin suppressant, demonstrates activity in subjects with stage III or IV melanoma*. 5th Int Symp Target Anticancer Ther (March 8-10, Amsterdam) 2007, Abst P405.

18. Karavasilis, V., Mita, A., Hudes, G. et al. *Phase II monotherapy study of YM155, a novel survivin suppressant, administered by 168-hour continous infusion in previously treated hormone refractory prostate cancer (HRPC)*. J Clin Oncol [43rd Annu Meet Am Soc Clin Oncol (ASCO) (June 1-5, Chicago) 2007] 2007, 25(18, Suppl.): Abst 5135.

19. Tolcher, A.W., Karavasilis, V., Hudes, G. et al. *YM155, a novel survivin suppressant demonstrates activity in subjects with hormone refractory prostate cancer (HRPC) previously treated with taxane chemotherapy*. 5th Int Symp Target Anticancer Ther (March 8-10, Amsterdam) 2007, Abst P404.

20. Giaccone, G., Zatloukal, P., Jaromir, R. et al. *A phase II, monotherapy study of YM155 in patients with advanced stage IIIb or IV non-small cell lung cancer (NSCLC)*. 5th Int Symp Target Anticancer Ther (March 8-10, Amsterdam) 2007, Abst P406.

21. *Study of YM155 in refractory diffuse large B-cell lymphoma (DLBCL) subjects (NCT00498914)*. ClinicalTrials.gov Web site, October 2, 2007.

22. *LUCY: A study for the treatment of non-small cell lung cancer (NSCLC) in patients previously treated with chemotherapy (NCT00328588)*. ClinicalTrials.gov Web site, October 2, 2007.

23. *A study for the treatment of unresectable stage III or metastatic stage IV melanoma (NCT00281541)*. ClinicalTrials.gov Web site, October 2, 2007.

Drugs of the Future 2011, 36(9): 663-667

CCC: 0377-8282/2011
DOI: 10.1358/dof.2011.36.9.1678337

MONOGRAPH

TH-302

DNA Alkylating Agent
Hypoxia-Activated Cytotoxic Prodrug
Oncolytic

HAP-302

N,*N*'-Bis(2-bromoethyl)phosphorodiamidic acid (1-methyl-2-nitro-1*H*-imidazol-5-yl)methyl ester

InChI: 1S/C9H16Br2N5O4P/c1-15-8(6-12-9(15)16(17)18)7-20-21(19,13-4-2-10)14-5-3-11/h6H,2-5,7H2,1H3,(H2,13,14,19)

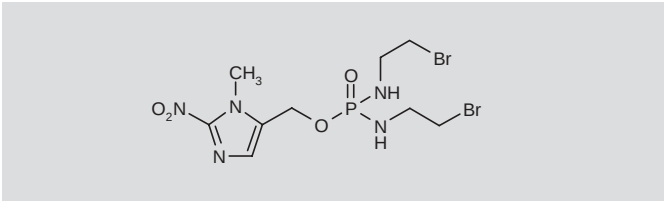

$C_9H_{16}Br_2N_5O_4P$
Mol wt: 449.036
CAS: 918633-87-1
CAS: 918632-75-4 (labeled)
EN: 442503

SUMMARY

Since cancer cells do not produce blood vessels, tumors usually contain regions of hypoxia with relatively low metabolic activity and regions with relatively normal oxygenation where cancer cells grow much more rapidly. Most current cytotoxic anticancer drugs inhibit the growth of highly metabolic cancer cells, while not affecting the hypoxic cancer cells, which remain to grow more aggressively following chemotherapy. TH-302 is a phosphoramidate-based prodrug which becomes activated by electron reduction involving NADPH cytochrome P450 or other reductases present in hypoxic tumor tissue. Preclinical studies have demonstrated the unique hypoxic specificity and therapeutic efficacy of TH-302 in a variety of common human cancer cells. The results of phase I and II clinical trials indicate that this compound has clinical promise in terms of pharmacokinetics, safety and effectiveness for the treatment of various solid tumors in human cancer patients.

J. Thomas Pento, Ph.D., Department of Pharmaceutical Sciences, College of Pharmacy, University of Oklahoma, Health Sciences Center, Oklahoma City 73117, Oklahoma, US. E-mail: tom-pento@ouhsc.edu.
*Synthesis prepared by S. ShankharaRaman, C. Estivill, R. Castañer. Thomson Reuters, Provença 398, 08025 Barcelona, Spain.

SYNTHESIS*

TH-302 is prepared by reaction of 2-bromoethylammonium bromide (I) with $POCl_3$ in the presence of Et_3N in CH_2Cl_2 to yield isophosphoramide mustard (II) (1), which then undergoes Mitsunobu reaction by means of PPh_3 and DIAD in THF (1, 2). Scheme 1.

INTRODUCTION

Since the tumor or cancer cell mass cannot produce endothelial cells necessary for the formation of lymphatic and blood vessels, when the cell mass becomes large enough that oxygen and nutrients do not diffuse adequately into the tumor tissue (usually when the cell mass is 1-2 mm in diameter), the cancer cells secrete several factors that stimulate endothelial cells in the surrounding normal tissue to produce new blood vessels, which grow into the tumor mass to deliver oxygen and nutrients and to carry away waste products, thus permitting the tumor mass to rapidly grow much larger (3). Therefore, angiogenesis or neovascularization is essential for tumor growth and metastatic progression. However, the angiogenesis which occurs in tumor tissue is usually disorganized and inefficient when compared to the vascularization of normal tissue, resulting in interspersed areas of hypoxia and normoxia within the tumor microenvironment (4-6).

There are a number of biochemicals produced by tumor cells and surrounding stromal cells that induce vascular growth, enhance the formation, migration and stability of endothelial cells and vascular formation referred to as vascular sprouting (7). The biochemicals known to be involved in tumor angiogenesis include vascular endothelial growth factor (VEGF), including VEGF-A to VEGF-E (8, 9), heparin-binding growth factor 1 (acidic fibroblast growth factor, aFGF) and heparin-binding growth factor 2 (basic fibroblast growth factor, bFGF) (10-12), platelet endothelial cell adhesion molecule (PECAM) (13, 14), thrombospondin-2 (15-17), various integrins (18-21), neuropilin-1 (22-25) and epidermal growth factor-like protein 7 (EGF-like protein 7, *EGFL7*) (26-28).

Bevacizumab is a humanized monoclonal antibody (MAb) that selectively binds to VEGF and inhibits tumor angiogenesis. Bevacizumab was approved in the U.S. in 2004 for the treatment of

Scheme 1. Synthesis of TH-302

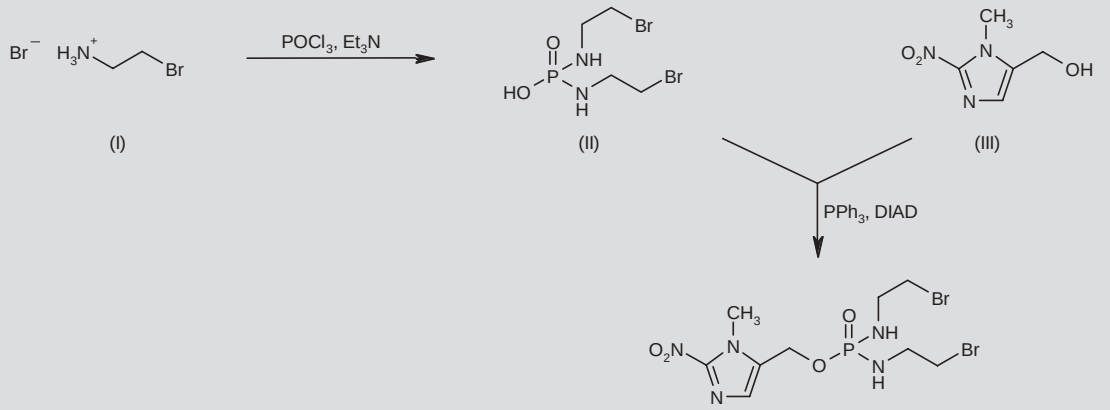

advanced or metastatic colon cancer. Later it was approved for non-small cell lung cancer, glioblastoma, metastatic renal cell cancer and metastatic breast cancer (29). Continued use in breast cancer is currently undergoing NIH review.

Tumor cells in areas of vascularization grow very rapidly and are most sensitive to conventional chemotherapy. However, the hypoxic regions within the tumor are known to be resistant to standard chemotherapy and radiation (2). Thus, hypoxia represents a critical therapeutic limitation and an opportunity for the development of drugs which are selectively activated by hypoxia; thus, these compounds hold the potential to eliminate dormant cancer cells within the hypoxic tumor microenvironment (30-34). It has been proposed that the use of a hypoxia-activated drug in combination with treatments such as radiation or standard cytotoxic chemotherapy, which are most effective within normoxic tumor regions, would produce a more complete therapeutic response, reduce relapse and enhance patient survival (35).

Since the density of hypoxia in the tumor microenvironment is known to be associated with resistance to current radiation and chemotherapy (36-38), the concept of targeting hypoxic tumor cells has developed during the past 10 to 15 years (30). The first hypoxia-activated DNA alkylating mustard compounds were reported by Borch et al. in 2000 (39, 40). Other hypoxia-activated compounds that are used in the treatment of cancer or undergoing clinical testing include tirapazamine (41), mitomycin C (42) and banoxantrone (43).

TH-302 was specifically designed to enhance the cytotoxicity, selectivity and safety of hypoxia-activated alkylating agents. Duan et al. synthesized TH-302 and examined the therapeutic efficacy of this compound and related derivatives on several cancer cell lines both in vitro and in vivo (2). The results of this study demonstrated that TH-302 has a high degree of cytotoxic potency and hypoxic selectivity when compared with other hypoxia-selective isophosphoramide mustard anticancer prodrugs. This compound significantly reduced the survival of human colon adenocarcinoma HT-29 and non-small cell lung carcinoma NCI-H460 cells in a clonogenic cytotoxic assay under selective hypoxic conditions.

PRECLINICAL PHARMACOLOGY

The anticancer activity of TH-302 in vivo was examined in a mouse orthotopic xenograft model of human pancreatic carcinoma MIA PaCa-2 (2). Three days after implantation of the cancer cells, the mice were treated with i.p. injections of either gemcitabine (200 mg/kg once a week for 3 weeks) or TH-302 (30 mg/kg 5 days a week for 15 days for 11 total doses) or a combination of gemcitabine and TH-302 (given 2 hours before gemcitabine on the days that both drugs were scheduled), or vehicle alone. The doses of TH-302 and gemcitabine were approximately one-third the maximum tolerated dose (MTD) of these compounds as single agents. Gemcitabine treatment alone was observed to produce an 82% decrease in primary tumor growth and TH-302 alone produced a 41% decrease in tumor growth, while the combination produced 96% inhibition. Furthermore, the therapeutic combination enhanced survival of the animals and did not produce gross cytotoxicity.

Another study examined the therapeutic efficacy and safety of TH-302 in combination with bortezomib for the treatment of multiple myeloma in a murine xenograft model (44). Preliminary results indicated synergistic cytotoxicity related to changes in Bcl-2 family members and provided a basis for clinical trials in myeloma patients.

Other preclinical studies have demonstrated a broad range of therapeutic efficacy for TH-302 either as a single agent or in combination with standard chemotherapeutic drugs in various murine xenograft models (2, 45-47). Tumor responsiveness to TH-302 monotherapy suggests that, following hypoxia-induced activation, this compound may diffuse away from hypoxic regions and destroy cancer cells within the normoxic regions of the tumor, referred to as the "bystander effect" (2, 35, 46). Furthermore, animal toxicological studies with TH-302 established the no-observable adverse effect level (NOAEL) at 12.5 mg/kg in rats and 8 mg/kg in dogs. These results formed the basis for the allometric scaled starting dose of 7.5 mg/m^2 used in the initial phase I human trials (35).

CLINICAL STUDIES

Weiss et al. completed a phase I dose-escalation study to determine the dose-limiting toxicity (DLT), MTD, safety, pharmacokinetics and

preliminary therapeutic oncolytic activity of TH-302 (35). The study was conducted in 57 patients with advanced solid tumors in whom standard anticancer therapy had failed. In this two-arm study, TH-302 was administered i.v. over 30-60 minutes. In arm A patients received doses that were escalated from 7.5 to 670 mg/m^2 (3 times weekly followed by 1 week off) and in arm B they received doses of 670-940 mg/m^2 (every 3 weeks). Adverse side effects most often observed were nausea, skin rash, fatigue, vomiting and mild hematological toxic events. In arm A the DLT was found to be 670 mg/m^2 and the MTD was reported to be 575 mg/m^2. In arm B the DLT was found to be 940 mg/m^2 and the MTD was reported to be 670 mg/m^2. Of the 57 patients enrolled in this study, partial responses were observed in 2 patients, with stable disease in 27 patients. The results of this study demonstrated a wide range of therapeutic effectiveness and served as the basis for other clinical trials.

In a separate phase I clinical trial, Ganjoo et al. conducted a study to determine the DLT, MTD, safety, pharmacokinetics and therapeutic efficacy of TH-302 when used in combination with doxorubicin in 16 patients with high-grade advanced soft tissue sarcoma (STS) (48). This study employed Response Evaluation Criteria in Solid Tumors (RECIST) criteria methodology for response assessment. In this study, TH-302 was administered i.v. on days 1 and 8 at a starting dose of 240 mg/m^2 and using a classic 3 + 3 dose escalation. Doxorubicin was administered at 2 hours following TH-302 at a dose of 75 mg/m^2 on the first day of every 3-week cycle. In several patients, prophylactic growth factor support was added due to grade 4 neutropenia. The MTD for TH-302 was determined to be 300 mg/m^2. The DLTs were neutropenia-associated infection and thrombocytopenia at a dose of 340 mg/m^2. Common adverse side effects included fatigue, nausea and skin rash. A partial response was observed in 5 patients. TH-302 appeared to enhance the hematological toxicity of doxorubicin, which could be alleviated with prophylactic growth factor support.

In a follow-up phase II trial, Cranmer et al. (49) examined the efficacy and safety of the combination of TH-302 and doxorubicin in patients with advanced or metastatic STS. The results of this study demonstrated that treatment with TH-302 at a dose of 300 mg/m^2 in combination with full-dose doxorubicin (75 mg/m^2) was associated with an acceptable safety profile, which included hematological, skin and mucosal adverse effects. In addition, the therapeutic response and progression-free survival were observed to be better than with single-agent doxorubicin. Based on these results, a trial was initiated to evaluate the efficacy of the combination as compared to doxorubicin alone, the current standard treatment for patients with STS.

In a phase IB study, Borad et al. examined the combination of TH-302 with gemcitabine, docetaxel or pemetrexed to determine the efficacy, MTD and DLT of these therapeutic combinations (50). The MTDs were determined to be 340 mg/m^2 for TH-302 plus gemcitabine, 340 mg/m^2 for TH-302 plus docetaxel and 480 mg/m^2 for TH-302 plus pemetrexed. Hemorrhagic toxicities were dose-limiting, while skin and mucosal side effects were common but manageable. The results indicate that TH-302 may be used to enhance or to complement standard cancer chemotherapy.

Borad et al. are conducting a multicenter, crossover phase II trial with TH-302 in combination with gemcitabine in 165 first-line pancreatic cancer patients (51). Three groups of patients are being treated with either TH-302 240 mg/m^2 plus gemcitabine, TH-302 340 mg/m^2 plus gemcitabine or gemcitabine alone. Patients who successfully complete six cycles without treatment-induced toxicity or disease progression may continue therapy. The results of this study will be analyzed for response rate, survival, event-free survival and safety, with the completion of a minimum of 144 events. Preliminary results indicate that TH-302 can be used safely with a full therapeutic dose of gemcitabine and that greater response rates are observed with the combination than with gemcitabine alone.

CONCLUSION

TH-302 is a cytotoxic prodrug that is selectively activated in hypoxic regions of the tumor microenvironment. When used in combination with radiation and/or standard cytotoxic chemotherapy, the therapeutic combination appears to effectively inhibit the growth, invasiveness and progression of a number of clinically important cancers. Initial clinical trials indicate that this agent is well tolerated and may be effective in combination chemotherapy for a broad range of human cancers.

SOURCE

Threshold Pharmaceuticals, Inc. (US).

DISCLOSURES

The author states no conflicts of interest.

REFERENCES

1. Matteucci, M., Duan, J.-X., Jiao, H., Kaizerman, J., Ammons, S. (Threshold Pharmaceuticals, Inc.). *Phosphoramidate alkylator prodrugs*. CA 2613312, EP 1896040, EP 2336141, JP 2009502743, US 2010137254, WO 2007002931.
2. Duan, J.X., Jiao, H., Kaizerman, J. et al. *Potent and highly selective hypoxia-activated achiral phosphoramidate mustards as anticancer drugs*. J Med Chem 2008, 51(8): 2412-20.
3. Folkman, J., Cotran, R. *Relation of vascular proliferation to tumor growth*. Int Rev Exp Pathol 1976, 16: 207-48.
4. Folkman, J. *Tumor angiogenesis: Therapeutic implications*. N Engl J Med 1971, 285(21): 1182-6.
5. Folkman, J. *Role of angiogenesis in tumor growth and metastasis*. Semin Oncol 2002, 29(6, Suppl. 16): 15-8.
6. Cavallo, T., Sade, R., Folkman, J., Cotran, R.S. *Tumor angiogenesis. Rapid induction of endothelial mitoses demonstrated by autoradiography*. J Cell Biol 1972, 54(2): 408-20.
7. Folkman, J. *Angiogenesis*. Annu Rev Med 2006, 57: 1-18.
8. Folkman, J. *Angiogenesis: Initiation and control*. Ann N Y Acad Sci 1982, 401: 212-27.
9. Nissen, L.J., Cao, R., Hedlund, E.M. et al. *Angiogenic factors FGF2 and PDGF-BB synergistically promote murine tumor neovascularization and metastasis*. J Clin Invest 2007, 117(10): 2766-77.
10. Schwertfeger, K.L. *Fibroblast growth factors in development and cancer: Insights from the mammary and prostate glands*. Curr Drug Targets 2009, 10(7): 632-44.

11. Abate-Shen, C., Shen, M.M. *FGF signaling in prostate tumorigenesis—New insights into epithelial-stromal interactions.* Cancer Cell 2007, 12(6): 495-7.
12. Demirkesen, C., Buyukpinarbasili, N., Ramazanoglu, R., Oguz, O., Mandel, N.M., Kaner, G. *The correlation of angiogenesis with metastasis in primary cutaneous melanoma: A comparative analysis of microvessel density, expression of vascular endothelial growth factor and basic fibroblastic growth factor*. Pathology 2006, 38(2): 132-7.
13. Nickoloff, B.J. *PECAM-1 (CD31) is expressed on proliferating endothelial cells, stromal spindle-shaped cells, and dermal dendrocytes in Kaposi's sarcoma.* Arch Dermatol 1993, 129(2): 250-1.
14. Delisser, H.M. *Targeting PECAM-1 for anti-cancer therapy*. Cancer Biol Ther 2007, 6(1): 121-2.
15. John, A.S., Hu, X., Rothman, V.L., Tuszynski, G.P. *Thrombospondin-1 (TSP-1) up-regulates tissue inhibitor of metalloproteinase-1 (TIMP-1) production in human tumor cells: Exploring the functional significance in tumor cell invasion.* Exp Mol Pathol 2009, 87(3): 184-8.
16. Yee, K.O., Connolly, C.M., Duquette, M., Kazerounian, S., Washington, R., Lawler, J. *The effect of thrombospondin-1 on breast cancer metastasis.* Breast Cancer Res Treat 2009, 114(1): 85-96.
17. Bastian, M., Steiner, M., Schuff-Werner, P. *Expression of thrombospondin-1 in prostate-derived cell lines*. Int J Mol Med 2005, 15(1): 49-56.
18. Giancotti, F.G. *Targeting integrin beta4 for cancer and anti-angiogenic therapy*. Trends Pharmacol Sci 2007, 28(10): 506-11.
19. Mitra, S.K., Schlaepfer, D.D. *Integrin-regulated FAK-Src signaling in normal and cancer cells*. Curr Opin Cell Biol 2006, 18(5): 516-23.
20. Koul, D., Shen, R., Bergh, S. et al. *Targeting integrin-linked kinase inhibits Akt signaling pathways and decreases tumor progression of human glioblastoma*. Mol Cancer Ther 2005, 4(11): 1681-8.
21. Jin, H., Varner, J. *Integrins: Roles in cancer development and as treatment targets*. Br J Cancer 2004, 90(3): 561-5.
22. Lu, L., Zhang, L., Xiao, Z., Lu, S., Yang, R., Han, Z.C. *Neuropilin-1 in acute myeloid leukemia: Expression and role in proliferation and migration of leukemia cells*. Leuk Lymphoma 2008, 49(2): 331-8.
23. Ellis, L.M. *The role of neuropilins in cancer*. Mol Cancer Ther 2006, 5(5): 1099-107.
24. Hansel, D.E., Wilentz, R.E., Yeo, C.J., Schulick, R.D., Montgomery, E., Maitra, A. *Expression of neuropilin-1 in high-grade dysplasia, invasive cancer, and metastases of the human gastrointestinal tract*. Am J Surg Pathol 2004, 28(3): 347-56.
25. Akagi, M., Kawaguchi, M., Liu, W. et al. *Induction of neuropilin-1 and vascular endothelial growth factor by epidermal growth factor in human gastric cancer cells*. Br J Cancer 2003, 88(5): 796-802.
26. Saito, Y., Friedman, J.M., Chihara, Y., Egger, G., Chuang, J.C., Liang, G. *Epigenetic therapy upregulates the tumor suppressor microRNA-126 and its host gene EGFL7 in human cancer cells*. Biochem Biophys Res Commun 2009, 379(3): 726-31.
27. Schmidt, M., De Maziere, A., Smyczek, T. et al. *The role of Egfl7 in vascular morphogenesis.* Novartis Found Symp 2007, 283: 18-28; discussion 28-36, 238-41.
28. Wu, F., Yang, L.Y., Li, Y.F., Ou, D.P., Chen, D.P., Fan, C. *Novel role for epidermal growth factor-like domain 7 in metastasis of human hepatocellular carcinoma*. Hepatology 2009, 50(6): 1839-50.
29. Cohen, M.H., Gootenberg, J., Keegan, P., Pazdur, R. *FDA drug approval summary: Bevacizumab (Avastin) plus carboplatin and paclitaxel as first-line treatment of advanced/metastatic recurrent nonsquamous non-small cell lung cancer*. Oncologist 2007, 12(6): 713-8.
30. Brown, J.M., Wilson, W.R. *Exploiting tumour hypoxia in cancer treatment*. Nat Rev Cancer 2004, 4(6): 437-47.
31. Gillies, R.J., Gatenby, R.A. *Hypoxia and adaptive landscapes in the evolution of carcinogenesis.* Cancer Metastasis Rev 2007, 26(2): 311-7.
32. McKeown, S.R., Cowen, R.L., Williams, K.J. *Bioreductive drugs: From concept to clinic.* Clin Oncol (R Coll Radiol) 2007, 19(6): 427-42.
33. Welsh, S.J., Koh, M.Y., Powis, G. *The hypoxic inducible stress response as a target for cancer drug discovery.* Semin Oncol 2006, 33(4): 486-97.
34. Williams, K.J., Cowen, R.L., Brown, L.M., Chinje, E.C., Jaffar, M., Stratford, I J. *Hypoxia in tumors: Molecular targets for anti-cancer therapeutics.* Adv Enzyme Regul 2004, 44: 93-108.
35. Weiss, G.J., Infante, J.R., Chiorean, E.G. et al. *Phase 1 study of the safety, tolerability, and pharmacokinetics of TH-302, a hypoxia-activated prodrug, in patients with advanced solid malignancies.* Clin Cancer Res 2011, 17(9): 2997-3004.
36. Brizel, D.M., Sibley, G.S., Prosnitz, L.R., Scher, R.L., Dewhirst, M.W. *Tumor hypoxia adversely affects the prognosis of carcinoma of the head and neck.* Int J Radiat Oncol Biol Phys 1997, 38(2): 285-9.
37. Shannon, A.M., Bouchier-Hayes, D.J., Condron, C.M., Toomey, D. *Tumour hypoxia, chemotherapeutic resistance and hypoxia-related therapies.* Cancer Treat Rev 2003, 29(4): 297-307.
38. Vaupel, P., Mayer, A. *Hypoxia in cancer: Significance and impact on clinical outcome*. Cancer Metastasis Rev 2007, 26(2): 225-39.
39. Borch, R.F., Liu, J., Schmidt, J.P., Marakovits, J.T., Joswig, C., Gipp, J.J., Mulcahy, R.T. *Synthesis and evaluation of nitroheterocyclic phosphoramidates as hypoxia-selective alkylating agents*. J Med Chem 2000, 43(11): 2258-65.
40. Freel Meyers, C.L., Hong, L., Joswig, C., Borch, R.F. *Synthesis and biological activity of novel 5-fluoro-2′-deoxyuridine phosphoramidate prodrugs.* J Med Chem 2000, 43(22): 4313-8.
41. Denny, W.A., Wilson, W.R. *Tirapazamine: A bioreductive anticancer drug that exploits tumour hypoxia.* Expert Opin Investig Drugs 2000, 9(12): 2889-901.
42. Alkis, N., Demirci, U., Benekli, M. et al. *Mitomycin-C in combination with fluoropyrimidines in the treatment of metastatic colorectal cancer after oxaliplatin and irinotecan failure*. J BUON 2011, 16(1): 80-3.
43. Lalani, A.S., Alters, S.E., Wong, A., Albertella, M.R., Cleland, J.L., Henner, W.D. *Selective tumor targeting by the hypoxia-activated prodrug AQ4N blocks tumor growth and metastasis in preclinical models of pancreatic cancer*. Clin Cancer Res 2007, 13(7): 2216-25.
44. Hu, J., Van Valckenborgh, E., Menu, E. et al. *Combination of TH-302 and bortezomib has synergistic activity in multiple myeloma.* 13th Int Myeloma Workshop 2011, 272.
45. Ahluwalia, D., Sun, C.J., Liu, Q., Ferraro, D., Wang, Y., Lewis, J.G. *Th-302, a novel hypoxia-activated prodrug, shows superior efficacy and less toxicity than ifosfamide (IFOS) in metastatic and ectopic human lung carcinoma models.* Proc Am Assoc Cancer Res (AACR) 2009, 50: Abst 4517.
46. Hart, C.P., Armstrong, A., Chiorean, E.G., Sun, C.J., Langmuir, V.K., Meng, F. *Bench to bedside experience with TH-302: A tumor selective hypoxiaactivated prodrug as a promising treatment for prostate cancer*. AACR-NCI-EORTC Int Conf Mol Targets Cancer Ther (Nov 15-19, Boston) 2009, Abst B185.
47. Hu, J., Handisides, D.R., Van Valckenborgh, E. et al. *Targeting the multiple myeloma hypoxic niche with TH-302, a hypoxia-activated prodrug.* Blood 2010, 116(9): 1524-7.
48. Ganjoo, K.N., Cranmer, L.D., Butrynski, J.E. et al. *A phase I study of the safety and pharmacokinetics of the hypoxia-activated prodrug TH-302 in combination with doxorubicin in patients with advanced soft tissue sarcoma*. Oncology 2011, 80(1-2): 50-6.

49. Cranmer, L.D., Ganjoo, K.N., Adkins, D. et al. *A phase II dose expansion of TH-302 in combination with doxorubicin in soft-tissue sarcoma.* 47th Annu Meet Am Soc Clin Oncol (ASCO) (June 3-7, Chicago) 2011, Abst 10024.

50. Borad, M., Mita, A., Infante, J. et al. *Complete phase 1B study of TH-302 in combination with gemcitabine, docetaxel or pemetrexed*. Ann Oncol [35th Congr Eur Soc Med Oncol (ESMO) (Oct 8-12, Milan) 2010] 2010, 21(Suppl. 8): Abst 525P.

51. Borad, M.J., Chiorean, E.G., Molina, J.R. et al. *Clinical benefits of TH-302, a tumor selective, hypoxia-activated prodrug and gemcitabine in first-line pancreatic cancer (PanC).* J Clin Oncol [Gastrointest Cancers Symp (Jan 20-22, San Francisco) 2011] 2011, 29(Suppl. 4): Abst 265.

Drugs of the Future 2013, 38(3): 163-167

CCC: 0377-8282/2013
DOI: 10.1358/dof.2013.38.3.1946379

MONOGRAPH

UMECLIDINIUM BROMIDE

Rec INN; USAN

Muscarinic Acetylcholine M_3 Receptor Antagonist
Treatment of COPD
Treatment of Asthma

GSK-573719

1-[2-(Benzyloxy)ethyl]-4-(1-hydroxy-1,1-diphenylmethyl)-1-azoniabicyclo[2.2.2]octane bromide

InChI: 1S/C29H34NO2.BrH/c31-29(26-12-6-2-7-13-26,27-14-8-3-9-15-27)28-16-19-30(20-17-28,21-18-28)22-23-32-24-25-10-4-1-5-11-25;/h1-15,31H,16-24H2;1H/q+1;/p-1

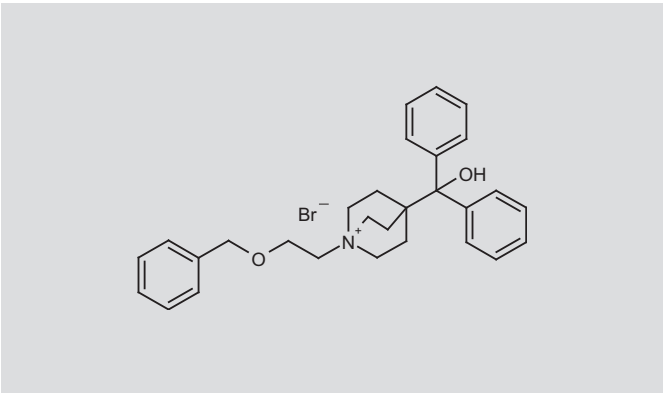

$C_{29}H_{34}NO_2.Br$
Mol wt: 508.49
CAS: 869113-09-7
EN: 447223

SUMMARY

Chronic obstructive pulmonary disease (COPD) is expected to become the third leading cause of death worldwide by 2030. Umeclidinium bromide (GSK-573719), a novel, potent, long-acting muscarinic acetylcholine M_3 receptor antagonist, is in phase III development for the treatment of COPD. It exhibits competitive antagonism for the human M_3 receptor, and competitive, long-lasting antagonism versus carbachol in human bronchial strips; in animals, it potently inhibited bronchoconstriction induced by cholinergic stimulation. In humans, umeclidinium bromide, which was rapidly absorbed by inhalation as dry powder, was well tolerated at doses up to 1000 µg. In a phase II trial in COPD patients, umeclidinium bromide administered once daily at 125, 250 or 500 µg significantly improved trough forced expiratory volume in 1 second (FEV1) and serial FEV1 measurements compared with placebo, and it reduced albuterol use as a rescue medication. Currently, there are eight ongoing trials for COPD for umeclidinium bromide, either alone or in combination with other agents.

Key words: Chronic obstructive pulmonary disease – M_3 receptor antagonist – Bronchoconstriction – Umeclidinium bromide – GSK-573719

SYNTHESIS*

Alkylation of ethyl isonipecotate (I) with 1-bromo-2-chloroethane (II) in the presence of K_2CO_3 in acetone yields ethyl 1-(2-chloroethyl)piperidine-4-carboxylate (III), which by treatment with LDA in THF cyclizes to the quinuclidine derivative (IV) (1, 2). Alternatively, quinuclidine (IV) can be prepared by alkylation of Boc-protected ethyl nipecotate (V) with 1-bromo-2-chloroethane (II) using LiHMDS in toluene to yield the 4-(2-chloroethyl)piperidine derivative (VI), which is then *N*-deprotected with HCl in water/dioxane, followed by cyclization of the resulting chloro amine (VII) by means of K_2CO_3 in refluxing toluene (3). Addition of phenyl lithium (VIII) to ester (IV) in THF affords 1-azabicyclo[2.2.2]oct-4-yl(diphenyl)methanol (IX), which finally undergoes quaternization with benzyl 2-bromoethyl ether (X) in acetonitrile/chloroform (1, 2). Scheme 1.

BACKGROUND

Chronic obstructive pulmonary disease (COPD) will become the third leading cause of death worldwide by 2030 (4); currently, 64 million people have COPD, and 3 million people died of COPD in 2005 according to WHO estimates. The primary cause of COPD is tobacco smoke (5).

COPD is a disease characterized by persistent airflow limitation, usually progressive, concomitant with a pulmonary enhanced chronic inflammatory response. Often, exacerbations and co-morbidities affect COPD patients, contributing to the severity of the disease (6). COPD, which represents an outstanding and increasing economical and social burden (7, 8), is a preventable and treatable disease, although not curable (5, 6).

Current guidelines for the pharmacological management of COPD recommend, as a first choice, the use of inhaled long-acting anti-

J. Gras. C/Roger de Flor 3, 08018 Barcelona. Spain. E-mail: jgrasescardo@hotmail.com.
*Synthesis prepared by J. Bolòs, R. Castañer. Thomson Reuters, Provença 398, 08025 Barcelona, Spain.

Scheme 1. Synthesis of Umeclidinium Bromide

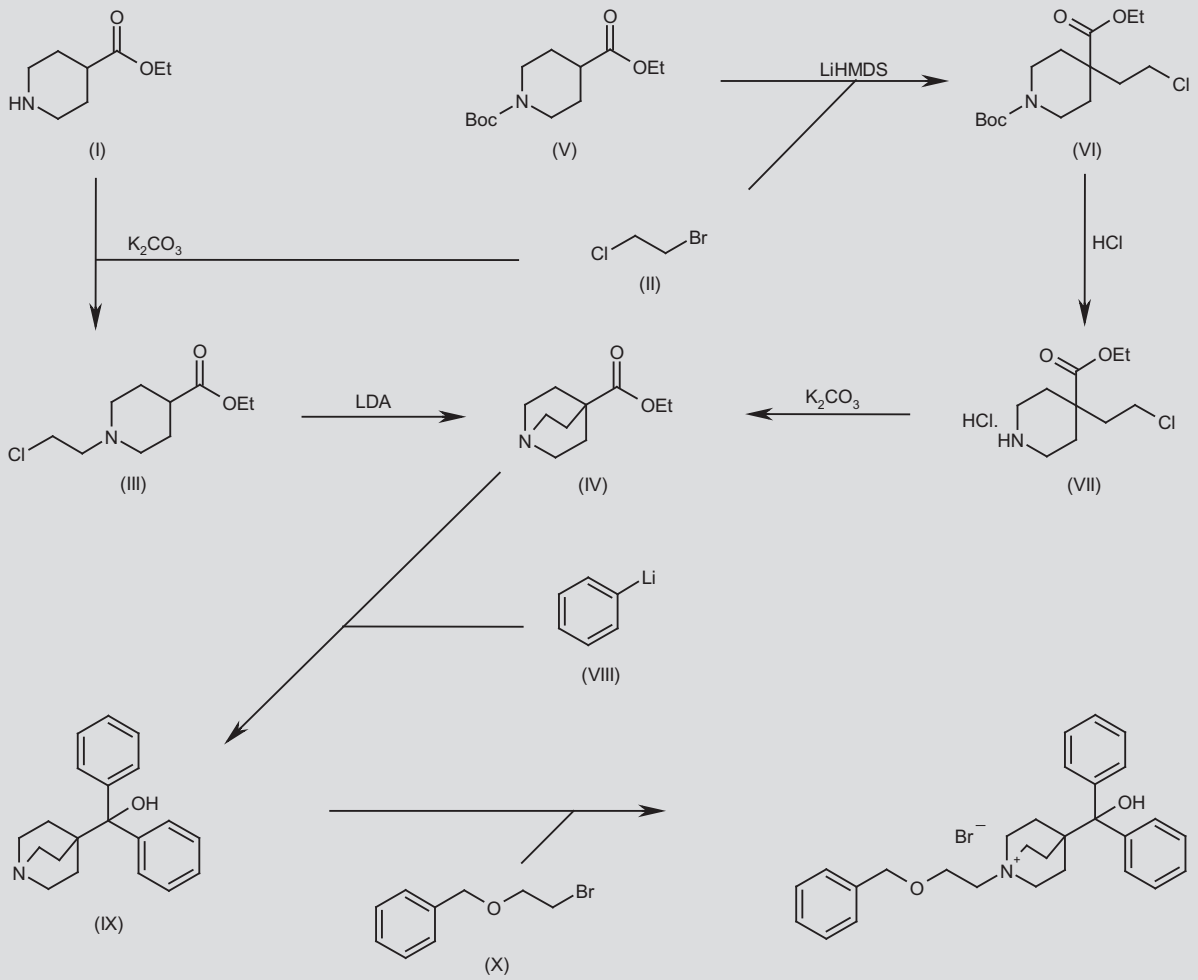

cholinergics or β_2-adrenoceptor agonist bronchodilators to treat COPD patients in the severity range from moderate to very severe (6, 9).

The pharmacological rationale for the use of anticholinergic agents in the treatment of COPD relies on the fact that vagal cholinergic tone is a major mechanism eliciting airway narrowing in COPD disease (10). Five different subtypes of muscarinic acetylcholine receptors have been identified so far (M_1-M_5), and the M_3 receptor, localized in airway smooth muscle, is responsible for mediating the bronchoconstrictor response to cholinergic nerve stimulation (11).

Putting aside tiotropium bromide, which was the first once-daily, long-acting muscarinic acetylcholine receptor antagonist for the maintenance treatment of COPD (12), several novel inhaled long-acting muscarinic acetylcholine M_3 receptor antagonists are currently being developed, or are already approved for the treatment of COPD, e.g., glycopyrronium bromide, aclidinium bromide, umeclidinium bromide, TD-4208, CHF-5407, QAT-370, BEA-2180BR, trospium, dexpirronium and PF-4522971 (13).

Umeclidinium bromide (GSK-573719) is a long-lasting muscarinic acetylcholine M_3 receptor antagonist in phase III clinical development for the treatment of COPD (14) at GlaxoSmithKline, with global filings expected to commence in 2013.

PRECLINICAL PHARMACOLOGY

In radioligand binding assays using cell membrane preparations from CHO cells expressing the human M_1, M_2 or M_3 receptor, umeclidinium bromide showed K_i values of 0.16, 0.15 and 0.06 nM, respectively (1).

Umeclidinium bromide also displayed potent (–log pA_2 = 23.9 pM) and competitive antagonism, with partial reversibility after drug washout, for the human M_3 receptor transfected into CHO cells in an acetylcholine-mediated Ca^{2+} mobilization assay (15). In an in vitro study in human bronchial strips, umeclidinium bromide demonstrated potent (–log pA_2 = 316 pM) and competitive antagonism versus carbachol. Bronchial strips superfused with carbachol showed reversibility in a concentration-dependent manner. The time to restore 50% of the contraction at 10 nM was > 600 minutes.

In a murine plethysmographic model, umeclidinium bromide administered intranasally showed an ED_{50} of 0.02 µg for inhibition of the airway responsiveness to methacholine, and when dosed at the ED_{80} (0.05 µg), bronchoprotection > 50% was observed at 48 hours (1, 15).

Finally, in conscious guinea pigs umeclidinium bromide administered intratracheally showed a dose-dependent blockade of acetylcholine-induced bronchoconstriction with a long duration of action, e.g., > 50% bronchoprotection for more than 24 hours at a dose of 2.5 µg. These results suggest a long duration of action in clinical practice, compatible with the once-daily regimen for the treatment of COPD (15).

PHARMACOKINETICS AND METABOLISM

A pharmacokinetic study in rats demonstrated that umeclidinium bromide has low oral bioavailability and high plasma clearance. These properties are suitable for a drug intended to act topically in the airways and to minimize systemic side effects (1).

The absorption, distribution, metabolism and elimination of [^{14}C]-umeclidinium bromide administered as a single dose intravenously or orally were assessed in an open-label, nonrandomized study in healthy adults. By the intravenous route, parent umeclidinium bromide accounts for 20% of total radioactivity in plasma, suggesting extensive metabolism. By day 8, around 58% and 22% of umeclidinium bromide radioactivity was eliminated in the feces and urine, respectively, and therefore umeclidinium bromide is cleared from plasma by metabolism and biliary excretion, and less by urinary excretion. Oral umeclidinium bromide is poorly absorbed, and 92% of total radioactivity was recovered in feces and < 1% in urine (16).

Healthy volunteers treated with umeclidinium bromide as a dry powder at single inhaled doses in the range of 10-350 µg showed a t_{max} of 5 minutes, a rapid plasma concentration decline and a moderate to high C_{max} variability (17). In another study in healthy adults, umeclidinium bromide administered as dry powder inhalation at 250, 750 and 1000 µg once daily for 14 days showed a rapid absorption (t_{max} = 5-15 minutes) and a mean elimination half-life of 26-28 hours. Approximately 1-1.5% of the dose of umeclidinium bromide was detected unchanged in the urine at day 1, and 3.9-4.5% at steady state. Based on plasma levels, a 1.5- to 3-fold accumulation was observed at day 14 versus day 1 (18).

In COPD patients treated with umeclidinium bromide as dry powder by inhalation at 250, 500 and 1000 µg as a single dose, a median t_{max} of 5-15 minutes and an elimination half-life of 11-12 hours based on urine concentration were reported (19). When umeclidinium bromide was administered repeatedly once daily for 7 days in a new dry powder formulation containing magnesium stearate at 250 and 1000 µg to COPD patients, rapid absorption (t_{max} = 5-15 minutes), 1-2% of the dose excreted unchanged in the urine and low accumulation were observed (14, 20).

Finally, a pharmacokinetic study of umeclidinium bromide administered to COPD patients using a multiple-dose powder inhaler at doses of 62.5, 125, 250, 500 and 1000 µg once daily and at 62.5, 125 and 250 µg twice daily for 14 days also showed rapid absorption (t_{max} = 5-15 minutes) and rapid elimination from plasma. Steady state was reached by day 7 (21).

CLINICAL STUDIES

In healthy male subjects, the safety, tolerability and pharmacodynamics of single doses of umeclidinium bromide (in the range of 10-350 µg) in comparison with tiotropium at 18 µg, both administered as dry powder inhalation, were evaluated in a randomized, double-blind, placebo-controlled, dose-ascending, crossover trial. Eighteen subjects completed all treatments, and most adverse events (AEs) observed were mild to moderate. Significant increases in specific airway conductance (sGaw) and forced expiratory volume in 1 second (FEV1) in comparison with placebo were observed with umeclidinium bromide at 100, 250 and 350 µg, and 100 and 350 µg, respectively. In this first-in-human study, umeclidinium bromide demonstrated the potential for once-daily administration in COPD patients (17).

The safety and tolerability of repeated doses of umeclidinium bromide administered as dry powder inhalation at 250, 750 and 1000 µg once daily for 14 days were studied in 36 healthy adults in a single-center, double-blind, parallel-group phase I trial (NCT00475436). Most AEs were mild, resolving during the study, headache and pharyngolaryngeal pain being the most frequent drug-related AEs. Neither clinically relevant abnormalities nor ECG changes were observed, and umeclidinium bromide was well tolerated even at the highest dose (18).

In COPD patients, the safety and pharmacodynamics of single doses of umeclidinium bromide at 250, 500 or 1000 µg in comparison with tiotropium 18 µg, both administered as dry powder inhalation, were evaluated in a randomized, double-blind, dose-ascending, placebo-controlled phase II trial (NCT00515502). AEs, observed in 31-41% of subjects treated with umeclidinium bromide, were in general mild or moderate in intensity, and no clinically relevant changes in clinical chemistry, vital signs or ECG were reported. All doses of umeclidinium bromide showed significantly higher values of sGaw and FEV1 compared with placebo (19).

The safety and tolerability of repeated doses of umeclidinium bromide administered as dry powder inhalation at 250 and 1000 µg once daily for 7 days in a new dry powder formulation containing magnesium stearate, were studied in 38 COPD patients in a randomized, double-blind, placebo-controlled phase II trial (NCT00732472). Of the 16 drug-related AEs detected, all mild or moderate, 5 were at the dose of 250 µg (arrhythmia, tachycardia, dysgeusia, hypertension, bronchospasm) and 7 at 1000 µg (blood pressure increase, thirst, oropharyngeal pain, headache, dry mouth, dyspnea, feeling abnormal). However, the highest dose showed increases in heart rate compared with the low dose; Holter monitoring for 24 hours showed no dose effect and small treatment effects (20).

Dose-related efficacy and safety for umeclidinium bromide administered as dry powder inhalation in comparison with tiotropium were examined in COPD patients in a randomized, double-blind, placebo-controlled phase II trial (NCT01372410). Umeclidinium was adminis-

tered once daily at 15.6, 31.25, 62.5 and 125 µg or twice daily at 15.6 and 31.25 µg, and tiotropium was administered once daily at 18 µg once daily; all treatments lasted for 7 days, and morning trough FEV1 was measured on day 8 as a primary endpoint. Umeclidinium bromide administered once daily showed a dose response on the order of 125 > 62.5 > 31.25 = 15.6 µg for increases in trough FEV1, with an estimated potency expressed as ED_{50} of 37 µg. No advantage of twice-daily over once-daily dosing was observed. AEs for umeclidinium bromide reached 18% at the highest dose (125 µg once daily) and between 5-12% for the rest of the doses, whereas tiotropium showed 4% and placebo 8% AEs (22).

The efficacy and safety of umeclidinium bromide administered as dry powder inhalation in comparison with tiotropium were also studied in COPD patients in a multicenter, randomized, double-blind, placebo-controlled phase II trial (NCT00950807). Treatments, which lasted for 14 days, were umeclidinium bromide once daily in the range of 62.5-1000 µg, or twice daily in the range of 62.5-250 µg, and tiotropium at 18 µg once daily as open-label therapy. The primary efficacy endpoint was trough FEV1 measured on day 15 and secondary efficacy endpoints were weighted mean FEV1 over 0 to 24 hours, trough forced vital capacity (FVC), weighted mean FVC over 0 to 24 hours and the use of albuterol as rescue. Safety assessments included AEs, vital signs, 12-lead ECG and 24-hour Holter, clinical laboratory tests and COPD exacerbations. Of the 135 patients who completed the study, umeclidinium bromide showed significant increases in trough FEV1 on day 15, expressed as adjusted mean differences compared with placebo of 128, 147, 95, 140 and 186 mL for the doses of 62.5, 125, 250, 500 and 1000 µg once daily, respectively, and 79, 134 and 172 mL for the doses of 62.5, 125 and 250 µg twice daily, respectively, 105 mL being the value for tiotropium. All doses of umeclidinium bromide also significantly improved the adjusted mean change from baseline in 0- to 24-hour weighted mean FEV1 compared with placebo on day 14. Similarly, all doses of umeclidinium bromide significantly improved trough FVC and the adjusted mean change from baseline in 0- to 24- hour weighted mean FVC compared with placebo on day 14. Both parameters, FEV1 and FVC, showed a flat dose–effect relationship. Most doses of umeclidinium bromide displayed significant reductions in rescue albuterol use compared with placebo. Concerning the safety assessment, the most commonly reported AEs in the study were headache and cough. Umeclidinium bromide was well tolerated, and no treatment-related changes were observed in any of the safety assessments, including ECG evaluations. However, to characterize the efficacy and safety profile of umeclidinium bromide, larger clinical trials will be required (21).

An analysis of pooled data from the two dose-ranging studies of umeclidinium bromide, the studies just summarized, i.e., NCT01372410, and NCT00950807, in order to assess the dose–response and dosing interval in COPD patients was reported. Data from 321 patients were examined, and all umeclidinium bromide doses significantly increased trough FEV1 values in comparison with placebo, with values ranging from 97 to 189 mL with once-daily dosing, and from 83 to 173 mL with twice-daily dosing. This analysis confirmed the suitability of once-daily dosing of umeclidinium bromide for the treatment of COPD patients (23).

Dose-related efficacy for repeated doses of umeclidinium bromide administered as dry powder inhalation at 125, 250 and 500 µg once daily for 28 days, were tested in COPD patients in a multicenter, randomized, double-blind, placebo-controlled phase II trial (NCT01030965). All doses of umeclidinium bromide trough FEV1 values after 28 days were increased significantly compared with placebo, umeclidinium bromide serial FEV1 and FVC measurements showed improvements over placebo, and the use of albuterol as a rescue medication was reduced (14, 24).

Currently, there are 11 trials ongoing for umeclidinium bromide, either alone or in combination, 8 of which are for the indication of COPD and 3 for the indication of asthma (14).

CONCLUSIONS

Umeclidinium bromide is a novel, potent, long-acting muscarinic acetylcholine receptor antagonist which is in phase III trials for the treatment of COPD and phase II trials for asthma. In preclinical studies, umeclidinium bromide demonstrated affinity for the human M_1, M_2 or M_3 receptors, competitive antagonism at the muscarinic acetylcholine M_3 receptor transfected into CHO cells, and competitive and long-lasting antagonism versus carbachol in human bronchial strips. In in vivo studies in experimental animals, umeclidinium bromide administered into the airways inhibited the bronchoconstriction induced by cholinergic stimulation in a potent and long-lasting manner. Pharmacokinetic studies in humans demonstrated that umeclidinium bromide was poorly absorbed orally, but rapidly absorbed by inhalation as dry powder. In clinical trials, umeclidinium bromide administered as a dry powder by inhalation proved to be well tolerated. In a phase II trial, umeclidinium bromide at doses of 125, 250 or 500 µg administered once daily for 28 days to COPD patients demonstrated significant efficacy at all doses, improving trough FEV1 and serial FEV1 measurements compared to placebo, and reducing albuterol use as a rescue medication. However, to characterize the efficacy and safety profile of umeclidinium bromide, larger clinical trials will be required.

SOURCE

GlaxoSmithKline (UK).

DISCLOSURES

The author states no conflicts of interest.

REFERENCES

1. Lainé, D.I., McCleland, B., Thomas, S. et al. *Discovery of novel 1-azoniabicyclo[2.2.2]octane muscarinic acetylcholine receptor antagonists.* J Med Chem 2009, 52(8): 2493-505.
2. Lainé, D.I., Palovich, M.R., McCleland, B.W., Neipp, C.E., Thomas, S.M. (GlaxoSmithKline plc). *Muscarinic acetylcholine receptor antagonists*. CA 2564742, CN 102040602, EP 1740177, JP 2007534769, KR 2011010841, US 200785155, US 7498440, US 8183257, US 2012157491, US 8309572, US 2013030015, WO 2005104745.
3. Carangio, A., Cheung, I., D'Souza, E.C.F., Leahy, J.H., Strachan, J.B. (GlaxoSmithKline plc). *Methods of preparation of muscarinic acetylcholine receptor antagonists.* WO 2011029896.
4. World Health Statistics 2008. Geneva: World Health Organization. (http://www.who.int/whosis/whostat/EN_WHS08_Full.pdf) (Accessed January 30, 2013).
5. Chronic obstructive pulmonary disease (COPD) Fact sheet N°315, November 2012. Geneva: World Health Organization. (http://www.who.

int/mediacentre/factsheets/fs315/en/index.html) (Accessed January 30, 2013).

6. Global Strategy for the Diagnosis, Management, and Prevention of Chronic Obstructive Lung Disease. Global Initiative for Chronic Obstructive Lung Disease (GOLD) (Updated) 2011, http://www.goldcopd.org. (Accessed January 30, 2013).
7. López, A.D., Shibuya, K., Rao, C. et al. *Chronic obstructive pulmonary disease: Current burden and future projections.* Eur Respir J 2006, 27(2): 397-412.
8. Mathers, C.D., Loncar, D. *Projections of mortality and burden of disease from 2002 to 2030.* PloS Med 2006, 3(11): e442.
9. Qaseem, A., Wilt, T.J., Weinberger, S.E. et al.; American College of Physicians; American College of Chest Physicians; American Thoracic Society; European Respiratory Society. *Diagnosis and management of stable chronic obstructive pulmonary disease: A clinical Practice guideline Update from the American College of Physicians, American College of Chest Physicians, American Thoracic Society, and European Respiratory Society*. Ann Intern Med 2011, 155(3): 179-91.
10. Belmonte, K.E. *Cholinergic pathways in the lungs and anticholinergic therapy for chronic obstructive pulmonary disease.* Proc Am Thorac Soc 2005, 2(4): 297-304.
11. Roffel, A.F., Elzinga, C.R., Zaagsma, J. *Muscarinic M3 receptors mediate contraction of human central and peripheral airway smooth muscle.* Pulm Pharmacol 1990, 3(1): 47-51.
12. Barnes, P.J. *The pharmacological properties of tiotropium.* Chest 2000, 117(2, Suppl.): 63S-6S.
13. Cazzola, M., Page, C.P., Calzetta, L., Matera, M.G. *Pharmacology and therapeutics of bronchodilators.* Pharmacol Rev 2012, 64(3): 450-504.
14. ClinicalTrials.gov web site. http://clinicaltrials.gov/ct2/results?term=GSK573719 http://clinicaltrials.gov/ct2/results?term=umeclidinium (Accessed January 29, 2013).
15. Lainé, D.I., Luttmann, M.A., Foley, J.J., Cehaas, C.J., Kotzer, C.J., Salmon, M., Rumsey, W.L. *The pre-clinical pharmacology of the inhaled muscarinic antagonist GSK573719 predicts o.d. clinical dosing.* Eur Respir J [Annu Congr Eur Respir Soc (ERS) (Sept 24-28, Amsterdam) 2011] 2011, 38(Suppl. 55): Abst 3450.
16. Kelleher, D., Hughes, S., Mehta, R., Tombs, L., Kelly, K., Church, A. *Absorption, distribution, metabolism, and elimination (ADME) of umeclidinium (UMEC) in healthy adults.* Eur Respir J [Annu Congr Eur Respir Soc (ERS) (Sept 1-5, Vienna) 2012] 2012, 40(Suppl. 56): Abst P2153.
17. Cahn, A., Lovick, R., Newlands, A. et al. *Safety, tolerability, pharmacodynamics (PD) and pharmacokinetics (PK) of GSK573719 inhalation powder in healthy subjects.* Eur Respir J [Annu Congr Eur Respir Soc (ERS) (Sept 24-28, Amsterdam) 2011] 2011, 38(Suppl. 55): Abst P3971.
18. Mehta, R., Hardes, K., Cahn, A. et al. *Safety, tolerability and pharmacokinetics (PK) of repeated doses of GSK573719 inhalation powder, a new long-acting muscarinic antagonist, in healthy adults*. Eur Respir J [Annu Congr Eur Respir Soc (ERS) (Sept 24-28, Amsterdam) 2011] 2011, 38(Suppl. 55): Abst P3972.
19. Mehta, R., Newlands, A., Kelleher, D., Preece, A., Cahn, A., Crater, G. *Safety, pharmacokinetics (PK) and pharmacodynamics (PD) of single doses of GSK573719 inhalation powder, a new long-acting muscarinic antagonist (LAMA), in patients with COPD.* Eur Respir J [Annu Congr Eur Respir Soc (ERS) (Sept 24-28, Amsterdam) 2011] 2011, 38(Suppl. 55): Abst P822.
20. Kelleher, D., Preece, A., Mehta, R., Donald, A., Hardes, K., Cahn, A., Crater, G. *Phase II study of o.d. GSK573719 inhalation powder, a new long-acting muscarinic antagonist, in patients with chronic obstructive pulmonary disease (COPD).* Eur Respir J [Annu Congr Eur Respir Soc (ERS) (Sept 24-28, Amsterdam) 2011] 2011, 38(Suppl. 55): Abst P834.
21. Donohue, J.F., Anzueto, A., Brooks, J., Mehta, R., Kalberg, C., Crater, G. *A randomized, double-blind dose-ranging study of the novel LAMA GSK573719 in patients with COPD.* Respir Med 2012, 106(7): 970-9.
22. Church, A., Beerahee, M., Brooks, J., Mehta, R., Shah, P. *Umeclidinium (GSK573719) dose response and dosing interval in COPD.* Eur Respir J [Annu Congr Eur Respir Soc (ERS) (Sept 1-5, Vienna) 2012] 2012, 40(Suppl. 56): Abst P2121.
23. Church, A., Kalberg, C., Shah, P., Beerahee, M., Donohue, J. *An analysis of the dose response of umeclidinium (GSK573719) administered once or twice daily in patients with COPD.* Chest [Annu Meet Am Coll Chest Physic (ACCP) (Oct 20-25, Atlanta) 2012] 2012, 142(4, Meeting Abstracts): Abst 672A.
24. Decramer, M., Maltais, F., Feldman, G., Brooks, J., Willits, L., Harris, S., Crater, G. *Dose-related efficacy of GSK573719, a new long-acting muscarinic receptor antagonist (LAMA) offering sustained 24-hour bronchodilation, in COPD.* Eur Respir J [Annu Congr Eur Respir Soc (ERS) (Sept 24-28, Amsterdam) 2011] 2011, 38(Suppl. 55): Abst P878.

Drugs of the Future 2012, 37(2): 99-109

CCC: 0377-8282/2012
DOI: 10.1358/dof.2012.37.2.1704836

BI-201335

Treatment of Hepatitis C Virus
Serine Protease NS3/Non-Structural Protein 4A (NS4A) Inhibitor

N-(Cyclopentyloxycarbonyl)-3-methyl-L-valyl-4(*R*)-[8-bromo-2-[2-(isobutyrylamino)thiazol-4-yl]-7-methoxyquinolin-4-yloxy]-*N*-[1(*R*)-carboxy-2(*S*)-vinylcyclopropyl]-L-prolinamide

InChI: 1S/C40H49BrN6O9S/c1-8-21-17-40(21,36(51)52)46-34(49)27-15-23(18-47(27)35(50)32(39(4,5)6)44-38(53)56-22-11-9-10-12-22)55-29-16-25(26-19-57-37(43-26)45-33(48)20(2)3)42-31-24(29)13-14-28(54-7)30(31)41/h8,13-14,16,19-23,27,32H,1,9-12,15,17-18H2,2-7H3,(H,44,53)(H,46,49)(H,51,52)(H,43,45,48)/t21-,23-,27?,32-,40-/m1/s1

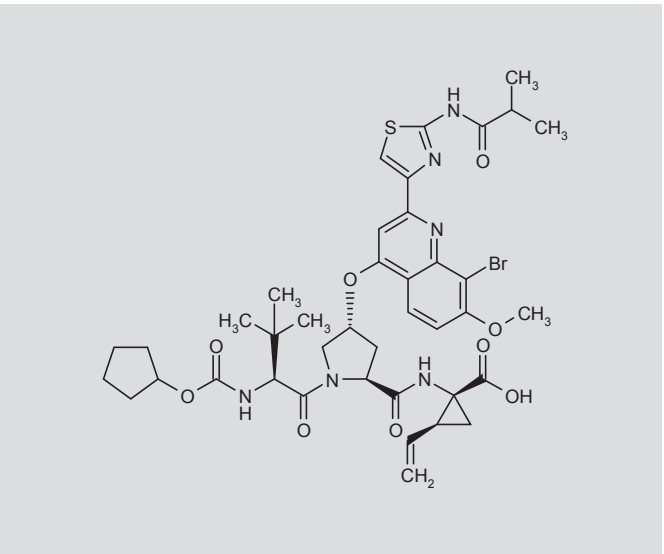

$C_{40}H_{49}BrN_6O_9S$
Mol wt: 869.821
EN: 644871

SUMMARY

Chronic hepatitis C affects an estimated 170 million people worldwide and is the leading indication for liver transplantation in the U.S. Until recently, eradication of chronic hepatitis C depended on the combination of pegylated interferon (pegIFN) and ribavirin (RBV). This combination is effective in only 40-50% of patients infected with hepatitis C virus (HCV) genotype 1, and 30-40% of patients co-infected with HIV. It also carries a high burden of side effects, mostly flu-like illness, fatigue, depression and anemia. This low-efficacy/high-toxicity regimen has motivated the search for a more potent treatment with an improved side effect profile. In this context, various therapeutic agents targeting viral enzymes critical to HCV replication have been identified. BI-201335 is a potent and selective HCV serine protease NS3/non-structural protein 4A (NS4A) inhibitor that recently entered phase III clinical trials. In phase II trials, cure rates above 80% were reported for previously untreated patients, with the majority being eligible for shorter treatment duration. Its high potency, once-daily dosing and good safety profile suggest it could be included in future interferon-free direct-acting antiviral combinations.

Key words: Hepatitis C virus – NS3/NS4A inhibitor – Protease inhibitor – BI-201335

Marie-Louise Vachon, MD, MSc. Research Center in Infectious Diseases, Centre Hospitalier Universitaire de Quebec and Laval University, CHUL, Rm. S-796, 2705 Blvd. Laurier, Quebec G1V 4G2, Canada. E-mail: marie-louise.vachon@mail.chuq.qc.ca.
*Synthesis prepared by C. Estivill, R. Castañer. Thomson Reuters, Provença 398, 08025 Barcelona, Spain.

SYNTHESIS*

BI-201335 can be synthesized by the following methods:

Cyclization of the α-bromoketone (I) with *N*-isobutyrylthiourea (II) in *i*-PrOH at 75 °C produces the thiazole derivative (III), which upon methyl ester hydrolysis using LiOH in H_2O/MeOH/THF gives directly BI-201335 (1, *2*). Scheme 1.

In an alternative method, the methyl ester precursor (III) is obtained by condensation of the dipeptide derivative (IV) with methyl 1(*R*)-amino-2(*S*)-vinylcyclopropanecarboxylate tosylate salt (Va) by means of EDC, HOBt and DIEA in DMF (*2*). Scheme 1.

In a different strategy, the tripeptide carbamate (VI) is coupled with the chloroquinoline derivative (VII) by means of *t*-BuOK in DMSO to afford BI-201335 (*2*). Scheme 1.

The bromoketone intermediate (I) is prepared as follows:

Alcohol (VIII) is converted to the corresponding brosylate (IX) by treatment with *p*-bromobenzenesulfonyl chloride in the presence of DMAP and Et_3N in CH_2Cl_2 (1, 3, 4). Subsequent displacement of the sulfonate group of compound (IX) with the quinolinol (X) in the presence of Cs_2CO_3 in NMP affords the ether adduct (XI) (1, 3). Selective hydrolysis of diester (XI) by means of NaOH in THF/H_2O generates the sodium salt (XII), which, after conversion to a mixed anhydride with *i*-BuOCOCl and Et_3N in THF, is treated in situ with CH_2N_2 to give the diazoketone (XIII). Finally, reaction of diazoketone (XIII) with concentrated HBr in THF yields the α-bromoketone (I) (1, 3). Scheme 2.

Scheme 1. Synthesis of BI-201335

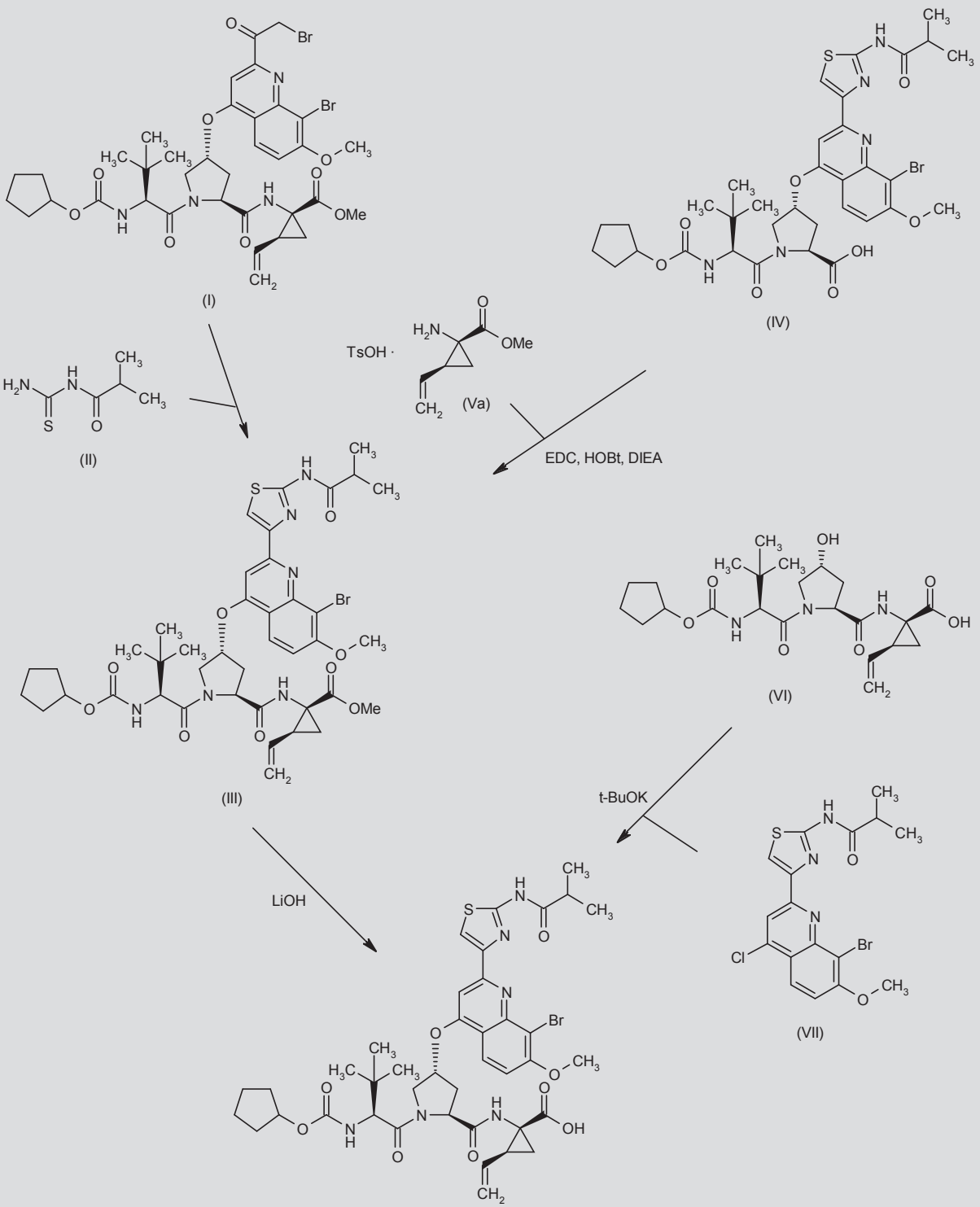

Scheme 2. Synthesis of Bromoketone Intermediate (I)

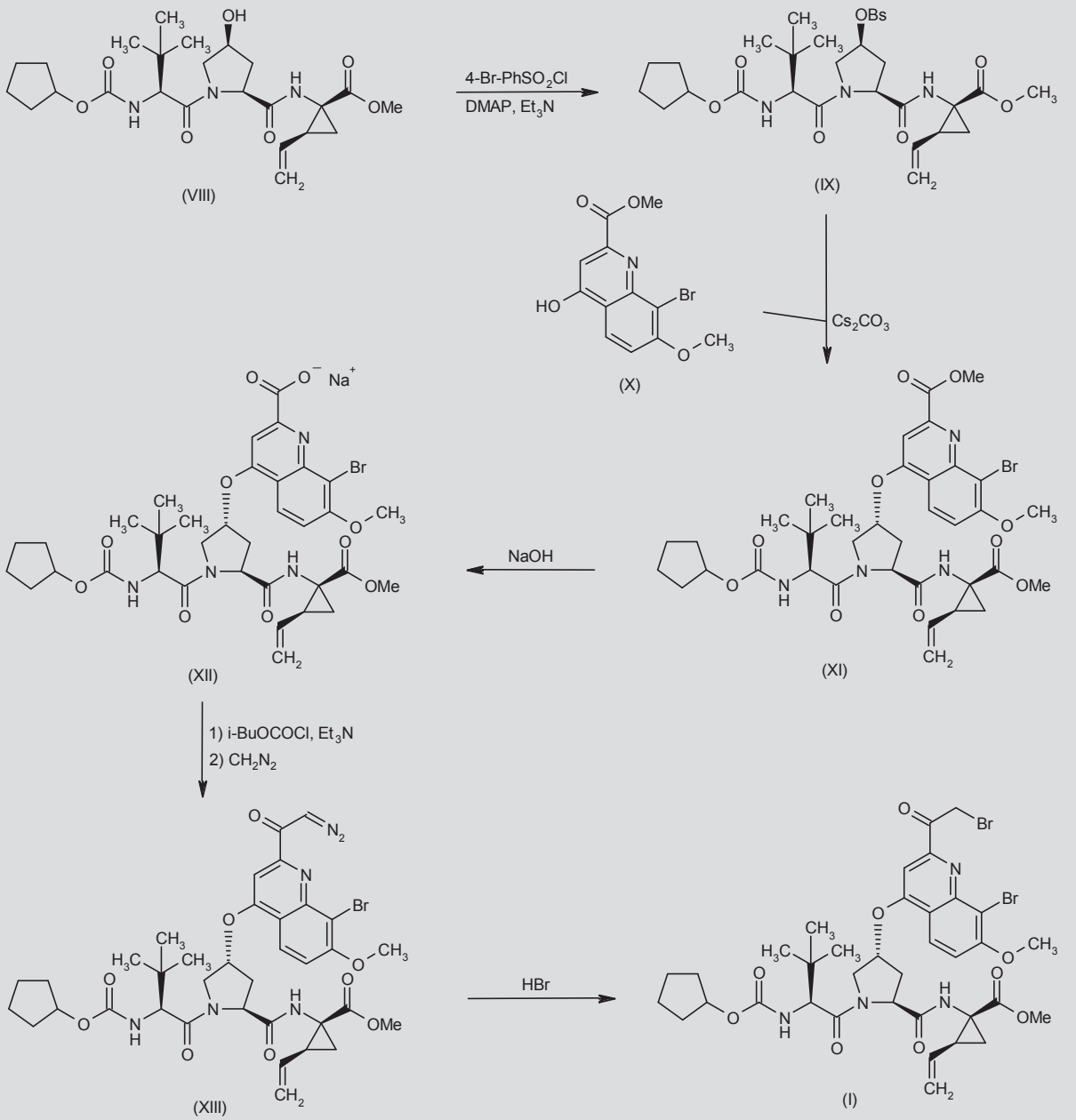

Tripeptide derivative (VIII) is obtained by coupling of *N*-Boc-4(*R*)-hydroxy-L-proline (XIV) with methyl 1(*R*)-amino-2(*S*)-vinylcyclopropanecarboxylate (Vb) by means of TBTU and DIEA in DMF to afford amide (XV). Subsequent Mitsunobu condensation of alcohol (XV) with *p*-nitrobenzoic acid (PNBA) in the presence of PPh_3 and DEAD in THF gives the fully protected dipeptide (XVI), from which the *N*-Boc group is removed by treatment with HCl in dioxane, yielding the corresponding amine (XVII) (3, 4). Coupling of dipeptide ester (XVII) with *N*-(cyclopentyloxycarbonyl)-3-methyl-L-valine (XVIII) [prepared by condensation of cyclopentyl succinimidyl carbonate

(XX) with 3-methyl-L-valine (XIX) by means of Et_3N in THF/H_2O (1, 4)] in the presence of TBTU and DIEA in CH_2Cl_2 provides tripeptide derivative (XXI), which by selective hydrolysis of the PNB ester (XXI) by means of LiOH in H_2O/THF produces the tripeptide derivative (VIII) (1, 3, 4). Scheme 3.

The peptide building blocks (IV) and (VI) are prepared as follows:

Coupling of 4(*R*)-hydroxy-L-proline methyl ester hydrochloride (XXII) with *N*-(cyclopentyloxycarbonyl)-3-methyl-L-valine (XVIII) by means of EDC, HOBt and DIEA in DMF affords the dipeptide derivative (XXIII), which is then subjected to methyl ester hydrolysis with LiOH in H_2O/MeOH/THF to yield dipeptide carbamate (XXIV) (isolated as solvate with MTBE). Subsequent condensation of compound (XXIV) with the chloroquinoline (VII) using *t*-BuOK in DMSO gives rise to the key intermediate (IV) (2). Scheme 4.

Coupling of the dipeptide carbamate (XXIV) with methyl 1(*R*)-amino-2(*S*)-vinylcyclopropanecarboxylate tosylate salt (Va) by means of EDC, HOBt and DIEA in DMF leads to the tripeptide ester (XXV), which by hydrolysis with LiOH in H_2O/MeOH/THF provides the carboxylic acid intermediate (VI) (2). Scheme 4.

Scheme 3. Synthesis of Tripeptide Derivative (VIII)

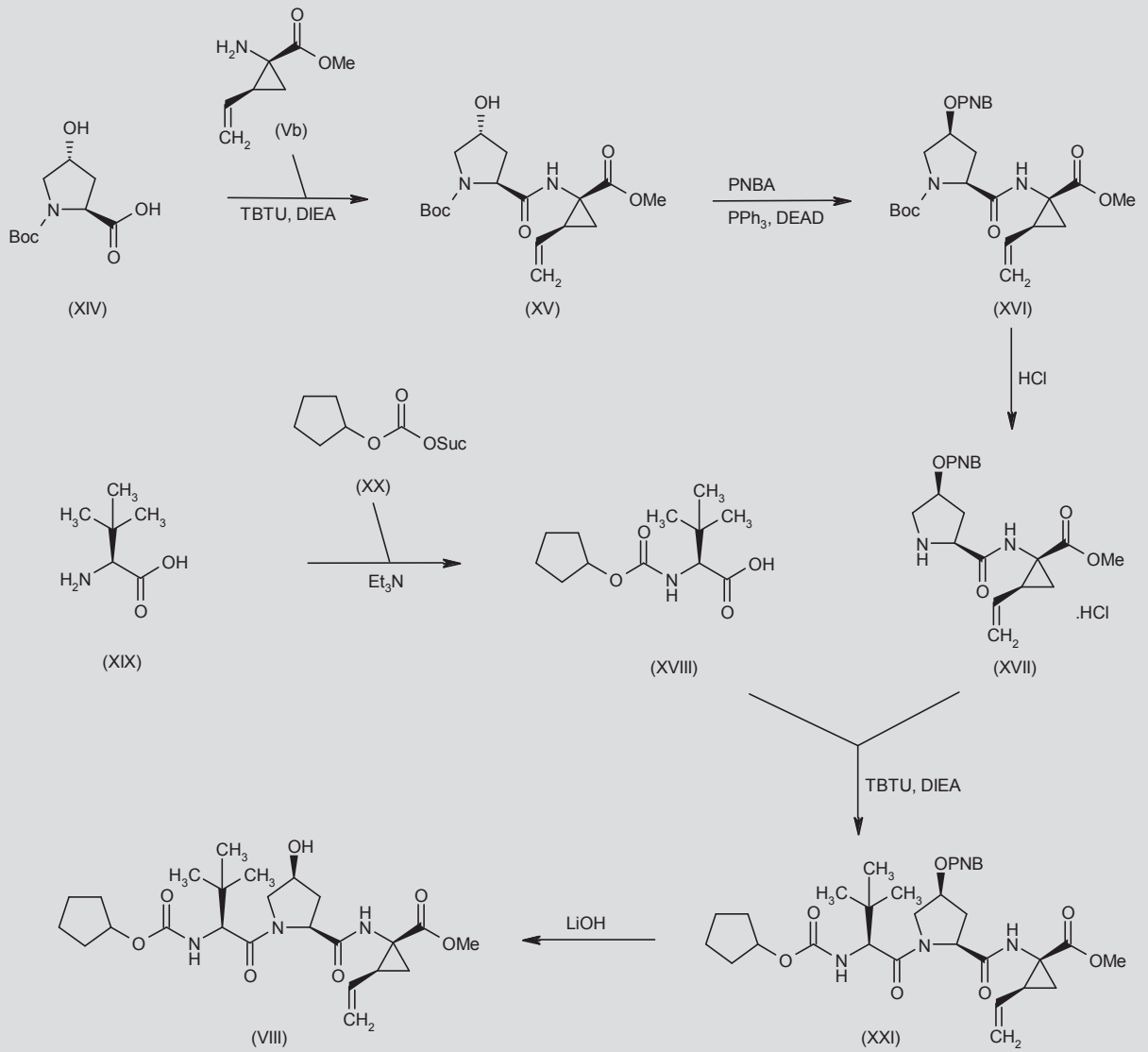

Scheme 4. Synthesis of Peptide Building Blocks (IV) and (VI)

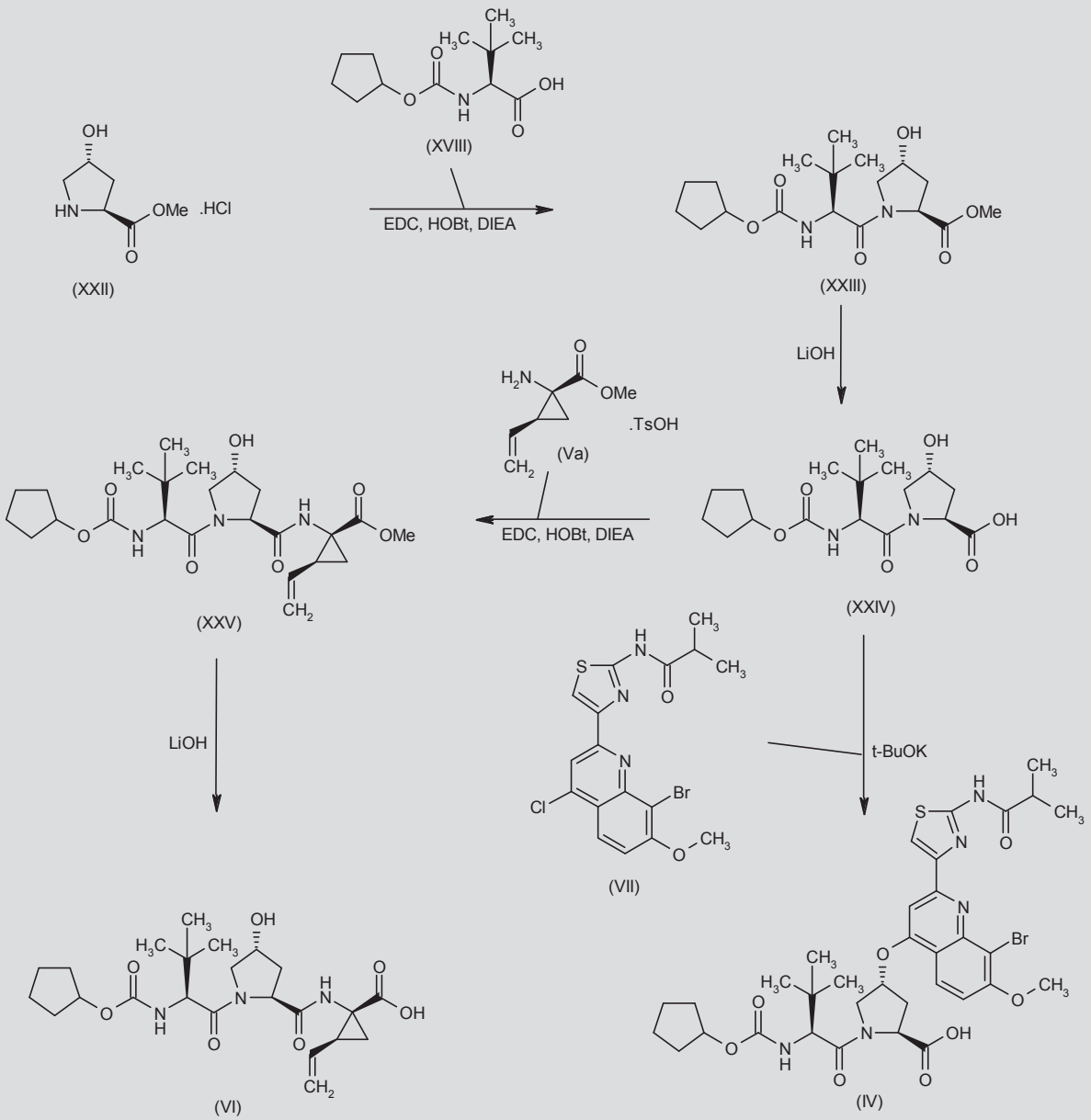

Hydroxyquinoline derivative (X) is obtained as follows:

Sandmeyer reaction of 2-amino-3-nitrophenol (XXVI) using $NaNO_2$ and HBr in the presence of CuBr in H_2O/dioxane gives 2-bromo-3-nitrophenol (XXVII), which by *O*-alkylation with MeI in the presence of Cs_2CO_3 in DMF affords the methyl ether (XXVIII). Subsequent reduction of the nitro derivative (XXVIII) with Fe powder in refluxing AcOH/EtOH provides 2-bromo-3-methoxyaniline (XXIX) (3, 4). Addition of aniline (XXIX) to dimethyl acetylene dicarboxylate (XXX) in refluxing MeOH produces the amino diester (XXXI), which by cyclization at 240 °C in diphenyl ether affords the quinoline (X) (1, 3, 4). Scheme 5.

The thiazolylquinoline intermediate (VII) is prepared by the following method:

ortho-Metalation of *N*-Boc-*m*-anisidine (XXXII) with BuLi in cold THF, followed by bromination with perfluorooctyl bromide, gives

Scheme 5. Synthesis of Hydroxiquinolone Derivative (X)

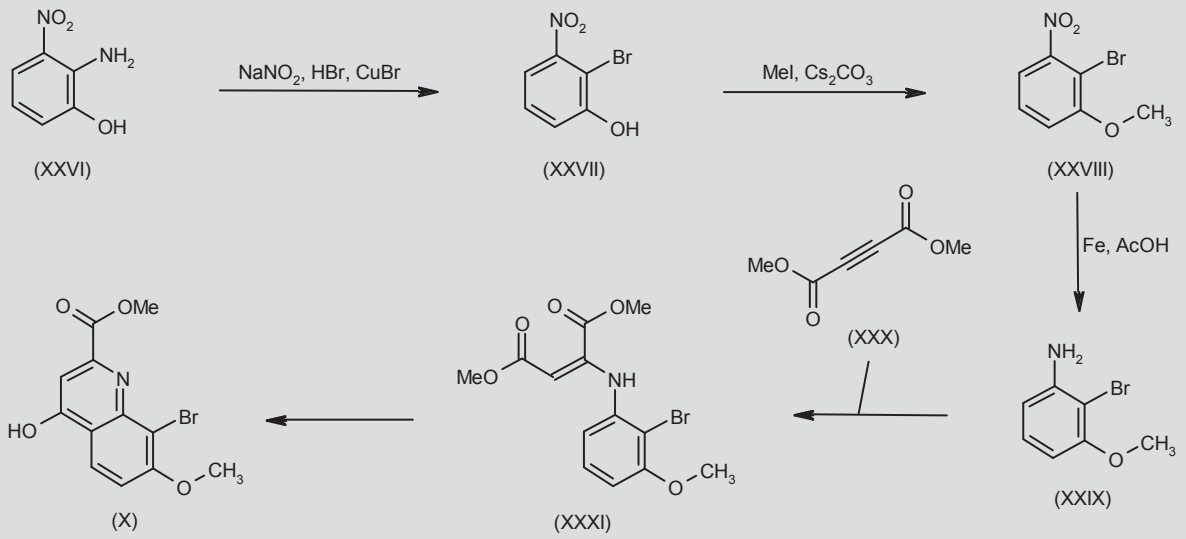

N-Boc-2-bromo-3-methoxyaniline (XXXIII), which by Boc group cleavage with HCl in diglyme at 100 °C provides 2-bromo-3-methoxyaniline hydrochloride (XXXIV). Friedel–Crafts acylation of bromoanisidine (XXXIV) with acetonitrile (XXXV) in the presence of BCl_3 and $AlCl_3$ in chlorobenzene at 100 °C affords 2′-amino-3′-bromo-4′-methoxyacetophenone (XXXVI) (4), which is then coupled with the acid chloride (XXXVII) [prepared by chlorination of 2-isobutyrylaminothiazole-4-carboxylic acid (XXXVIII) with either $(COCl)_2$ in DMF/THF (4, 5) or $SOCl_2$ in NMP (5)] by means of Et_3N and DMAP in THF (2) to provide the corresponding carboxamide (XXXIX) (2, 5). Intramolecular cyclocondensation of the ketoamide (XXXIX) in the presence of either *t*-BuOK in DME at 80-85 °C (2) or KOH in *t*-BuOH (5) yields the quinolinol (XL), which is then chlorinated with $POCl_3$ in dioxane at 75 °C to obtain the 4-chloroquinoline derivative (VII) (2, 5). Scheme 6.

BACKGROUND

Chronic hepatitis C affects an estimated 170 million people worldwide and is the leading indication for liver transplantation in the U.S. (6). Since the beginning of the 21st century, hepatitis C virus (HCV) drug development has been a very active field of clinical research. Until recently, eradication of chronic HCV depended on the combination of pegylated interferon (pegIFN) and ribavirin (RBV), which was approved by the Food and Drug Administration (FDA) in 1998. While this combination is effective in only 40-50% of patients infected with HCV genotype 1 (7), and 30-40% of patients co-infected with HIV (8), it also carries a high burden of side effects, mostly flu-like illness, fatigue, depression and anemia (7). This low-efficacy/high-toxicity regimen has motivated the search for a more potent treatment with an improved side effect profile. The lack of a tissue culture model had been a major obstacle to HCV drug development until recently. Production of infectious HCV in tissue culture is now possible and allows analysis of host–virus interactions (9-11). This was a huge step forward that facilitated anti-HCV drug discovery. Therefore, in the last decade, the HCV pipeline has dramatically grown and various therapeutic agents have been identified that target viral enzymes critical to HCV replication (12, 13).

There are several classes of direct-acting antivirals (DAAs), including the serine protease NS3/non-structural protein 4A (NS4A) inhibitors, the RNA-directed RNA polymerase 5B (NS5B) inhibitors and the non-structural protein 5A (NS5A) inhibitors. NS3/NS4A inhibitors are the farthest ahead in terms of clinical development. The first HCV DAA to have shown clinical proof of principle was BILN-2061, a reversible inhibitor of HCV NS3/NS4A (14, 15). Development of BILN-2061 was stopped following safety studies conducted in rhesus monkeys showing cardiotoxicity, specifically myocardial vacuolation at light microscopy, within 4 weeks of starting daily dosing (16). Boceprevir (SCH-503034) and telaprevir (VX-950), two linear α-ketoamide derivatives, have successfully gone through phases I to III of clinical development and were approved by the FDA in May 2011 to be used in combination with pegIFN and RBV (17). The combination of one of these protease inhibitors with pegIFN/RBV nearly doubles the chance of cure and allows for shorter treatment duration in the majority of patients (18-21). Although highly effective, this triple combination leads to increased side effects, mostly anemia and dysgeusia with boceprevir and skin reactions and anorectal dis-

Scheme 6. Synthesis of Thiazolylquinoline Intermediate (VII)

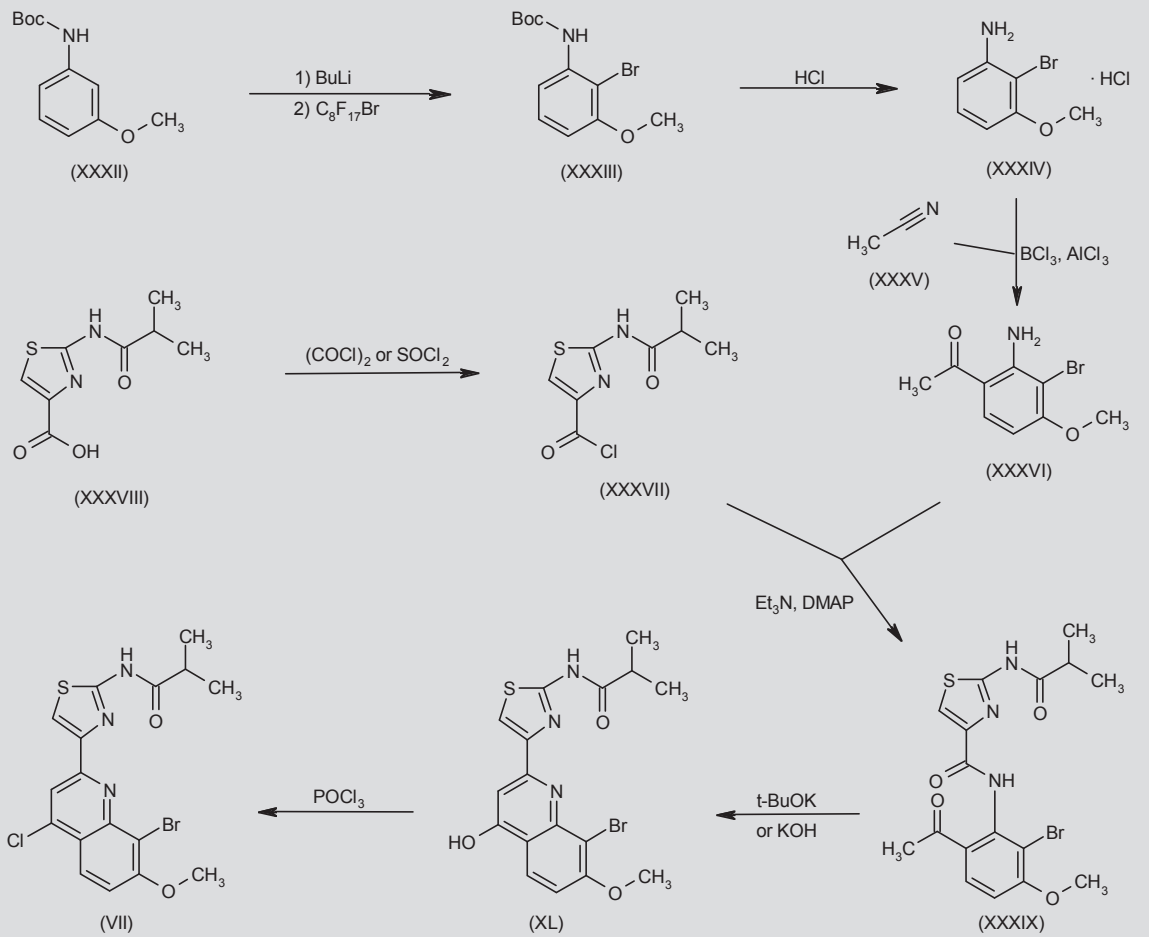

comfort with telaprevir. These two protease inhibitors, which have to be taken three times daily, are classified as first-generation, first-wave protease inhibitors. The second-generation protease inhibitors feature linear and macrocyclic noncovalent inhibitors of HCV NS3/NS4A. These second-wave protease inhibitors offer the advantages of convenience, being administered once or twice daily, and improved side effect profiles. Broader genotypic coverage and improved resistance profiles are true characteristics of the second-generation protease inhibitors (22).

BI-201335 is a linear tripeptide carboxylic acid inhibitor of the NS3/NS4A proteases that noncovalently interacts with the enzymes, resulting in high binding affinity. Its carboxylic acid at the *C*-terminus allows for selective interaction with the HCV NS3 protease active site, contributing to its potency (11, 23, 24). The combination of the carboxylic acid at the *C*-terminus and a bromo-quinoline substitution on its proline residue is responsible for its high potency (1). BI-201335 has shown favorable results in preclinical and early clinical phases of development (25-28). It is a potent protease inhibitor administered once daily that appears to have an improved side effect profile compared to the two α-ketoamide derivatives boceprevir and telaprevir.

PRECLINICAL PHARMACOLOGY

A detailed preclinical characterization of BI-201335 has been published (25). In biochemical assays, the median 50% inhibitory concentration (IC_{50}) was determined and converted to apparent K_i values (binding affinity for inhibition) to allow direct comparison of binding affinity across HCV genotypes. BI-201335 showed the great-

est inhibitory potency against HCV genotypes 1a, 1b and 4a (K_{iapp} ± standard deviation [SD] = 1.2 ± 0.2, 2.8 ± 0.5 and 1.8 ± 0.5 nM, respectively). It also inhibits the NS3/NS4A proteases of HCV genotypes 5a and 6a (K_{iapp} ± SD = 5.8 ± 1.0 and 6.1 ± 0.9 nM, respectively). Its inhibitory potency is weaker for HCV genotypes 2a, 2b and 3a (20-, 50- and 190-fold, respectively, vs. genotype 1a). When compared with telaprevir and boceprevir, BI-201335 had similar inhibitory potency against HCV genotypes 1a and 1b. BI-201335 had no activity against the human serine and cysteine proteases elastase and cathepsin B, and little or no activity against 39 proteases tested, which is consistent with its NS3-selective property conferred by the *C*-terminal carboxylic acid (24).

Similar to enzymatic assays, in replicon assays, BI-201335 had low-nanomolar activity against HCV genotypes 1a and 1b. The 50% effective concentrations (EC_{50}) ± SD of BI-201335 against HCV genotypes 1a and 1b in replicon assays were 6.5 ± 0.9 and 3.1 ± 1.2 nM, respectively. For comparison, in that experiment, telaprevir and boceprevir EC_{50} values against genotype 1a were 108- and 85-fold those of BI 201335, respectively, and 174- and 168-fold those for genotype 1b, respectively, despite their excellent enzymatic activity (25). When BI-201335 was combined with either interferon alfa or RBV in replicon assays, additive effects were observed.

PHARMACOKINETICS AND METABOLISM

In animal studies, a good absorption, distribution, metabolism and excretion (ADME) profile was seen. After a single oral administration of BI-201335 at a dose of 5 mg/kg in rats, monkeys and dogs, the drug was rapidly absorbed, as demonstrated by a time to maximum concentration of drug in serum (t_{max}) value of 1-2 hours (25). The oral maximum concentration of drug in serum (C_{max}) ± standard error (SE) was lowest in rats (0.41 µM), intermediate in monkeys (2.0 ± 0.3 µM) and highest in dogs (3.8 ± 0.3 µM). The area under the curve (AUC) ± SE also increased from 1.55 µM·h in rats to 8.3 ± 0.9 µM·h in monkeys and 13 ± 3 µM·h in dogs. In rats, drug levels were higher in liver than plasma, with a mean liver to plasma ratio of 42 in 1 hour. The same favorable distribution was not reported in dogs and monkeys.

In humans, the pharmacokinetics of BI-201335 have been studied in both HCV treatment-naive and treatment-experienced patients in a randomized, placebo-controlled, successive cohort study (26). Treatment-naive patients received BI-201335 monotherapy for 14 days (20, 48, 120 and 240 mg once daily) or matching placebo followed by combination with pegIFN/RBV through day 28. Treatment-experienced patients received BI-201335 at a dose of 48, 120 or 240 mg once daily in combination with pegIFN/RBV for 28 days. The mean t_{max} ranged from 2.0 to 5.57 hours. C_{max}, minimal concentration of drug in serum (C_{min}) and $AUC_{0-\delta}$ increased supraproportionally with the BI-201335 dose. The mean elimination half-life ($t_{1/2}$) was approximately 20-30 hours, with the lowest value being 17.8 hours and the highest value 38.7 hours. This suggested that once-daily dosing was appropriate. No difference was seen between treatment-naive and -experienced patients, although there was significant interindividual variability in pharmacokinetic parameters. The coefficient of variation, which measures the amount of variation in a data set, reached 61% for t_{max}, 65% for C_{max}, 68% for C_{min}, 65% for $AUC_{0-\delta}$ and 31% for $t_{1/2}$.

SAFETY

Results of the phase Ia multiple-rising-dose study in healthy volunteers of BI-201335 at doses of 20-240 mg once daily for 21-28 days demonstrated that the drug was safe and well tolerated and justified continuation into phase Ib (26). These results have not yet been published. In a phase Ib multiple-ascending-dose study of BI-201335 in 34 treatment-naive and 19 treatment-experienced patients, the drug was generally well tolerated. During the first 14 days during which the drug was administered as monotherapy, the frequency of adverse events was not higher in the BI-201335 group compared to the placebo group. Dose-dependent, mild unconjugated hyperbilirubinemia occurred with BI-201335, with a maximal median increase of 0.8 mg/dL in the 24-mg once daily group. When BI-201335 was combined with pegIFN/RBV, the most common adverse events were fatigue, nausea, headache, gastrointestinal discomfort and anemia. Four patients experienced a mild rash or photosensitivity that spontaneously resolved. Two severe adverse events (SAEs) were reported (asthenia and cataract), both of which were thought to be unrelated to BI-201335.

In a phase Ib trial of BI-201335 in HCV genotype 1 patients with compensated liver cirrhosis and prior non-response to pegIFN/RBV (29), there was good safety and tolerability in the once daily dosing group, comparable to non-cirrhotic patients (26). Isolated unconjugated hyperbilirubinemia was more common and more pronounced in the group that received twice daily dosing. Two severe adverse events and two treatment discontinuations occurred in the twice daily dosing group. In the interferon-free SOUND-C1 trial (discussed below), the reported adverse events during the first 28 days were mild gastrointestinal effects (diarrhea, nausea and vomiting), rash and photosensitivity.

In the phase IIb trials, several adverse events were reported in a higher proportion of patients receiving BI-201335 compared to those on placebo and were dose-dependent (27, 28). Jaundice, skin manifestations, including rash, photosensitivity reactions, pruritus and dry skin, and gastrointestinal side effects, mostly nausea, vomiting and diarrhea, were reported in the BI-201335 arms in a proportion exceeding 10% of the placebo/pegIFN/RBV group. Jaundice was secondary to predominantly indirect or unconjugated hyperbilirubinemia. The mechanism of action of this unconjugated hyperbilirubinemia is inhibition of hepatic uptake of UDP-glucuronosyltransferase 1-1 (*UGT1A1*) (30). In all trials of BI-201335, hyperbilirubinemia was dose-dependent, unconjugated, isolated and rapidly reversible at the time of drug discontinuation.

CLINICAL STUDIES

Activity in cell culture is usually predictive of in vivo efficacy. As previously discussed, BI-201335 exhibited similar and strong activity in enzymatic and cellular assays (25). The results of a phase Ib multiple-ascending-dose study of BI-201335 in 34 treatment-naive patients with HCV genotype 1 and 19 treatment-experienced patients were recently published (26). In this study, the treatment-naive patients were randomized to BI-201335 monotherapy 20-240 mg once daily versus placebo for 14 days, followed by combination with pegIFN/RBV for 14 days when a ≥ 1 $\log_{10}$ international units (IU)/mL decline in HCV RNA was reached following 14 days of treat-

ment. The treatment-experienced patients received 48-240 mg of BI-2101335 once daily in combination with pegIFN/RBV for 28 days. Monotherapy was not allowed in this group. All patients receiving BI-201335 (n = 25; 96%), except one in the 20-mg treatment group, achieved the primary efficacy endpoint of ≥ 2 $\log_{10}$ IU/mL HCV RNA reduction in the first 14 days. Among treatment-naive patients, median maximal HCV RNA reductions during 14-day monotherapy were −3.0, −3.6, −3.7 and −4.4 $\log_{10}$ IU/mL for the 20-, 48-, 120- and 240-mg groups. This −4.4 $\log_{10}$ IU/mL median maximal decline in HCV RNA at the dose of 240 mg once daily is comparable to what has been reported with telaprevir (maximal median decline of −4.4 $\log_{10}$ IU/mL at 750 mg every 8 hours for 14 days) (31) and boceprevir (maximal mean HCV RNA decline of −2.06 $\log_{10}$ IU/mL at 400 mg 3 times daily for 14 days) (32). As expected with protease inhibitor monotherapy, virological breakthrough occurred in most of the patients in the first 14 days. The proportion of patients with viral breakthrough by day 14 was 83.3%, 71.4%, 71.4% and 83.3%, respectively, in the 20-, 48-, 120- and 240-mg BI-201335 groups. At the time of breakthrough, NS3/NS4A-resistant variants (R155K with HCV genotype 1a and D168V with HCV genotype 1b) known to confer in vitro resistance to BI-201335 were found. When the R155K mutation was selected, sensitivity to BI-201335 was less, with EC_{50} values of 1.8-6.5 µM, whereas the EC_{50} for D168V mutants was 3.6-15 µM. These variants are also selected with the use of other protease inhibitors, such as the first-generation, first-wave protease inhibitors boceprevir and telaprevir, which strongly suggests cross-resistance (33-35). Second-generation protease inhibitors, such as MK-5172, which has pan-genotypic activity, do not share the same resistance mutations and retain activity against common first-generation protease inhibitor resistance-associated variants. It is known that naturally occurring variants resistant to HCV protease inhibitors exist in about 2% of treatment-naive patients at baseline (V36M, R155K, V170A and R109K) (36). The effect of pre-existing resistant mutants in patients treated with BI-201335 has not yet been reported.

Following 14 days of monotherapy, pegIFN/RBV was added in those patients with a ≥ 1 $\log_{10}$ IU/mL reduction in HCV RNA at day 6 or day 10, which was seen in all patients on BI-201335, but in none of the patients on placebo. After addition of pegIFN/RBV, 4 of 6, 4 of 7, 6 of 7 and 6 of 6 patients, respectively, treated with BI-201335 at 20, 48, 120 or 240 mg showed ≥ 1 $\log_{10}$ IU/mL HCV RNA reductions between day 15 and 28. Of the 19 treatment-experienced patients treated with BI-201335 and pegIFN/RBV, 3 of 6, 4 of 7 and 5 of 6 patients, respectively, in the 48-, 120- and 240-mg dose groups achieved HCV RNA < 25 IU/mL at day 28. All patients achieved the primary efficacy endpoint of ≥ 2 $\log_{10}$ IU/mL reduction in HCV RNA from baseline during treatment. The mean HCV RNA reduction was 5.3 $\log_{10}$ IU/mL for BI-201335 given as 240 mg once daily after 28 days in combination with pegIFN/RBV. Of the 19 patients, 3 experienced virological breakthrough during triple combination, but none in the 240 mg once daily group.

A different phase Ib trial assessed safety, short-term efficacy and pharmacokinetics of BI-201335 in HCV genotype 1 patients with compensated liver cirrhosis and prior partial response (maximum HCV RNA reduction > 1 $\log_{10}$ IU/mL from baseline but never achieved undetectable HCV RNA at any time) or null response (maximum HCV RNA reduction < 1 $\log_{10}$ IU/mL from baseline at any time) to pegIFN/RBV therapy (29). This was an open-label, sequential-group, dose-escalating comparison of 240 mg BI-201335 once daily (n = 6) or twice daily (n = 7) for 28 days in combination with pegIFN/RBV. All patients showed a rapid and continuous decline in HCV RNA, with mean HCV RNA declines on day 28 of −4.8 and −5.0 $\log_{10}$ IU/mL, respectively, in the 240-mg once daily and twice daily groups. At day 28, 5 of 6 and 6 of 7 patients achieved HCV RNA < 25 IU/mL in the once daily and twice daily groups.

SOUND-C1 was a phase Ib study that evaluated an interferon-free regimen consisting of BI-201335, BI-207127 (an NS5B inhibitor) and RBV in patients with HCV genotype 1, naive to HCV treatment. This was a randomized, open-label trial evaluating the combination of BI-201335 120 mg once daily plus BI-207127 400 or 600 mg 3 times daily and weight-based RBV (in 2 divided doses) for 28 days. At day 29, patients were switched to BI-201335 in combination with pegIFN and RBV, as specified in the protocol. The 28-day results have been presented (37). All but two patients experienced a rapid first-phase decline in HCV viral load in the first 2 days, followed by a slower second-phase decline. Patients with HCV genotype 1a had lower response rates when receiving BI-207127 400 mg three times daily compared to patients with HCV genotype 1b, while HCV subtype did not impact response rates in those receiving the dose of 600 mg three times daily. In the lower dose group, 4 of 15 patients had undetectable HCV RNA (< 25 IU/mL) at day 8, 6 of 15 at day 15, 10 of 15 at day 22 and 11 of 15 at day 29. In the higher dose group, at the same time points, 3 of 17, 14 of 17, 17 of 17 and 17 of 17 patients, respectively, had undetectable HCV RNA.

The phase IIb SILEN-C1 trial was conducted in patients with HCV genotype 1 naive to HCV treatment to evaluate the safety and efficacy of BI-201335 given once daily at a dose of 120 or 240 mg for 24 weeks in combination with pegIFN and RBV for 24 versus 48 weeks (27). A lead-in of pegIFN and RBV for 3 days was also evaluated in two of the four arms (with 120 and 240 mg once daily). In the two arms using BI-201335 at a dose of 240 mg (with and without a lead-in), patients achieving extended rapid virological response (eRVR) were re-randomized to either stop treatment at week 24 or continue with pegIFN/RBV for a total of 48 weeks. Patients receiving 240 mg once daily without a lead-in achieved the highest eRVR rate of 87% and were thus eligible for shortened treatment duration. This arm had the highest SVR rate of 83% versus 73% of patients receiving 240 mg with a lead-in and 56% of patients in the pegIFN/RBV control group. Prolonging treatment to 48 weeks in those patients achieving eRVR did not result in higher SVR rates. Of those who completed 24 weeks, 93% achieved SVR versus 90% of those who completed 48 weeks. Viral breakthroughs occurred in 2.8-5.8% of patients receiving BI-201335, with the highest rate in those in the 120-mg daily with lead-in arm. There was no difference in SVR according to HCV genotype 1 subtypes. In the 240-mg once daily arm, 82% of patients infected with HCV genotype 1a achieved SVR compared to 84% of those infected with HCV genotype 1b (38).

The phase IIb SILEN-C2 trial evaluated BI-201335 for 24 weeks in combination with pegIFN/RBV for 24 versus 48 weeks, with or without a 3-day lead-in of pegIFN/RBV in previous partial and null responders infected with HCV genotype 1 (28). The dose of 240 mg once daily (with and without a lead-in) was compared to 240 mg twice daily with a lead-in. Patients in the 240-mg once daily group

with lead-in achieving eRVR were re-randomized to stopping therapy or continuing 48 weeks with pegIFN/RBV. Similar to the SILEN-C1 trial, the lead-in did not appear to be useful. The 240-mg once daily dosing without a lead-in led to the highest SVR rates. Overall, eRVR was achieved by 45% of patients and SVR was achieved by 27-41% of patients. The lowest SVR rate was observed in the 240-mg once daily with lead-in arm, the one group that used response-guided therapy (RGT) for those achieving eRVR. In comparison to the good results observed with 24 weeks of treatment in the naive patients achieving eRVR in the SILEN-C1 trial (27), prior partial and null responders achieving eRVR in SILEN-C2 achieved lower SVR rates when stopped at week 24. Only 40% of patients achieved SVR when stopped at week 24 compared to 72% of those who completed 48 weeks of treatment. The additional 24 weeks of pegIFN/RBV greatly impacted the relapse rate. Sixty percent of those who stopped at week 24 relapsed compared to 21% of those who completed 48 weeks of treatment. Viral breakthroughs occurred predominantly on BI-201335 compared to pegIFN/RBV (17-28% vs. 5-7%).

SILEN-C3 was an open-label phase IIb study in treatment-naive HCV genotype 1 patients (39). The objective was to evaluate the efficacy and safety of 12 versus 24 weeks of BI-201335 with RGT. Seventy-nine patients were randomized to 120 mg BI-201335 once daily with pegIFN/RBV for 24 weeks followed by pegIFN/RBV alone for up to 48 weeks. Eighty-one patients were randomized to 120 mg BI-201335 once daily with pegIFN/RBV for 12 weeks followed by pegIFN/RBV alone for a total of 24-48 weeks. The total duration of pegIFN/RBV tail depended on achievement of eRVR (HCV RNA below lower limit of quantification at week 4 and HCV RNA below lower limit of detection from week 8 to 18). In the 12-week triple therapy arm, 65% of patients achieved SVR compared to 73% of those who received 24 weeks of triple therapy. More than 70% of patients achieved eRVR and received 24 weeks of total treatment.

Currently, patients are being recruited in phase III clinical trials. In treatment-naive patients with HCV genotype 1, a randomized, double-blind, placebo-controlled phase III study of once-daily BI-201335 120 mg for 12 or 24 weeks or BI-201335 240 mg for 12 weeks in combination with pegIFN/RBV will enroll 625 patients. A different randomized, double-blind, placebo-controlled phase III study also in treatment-naive patients will enroll 625 patients to compare BI-201335 120 mg once daily for 24 weeks to 240 mg once daily for 12 weeks in combination with pegIFN/RBV. In treatment-experienced patients with HCV genotype 1, a randomized, double-blind, placebo-controlled phase III study of BI-201335 240 mg once daily for 12 or 24 weeks in combination with pegIFN/RBV will enroll 625 patients.

In HIV/HCV co-infected patients, a multinational phase III trial started enrollment in the fall of 2011. This trial is evaluating the efficacy and the safety of BI-201335 for 12 or 24 weeks in combination with pegIFN/RBV for 24-48 weeks in HCV treatment-naive patients or prior relapsers who are co-infected with HIV. This trial is among the first to evaluate a shorter than 48-week treatment (response-guided therapy) with DAA in HIV co-infected patients.

DRUG INTERACTIONS

Three different drug interaction studies of BI-201335 have been conducted evaluating potential drug interactions with darunavir/ritonavir, tenofovir and efavirenz. The results have not yet been published.

SOURCE

Boehringer Ingelheim Pharma GmbH & Co. KG (DE).

DISCLOSURES

The author states no conflicts of interest.

REFERENCES

1. Llinas-Brunet, M., Bailey, M.D., Goudreau, N. et al. *Discovery of a potent and selective noncovalent linear inhibitor of the hepatitis C virus NS3 protease (BI 201335).* J Med Chem 2010, 53(17): 6466-76.
2. Berkenbusch, T., Busacca, C.A., Jaeger, B., Varsolona, R.J. (Boehringer Ingelheim Pharma GmbH & Co. KG). *Crystalline forms of a 2-thiazolyl-4-quinolinyl-oxy derivative, a potent HCV inhibitor*. CN 102159571, EP 2331538, JP 2012502910, KR 2011059841, US 2010093792, WO 2010033444.
3. Llinas-Brunet, M., Bailey, M., Bhardwaj, P. et al. (Boehringer Ingelheim International GmbH & Co. KG). *Hepatitis C inhibitor compounds*. US 7585845.
4. Bhardwaj, P., Forgione, P., Goudreau, N. et al. (Boehringer Ingelheim International GmbH). *Hepatitis C inhibitor compounds*. EP 1654261, JP 2006528937, JP 2010043129, US 2005020503, US 2011177030, US 8067438, WO 2004103996.
5. Patel, N., Senanayake, C.H., Wei, X., Yee, N.K. (Boehringer Ingelheim Pharma GmbH & Co. KG). *Process for preparing sulfonyl quinolines*. EP 2408768, WO 2010107965.
6. Annual Report of the U.S. Organ Procurement and Transplantation Network and the Scientific Registry of Transplant Recipients: Transplant Data 1999-2008. U.S. Department of Health and Human Services, Health Resources and Services Administration, Healthcare Systems Bureau, Division of Transplantation, Rockville, MD.).
7. Manns, M.P., McHutchison, J.G., Gordon, S.C. et al. *Peginterferon alfa-2b plus ribavirin compared with interferon alfa-2b plus ribavirin for initial treatment of chronic hepatitis C: a randomised trial. Lancet 2*001, 358(9286): 958-65.
8. Torriani, F.J., Rodriguez-Torres, M., Rockstroh, J.K. et al. *Peginterferon alfa-2a plus ribavirin for chronic hepatitis C virus infection in HIV-infected patients.* N Engl J Med 2004, 351(5): 438-50.
9. Lindenbach, B.D., Evans, M.J., Syder, A.J. et al. *Complete replication of hepatitis C virus in cell culture.* Science 2005, 309(5734): 623-6.
10. Wakita, T., Pietschmann, T., Kato, T. et al. *Production of infectious hepatitis C virus in tissue culture from a cloned viral genome.* Nat Med 2005, 11(7): 791-6.
11. Zhong, J., Gastaminza, P., Cheng, G. et al. *Robust hepatitis C virus infection in vitro*. Proc Natl Acad Sci U S A 2005, 102(26): 9294-9.
12. Kwong, A.D., McNair, L., Jacobson, I., George, S. *Recent progress in the development of selected hepatitis C virus NS3.4A protease and NS5B polymerase inhibitors.* Curr Opin Pharmacol 2008, 8(5): 522-31.
13. Dore, G.J., Matthews, G.V., Rockstroh, J. *Future of hepatitis C therapy: Development of direct-acting antivirals*. Curr Opin HIV AIDS 2011, 6(6): 508-13.

14. Lamarre, D., Anderson, P.C., Bailey, M. et al. *An NS3 protease inhibitor with antiviral effects in humans infected with hepatitis C virus.* Nature 2003, 426(6963): 186-9.
15. Hinrichsen, H., Benhamou, Y., Wedemeyer, H. et al. *Short-term antiviral efficacy of BILN 2061, a hepatitis C virus serine protease inhibitor, in hepatitis C genotype 1 patients.* Gastroenterology 2004, 127(5): 1347-55.
16. Stoltz, J.H., Stern, J.O., Huang, Q., Seidler, R.W., Pack, F.D., Knight, B.L. *A twenty-eight-day mechanistic time course study in the rhesus monkey with hepatitis C virus protease inhibitor BILN 2061.* Toxicol Pathol 2011, 39(3): 496-501.
17. Pawlotsky, J.M. *The results of phase III clinical trials with telaprevir and boceprevir presented at the Liver Meeting 2010: A new standard of care for hepatitis C virus genotype 1 infection, but with issues still pending*. Gastroenterology 2011, 140(3): 746-54.
18. Jacobson, I.M., McHutchison, J.G., Dusheiko, G. et al. *Telaprevir for previously untreated chronic hepatitis C virus infection.* N Engl J Med 2011, 364(25): 2405-16.
19. Poordad, F., McCone, J. Jr., Bacon, B.R. et al. *Boceprevir for untreated chronic HCV genotype 1 infection*. N Engl J Med 2011, 364(13): 1195-206.
20. Zeuzem, S., Andreone, P., Pol, S. et al. *Telaprevir for retreatment of HCV infection*. N Engl J Med 2011, 364(25): 2417-8.
21. Bacon, B.R., Gordon, S.C., Lawitz, E. et al. *Boceprevir for previously treated chronic HCV genotype 1 infection.* N Engl J Med 2011, 364(13): 1207-17.
22. Ciesek, S., von Hahn, T., Manns, M.P. *Second-wave protease inhibitors: Choosing an heir.* Clin Liver Dis 2011, 15(3): 597-609.
23. Tsantrizos, Y.S., Bolger, G., Bonneau, P. et al. *Macrocyclic inhibitors of the NS3 protease as potential therapeutic agents of hepatitis C virus infection.* Angew Chem Int Ed Engl 2003, 42(12): 1356-60.
24. Llinas-Brunet, M., Bailey, M., Deziel, R. et al. *Studies on the C-terminal of hexapeptide inhibitors of the hepatitis C virus serine protease.* Bioorg Med Chem Lett 1998, 8(19): 2719-24.
25. White, P.W., Llinas-Brunet, M., Amad, M. et al. *Preclinical characterization of BI 201335, a C-terminal carboxylic acid inhibitor of the hepatitis C virus NS3-NS4A protease.* Antimicrob Agents Chemother 2010, 54(11): 4611-8.
26. Manns, M.P., Bourliere, M., Benhamou,Y. et al. *Potency, safety, and pharmacokinetics of the NS3/4A protease inhibitor BI201335 in patients with chronic HCV genotype-1 infection*. J Hepatol 2011, 54(6): 1114-22.
27. Sulkowski, M.S., Ceasu, E., Asselah, T. et al. *SILEN-C1: Sustained virologic response (SVR) and safety of BI 201335 combined with peginterferon alfa-2a and ribavirin (P/R) in treatment-naive patients with chronic genotype 1 HCV.* J Hepatol [46th Annu Meet Eur Assoc Study Liver (EASL) (March 30-April 3, Berlin) 2011] 2011, 54(Suppl. 1): Abst 60.
28. Sulkowski, M.S., Bourliere, M., Bronowicki, J.P. et al. *SILEN-C2: Sustained virologic response (SVR) and safety of BI201335 combined with peginterferon alfa-2a and ribavirin (P/R) in chronic HCV genotype-1 patients with non-response to P/R.* J Hepatol [46th Annu Meet Eur Assoc Study Liver (EASL) (March 30-April 3, Berlin) 2011] 2011, 54(Suppl. 1): Abst 66.
29. Pol, S., Berg, T., Bonacini, M. et al. *Virological response and safety of BI 201335 protease inhibitor, peginterferon alfa 2a and ribavirin treatment of HCV genotype-1 patients with compensated liver cirrhosis and non-response to previous peginterferon/ribavirin*. Hepatology 2009, 50: 228A.
30. Sane, R., Podila, L., Mathur, A. et al. *Mechanisms of isolated unconjugated hyperbilirubinemia induced by the HCV NS3/4A protease inhibitor BI201335.* J Hepatol [46th Annu Meet Eur Assoc Study Liver (EASL) (March 30-April 3, Berlin) 2011] 2011, 54(Suppl. 1): Abst 1236.
31. Reesink, H.W., Zeuzem, S., Weegink, C.J. et al. *Rapid decline of viral RNA in hepatitis C patients treated with VX-950: A phase Ib, placebo-controlled, randomized study.* Gastroenterology 2006, 131(4): 997-1002.
32. Zeuzem, S., Sarrazin, C., Rouzier, R. et al. *Anti-viral activity of SCH 503034, a HCV protease inhibitor, administered as monotherapy in hepatitis C genotype-1 patients refractory to pegylated interferon (PEGIFN-alfa).* Hepatology [56th Annu Meet Am Assoc Study Liver Dis (Nov 11-15, San Francisco) 2005] 2005, Abst 94.
33. Susser, S., Welsch, C., Wang, Y. et al. *Characterization of resistance to the protease inhibitor boceprevir in hepatitis C virus-infected patients.* Hepatology 2009, 50(6): 1709-18.
34. Sarrazin, C., Kieffer, T.L., Bartels, D. et al. *Dynamic hepatitis C virus genotypic and phenotypic changes in patients treated with the protease inhibitor telaprevir.* Gastroenterology 2007, 132(5): 1767-77.
35. Lin, C., Gates, C.A., Rao, B.G. et al. *In vitro studies of cross-resistance mutations against two hepatitis C virus serine protease inhibitors, VX-950 and BILN 2061.* J Biol Chem 2005, 280(44): 36784-91.
36. Bartels, D.J., Zhou, Y., Zhang, E.Z. et al. *Natural prevalence of hepatitis C virus variants with decreased sensitivity to NS3/4A protease inhibitors in treatment-naïve subjects.* J Infect Dis 2008, 198(6): 800-7.
37. Zeuzem, S., Asselah, T., Angus, P. et al. *Strong antiviral activity and safety of IFN-sparing treatment with the protease inhibitor BI201335, the HCV polymerase inhibitor BI207127 and ribavirin in patients with chronic hepatitis C*. Hepatology 2010, 52(4): Abst LB-7.
38. Sulkowski, M.S., Asselah, T., Ferenci, P. et al. *Treatment with the 2nd generation HCV protease inhibitor BI 201335 results in high and consistent SVR rates - Results from SILEN-C1 in treatment-naïve patients across different baseline factors.* Hepatology [62nd Annu Meet Am Assoc Study Liver Dis (Nov 4-8, San Francisco) 2011] 2011, 54(4, Suppl. 1):473A.
39. Dieterich, D., Asselah, T., Guyader, D. *SILEN-C3: Treatment for 12 or 24 weeks with BI 201335 combined with peginterferon alfa-2a and ribavirin in treatment-naïve patients with chronic genotype-1 HCV infection.* Hepatology [62nd Annu Meet Am Assoc Study Liver Dis (Nov 4-8, San Francisco) 2011] 2011, 54(4, Suppl. 1): Abst 378A.